PACIFIC EARTHQUAKE ENGINEERING
RESEARCH CENTER

Integrated Probabilistic Performance-Based Evaluation of Benchmark Reinforced Concrete Bridges

Kevin R. Mackie
University of Central Florida

John-Michael Wong
Božidar Stojadinović
University of California, Berkeley

PEER 2007/09
JANUARY 2008

Integrated Probabilistic Performance-Based Evaluation of Benchmark Reinforced Concrete Bridges

Kevin R. Mackie
Department of Civil and Environmental Engineering
University of Central Florida

John-Michael Wong
Department of Civil and Environmental Engineering
University of California, Berkeley

Božidar Stojadinović
Department of Civil and Environmental Engineering
University of California, Berkeley

PEER Report 2007/09
Pacific Earthquake Engineering Research Center
College of Engineering
University of California, Berkeley
January 2008

ABSTRACT

Multiple-span reinforced concrete highway overpass bridges constitute a large portion of the total inventory of bridges in California, particularly among bridges of new design. Probabilistic valuation of performance of these bridges under rare but strong ground motions is therefore essential for successful evaluation of the entire regional transportation network performance during and after an earthquake. Additionally, probabilistic quantification of bridge seismic performance and vulnerability provides insight into the shortcomings of current designs and into the potential advantages of proposed new technologies at varying levels of seismic hazard and for different site conditions.

Performance of bridges at the demand, damage, and loss levels can be evaluated using the Pacific Earthquake Engineering Research (PEER) Center's probabilistic performance-based seismic evaluation framework. Use of this framework to evaluate two classes of benchmark reinforced concrete bridge types typical of new construction in California is presented. Each bridge type has a variety of column designs for different seismic demands. Models of these structures are created that account for the nonlinear behavior of the columns, deck, abutments, and expansion joints at the abutments. Seismic demand models are then developed using nonlinear time history analysis, considering both near- and far-field excitation types. Damage in the bridge components is determined using experimental and empirical databases. Structural components are then classified into performance groups according to the repair methods corresponding to their damage states. Finally, approximate repair cost ratios and repair durations are estimated from both discrete bridge-level damage states and the assembly of discrete damage states from all performance groups.

Three realistic damage scenarios are developed to calibrate the repair cost and the repair working days estimate data. The results are presented in the forms of repair cost ratios and repair time loss models and fragilities. The performance of the benchmark bridges, particularly bridge Type 1A, is intended to serve as a baseline for other PEER researchers to measure the change of bridge seismic performance due to the use of new experimentally calibrated models of column, abutment, and foundation components; due to the use of new enhanced-performance structural elements and response modification devices; and due to explicit consideration of liquefaction and lateral spreading. The performance of the benchmark bridges is also intended to serve as a baseline for transportation network studies by other PEER researchers.

An implementation of the PEER Center's probabilistic performance-based seismic evaluation framework is also presented in this report. This implementation, developed for the testbed bridges, is modular to allow plug-and-play incorporation of emerging structural components, response modification technologies, analysis methods, and repair techniques. The implementation is founded on a general closed-form solution of the PEER framework total probability integral based on the demand, damage, and loss models developed in this report for the benchmark bridges. A method for developing such models for other structures is presented. A Matlab-based tool is developed to facilitate the integration of the PEER framework total probability integral. Finally, a data structure designed to efficiently organize and store the data and interim results is presented. Together, the implemented tools and data structures form a solid basis for conducting probabilistic performance-based seismic evaluations of any structure using the PEER Center framework.

ACKNOWLEDGMENTS

This work was supported primarily by the Earthquake Engineering Research Centers Program of the National Science Foundation under award number EEC-9701568 through the Pacific Earthquake Engineering Research Center (PEER).

Any opinions, findings, and conclusions or recommendations expressed in this material are those of the author(s) and do not necessarily reflect those of the National Science Foundation.

This project would not have been possible without collaboration with the California Department of Transportation. In particular, Mike Keever, Steve Sahs, Tom Shantz, and Richard Porter contributed the data needed to complete the simulations and to establish the repair cost and repair time databases. Contributions, guidance, and feedback from PEER researchers working within the PEER Bridge Group, led by Professors Ross Boulanger and Stephen Mahin, are gratefully acknowledged.

CONTENTS

LIST OF FIGURES

LIST OF TABLES

LIST OF SYMBOLS

The following symbols or acronyms are used in this paper:

A, B, a, b	=	demand model coefficients in Equation (2.6);
AC	=	asphalt concrete;
A_g	=	column gross area;
BB	=	beginning of bridge;
BDA	=	Caltrans Bridge Design Aids (Division of Engineering Services, 2005);
BDD	=	Caltrans Bridge Design Details (Division of Engineering Services, 1994);
C, D, c, d	=	damage model coefficients in Equation (2.8);
C_L	=	wing wall effectiveness coefficient;
Cu	=	unit cost;
C_w	=	wing wall participation coefficient;
CF	=	cubic foot;
CY	=	cubic yard;
d_0	=	linearization point in DM space;
d_b	=	column longitudinal rebar diameter (m);
D_c	=	column diameter (m);
D_s	=	superstructure depth (m);
DM	=	damage model;
DS	=	damage state;
DV	=	decision variable;
e_{lin}, f_{lin}	=	linear loss model coefficients in Equation (2.22);
E, F, e, f	=	loss model coefficients in Equation (2.9);
E', F'	=	linearized loss model coefficients in Equations (2.24) and (2.25);
EA	=	each;
EB	=	end of bridge;
EDP	=	engineering demand parameter;
f'_c	=	unconfined concrete compressive strength (kPa);

f_y = steel yield strength (kPa);

GAL = gallon;

H = column height above grade (m);

H_c = equivalent column cantilever length (m);

IM = intensity measure;

k, k_0 = hazard curve constants in Equation (2.4)

l = lth performance group ranging from 1 to N_{PG};

L = span length (m);

LB = pound;

LF = linear foot;

LS = limit state;

m = mth damage state/measure;

M_w = moment magnitude;

MTD = Caltrans Memo to Designers (Division of Engineering Services, 2004);

n = nth repair quantity ranging from 1 to N_Q;

N = column axial load (kN);

N_{PG} = number of performance groups;

N_Q = number of repair quantities;

PCC = Portland cement concrete;

PDM = probabilistic damage model;

PGA = peak ground acceleration (g);

PGV = peak ground velocity (cm/s);

PLM = probabilistic loss model;

PSDM = probabilistic seismic demand model;

Q = repair quantity;

R = closest distance to fault;

RCR = repair cost ratio;

RT = repair time;

Sa, Sa_{el} = pseudo-spectral acceleration (g);

Sd = spectral displacement (cm);

SF	=	square foot;
T	=	structural period (sec);
TC	=	total cost;
TON	=	ton = 2,000 LB;
u_{max}	=	maximum column displacement (m);
V_s	=	shear strength contribution from steel reinforcement (kN);
V_c	=	shear strength contribution from concrete (kN);
W	=	participating bridge weight (kN);
y	=	standard normal variate;
β	=	lognormal standard deviation;
Δ	=	drift ratio (%);
ϵ	=	number of standard deviations away from an attenuation curve;
λ	=	lognormal distribution parameter (median);
μ	=	displacement ductility;
ν	=	mean annual frequency of exceedance;
ξ	=	damping ratio (%);
ξ_{eff}	=	effective damping ratio (%);
$\rho_{s,long}$	=	column longitudinal reinforcement ratio (%)
$\rho_{s,trans}$	=	column transverse reinforcement ratio (%); and
σ	=	dispersion.

1 Introduction

Since its inception, the Pacific Earthquake Engineering Research (PEER) Center has devoted considerable effort to addressing the seismic safety and economic needs of a society living in a modern built environment exposed to earthquake hazard. The main goals of the multi-disciplinary research teams that constitute the PEER Center have been to develop a performance-based earthquake engineering (PBEE) methodology and probabilistic framework, and to apply them to increase the seismic safety of our society.

Performance-based earthquake engineering aims to quantify the seismic performance of engineered facilities using metrics that are of immediate use to both engineers and stakeholders. The PEER PBEE methodology considers seismic hazard, structural response, resulting damage, and repair costs associated with restoring a structure to its original function, using a fully consistent, probabilistic analysis of the associated parts of the problem (Cornell and Krawinkler, 2000). The uncertainty surrounding the constitutive elements of the PBEE framework, stemming from both lack of knowledge and sheer randomness, necessitates a probabilistic approach and acceptance criteria based on levels of confidence that probabilities of failure are acceptably small. Adoption of such PBEE methodology in practice requires abandonment of prescriptive seismic safety specifications and acceptance of performance objectives defined in terms of quantities familiar to engineers, owners, managers, and stake-holders alike. This approach to earthquake engineering is, above all, sustainable because the underlying framework is independent of the performance objectives selected for the particular evaluation or design project, thus allowing for seamless adaptation to specific project needs and smooth adoption of new design methods and innovative structural systems.

A rigorous yet practical implementation of a performance-based earthquake engineering meth-

odology is developed and demonstrated for benchmark reinforced concrete bridges. To define performance objectives, performance quantities are defined by the probability of exceeding threshold values of socio-economic decision variables (DVs) in the seismic hazard environment under consideration. However, creating a general probabilistic model directly relating DVs to measures describing the site seismicity is too complex. Instead, the PEER PBEE framework utilizes the total probability theorem to disaggregate the problem into several intermediate probabilistic models that address sources of randomness and uncertainty more objectively. This disaggregation of the decision-making framework outcome involves the following intermediate variables: damage measures (DMs), engineering demand parameters (EDPs), and seismic hazard intensity measures (IMs). Consequently, engineers may choose to scrutinize probabilities of exceeding an engineering demand parameter, such as strain, while an owner may choose to scrutinize probabilities of exceeding a decision variable, such as repair cost. An important step enabling effective aggregation of decision data is the association of structural elements and assemblies into performance groups (PGs) following the correlations imposed by the commonly used repair methods.

1.1 BENCHMARK BRIDGES

Effective tools have been developed to analyze the economic impact of damage to transportation systems in an urban area due to extreme events such as earthquakes (HAZUS, 1999; Werner et al., 2004). Direct losses to the region include damage to components (bridges) as well as time delays in the damaged network. Indirect losses include the interruption of goods and services to those businesses affected by the earthquake. Highway network risk assessment is performed as a decision-making aid in both the pre-earthquake and post-earthquake settings for better-informed decisions on the allocation of resources for retrofit, design, and the improved redundancy of a network. Similarly, post-earthquake repair and capacity management are improved by the outcome of network analysis. Bridges are the critical links in any highway network, yet they are vulnerable to earthquake hazard from ground shaking and ground deformation. The prevalence of certain types of highway bridges in the inventory of particular urban areas within California makes it essential to better quantify the vulnerability of these benchmark bridge types.

A large portion of bridges in the current California bridge inventory share similar construction characteristics, especially those owned and maintained by the California Department of Trans-

portation (Caltrans). Specifically, 85% of all bridges are made from either concrete and prestressed concrete according to the 2005 National Bridge Inventory, and 90% of Caltrans bridges are concrete I-beam or box girder bridges according to Ketchum et al. (2004). To classify a bridge as an "ordinary standard bridge" by the Caltrans Seismic Design Criteria (Caltrans, 2004), a bridge must be of standard concrete construction, less than 90m (300 ft) long, and have no special devices, bearings, or eccentricities. The most prevalent ordinary construction types for new California bridges were selected for a study on the relationship between bridge construction cost and design ground motion level (Ketchum et al., 2004). Designs conforming to the SDC were generated for each of the 11 bridge types, including column and superstructure reinforcement details of sufficient resolution to allow complete demand, damage, and loss models to be generated without the necessity of obtaining as-built details from an existing structure. Of the 11 typical types and configurations developed by Ketchum, two continuous, five-span, straight, post-tensioned, cast-in-place, box girder bridges on monolithic piers were selected for this study. They are designated Type 1 and Type 11 benchmark bridges.

The PEER PBEE framework provides a method for evaluating the vulnerability, or fragility, of these benchmark bridges. Outcomes of an engineering implementation of the PEER PBEE framework are the inputs essential for accurate traffic network simulations: these are bridge-level assessments of repair costs, repair durations, and degrees of bridge traffic capacity loss. More specifically, the probabilities of exceeding certain damage and decision limit states are required for each level of seismic hazard experienced at all bridge sites geographically distributed throughout the network. Using this information, the traffic network assessment tools calculate a direct loss (repair cost) for the network bridges, and then perform post-earthquake traffic analysis to assess indirect losses.

1.2 BRIDGE FRAGILITY CURVES

A fragility curve is used in this report to define the conditional probability of exceeding a benchmark bridge limit state given an earthquake intensity as a fragility curve. Previous attempts to develop fragility curves for bridge decision or damage limit states, such as repair cost or damage state, were based on heuristic extensions of computed bridge demand fragility curves. The main goal of this report is to present a method to generate decision-level repair cost and repair duration

fragility curves directly, using a fully consistent probabilistic implementation of the PEER PBEE framework.

Three different approaches are used to compute the decision-level fragilities for the Type 1 and Type 11 benchmark bridges. All approaches make use of seismic demand models relating EDPs to IMs generated using nonlinear dynamic finite element analysis on the bridge structural model as a whole. The first approach is an approximate (scalar) analysis that assumes that the damage to the bridge structural elements can be quantified into discrete damage states that adequately capture the damage to the bridge in aggregate. A database of experimental data for bridge columns is utilized to generate the damage model relating DMs to the demand model EDPs (drift ratios in this approach). Similar damage models are created for other bridge structural elements (abutments, joints, etc.) using heuristics and Caltrans engineer experience. These bridge-level damage states are then related to bridge repair cost data obtained during the 1994 Northridge earthquake. The other two (vector) approaches consider a series of bridge components, or performance groups, that each experience demand, undergo damage, and are consequently repaired. Probabilistic seismic demand and damage/capacity models are developed for each of the performance groups in this second approach. Each performance group then has a repair method and repair materials associated with it. All the individual repair costs are recombined into the total bridge repair cost taking into account the correlation between the individual performance groups. Results for all approaches are presented in the form of benchmark bridge damage fragilities and decision/loss fragilities. In addition, the repair time (duration) loss models are developed using the vector approaches.

The particular fragility curves computed for the selected benchmark bridges presented in this report are valid and can be used as input for traffic network evaluation or other studies. However, a wider use of the fragility curves presented in this report is limited by the selection of the benchmark bridges. This selection was made to demonstrate applicability of performance-based earthquake engineering concepts to commonly occurring structures rather than to provide data for specific bridges with unique geometric configurations or design and functional constraints (such as "important bridges"). The primary outcome of the work presented in this report is a method to enable engineers to generate the relevant fragility curves for the particular bridge with the fidelity required for the particular practical application.

While bridge repair cost and repair time fragility curves provide important information regard-

ing the effort required to return the bridge to full functionality (if repaired or replaced), they do not provide direct information on the degree of bridge functionality immediately after an earthquake. An example of such post-earthquake functionality is an assessment of the probability that a damaged bridge can safely carry emergency vehicles or limited traffic loads. An attempt to evaluate such post-earthquake functionality was made using finite element models, but was severely hampered by the lack of confidence in the ability of these models to accurately simulate the effect of traffic loads on a damaged bridge. An ongoing Caltrans project is expected to provide the calibrated models needed to complete the post-earthquake bridge functionality study.

1.3 PEER PBEE FRAMEWORK IMPLEMENTATION

An implementation of the PEER PBEE framework is also presented in this report. This implementation is based on a closed-form integration of the total probability framing equation: thus, this implementation does not require the use of the Monte Carlo technique. However, the intermediate demand, damage and decision models must be formulated as analytical functions. Methods to derive these functions are presented in this report and illustrated using the benchmark bridge examples.

Modularity is a very important feature of the closed-form implementation of the PEER PBEE framework. Such design allows plug-and-play change of the demand, damage, or decision models and enables PEER researchers to investigate the consequences of changing foundation assumptions, modeling and analysis assumptions, bridge elements, damage estimates, or repair methods. Such modular approach is extended to the finite element model of the benchmark bridges developed in OpenSees for this study. Consistent with the object-oriented design philosophy, the OpenSees bridge model allows for easy replacement of the default bridge components with those designed for enhanced seismic performance, or easy coupling of the bridge model with soil models for soil-foundation-structure interaction studies.

Two computer tools are developed to facilitate practical use of the closed-form implementation of the PEER PBEE framework. First, a Matlab based software tool for numerical integration of the PEER framing integral, called Fourway, is presented. This tool features a graphical user interface that enables the user to input the parameters of the analytical demand, damage, and decision models and investigate the effect of model parameter changes on the resulting fragility curves. Second,

a data structure was designed and implemented in Excel to facilitate organization and storage of the data for the demand, damage, and decision models. Together, these tools are a computer foundation for customizing the PEER PBEE framework to particular structures and applications and for transfer of the PEER PBEE methodology into engineering practice.

1.4 RELATION TO OTHER PEER RESEARCH PROJECTS

The study presented in this report builds on the work done by PEER researchers. The formulation of the PEER PBEE framework and the development of the closed-form integration procedure is based on the fundamental work of Professor Cornell and his colleagues and students (Cornell and Krawinkler, 2000; Cornell et al., 2002; Jalayer, 2003). Selection of intensity measures and development of finite element models in OpenSees used subsequently for the benchmark bridges was done by the authors (Mackie and Stojadinović, 2003) in parallel with similar work on PEER benchmark buildings. Valuable modeling experience was gained through the PEER I-880 benchmark study (Kunnath, 2006). Damage models for reinforced concrete bridge columns were obtained using a PEER column structural performance database (Berry and Eberhard, 2003). Damage fragility curves for typical California overpass bridges were developed by combining the bridge demand and damage models (Mackie and Stojadinović, 2005). An extension of the framework to encompass decision models was made in parallel with similar PEER Center work on buildings (Yang et al., 2006).

All of the PEER research teams within the bridge group adopted the same benchmark bridges for investigation, providing continuity between the projects and results. In particular, bridge Type 1A was used by the geotechnical teams from the University of California, Berkeley (Ledezma and Bray, 2008) and the University of Washington (Kramer et al., 2008) to analyze the increased vulnerability of the bridges when located on site conditions susceptible to liquefaction and lateral spreading. The structural team from Stanford (Lee and Billington, 2008) used both Types 1 and 11 to investigate the mitigation of damage and costs due to performance-enhanced structural elements and materials. Self-centering columns were tested experimentally on the shake table (Jeong et al., 2008). The benchmark bridges are also used in several ongoing PEER-Lifelines and Caltrans projects.

1.5 REPORT OUTLINE

The document is organized such that the methodology and data structure are separate from the sample application and data particular to the Types 1 and 11 bridges. The data flows are covered in Chapter 3, and both the scalar and vector approaches to generating fragilities are covered in Chapter 2. Specific details regarding the example bridges first designed in Ketchum et al. (2004) are summarized in Chapter 4. For these bridges, and particularly Type 1A, performance groups were defined and demands measured using nonlinear analysis, discrete damage states were defined for each performance group, repair methods and repair quantities were associated with each damage state, and unit costs and production rates were determined for these repair quantities. The definition of performance groups, damage states, and repair quantities are detailed in Chapter 5. Rather than utilize generic data for classes of bridges, damage scenarios pertaining to bridge Type 1A were generated for the purpose of quantifying cost estimates and working days estimates. These damage scenarios and the remaining data necessary for repair cost and repair time estimation are contained in Chapter 6. Finally, application of the methodology in Chapter 2 to the data contained in the previously mentioned chapters is illustrated in Chapter 7.

2 Methodology

The Pacific Earthquake Engineering Research (PEER) Center was conceived as a multi-disciplinary organization to address the seismic safety and economic needs of society exposed to earthquake hazard. A core feature of the PEER Center is the development of a performance-based earthquake engineering (PBEE) methodology and probabilistic framework to provide a unified approach to the seismic risk assessment of engineered systems (Cornell and Krawinkler, 2000). Probabilistic methods allow for the definition of performance objectives under uncertain hazard levels. Performance objectives are defined in terms of threshold values of socio-economic decision variables (DVs) being exceeded in the seismic hazard environment under consideration. A general probabilistic model directly relating DVs to measures describing the site seismicity is too complex. Instead, the PEER framework utilizes the total probability theorem to disaggregate the problem into several intermediate probabilistic models that address sources of randomness and uncertainty more objectively. This disaggregation of the decision-making framework outcome involves the following intermediate variables: damage measures (DMs), engineering demand parameters (EDPs), and seismic hazard intensity measures (IMs).

Typical DVs used to evaluate conventional building structures include repair cost, downtime, repair time, and loss of life. For bridges, additional DVs include load rating and lane closures. DMs are, usually, observable states of structural component or system damage. Alternatively, DMs may include the loss of live-load or gravity-load-carrying capacity. EDPs are numerous and varied based on the size and complexity of the system under consideration. Typical EDPs include displacements, drifts, strains, curvatures, moments, and residual deformations. Finally, IMs are also numerous; however, the most commonly used IMs are peak ground acceleration (PGA), peak ground velocity (PGV), and first-mode pseudo-spectral acceleration ($Sa(T_1)$). Note that

the methodology is not limited to structural systems: geotechnical, infrastructure, and combined systems can be evaluate using an appropriate selection of IMs, EDPs, DMs, and DVs.

One possible outcome of the PEER probabilistic PBEE evaluation methodology is a scalar decision (or loss) fragility curve, defined as the conditional probability of exceeding a single (scalar) decision limit state (dv^{LS}) given an earthquake intensity value im:

$$P(DV > dv^{LS}|IM = im) = \iint G_{DV|DM}(dv^{LS}|dm)|dG_{DM|EDP}(dm|edp)||dG_{EDP|IM}(edp|im)| \quad (2.1)$$

Lowercase variables in Equation (2.1) imply individual realizations of their capitalized random variable counterparts. The complementary cumulative distribution function (CDF) of intermediate variable X (DV, DM, or EDP) conditioned on intermediate variable Y (DM, EDP, or IM) is denoted $G_{X|Y}$. The probability density function (PDF) of intermediate variable X conditioned on intermediate variable Y is denoted $dG_{X|Y}$.

Another possible outcome of the methodology is the mean annual frequency (MAF) of exceeding the same scalar decision limit state (dv^{LS}). The MAF of exceedance, ν, is written as

$$\nu_{DV}(dv^{LS}) = \int G_{DV|IM}(dv^{LS}|im)|d\nu_{IM}(im)| \quad (2.2)$$

Absolute value signs are required for terms in which the derivatives will be negative. It is not necessarily correct to assume that the MAF is equal to the annual probability of exceedance (Der Kiureghian, 2005).

By disaggregating the final probability or MAF as defined by the PEER framing equations, it is possible to more carefully address the sources of both aleatory and epistemic uncertainties in each intermediate probabilistic model. While it is sometimes possible to quantify these two sources separately (usually in demand models), they are often lumped together. Such is the case with experimentally based damage models, and most loss models. However, quantifying the uncertainty is based on the assumption that the conditional probability distributions are (for example) lognormal, which is a source of uncertainty in the procedure that is not captured. In addition, the methodology does not explicitly account for changes in the state of the structure or the state of knowledge. In addition, the MAFs of exceedance are sensitive to reassessment of the site-specific hazard, construction oversights, damage due to earthquakes, other hazards, or operations, and changes to non-structural components.

The PEER Center methodology is certainly not limited to scalar variables. This report investigates several different ways of applying the PEER framework to the problem of post-earthquake highway bridge loss modeling. In this context, the DVs are limited to the post-earthquake repair cost and repair time. The three approaches followed include (1) a scalar approach (Eq. 2.1) at estimating repair cost ratios, (2) a vector approach based on closed-form solutions and the Fourway procedure (Mackie and Stojadinović, 2006b), and (3) a vector approach proposed in this project based on damage model linearization. The scalar approach treats the response of, and damage to, the bridge as a whole system, while the two vector approaches disaggregate the bridge into all relevant structural components.

A feature unique to the two vector-based approaches is the disaggregation of the bridge system into individual components, such as the columns, denoted as performance groups. The concept of disaggregating structures into structural and non-structural components, or assemblies, has been investigated previously for buildings by Porter and Kiremidjian (2001) and Yang et al. (2006). In the disaggregation approach taken in this report, it was necessary to insert an additional intermediate probabilistic model into the framework that relates damage to repair quantities (Qs). The repair quantities are then combined for all components, taking into account correlation, by way of a unit cost or unit time function before producing the eventual DV. The vector approaches are summations over all of the pertinent bridge components l (denoted performance groups), all of the discrete damage states m applicable to each component, and all of the repair quantities n necessary to repair damage of type m to component l. Each repair quantity $Q_{n,l}$ is then treated in a probabilistic manner with a form similar to Equation (2.1), defined as:

$$P(Q_{n,l} > q^{LS} | IM = im) = \sum_{m} \int G_{Q_{n,l}|DM_{m,l}}(q^{LS}|dm_{m,l}) G_{DM_{m,l}|EDP_l}(dm_{m,l}|edp_l) |dG_{EDP_l|IM}(edp_l|im)| \quad (2.3)$$

All three approaches are dependent on a full definition of the intermediate probabilistic demand, damage, and loss models. Therefore, a brief discussion of the origin and form of the probabilistic models precedes a full description of the three analytical approaches. In addition, both the scalar and vector approaches make use of the probabilistic solution of Equation (2.1). Details on a closed-form solution, a Fourway solution, and a numerical integration solution to this equation are presented after the intermediate probabilistic models. Numerical tools are provided to

facilitate both the closed-form and the numerical integration of the PEER framing equations. The closed-form tool is used to automate the computation of Equation (2.3) for the vector approaches.

2.1 PROBABILISTIC MODELS

Whether the desired outcome of a performance-based study is a fragility curve or MAF of exceedance data, a mathematical relation between the intermediate variables, i.e., the complementary CDFs $G_{X|Y}$, must be specified in order to solve the framing equations (Eqs. 2.1, 2.2, or 2.3). These CDFs will be referred to as the intermediate probabilistic models. The two probabilistic moments utilized in the intermediate models, based on the assumption that the variables are lognormally distributed as described below, are the median and dispersion. The best estimate of the resulting model is defined as the median, or the mean of the natural log of the data points, and is denoted with a superscript "hat" ($\hat{x}$). The mean of a variable is denoted with a superscript bar ($\bar{x}$). The log standard deviation of the model error is termed dispersion (σ). Solutions of Equations (2.1), (2.2), and (2.3) can be obtained by numerical integration or Monte Carlo simulation for any form of such intermediate models. However, closed-form and simplified solutions will greatly enhance the utility of the PEER methodology and are, therefore, the focus of this testbed.

Two primary assumptions made to facilitate the solution of the PEER framing equations (Eqs. 2.1, 2.2, and 2.3) are: (1) the conditional distribution of intermediate variable X given intermediate variable Y can be modeled by the lognormal distribution and (2) the conditional dispersion of intermediate variable X given intermediate variable Y is constant (homoskedastic) over the range of Y considered. These two assumptions are independent of the mathematical form selected for the relationship between intermediate variables, and remain true even in the absence of a "best-fit" relationship between the intermediate variables. The assumptions can be verified during the course of intermediate model generation. Goodness-of-fit tests, such as the Kolmogorov-Smirnov or Lilliefors tests, can be used to accept or reject the hypothesis that conditional distributions (for example: EDP given IM) can be described by the lognormal distribution. Alternatively, the residuals surrounding the best estimate can be examined or fitted for a lognormal distribution (normal distribution in log space). The conditional dispersion can be evaluated for consistency over the range of input parameters. This is accomplished by comparing individual conditional dispersions (for example: at a given IM value) to the dispersion obtained from the model fitted to

all the data.

Two strategies for solving Equations (2.1), (2.2), and (2.3) are presented in this chapter. The first is a closed-form approach, made possible by assuming that the conditional mean of intermediate variable X is locally linear with respect to intermediate variable Y in (natural) log space. In linear space, this is equivalent to assuming a power-law relationship between X and Y. The parameters to the power-law fit can easily be determined using least-squares regression on the data in natural-log space. This assumption also implies, in log space, that the nonlinear intermediate models are linearized locally over a finite interval of the independent variable values. Therefore, care should be taken when extrapolating the results beyond the range accurately represented by the linearized intermediate models. The second, numerical, solution strategy is motivated by the limitations of the first strategy: it yields a numerical solution to the same equations for arbitrary intermediate model median mathematical forms.

2.1.1 Seismic Hazard Model

Seismicity at the site of the structure that is being evaluated is described by the probable intensity of ground motion and a selected suite of representative ground motion records. There are numerous ways of obtaining such site-specific probabilistic seismic hazard data. The following is a short description of a method to compute the probable intensity of ground motion using the median seismic hazard curve obtained from USGS hazard maps (USGS, 2002). Pseudo-spectral acceleration at the fundamental period and damping of the structure, i.e., $Sa(T, \zeta)$, is chosen as the ground motion IM. The median seismic hazard curve for this IM is computed using the ordinates of the pseudo-acceleration equal hazard spectra with 2%, 5%, and 10% median probability of exceedance in 50 years obtained using the USGS hazard maps and a spectra construction procedure for the chosen site. The median hazard curve is also assumed to have a power-law form with two unknown parameters (Eq. 2.4) in the range of the ground motion intensities bracketed by the 2%- and 10%-probability of exceedance IM values.

$$\hat{\nu}_{IM}(im) = k_0(im)^{-k} \tag{2.4}$$

$$\ln(\hat{\nu}_{IM}(im)) = \ln(k_0) - k\ \ln(im) \tag{2.5}$$

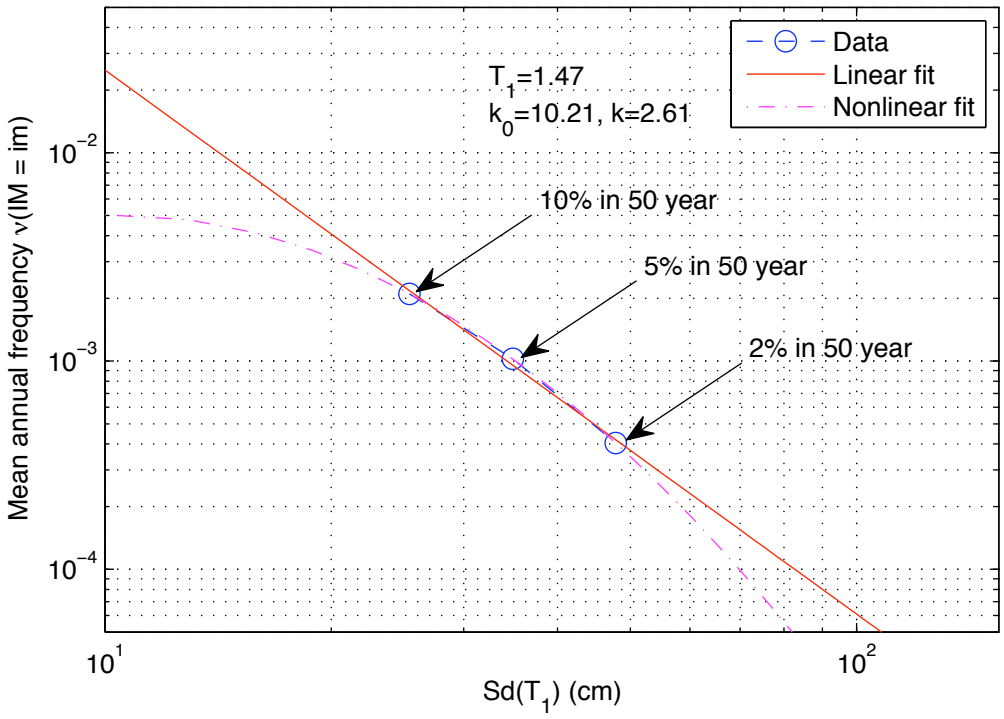

Fig. 2.1 Annual seismic hazard curve for T_1 = 1.47 sec in Berkeley, CA showing three hazard data points sampled from USGS maps and the linear fit from Eq. (2.5).

The two-parameter fit (linear in log space) to the nonlinear (in log space) hazard curve tends to overpredict frequencies of exceedance for IM extremes both above and below the range of intensities considered. Therefore, care should be taken when extrapolating any resultant hazard curves to extremely low (or high) frequencies of exceedance. Using a least-squares fit in log space (Eq. (2.5)), the unknown parameters can be determined numerically. An example of the resulting hazard curve approximation is shown in Figure 2.1.

Additionally, there are uncertainties inherent in derivation of the hazard curve. If the uncertainty in the hazard is assumed to be a lognormal random variable with dispersion σ_H, then the MAF of exceeding an IM is also a random variable with mean $\bar{\nu}_{IM} = \hat{\nu}_{IM} e^{1/2\sigma_H^2}$ (Jalayer, 2003). Alternatively, the mean hazard curve can be derived statistically from the hazard data directly, $\bar{\nu}_{IM}(im) = \bar{k_0}(im)^{-\bar{k}}$. Oftentimes the mean hazard curve is provided directly for a given site and project; therefore the user should be aware of which hazard curve (mean or median) is being used.

There is a plethora of scalar intensity measures (IMs) to select from Mackie and Stojadinović

(2005). Two classes of IMs are distinguished. The first class comprises the IMs that are period- (and structure-) independent, calculated directly from the ground motion record being utilized. Alternatively, these IMs can be viewed as responses from a single-degree-of-freedom (SDOF) oscillator with zero period. Familiar IMs from this class include peak ground acceleration (PGA) and cumulative absolute velocity (CAV). The second class of IMs comprises those derived by applying an elastic or inelastic SDOF filter to the original ground motion records. Any of the original class I IMs can be calculated from such SDOF-filtered records. Familiar IMs from this class include spectral acceleration (Sa) and displacement (Sd). Also included in class II IMs are any elastic or inelastic spectral ordinate combinations, or other combinations of class I and II IMs with, possibly, different SDOF filter periods. Similarly, averaged quantities over a band-range of interest, such as Housner intensity, are also included in this class. Recent research has shown that vectors of IMs can be beneficial in predicting structural response (Baker and Cornell, 2005).

Two primary matters are of concern for selection of the IM. First, hazard data should be available for the IMs, usually in the form of attenuation relationships for the specific site. Currently, this limits the selection to IMs such as PGA, Sa, and Arias intensity. Second, the choice of IM more often than not dictates the efficiency of the corresponding demand (IM-EDP) intermediate models. Efficiency is a measure of aleatory uncertainty (Shome and Cornell, 1999). It is defined in terms of dispersion of the demand intermediate model, 0.30 or less being considered good. Experience has shown that first-mode spectral acceleration is an efficient choice of IM for most structures. However, this does not imply that $Sa(T_1)$ provides a demand model with lowest possible dispersion for a given structure.

Numerous factors should be considered when selecting a suite of representative site-specific recorded ground motions for use in seismic hazard analysis. Disaggregation of the hazard for a given site includes determination of the contribution of ground shaking due to predominant faults with given magnitudes and distances. Representative motions with these magnitude (M_w), distance (R), local soil type characteristics, and faulting mechanisms should be selected, or binned, where feasible. Selection is more critical for sites with poor soil, expected near-fault and directivity effects, and structures that are expected to experience highly nonlinear response. Otherwise, the response of certain building structures has been shown to be insensitive to the choice of ground motion bin characteristics (Iervolino and Cornell, 2005). Additionally, the use of ϵ to select ground

motions has also been shown to provide favorable results when scaling ground motion records (see Stewart et al. (2001); Baker and Cornell (2005)). The standard normal variate, ϵ, is the number of standard deviations a spectral ordinate falls away from a mean attenuation relation value.

2.1.2 Demand Model

The demand intermediate model describes the probable effect of site-specific ground motions with a given intensity (IM) on a structure in terms of engineering demand parameters (EDPs). The effect of a ground motion on the structure is determined using a mathematical model of a structure (linear or nonlinear) and an appropriate structural analysis method (static or dynamic). A relation between IMs and EDPs is derived using the response data for each of the ground motions in the selected site-specific suite. A nonlinear model and time-history dynamic analysis are assumed to minimize epistemic uncertainty by providing the best estimate of structural response. Other models and analysis methods may be used, provided that bias in median and dispersion values obtained using such models is adequately accounted for.

There are three common analysis procedures for obtaining a demand model. The first procedure, the "cloud" or direct (Shome and Cornell, 1999) method, attempts to represent the site seismicity through a wide selection of many representative ground motions. The cloud analysis method uses the selected ground motions without any prior scaling. Therefore, the demand model is derived from a cloud of data points in the IM-EDP space. Derivatives of the cloud method include binning of the ground motions into distinct magnitude and distance bins to disaggregate the source of the seismic hazard, scaling the cloud of records to a function of the median intensity for each bin, or simply scaling all constituent records by a constant (e.g., 1.5 or 2). The second procedure, known as incremental dynamic analysis (IDA), involves stepwise increase of the intensity of a select few ground motion records. The intensity of the ground motion is increased in each analysis, and the extreme values of an EDP are plotted against the corresponding IM for each intensity level to produce a dynamic pushover curve for the structure and the chosen earthquake record (Vamvatsikos and Cornell, 2002). To achieve comparison with an equivalent set of cloud results, several motions are required, and IDA intensities must cover a similar range. Finally, the third procedure, called the stripe method, scales all ground motions to the same intensity at a select few intensity levels or "stripes." For each selected IM level all ground motions are scaled first,

structural analyses are conducted to compute the EDPs, and then the EDPs are plotted to give a "stripe" of response data. Stripe analysis is, thus, a special case of IDA.

Regardless of the method used to obtain the demand model, the primary assumptions discussed above are applied in order to pursue a closed-form solution of Equations (2.1) and (2.2). Namely, the EDP data are assumed to have a lognormal distribution when conditioned on IM, the conditional mean of EDP given IM is linear in log space, and the conditional dispersion of EDP given IM is constant. The resulting demand model is represented by Equation (2.6) in log space and Equation (2.7) in linear space. The two unknown coefficients in Equation (2.6) and the unknown dispersion $\sigma_{EDP|IM}$ can be computed using least-squares regression. In linear space, the demand model coefficients become $a = exp(A)$ and $b = B$.

$$\ln(\widehat{EDP}) = A + B\ln(IM) \tag{2.6}$$

$$\widehat{EDP} = a(IM)^b \tag{2.7}$$

For linear elastic response and nonlinear response for which elastic and inelastic displacements are approximately equal, the form of Equation (2.6) is exact when $B = 1$. The power-law form of the demand model is often a good structural response predictor for nonlinear response when $B \neq 1$; however, it does not necessarily accurately capture the structural response over the complete range of intensities considered. Errors arise when considering highly nonlinear behavior, global instability, or collapse (see Jalayer (2003); Krawinkler and Ibarra (2003); Baker and Cornell (2005)). In these instances, the probability mass of, for example, collapse needs to be accounted for explicitly. Therefore, the power-law form of the demand model should be understood as a local approximation, as discussed above. However, it is possible to use several piecewise linear fits (in log space) to formulate a demand model using the same functional form to better capture the entire range of structural response (Mackie and Stojadinović, 2003).

The selection of an EDP for the demand model is largely dependent on the structure at hand. Generally speaking, EDPs that describe the global behavior of a structure have resulted in demand models with lower uncertainty than localized demand measures. For bridges and buildings such global EDPs are global drift ratios, or interstory drift ratios. See Mackie and Stojadinović (2003, 2005) for more information regarding IMs and EDPs for highway bridges. For buildings, numerous researchers have addressed the IM and EDP issue (e.g., Shome and Cornell (1999); Luco and

Cornell (2003); Baker and Cornell (2003); Medina and Krawinkler (2003); Alavi and Krawinkler (2004)).

2.1.3 Damage Model

The damage intermediate model describes the probable damage state of a structure, described in terms of damage measures (DMs), given a level of engineering demand parameters (EDPs) using a mathematical relation between EDPs and DMs. DMs are usually discrete rather than continuous quantities, defined as observations of the onset of certain damage states. Examples of damage states of reinforced concrete columns include cracking, spalling, and transverse reinforcement fracture (see *http://nisee.berkeley.edu/spd/*).

Damage models can be obtained from a variety of sources. The most common source is experimental tests of structural components, subassemblies, or systems where observed damage and measured capacity of the specimens is correlated to the level of applied demand. In this context, damage models are often termed capacity models. Databases of collected experimental results on similar-type specimens are often used to develop such descriptive equations that involve geometric and material properties of the specimen. For example, several damage models for reinforced concrete columns already exist (Berry and Eberhard, 2003; Panagiotakos and Fardis, 2001; Hose et al., 2000). The shortcoming of the database approach is the lack of test data for the multitude of materials and structural components, subassemblies, and structures encountered in practice. Alternatively, damage states can be taken from resistances (or capacities) for components of structural systems specified in pre-standard documents such as FEMA-356. Care should be taken when using these damage states because implied levels of uncertainty are already built in. For example, lower-bound strength in FEMA-356 is defined as the statistical mean minus one standard deviation of the strength data set.

Damage models may, sometimes, be obtained analytically using finite element reliability analysis. Finite element reliability analysis couples predictions of structural response using finite element analysis with reliability procedures to calculate, for example, failure probabilities and response sensitivities due to uncertain input. This is particularly useful when considering structural systems rather than individual components because little experimental data are available for systems or large subassemblies. Reliability analysis also allows development of a damage model for

the specific structure, rather than interpolating between geometry and material properties in the experimental database. Finally, reliability analyses make it possible to address continuous DMs, such as loss of lateral-load-carrying capacity. However, care should be taken in the consideration of uncertainties modeled analytically during reliability analysis and those uncertainties captured experimentally. Uncertainties due to loading, materials, and geometry can be specifically represented, but epistemic uncertainties due to modeling choices are subject to the same epistemic uncertainties that should be considered in the demand model.

In the case of a continuous DM, the median relationship between EDP and DM (Eq. 2.8) and the associated dispersion ($\sigma_{DM|EDP}$) completely define the damage model. Once again, to obtain a closed-form solution of the framing equations (Eqs. 2.1 and 2.2), a power-law relationship was assumed to apply over the range of values considered. In linear space, the damage model coefficients become $c = exp(C)$ and $d = D$. As with the demand models, Equation (2.8) may not be accurate when considering high levels of damage such as collapse.

$$\ln(\widehat{DM}) = C + D\ln(EDP) \tag{2.8}$$

Assuming that a continuum of damage states is akin to assuming there is a continuous progression of physical damage in the structure: then, all intermediate points between the discretely observed damage states can be used in the fragility analysis. Due to the discrete nature of most DMs it is often difficult to formulate a damage model in terms of a median DM value conditioned on EDP, as was done in the continuous DM case because the cumulative distribution function describing the observed discrete DMs is a step rather than a continuous function. The remainder of the report assumes that damage models can be cast in the continuous form. This simplification can be made for the discrete DM case when the coefficients of variation (c.o.v.) for each of the discrete damage states are approximately equal. In this case, the regression constants in Equation (2.8) are assumed to be $C = 0$, $D = 1$, and $\sigma_{DM|EDP}$ = c.o.v. Such an approximation is consistent with assuming that damage limit states can be defined at discrete (median) levels of demand; however, it increases the overall uncertainty by the uncertainty from the damage model.

2.1.4 Decision Model

The decision intermediate model describes the likely engineering decision pertaining to the use of a structure given a level of sustained damage. Decision models are mathematical relations be-

tween damage measures (DMs) and decision variables (DVs). Commonly used decision variables describe losses in terms of dollars (repair cost), interruption in service (downtime or repair time), or loss of life: thus, decision models are also called loss models. As mentioned earlier, the decision model may have several parts—those that relate DMs to repair quantities (Q) and those that relate Q back to repair cost or repair time. A completely different set of decision variables focuses on the remaining capacity of the structure to function as intended. For example, the return of a highway bridge to differing degrees of functionality in a highway network is also an important loss criterion. Functionality may be measured in terms of lateral load resistance in aftershocks, traffic volume, lane and speed reductions, or access for emergency vehicles.

Empirical and analytical sources of loss data needed to formulate a decision model are sparse. Data can be obtained from professional surveys and opinion (Porter, 2004; Padgett, 2007), reconnaissance data from previous earthquakes, repair data from post-earthquake reconstruction (Basöz et al., 1997), or cost estimators (Yang et al., 2006). Repair cost data may also be obtained by construction cost estimation or data collected during past earthquakes. Further complexities arise because repair cost estimation (and loss modeling in general) is almost always a structural system problem, not simply determined at the component level. Therefore, it is often necessary to combine (sum) numerous scalar values in order to obtain, for example, a total cost figure. When such summations are performed, due treatment of the correlations between spatially distributed components or statistical quantities is required (Miranda and Aslani, 2003; Baker and Cornell, 2003). In this study, the problem of computing repair-related decision variables at the structural system level accounting for the correlations imposed by the selected repair methods is treated using the notion of Performance Groups (Chapter 5). A Performance Group is a collection of discrete damage states, associated with different structural elements, correlated because they are affected by the selected repair procedure.

As with probabilistic damage models, it may not be possible to formulate a continuous relationship between DMs and DVs, further compounded by the fact that both the DM and the DV may be discrete variables. Decision quantities in particular are highly likely to be binary in nature: for example, a bridge may be categorized as either open or closed. Therefore, loss models are often also in the form of probabilities of exceeding explicit discrete decision states given different DMs derived from step-wise CDFs. However, when both the DM and DV are chosen as continuous

variables, the median relationship between DM and DV (Eq. 2.9) and the associated uncertainty ($\sigma_{DV|DM}$) completely define the loss model.

$$\ln(\widehat{DV}) = E + F\ln(DM) \tag{2.9}$$

Once again, the power-law relationship is assumed to apply locally in the region of values of interest. Thus, it may be more accurate to consider piecewise linear fits across the complete ranges of the variables. For example, a repair cost DV may be simply related to the amount of damage (DM) using a constant mobilization cost and modeling the cost of repair materials as decreasing linearly with increasing repair material quantities. In linear space, the decision model coefficients become $e = exp(E)$ and $f = F$.

2.2 SOLUTION STRATEGIES

As mentioned previously, all of the approaches used in this testbed require the solution of one or more of the framing equations (Eqs. 2.1, 2.2, or 2.3). Therefore, two different solution strategies are presented in this section. The closed-form strategy is limited by numerous assumptions, but is the most readily implementable in extensive loss simulations by computer. The numerical strategy is more general but requires more input parameters for each of the intermediate models and is more computationally demanding. A final strategy, based on the Fourway procedure (Mackie and Stojadinović, 2006b), is not discussed further in this report because it is based on a graphical technique for estimating the parameters of the lognormal distribution describing DVs. Under the same assumptions discussed in the closed-form strategy, the Fourway strategy simplifies to the closed-form solution; therefore, it is assumed that the two methods produce equivalent results for this study.

Finally, it is also always possible to use simulation (i.e., Monte Carlo simulation) to generate loss fragilities and MAFs. This strategy has been taken recently by Yang et al. (2006) in a building study that follows a similar decomposition of a building system into independent performance groups. However, the approach makes use of stripe demand analysis at a select few hazard levels, rather than developing the probabilistic moments that describe the distribution of a DV at an arbitrary IM. A comparison of the simulation strategy and the approach in this report based on the closed-form (or Fourway) strategy is presented in Mackie and Stojadinović (2006c,d).

2.2.1 Closed-Form Solution

The fragility formulation of the PEER framing integral (Eq. 2.1) requires numerical integration in order to generate a complete conditional CDF of DV given IM. However, when the intermediate models (CDFs) are assumed to be lognormal, DV can be conditioned directly on IM and is also a lognormal random variable. Additionally, both parameters (median and dispersion) of any decision fragility curve specified by Equation (2.1) can be determined in closed form. The median decision fragility curve (complementary CDF) for an arbitrary DV limit state (dv^{LS}) is given by Equation (2.10). This makes the generation of decision fragility curves merely an exercise in plotting with a program such as Matlab.

$$P[DV > dv^{LS}|IM = im] = 1 - \Phi[\frac{\ln(dv^{LS}) - (E + FC + FDA + FDB\ln(im))}{\sqrt{d^2 f^2 \sigma^2_{EDP|IM} + f^2 \sigma^2_{DM|EDP} + \sigma^2_{DV|DM}}}] \quad (2.10)$$

The PEER framing integral formulated in terms of the MAF of exceedance (Eq. 2.2) can be used to extend the seismic hazard curve to demand hazard curve by integrating the derivative of the hazard (Eq. 2.4) and the demand (Eq. 2.6) models. The result is still an annual hazard curve; however, it shows the MAF of exceeding a demand level. The integral can be evaluated numerically (using the demand data) or in closed form (using the coefficients of the linear fit to the demand model). Details on the integration by parts are demonstrated by other researchers (e.g., Jalayer (2003)). The resulting closed-form demand hazard curve form is shown in Equation (2.11).

$$\nu_{EDP}(edp) = k_0[(\frac{edp}{a})^{\frac{1}{b}}]^{-k} exp(\frac{k^2}{2b^2}\sigma^2_{PSDM,T}) \quad (2.11)$$

Equation (2.11) includes the uncertainty in the seismic hazard curve when the coefficients ($\bar{k}$, $\bar{k_0}$) describing the mean (instead of the median) hazard curve are used (Cornell et al., 2002). The dispersion term in Equation (2.11) is the square root of the sum of the squares (SRSS) of the aleatory ($\sigma_{EDP|IM}$) and epistemic ($\sigma_{U,PSDM}$) uncertainties associated with the demand model $\sigma_{PSDM,T} = \sqrt{\sigma^2_{EDP|IM} + \sigma^2_{U,PSDM}}$. When the epistemic uncertainty in the demand model is included, the MAF is also a random variable: therefore Equation (2.11) provides a mean estimate of the MAF. Typical values for $\sigma_{EDP|IM}$ range from 0.25–0.35 for efficient demand models. Values for $\sigma_{U,PSDM}$ depend on the complexity and assumptions of the model, failure modes captured, and the hazard intensity level; however they can be minimized using finite elements modeled calibrated to experimental data.

Similarly, it is possible to obtain a closed-form expression for the MAF of exceeding different damage (DM) values by integrating the damage model (Eq. 2.8) with the derivative of the demand hazard (Eq. 2.11). The hazard curve describing the MAF of exceeding a damage level is shown in Equation (2.12). As with the demand hazard, the total uncertainty from the damage model can be obtained by the SRSS combination of the aleatory ($\sigma_{DM|EDP}$) randomness and epistemic uncertainty ($\sigma_{U,PDM}$) as $\sigma_{PDM,T} = \sqrt{\sigma^2_{DM|EDP} + \sigma^2_{U,PDM}}$.

$$\nu_{DM}(dm) = k_0[\frac{1}{a}(\frac{dm}{c})^{\frac{1}{d}}]^{-\frac{k}{b}} exp(\frac{k^2}{2b^2d^2}(d^2\sigma^2_{PSDM,T} + \sigma^2_{PDM,T})) \tag{2.12}$$

Continuing from the damage hazard curve, it was also possible to obtain a closed-form expression for the MAF of exceeding different DV values by integrating the derivative of Equation (2.12) with the loss model (Eq. 2.9). The loss hazard curve for exceeding varying loss levels (dv) is described by Equation (2.13). The total uncertainty is $\sigma_{PLM,T} = \sqrt{\sigma^2_{DV|DM} + \sigma^2_{U,PLM}}$, or the SRSS combination of loss model aleatory ($\sigma^2_{DV|DM}$) and epistemic ($\sigma^2_{U,PLM}$) uncertainty. As mentioned in the previous section, $c = exp(C)$, $d = D$, $e = exp(E)$, and $f = F$ when the power-law assumption is made (Eqs. 2.8, 2.9).

$$\nu_{DV}(dv) = k_0[\frac{1}{a}(\frac{1}{c}(\frac{dv}{e})^{\frac{1}{f}})^{\frac{1}{d}}]^{-\frac{k}{b}} exp(\frac{k^2}{2b^2d^2f^2}(d^2f^2\sigma^2_{PSDM,T} + f^2\sigma^2_{PDM,T} + \sigma^2_{PLM,T})) \tag{2.13}$$

Armed with the coefficients of the power-law fit to all of the intermediate models (demand, damage, and decision), the solutions to Equations (2.10) and (2.13) are computed and presented visually using a Matlab tool (Mackie, 2007a). The results shown in Figure 2.2 pertain to a highway overpass bridge (not the same testbed bridge defined in Chapter 4) where the DV was the loss of traffic-load-carrying capacity (Mackie and Stojadinović, 2004b). The demand model is plotted in the upper-right pane of the four-plot box in the lower half of the figure. The damage and loss models follow in the lower-right and lower-left panes, respectively. The reason for this layout is detailed in Mackie and Stojadinović (2006b). The final result obtained by the Matlab tool is the two-moment (first and second moments are the median and dispersion of the lognormal CDFs) plot of DV versus IM, shown in the upper-left pane of the four-plot box.

Given this result, the entire complementary CDF surface of DV given IM, or $G_{DV|IM}(dv|im)$, can be plotted (Eq. 2.10) and is shown as the surface in the top-left plot in Figure 2.2. Lines of equal probability (16%, 50%, and 84%) are also shown on the surface to facilitate comparison

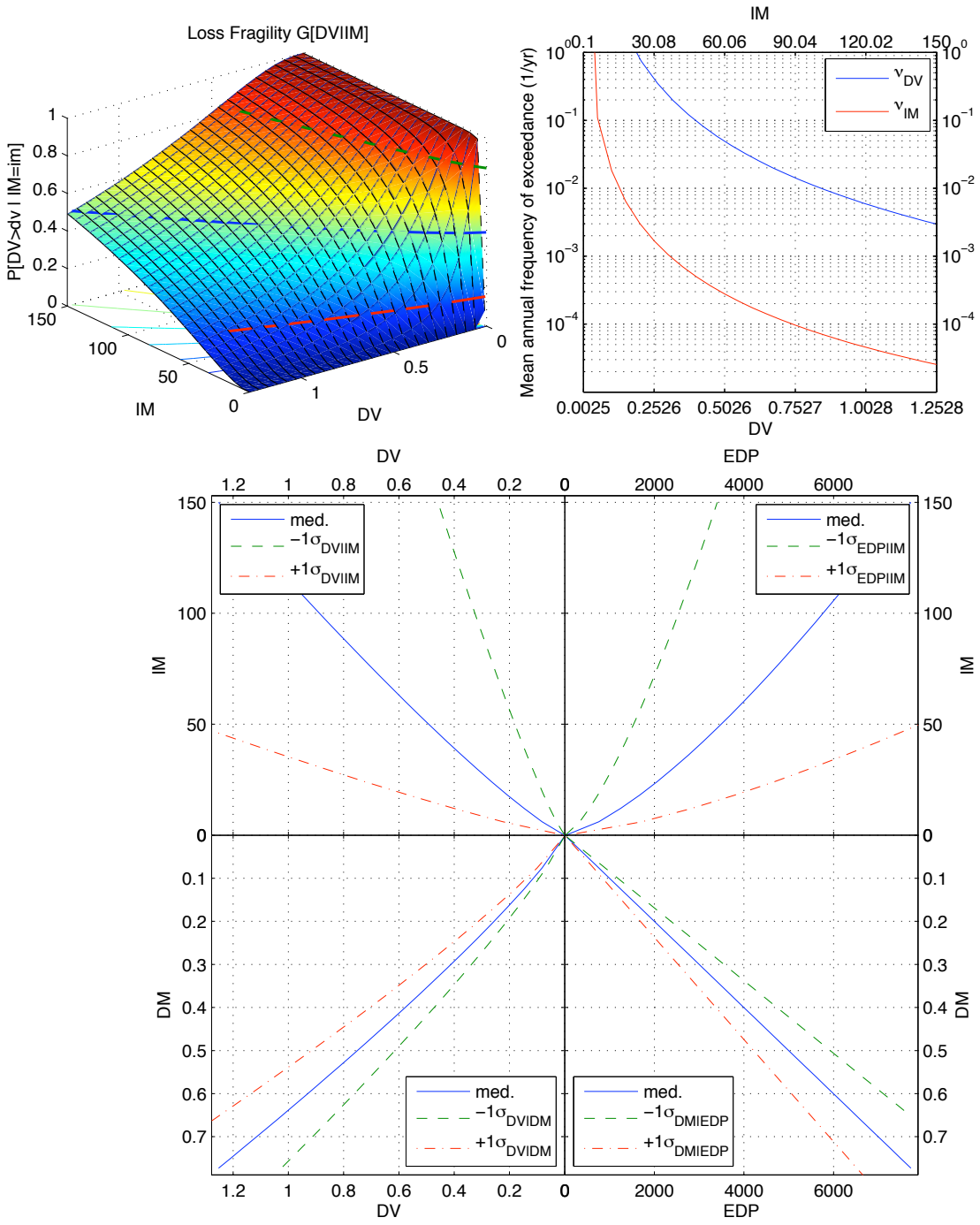

Fig. 2.2 Bridge performance evaluation results using power-law interim model functions and closed-form solutions integrated using the Matlab tool. IM = $Sd(T_1)$ (cm). EDP = loss of vertical-load-carrying capacity (k). DM = loss of vertical-load-carrying capacity (decimal). DV = loss of traffic-load-carrying capacity (decimal).

with the upper-left pane. The decision hazard curve (MAF of exceeding different DV values, Equation (2.13)) is plotted in the top-right plot in Figure 2.2. For example, using the median curve of DV given IM in the upper-left pane, an IM of 72 cm corresponds to a DV of 67%. The hazard curve can be entered using the IM axis, and the MAF of exceeding the given IM (72 cm) obtained from the red curve as $\nu_{IM} = 1.7e^{-4}$. Similarly, the hazard curve can be entered using the DV axis, and the MAF of exceeding the given DV (67% RCR) obtained from the blue curve as $\nu_{DV} = 2e^{-2}$. The increase in the MAF of exceedance of the DV is due to the randomness and uncertainty of the specified problem. This increase can be minimized by reducing the uncertainty in each intermediate probabilistic model (particularly the demand model in this example). Another useful feature of the hazard curve plot is that a constant hazard level (e.g., a MAF of $1e^{-3}$) can be selected and the corresponding value of the ratio between DV (which is a function of IM) and IM immediately obtained. This is appropriate for performance-checking criterion in performance-based design codes such as FEMA-350. However, due to the nonlinear scale of IM relative to DV, it is not possible to draw a vertical line through the hazard curve to compare the ratio of ν_{DV} and ν_{IM} at a common IM value. Each hazard curve must be entered individually as illustrated by the numerical example in this paragraph.

The Matlab tool (Mackie, 2007a) interface makes it possible to easily modify any of the intermediate model coefficients by manually editing values or by using sliders to generate new families of plots. Thus, it is easy to directly assess the effect of intermediate model changes on the decision fragility or MAF results. To facilitate comparison, the previous family of plots is retained in grey. For example, for a bridge with performance-enhanced columns, the demand model (EDP is a drift ratio) might remain essentially the same as for the case of conventional columns. However, the damage and decision models would necessarily be different. Thus, the corresponding intermediate model coefficients will be changed to generate a new family of plots to demonstrate the gains of using performance-enhanced over traditional bridge columns by, for example, achieving a significantly smaller mean annual frequency of exceeding a given repair cost value for the enhanced system. Alternatively, if the bridge were to be placed on a site with the potential for liquefaction or lateral spreading, it would be anticipated that the demand model for such bridge would change significantly compared to a bridge on firm soil. However, the remaining models (for structural components) would likely remain the same. Therefore, it would once again be a simple matter to

compare decision fragility outcomes of these two scenarios.

2.2.2 Numerical Solution

The power-law form of the demand, damage, and decision models is, at best, only a good estimate of the behavior of a structure under earthquake excitation in the interval of values where the locally linear fits were made. Other functional forms, such as a piecewise linear function in log space, may provide a better description of the behavior of the structure across the entire range of the variables involved in a probabilistic response evaluation. Note that the two primary assumptions (the demand, damage, and decision variables are conditionally lognormal and homoskedastic) must be retained in this generalized strategy.

A generalized Matlab tool (Mackie, 2007b) allows using arbitrary mathematical functions to specify the hazard, demand, damage, and decision models. However, numerical integration is now necessary to obtain the solutions of the PEER framing integrals and other intermediate results. The hazard, demand, damage, and decision models are described using Equations (2.14) through (2.17), respectively. The hazard is defined in terms of the mean MAF of exceeding a given IM. The remaining models are defined in terms of the median EDP, DM, and DV.

$$\bar{\nu}_{IM} = f_{hazard}(im) = hazard(im) \tag{2.14}$$

$$\widehat{EDP} = f_{psdm}(im) = psdm(im) \tag{2.15}$$

$$\widehat{DM} = f_{pdm}(edp) = pdm(edp) \tag{2.16}$$

$$\widehat{DV} = f_{plm}(dm) = plm(dm) \tag{2.17}$$

Numerical integration of Equation (2.1) is performed as indicated by the pseudo code below. The result of the numerical integration ($outp \in \Re^{dim(DV)\times dim(IM)}$) is the conditional CDF of DV given IM. This surface is plotted in the top-left corner of the Matlab tool plotting window. Numerical integration to obtain the decision hazard curve uses finite differences for the seismic hazard curve and sampled values at the $G_{DV|IM}$ surface (or can be computed using a user-specified function).

$$dP_{EDP}(IM_i) = lognpdf(EDP, log(psdm(IM_i)), \sigma_{PSDM})$$
$$dP_{DM} = lognpdf(DM, log(pdm(\widehat{EDP})), \sigma_{PDM})$$
$$temp = integrate(dP_{DM} .* [dP_{EDP}^T \ldots]_{dim(dP)\times dim(DM)})$$

$$P_{DV} = 1 - logncdf(DV, log(plm(\widehat{DM})), \sigma_{PLM})$$
$$outp_i = integrate(P_{DV} .* [temp^T \ldots]_{dim(temp)\times dim(DV)})$$

A particularly pertinent use of the generalized Matlab tool is to accurately account for the nonlinearity of the seismic hazard curve in log space. Furthermore, it may be expected that the demand model will be different for the low and the high ground motion intensities. Therefore, it may be desirable to fit a nonlinear form to the demand model or, alternatively, to fit a piecewise linear approximation to the data (in log space). Both of these alternatives are easily incorporated into the generalized Matlab tool as long as only a single output corresponds to a given input (i.e., the intermediate models are mathematical functions, not relations).

The same highway overpass bridge for which the loss of lateral-load-carrying capacity was evaluated using power-law intermediate models and closed-form solutions in Figure 2.2 is re-evaluated using the intermediate models formulated with more appropriate mathematical functions and the generalized Matlab tool: the results are presented in Figure 2.3. The seismic hazard curve was modeled as a parabolic function in log space using USGS map values over the range of spectral displacement ground motion intensities between Sd = 2 to 12 cm (Fig. 2.4a). The demand model was taken as bilinear to account for the elastic behavior of the bridge at low ground motion intensities when its load-carrying-capacity loss is minimal (Fig. 2.4b). Similarly, the loss model was also bilinear, calibrated to prevent the loss of traffic-load-carrying capacity from exceeding 100% (Fig. 2.4c). A comparison of the closed-form and generalized probabilistic performance-based seismic response evaluations is shown in Figure 2.4d. This plot shows the MAF of exceeding a given DV value (for example, loss of more than 25% of the lateral-load-carrying capacity) is substantially smaller when computed using more realistic bilinear intermediate models.

2.3 APPROACH 1: SCALAR

The scalar approach is a straightforward application of Equations (2.1) and (2.2) and uses the intermediate variables IM-EDP-DM-DV. To facilitate this approach, a loss model is developed that directly relates the bridge-level damage states to repair costs. The repair cost ratio (RCR), or ratio of repair cost to replacement cost, is used to define the losses (DV). Discrete column damage states are matched to the HAZUS damage (bridge-system level) states to accomplish this. This matching provided a mapping of the component level damage of the column to observed bridge

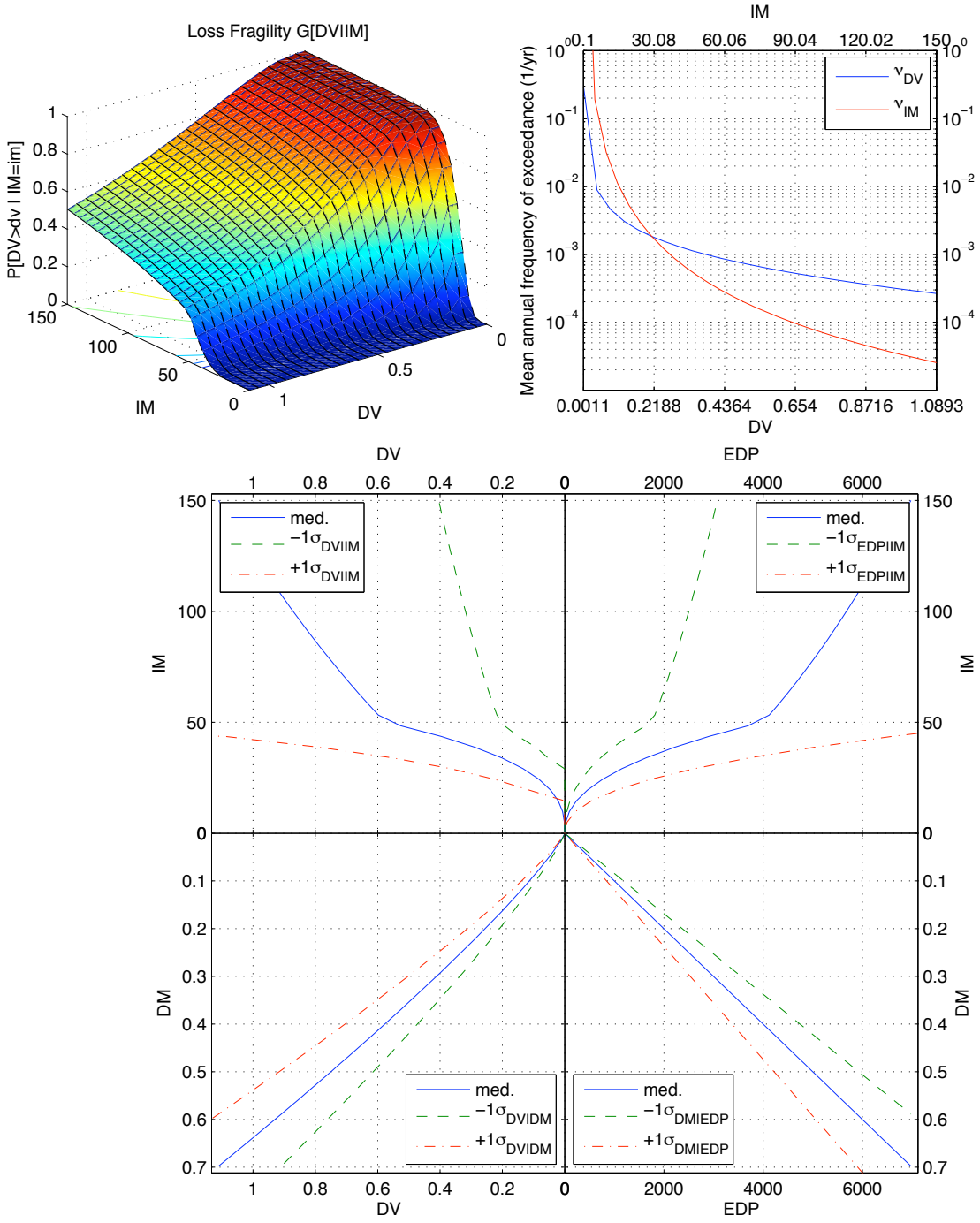

Fig. 2.3 Bridge performance evaluation using arbitrary forms of the interim models and the generalized Matlab tool. IM = $Sd(T_1)$ (cm). EDP = loss of vertical-load-carrying capacity (k). DM = loss of vertical-load-carrying capacity (decimal). DV = loss of traffic-load-carrying capacity (decimal).

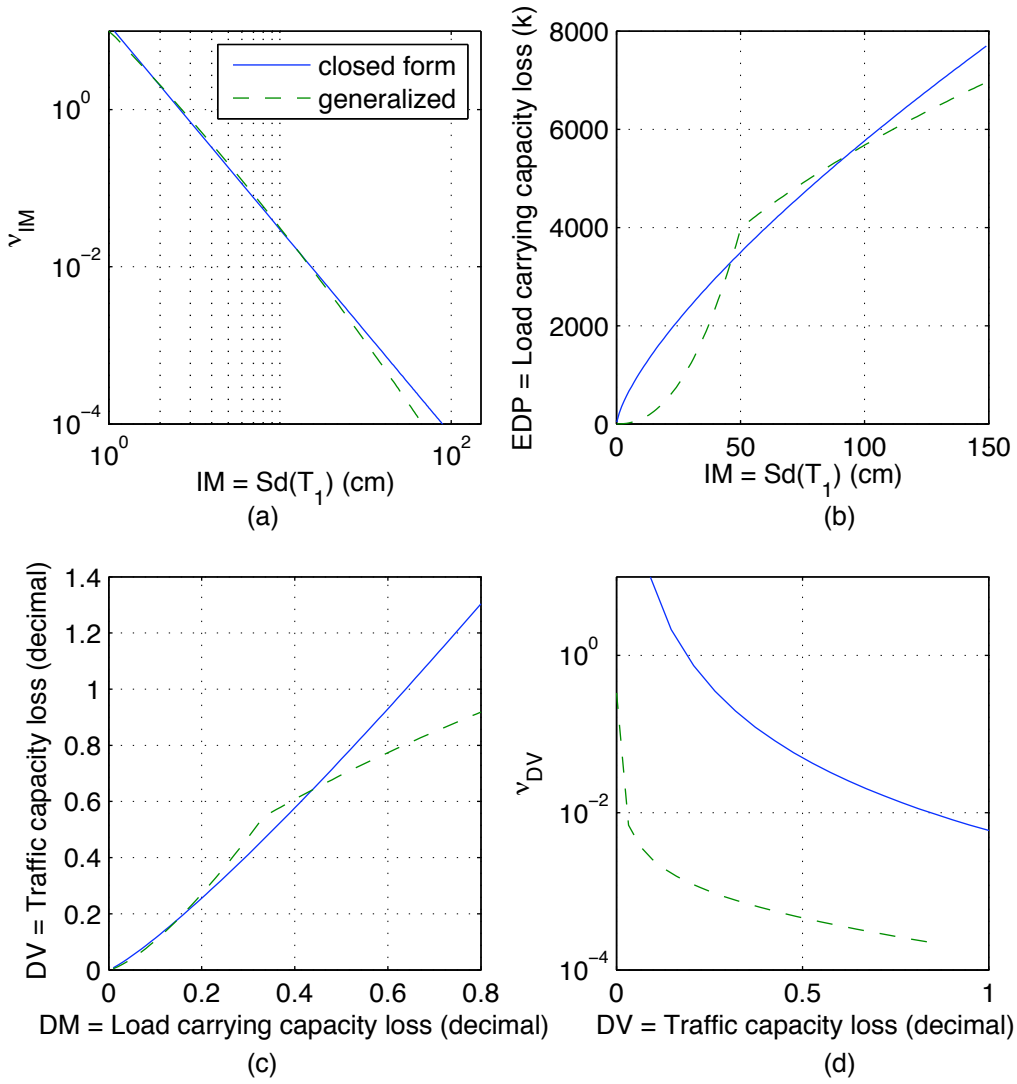

Fig. 2.4 Comparison of results obtained using closed-form and generalized numerical performance evaluation methods.

level damage that impacted the total repair cost, and it limits all variables to scalar quantities. Solutions to the scalar approach can be derived using any of the solution strategies mentioned previously (closed-form, Fourway, or numerical integration). Applications of the scalar approach are shown in Chapter 7 and sensitivities of the resulting loss fragilities to the solution strategy chosen in Mackie and Stojadinović (2006c).

2.4 APPROACH 2: VECTOR WITH CLOSED-FORM/FOURWAY SOLUTION

As mentioned previously, the vector approaches are not a straightforward implementation of the PEER methodology using only the intermediate variables IM-EDP-DM-DV, due to the inclusion of repair quantities (Qs) and repair costs/times as intermediate variables. However, for each structural component of the bridge (or performance group) and repair quantity, a single scalar-type analysis is performed, modeled in IM-EDP-DM-Q space. When solved using the closed-form or Fourway solution strategies, the expectation and variance of each repair quantity $q_{n,l}$ for the repair item n and performance group l are obtained. The first moment and second central moment are denoted $E[q_{n,l}]$ and $Var[q_{n,l}]$, respectively. These two quantities are lognormal distribution parameters due to the assumptions surrounding the Fourway process (technically, the second lognormal parameter is the square root of the variance). Because the repair quantity loss model cannot be assumed to be a power-law relationship, a different median relationship between Q and DM must be derived. A power-law relationship would grow exponentially beyond the data provided, and would not accurately define distinct plateaus of repair data. Choosing instead to use a log-linear relationship between discrete repair quantities is an intuitive choice because earthquake damage and the resulting repair methods and quantities are, by nature, continuous processes that are not completely defined by the discrete damage states and repair quantities for which data exist. So, the general form of the Q-DM model used is a piecewise linear relationship in log space.

Two additional considerations are necessary for formulating the Q-DM relationship. First, the repair quantities are not necessarily increasing with greater damage. For example, from low to moderate damage, the amount of patching for concrete cover spalling on a column increases. However, beyond a certain damage measure value, the amount of patching drops to zero because the preferred repair method becomes complete replacement instead of rehabilitation. This necessitates the use of a curtailed Q-DM relationship for certain items. By curtailing a repair quantity

loss model, it may be possible for the overall repair cost to be discontinuous (a decrease) with increasing IM. Second, because no simulations are performed in this method, the outcome is dependent on the ability to discern first and second moments of Q. This prevents the use of zero- or large-slope Q-DM models because the variance is dependent on these slopes.

The available Q-DM models were observed by plotting the repair quantity against the median EDP at which a discrete damage state occurs. Four general categories of Q-DM model behavior were then developed. The four categories of log-linear repair quantity loss models used in this report are the same as those derived for a similar study on the repair costs of buildings (Mackie and Stojadinović, 2006d). In summary, type I is for quantities that increase initially but plateau, type II is for quantities that do not trigger until higher damage states, type III is for quantities that have small initial quantity magnitudes compared to the ultimate quantity magnitude, and type IV is a combination of type I and type II. The four types are illustrated in Figure 2.5.

Once the quantities for individual items and performance groups can be determined, the total quantity of the same repair item across all performance groups can be computed. A total number of N_{PG} performance groups and N_Q repair items were used. The expected value and variance of each of the repair quantities was then computed, rather than the complete probability distribution for each repair quantity. The expectation of the total repair quantity Q_n for each item n remains a linear combination of the expected performance group-dependent quantities:

$$E[Q_n] = \sum_{l=1}^{N_{PG}} E[q_{n,l}] \tag{2.18}$$

The corresponding variances are not simple linear combinations due to the correlation between response quantities and performance groups. For a summation of correlated random variables, the variance is given as:

$$Var[Q_n] = \sum_{l=1}^{N_{PG}} Var[q_{n,l}] + 2 \sum_{l=1}^{N_{PG}} \sum_{p>l}^{N_{PG}} Cov[q_{n,l}, q_{n,p}] \tag{2.19}$$

The covariance is obtained from the correlation coefficient relating performance groups l and p from the nonlinear bridge analysis results. The simple summation of Q_n between performance groups is possible only if the quantities are assumed to be (or converted to) normal distributions. Addition of lognormally distributed variables is not as straightforward (Naus, 1969; Beaulieu et al., 1995). The unit cost Cu_n of each item n was considered to be constant regardless of the quantity

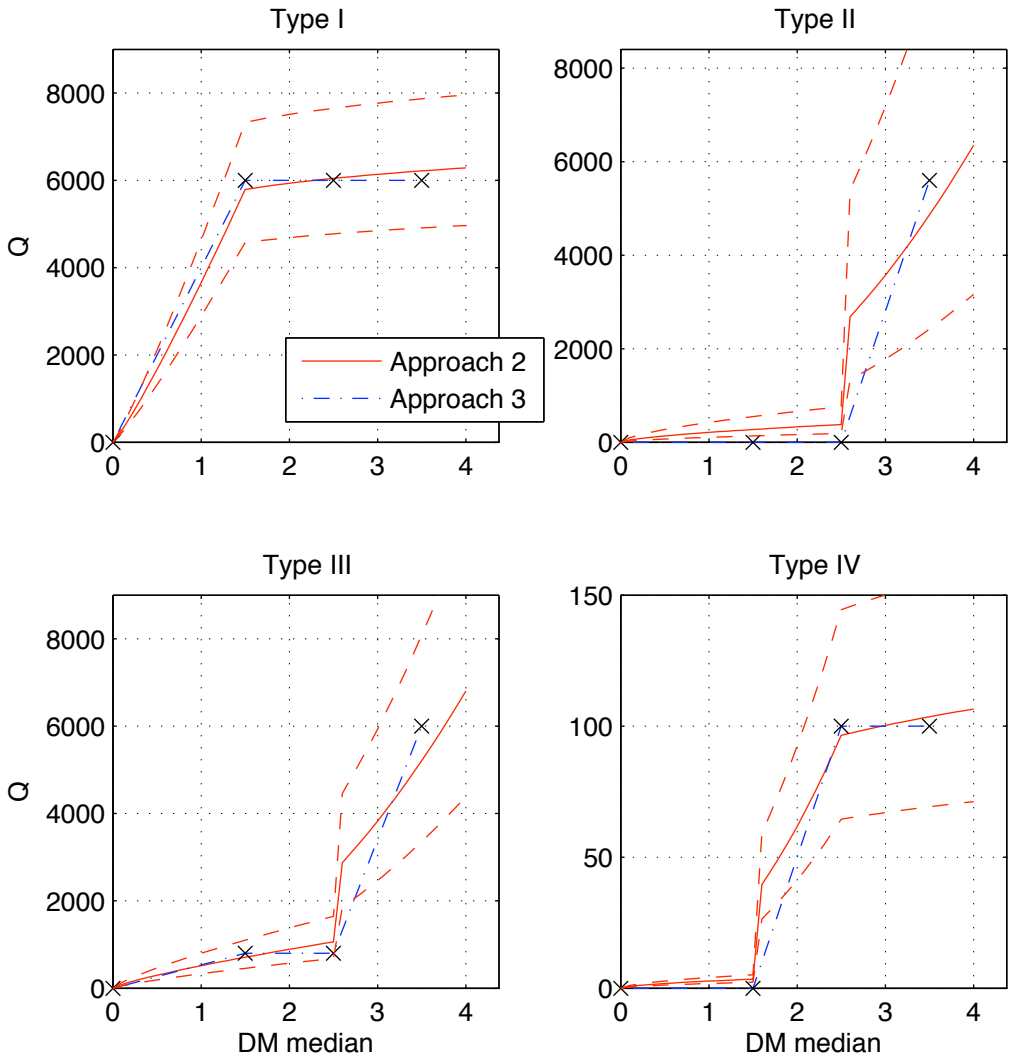

Fig. 2.5 Four categories of non-power-law quantity-damage (Q-DM) relationships.

Q_n. Costs associated with mobilization and contingencies can be estimated later as lump sum percentages of the total cost. The resolution of the cost data at present does not lend itself to developing a nonlinear unit cost function; however, this addition will be pursued in future studies. The total cost for each repair item is obtained by multiplying the unit cost by the repair quantity. Similarly, the variance of the cost is also dependent on $E[Q_n]$ and $Var[Q_n]$. The total expected cost of repair $E[TC]$ was then determined from:

$$E[TC] = \sum_{n=1}^{N_Q} Cu_n(E[Q_n]) \tag{2.20}$$

The total cost variance was obtained by summation of the individual material variances and adding an additional term due to the uncertainty in the unit cost. Because the repair items were assumed to be statistically independent, the covariance term, similar to that in Equation (2.19), is zero. Based on the central limit theorem, it is likely that the total cost will approach a normal distribution due to the number of Qs being summed (N_Q Qs varied within N_{PG} PGs). The process described in this section is easily automated by computer. If the intermediate IM-EDP-DM-Q relationships are assumed to all follow power-law relationships or one of the four types in Mackie and Stojadinović (2006d), are conditionally lognormal, and have constant conditional dispersion, then the values of $E[q_{n,l}]$ and $Var[q_{n,l}]$ can be determined in closed-form automatically by a computer implementation of the method. If these conditions do not hold for a given realization of the intermediate variables, the approximate Fourway solution can be applied directly.

The production rate PR_n of each item n is also considered constant regardless of the quantity Q_n. Therefore, the production rate specified in this report is in units of crew working days (CWD), and not the normalized quantity of CWD over total output. In addition, the magnitude (or distribution) of Q_n is not used explicitly in the repair time analysis, but rather as a trigger for adding a repair activity to the total number of crew working days (CWD) required. For the purposes of this report, each repair activity is triggered if the probability that $P[Q_n \geq tol] > 0.5$, where the tolerance is set at a value minimally larger than zero. The total expected repair time $E[RT]$ is then obtained from:

$$E[RT] = \sum_{n=1}^{N_Q} PR_n \tag{2.21}$$

The variance of the repair time was assumed to also be an addition of the individual variances of PR_n. The individual random variables in Equation (2.21) are assumed to follow the PERT (pro-

gram evaluation and review technique) criteria for mean and standard deviation. The simplification of the repair time analysis does not account explicitly for critical paths and other dependencies between repair activities. Research is ongoing to account for these dependencies/correlations while retaining the ability to perform simulations using the data structure detailed in Chapter 3.

Approach 2 was originally developed (Mackie and Stojadinović, 2006d) as an alternative loss modeling procedure to the simulation approach taken by Yang et al. (2006) for buildings. It was modified to suit the bridge data available at the time (Mackie et al., 2006, 2007a) and applied to the prediction of post-earthquake repair cost ratios for the testbed bridges described in Chapter 4. The data structure, number of performance groups, repair methods, repair quantities, and unit costs were not as complex, nor as up-to-date as the material presented in the following chapters of this report. However, an example of Approach 2, using all of the original data presented in Mackie et al. (2006, 2007a), is retained in Chapter 7 to illustrate the similarities and differences between Approach 2 and 3, as well as the improved data flows described in Chapter 3.

2.5 APPROACH 3: VECTOR WITH DAMAGE MODEL LINEARIZATION

The basic methodology of the two vector approaches (Approaches 2 and 3) are the same, i.e., Approach 3 also employs Equations (2.18)–(2.21). However, development of Approach 3 was motivated by the unpredictable behavior of Approach 2 at demands beyond the last damage state and the difficulty of extending the approach to user-specified Q-DM models without recognition of new piecewise types such as those shown in Figure 2.5. Approach 2 also often results in extremely large (and unlikely) values of dispersion for the repair quantities when there are large jumps in the quantity magnitudes between damage states, and occasionally leads to discontinuities in the median Q-DM relationship when trying to best fit linear curves in log space to the data points. However, the benefit of Approach 2 is that the closed-form solution strategy can easily be applied to each piecewise linear (in log space) portion of the Q-DM model. Therefore, a new approach was developed for this testbed that overcomes all of the issues experienced by Approach 2, plus it retains the simplicity of automated closed-form solutions. Approach 3 is based on linearization of the Q-DM model (linear in linear space).

Rather than assuming that the loss model follows a power-law relationship, as in Equation (2.9),

a loss model that is linear in linear space can be written as:

$$Q = e_{lin}DM + f_{lin} \tag{2.22}$$

The first-order expansion of $ln(Q)$ in Equation (2.22) about a point in DM space denoted d_0 can be written as:

$$ln(Q) = ln(e_{lin}d_0 + f_{lin}) + \frac{e_{lin}}{e_{lin}d_0 + f_{lin}}(DM - d_0) + h.o.t. \tag{2.23}$$

Similarly DM and d_0 can be related to $ln(DM)$ and $ln(d_0)$ and combined with Equation (2.23) to obtain the same form as Equation (2.9), but with new parameters E' and F' replacing the previous parameters E and F.

$$E' = ln(e_{lin}d_0 + f_{lin}) - \frac{e_{lin}d_0 ln(d_0)}{e_{lin}d_0 + f_{lin}} \tag{2.24}$$

$$F' = \frac{e_{lin}d_0}{e_{lin}d_0 + f_{lin}} \tag{2.25}$$

While easy to implement, the new parameters still require selection of an expansion point d_0 and do not guarantee that $e_{lin}d_0 + f_{lin} \neq 0$ or that the resulting piecewise Q-DM function is continuous at the end-points of the intervals used. The result of using Approach 3 is demonstrated in Figure 2.5 to contrast with Approach 2.

Approach 3 is complete as implemented for this testbed by continuously updating the location of the linearization point d_0 to be at every DM input desired. This results in well-behaved Q-DM models that are in fact linear in linear space but are compatible with the previous closed-form approach. A final improvement that is implemented in Approach 3 but none of the other approaches is the concept of DS0 and DS∞. However, this improvement is in the data flow and not unique to Approach 3; therefore, the discussion is included in the chapters on the data structure (Chapter 3) and on repair methods (Chapter 5).

Most of the repair cost, and all of the repair time, outcomes shown in Chapter 7 were generated using Approach 3. Approach 3 exclusively uses the updated data structure, performance groups, repair methods, repair quantities, unit costs, and production rates described in the following four chapters of this report.

3 Data Structure

This chapter describes the data required to support repair cost and repair time bridge fragility analysis. Geometric and design information for the bridge structure needs to be available in order to compute the quantities associated with the bridge damage states. The information about the bridge structure can be thought of as a very simple building information model (BIM) for the testbed bridge, or as a specific kind of bridge maintenance database (Branco and de Brito, 2004). Although it does not contain enough information to support graphical views, it does contain sufficient information to support the computation of repair time and repair cost. Queries on this information model are implemented in Excel using spreadsheet references. An implementation in a database management system could retrieve information through SQL SELECT statements.

In the Excel spreadsheets, two different pieces of information are implemented in the same location: the geometric and design information for the bridge, and the formula used to estimate repair quantities. The formula is generally hidden unless one clicks on the cells in the spreadsheet. This feature of spreadsheets makes it easy to perform multiple updates in multiple locations with only one change a cell. The referring cells are automatically recalculated when one cell is updated.

Considering the data structure in this manner allows a reformulation of the Excel spreadsheet data as an abstract data model. This abstract data model uses Excel spreadsheets serving as one possible instantiation of this data model. Formulating the data structure in this manner allows future extension and linking with other advances in BIM-related technologies.

3.1 DATABASE TABLES

Each item used in the methodology (Chapter 2) needs to have a corresponding entity in a database in order to programmatically obtain its values during computation. For example, for each perfor-

mance group there are multiple damage states and with each damage state there are multiple repair items each with different quantities. This data model is defined using tables that can be used to store the information (Fig. 3.1). Relationships are illustrated using foreign keys for simplicity; however, an actual implementation would use junction tables for one-to-many relationships. Defining the model with tables allows the usage of a query language to precisely define the queries needed to support the methodology. The table structure also serves as a backbone for future expansion. Each of the tables in the data model is described in detail below.

3.1.1 Bridge Information

Information about the dimensions, materials, and geometry of the bridge are important for computing repair quantities for the bridge damage states. The information about the bridge can be subdivided into 5 major areas: Column (Tables 3.1–3.2), Deck and Superstructure (Tables 3.3–3.4), Abutment and Joint (Tables 3.5–3.6), Column Foundation (Tables 3.7–3.8), and Abutment Foundation (Tables 3.9–3.10).

The bridge information shown is for the Type 1A bridge model which has 22′ tall circular columns. Each input variable is a unique short name that describes the quantity of interest. Each piece of information has a short variable name and a description of how it is measured or calculated from other variables.

The columns of the Bridge Information table include: `name`, `value`, `unit`, `metricValue`, and `metricUnit`. The `name` column contains the short name of the input variable for each bridge information quantity. The `value` and `unit` columns store the value of the information quantity as a floating point number along with the unit of measurement using US Imperial units. The `metricValue` and `metricUnit` are similar but using metric units instead. No relationships are defined for this table within the database.

3.1.2 Unit Costs

The unit costs are stored in the Unit Cost table with the following columns: `cost_id`, `unit`, `unitCost`, `unitCostSD`, `notes`. The `cost_id` column is the primary key and is an integer number. The unit costs could be linked to multiple repair quantities if some quantities have identical unit cost structures. In the methodology, the unit costs are assumed to be constant regard-

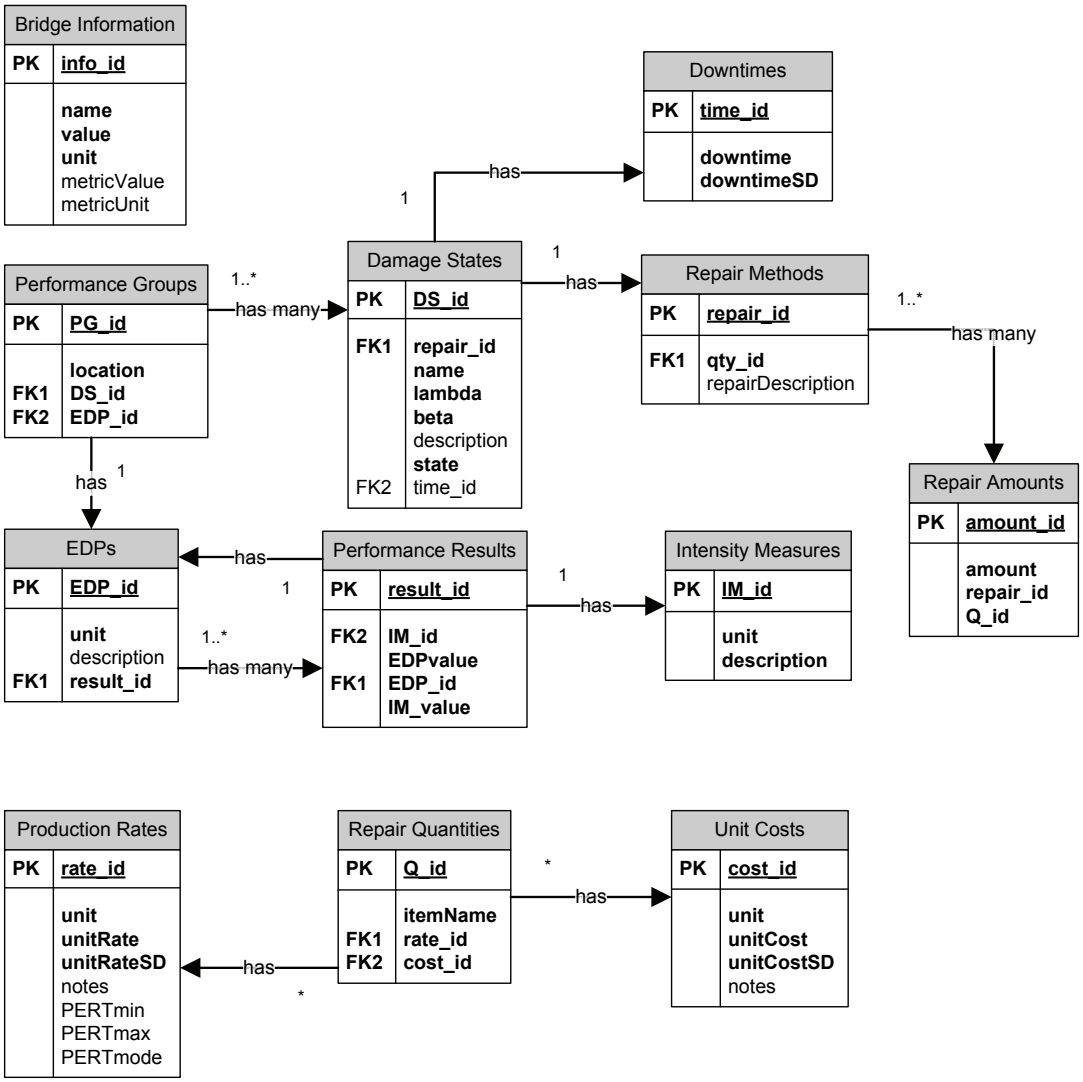

Fig. 3.1 Database tables.

Table 3.1 Column information.

Input Variable (`name`)	Description and Computation
column diameter	outer diameter of a circular column
column surface area	
number of columns	total count of columns in single bent configuration
required column casing thickness	thickness of column casing based on diameter of column and Caltrans detail sheet XS7-010e
column height	total column height from pile cap to bottom of superstructure
bar area	total cross-sectional area of longitudinal steel in the column
diameter of longitudinal bars	diameter of longitudinal steel
number of longitudinal bars	total count of individual longitudinal steel bars
percent transverse reinforcement	
percent long. reinforcement	
column dead load (bottom)	gravity dead load at the bottom of the column, including the self-weight of the column
col gross area (A_g)	(column diameter)$^2 \times \pi$
column cover	minimum cover from outside of transverse steel hoops
total column bar volume (long.)	total volume of longitudinal bars calculated using nominal area
total column bar weight (long.)	total weight of longitudinal bars calculated using nominal weight per foot
steel (f_{ye})	yield stress of bar reinforcing steel
concrete (f'_{ce})	compressive strength of concrete at 28 days
steel weight	unit weight of reinforcing steel
concrete weight	unit weight of concrete
steel weight estimate (BDA 11-5)	total weight of reinforcing steel per volume assumed for estimating purposes
total column gross volume	gross volume computed using $A_g \times$ (column height)

Table 3.2 Column quantity.

Input Variable (`name`)	Value (`value`, `unit`)		Metric Value		Notes
column diameter	48	in.	1.22	m	
column surface area	276	sf	25.68	m^2	
number of columns	4	ea	4	ea	
required column casing thickness	0.375	in.	0.0095	m	XS7-010e
column height	22	ft	6.706	m	
bar area	1.27	$in.^2$	0.00082	m^2	US #10 bars
diameter of longitudinal bars	1.272	in.	0.0323	m	US #10 bars
number of longitudinal bars	28	ea	28	ea	
percent transverse reinforcement	1.59	%	1.59	%	
percent long. reinforcement	2.0	%	2.0	%	
column dead load (bottom)	1837	k	8171	kN	
col gross area (A_g)	1810	$in.^2$	1.168	m^2	
column cover	1.5	in.	0.038	m	
total column bar volume (long.)	5.43	cf	0.154	m^3	
total column bar weight (long.)	2662	lb	1207	kg	
steel (f_{ye})	68	ksi	468843	kPa	
concrete (f'_{ce})	5.20	ksi	35853	kPa	
steel weight	490	lb/ft^3	76973	N/m^3	
concrete weight	150	lb/ft^3	23563	N/m^3	
steel weight estimate (BDA 11-5)	16.72	lb/ft^3	268.0	kg/m^3	BDA 11-5
total column gross volume	276.53	ft^3	7.826	m^3	

Table 3.3 Deck and superstructure information.

Input Variable (`name`)	Description and Computation
deck area, total	total deck area = (deck width) $\times$ 2 $\times$ (ext. span length) $\times$ 2 (int. span length)
deck width	constant width of deck
deck depth	depth from top of deck to bottom
ext. span length	span length of interior spans—segments between the abutments and adjacent column bent
int. span length	span length of exterior spans—the segments between column bents
deck area per column	average deck area per column = (deck area, total) / (number of columns)
deck area, ext. span	deck area of exterior span segment = (deck width) $\times$ (ext. span length)
deck area, int. span	deck area of interior span segment = (deck width) $\times$ (int. span length)
deck cross-sectional area	gross cross-sectional area of deck
superstructure bottom width	cross-sectional width of superstructure bottom
spalling strain	strain where concrete spalling initiates

Table 3.4 Deck and superstructure quantity.

Input Variable (`name`)	Value (`value`, `unit`)		Metric Value	
deck area, total	26910	sf	2500	m^2
deck width	39	ft	11.89	m
deck depth	6	ft	1.83	m
ext. span length	120	ft	36.58	m
int. span length	150	ft	45.72	m
deck area per column	6728	sf	625.0	m^2
deck area, ext. span	4680	sf	434.8	m^2
deck area, int. span	5850	sf	543.5	m^2
deck cross-sectional area	61.59	sf	5.72	m^2
superstructure bottom width	23	ft	7.01	m
spalling strain	0.005	in./in.	0.005	m/m

Table 3.5 Abutment and joint information.

Input Variable (`name`)	Description and Computation
number of bearings/joint	number of bearings at each abutment, one bearing under each box web
bearing height	total height of entire bearing assembly
expansion joint gap	gap between superstructure and abutment back wall
expansion joint blockout height	height of joint seal assembly blockout specified in MTD 7-20
expansion joint blockout width	width of joint seal assembly blockout specified in MTD 7-20
expansion joint blockout steel	weight of reinforcing steel per unit volume assumed for estimating purposes in BDA 11-5 for the blockout
back wall steel	weight of reinforcing steel per unit volume assumed for estimating purposes in BDA 11-5 for the back wall
abutment dead load	abutment dead load due to weight of ext. span = (ext. span length) / 2 $\times$ (deck cross-sectional area) $\times$ (concrete weight)
number of shear keys	count of shear keys at each abutment
approach slab length	approach slab length according to Caltrans standards
approach slab width	approach slab width = (deck width)
approach slab thickness	thickness of approach slab concrete
approach slab area	top surface area of approach slab = (approach slab length) $\times$ (approach slab width)
approach slab roadway volume	gross volume of approach slab = (approach slab area) $\times$ (approach slab thickness)
wing wall length	length of wing wall at deck grade level
wing wall thickness	wing wall thickness
shortest wing wall height	height of wing wall at shortest point away from the bridge
back wall thickness	back wall thickness
back wall height	back wall height measured from top of deck, including joint seal assembly blockout = (deck height)
stem wall thickness	stem wall thickness
stem wall height	stem wall height
shear key thickness at top	shear key thickness at top assuming trapezoidal shape
shear key height	shear key height
embankment slope	embankment slope ratio (V/H)

Table 3.6 Abutment and joint quantity.

Input Variable (`name`)	Value (`value`, `unit`)		Metric Value		Notes
number of bearings/joint	3	ea	3	ea	bearing under each box web
bearing height	2	in.	0.051	m	
expansion joint gap	4	in.	0.102	m	
expansion joint blockout height	12	in.	0.305	m	
expansion joint blockout width	10	in.	0.254	m	
expansion joint blockout steel	2.995	lb/ft^3	48.00	kg/m^3	BDA 11-5
back wall steel	3.370	lb/ft^3	54.00	kg/m^3	BDA 11-5
abutment dead load	554.31	k	2466	kN	
number of shear keys	2	ea	2	ea	
approach slab length	30	ft	9.14	m	Caltrans standard length
approach slab width	39	ft	11.89	m	deck width
approach slab thickness	1	ft	0.30	m	
approach slab area	1170	sf	108.7	m^2	
approach slab roadway volume	1170	cf	43.3	m^3	
wing wall length	19.0	ft	5.79	m	
wing wall thickness	1.0	ft	0.30	m	
shortest wing wall height	3.0	ft	0.91	m	
back wall thickness	1.0	ft	0.30	m	
back wall height	6.0	ft	1.83	m	deck depth
stem wall thickness	4.0	ft	1.22	m	
stem wall height	8.0	ft	2.44	m	
shear key thickness at top	3.0	ft	0.91	m	
shear key height	5.0	ft	1.52	m	
embankment slope (V/H)	2.0	–	2.0	–	

Table 3.7 Column foundation information.

Input Variable (`name`)	Description and Computation
pile cap dimension 1	longitudinal length of pile cap
pile cap dimension 2	transverse length of pile cap
pile cap depth	depth of pile cap measured from bottom of column to top of pile, not embedment under grade
pile cap steel reinforcement %	reinforcement ratio for all steel in the pile cap
pile cap volume	gross volume of pile cap = (pile cap dimension 1) $\times$ (pile cap dimension 2) $\times$ (pile cap depth)
column pile diameter	outer diameter of circular pipe pile
column pile thickness	thickness of circular pipe pile
column pile (f_{ye})	yield strength of pipe pile
column pile spacing	nominal center-to-center spacing of piles = 3 $\times$(column pile diameter)
pile length	
number of piles	
enlarged pile cap dimension 1	longitudinal length of enlarged pile cap for repair = (pile cap dimension 1) + 2 $\times$ (pile cap dimension 1)
enlarged pile cap dimension 2	transverse length of enlarged pile cap for repair = (pile cap dimension 2) + 2 $\times$ (pile cap dimension 2)
pile cap embedment depth	embedment of pile cap from grade to bottom of column
steel weight estimate footing	weight of reinforcing steel per unit volume assumed for estimating purposes

Table 3.8 Column foundation quantity.

Input Variable (`name`)	Value (`value`, `unit`)		Metric Value		Notes
pile cap dimension 1	15	ft	4.57	m	
pile cap dimension 2	10	ft	3.05	m	
pile cap depth	3.25	ft	0.99	m	
pile cap steel reinforcement %	3.65	%	3.65	%	
pile cap volume	18.06	cy	13.80	m^3	
column pile diameter	24	in.	0.610	m	
column pile thickness	0.50	in.	0.0127	m	
column pile (f_{ye})	68	ksi	468843	kPa	
column pile spacing	72	in.	1.829	m	3 $\times$ D
pile length	60	ft	18.3	m	
number of piles	6	ea	6	ea	3 $\times$ 2 group
enlarged pile cap dimension 1	27	ft	8.23	m	original + 2 $\times$ spacing
enlarged pile cap dimension 2	22	ft	6.71	m	original + 2 $\times$ spacing
pile cap embedment depth	2	ft	0.61	m	
steel weight estimate footing	6.552	lb/ft^3	105.00	kg/m^3	BDA 11-5

Table 3.9 Column foundation information.

Input Variable (`name`)	Description and Computation
abutment pile cap dimension 1	longitudinal length of pile cap
abutment pile cap dimension 2	transverse length of pile cap
abutment pile cap depth	depth of pile cap measured from bottom of column to top of pile, not embedment under grade
abutment pile cap reinforcement %	reinforcement ratio for all steel in the pile cap
abutment pile diameter	outer diameter of circular pipe pile
abutment pile thickness	thickness of circular pipe pile
abutment pile (f_{ye})	yield strength of pipe pile
abutment pile spacing	nominal center-to-center spacing of piles = 4 $\times$ (column pile diameter)
abutment pile length	
abutment number of piles	

Table 3.10 Abutment foundation quantity.

Input Variable (`name`)	Value (`value`, `unit`)		Metric Value		Notes
abutment pile cap dimension 1	45	ft	13.72	m	
abutment pile cap dimension 2	10	ft	3.05	m	
abutment pile cap depth	3	ft	0.91	m	
abutment pile cap reinforcement %		%	0	%	
abutment pile diameter	24	in.	0.610	m	
abutment pile thickness	0.5	in.	0.013	m	
abutment pile (f_{ye})	68	ksi	468843	kPa	
abutment pile spacing	96	in.	2.438	m	4 $\times$ D
abutment pile length	70	ft	21.34	m	
abutment number of piles	6	ea	6	ea	6$\times$1 group

less of the amount of repair quantities used. With this assumption, it would have been possible to define the unit costs and repair quantities in a single table. However, separating the unit cost table provides more opportunity for expansion and expressing dependency between the costs as the methodology is further developed. For example, using separate tables could support repair quantities having multiple different unit costs.

The unit column gives the measurement unit for the unit cost using cost estimating notation. The `unitCost` column provides the mean value of the unit cost as a floating point number and the `unitCostSD` column gives its standard deviation σ. The `notes` column is there to add commentary describing the derivation of the unit cost and possible limitations on its validity for extremely large or small quantities.

3.1.3 Damage States, Repair Methods, and Repair Amounts

The damage states themselves are defined by limit states conditioned on EDP values. This limit state information is stored in the Damage States table which has columns for `DS_id`, `repair_id`, `time_id`, `name`, `lambda`, `beta`, `state`, and `description`. The `DS_id` column is the primary key and is an integer value identifying each damage state individually. The `name` column contains a short name of the damage state and the description column contains a description of the The `repair_id` and `time_id` columns link the damage state to its corresponding downtimes and repair methods. In the current methodology, each damage state has only one downtime estimate and only one repair method. Future expansion could link damage states to different repair options. In that case, the damage state could be linked to repair methods in a one-to-many relationship through an intermediate junction table instead of a simple foreign key column.

The `lambda` and `beta` columns store the lognormal distribution parameters λ and β expressing the fragility curve for the damage state based on the corresponding EDP. The `state` column is either zero or a small positive integer representing the damage state number. A value of 0 corresponds to the DS0 trigger state indicating the onset of repair cost, a value of 1 indicates DS1, etc. A value of 10 can be used to represent the state of DS∞ since there are typically only up to 3 or 4 damage states. If more damage states are needed, then a higher value could be used to represent DS∞.

The damage states are also linked to repair methods through the `repair_id` column and

to expected bridge downtime through the time_id column. The Downtimes table contains a downtime column containing the expected amount of downtime in days and downtimeSD column for its standard deviation σ. The Repair Methods table has a description column for storing a summary of the repair method.

The computation of the quantity amounts for the damage states is described in Chapter 5. These amounts are stored in the Repair Amounts table. This table functions much like a junction table between Repair Methods and Repair Quantities, while also adding the amount of each quantity used by each repair method. The Repair Amounts table has columns amount_id, amount, repair_id, and Q_id. The column amount_id serves as the primary key and is an integer value. The amount column is a floating point number which gives the amount of repair quantity identified by Q_id that is used by the repair method identified by repair_id.

3.1.4 Performance Groups

The performance groups are stored in the Performance Groups table with columns: PG_id, location, DS_id, and EDP_id. The PG_id column is the primary key and is an integer number corresponding to performance group l or p in the methodology. The location column is a short text description of which part of the bridge is represented by the performance group. For example, this would give a text description differentiating the left abutment from the right abutment performance groups. The other fields are foreign keys pointing to the damage states and EDPs related to this performance group. Junction tables could be used to implement these as one-to-many relationships.

3.1.5 Production Rates and Repair Times

The production rates for bridge repairs are stored in the Production Rates table with columns: rate_id, unit, unitRate, unitRateSD, PERTmin, PERTmode, PERTmax, and notes. The column rate_id is the primary key and is an integer number. The value for the unit field is the unit of measurement for the production. Currently, this unit is always crew-work-days (CWD), which represents one working day for a normal sized crew. With additional data, these values could be refined to material level quantities with variation depending on the complexity of the work to be performed. The unitRate column gives the mean amount of time needed to complete a unit

of work and `unitRateSD` gives its standard deviation.

The mean and standard deviation are estimated using the PERT criteria (Harris, 1978; Perry and Grieg, 1975). This distribution uses estimates on the most likely duration for completing work and minimum and maximum values. With these parameters, the mean and standard deviation can be estimated. These parameters can be stored in the database using the `PERTmin`, `PERTmode`, and `PERTmax` columns.

3.1.6 Repair Quantities

The individual repair quantities are defined in the Repair Quantities table which contains columns `Q_id`, `itemName`, `rate_id`, and cost_id. The column `Q_id` is the primary key and is an integer number. The value for `Q_id` is the same as n for every Q_n in the methodology notation. The name of the quantity is stored in the `itemName` column. This name approximates the names of quantities used in Caltrans cost estimates. The Repair Quantities table does not need to contain much information on its own because many of the data values are stored in other tables which are referenced by the `rate_id` and `cost_id` foreign key columns. This table is referenced by repair amounts in order to link the quantities to the repair methods, damage states, and performance groups.

3.1.7 Downtimes

The data on the downtimes needed for emergency bridge repair are stored in the Downtimes table with columns: `time_id`, `downtime`, and `downtimeSD`. The `time_id` column acts as the primary key and is an integer number. The `downtime` column represents an estimate of the median downtime and `downtimeSD` represents the standard deviation of the downtime, all in units of days. The Downtimes table is designed to be linked to individual rows in the Damage States table so that each damage state has a corresponding downtime associated with it.

3.1.8 EDPs

The EDPs table stores a list of all the engineering demand parameters used in the bridge analysis using columns: `EDP_id`, `unit`, `description`, and `result_id`. The `EDP_id` column is the primary key and is an integer number. The unit used for the values of the EDP are stored in

`unit` and a short description of the EDP in `description`. This table does not actually store the analysis outcomes but only a list of the EDPs themselves. The analysis results are stored in the Performance Results table and linked to the EDPs by the `results_id` foreign key, or via a junction table when many performance results are present.

3.1.9 Intensity Measures

Similar to the EDPs table, the Intensity Measures table lists all the IMs used in the bridge analysis using columns: `IM_id`, `unit`, and `description`. The `IM_id` columns is the primary key and is an integer number. The unit of measurement for each IM is stored in `unit` and a short description is given in `description`. Entries in this table are meant to be linked to the Performance Results table.

3.1.10 Performance Results

The Performance Results table stores the analysis results with values of each EDP for each ground motion with different IMs. The table has primary key `results_id` and columns `IM_value` and `EDP_value` for storing the numerical values of the IM and EDP for each ground motion run. Each row in the table is linked to a corresponding EDP and IM through the `IM_id` and `EDP_id` foreign keys.

3.2 SPREADSHEET IMPLEMENTATION

The database for the performance-based assessment of bridges is implemented using a series of Excel spreadsheets. Excel sheets were chosen for their portability and ease of editing. Spreadsheets also make it easy to capture the dependencies between pieces of information through the use of cell references. For example, volumes can be automatically recomputed if values for length dimensions are changed. Formulas can be entered rapidly and edited quickly. The cell references take care of the logic for performing update operations within the data model. Another advantage of spreadsheets is the ability to display the data in a manner that summarizes a lot of data on a single page.

The spreadsheets can be thought of as different views of the database tables. Thinking of the data model in terms of tables shows the relationships between the spreadsheets in an explicit

Table 3.11 List of Excel spreadsheets.

	Filename	Description	Appendix
1	Cost.xls	Unit costs for each Q	A.1
2	Damage.xls	Limit states for each performance group EDP	A.2
3	EDP.xls	EDP results from structural analysis at various IMs	A.3
4	Info.xls	Bridge information, dimensions, quantities for estimation	A.4
5	Production.xls	Repair item production rate for each Q	A.5
6	Repair.xls	Repair quantities Q for each damage state and performance group	A.6
7	Time.xls	Downtime for each damage state and performance group	A.7

manner. A list of spreadsheets used by the methodology are in Table 3.11. At this time, the data model is implemented only in spreadsheets; however, future research could use the table definitions to implement the information in a database management system, such as MySQL or Microsoft Access. This would allow spreadsheets to be automatically generated from the database by using a series of SQL queries and output templates.

Screenshots of the Excel spreadsheets are provided in Appendix A.

3.2.1 Cost

The item names are presented in column A, the units in column B, mean cost in column C, and standard deviation in column D. Column E contains explanatory notes such as conditions when the unit costs are valid. The entries begin at row 4 and end at row 32. The items are listed in the order of `Q_id` which matches the order in which the items are presented in the other spreadsheets.

3.2.2 Damage

The damage spreadsheet contains a list of all the damage states for each performance group along with the short name and the lognormal distribution parameters λ and β for each damage state.

Column A contains the performance group number `PG_id`, and column B contains the location of the performance group. Each damage state takes the next two columns in order of ascending state severity. The first column contains the λ value and the second column the β value. For example, DS0 has its λ value in column C and β in column D. Subsequently, DS3 has its λ in column I and β in column J.

3.2.3 EDP

The EDP spreadsheet contains a view involving multiple different entities. The EDP spreadsheet combines a list of all the performance groups, all the performance results, and all the EDPs for a particular IM.

Column A has the IM values and columns B–AB have the corresponding EDP values for a single ground motion. Row 1 contains a description of the IM and EDPs, row 2 contains the units used to measure the IM and EDPs, and row 3 has the `PG_id` that the EDP is linked to. The values begin at row 4 and continue until row 107 (or as many rows of data available based on the number of individual ground motion analyses performed).

3.2.4 Information

Column A has the item names and group names, column B has the US Imperial value with units in column C, column D has the metric value with units in column E, and column F contains explanatory notes. Quantities related to the columns are groups in rows 4–24, deck quantities in rows 27–37, abutment and joint quantities in rows 40–63, column foundation quantities in rows 66–80, and abutment foundation quantities in rows 83–92.

3.2.5 Production

Column A contains the repair quantity name, column B has the measurement unit of production rate, column C contains the mean, column D has the standard deviation, and columns E–G contain the mode, minimum, and maximum duration in days used to estimate the mean and standard deviation. Explanatory notes for the computation of repair durations are in column H. The items are in rows 4–32 and are ordered by `Q_id`, which is the same order as in the other spreadsheets.

3.2.6 Repair

The repair spreadsheet contains a view showing all the repair quantities and their corresponding amounts for each damage state of each performance group. Row 1 contains the name of each repair quantity ordered by `Q_id` which is the same order as in the other spreadsheets. Row 2 has the units that are used by each repair amount. Column A contains the name of the performance group and the `PG_id`. Column B has the damage state level for each performance group. Each performance

group takes up the number of rows equal to the number of damage states from DS1 to DS∞. DS0 is not included, since this damage state represents the onset of repairing damage only. Columns C–AE and rows 4–103 contain the repair amounts corresponding to the intersecting damage state, performance group, and repair quantity.

3.2.7 Time

The time spreadsheet contains a list of all the damage states for each performance group. For each damage state, the mean and standard deviation of the bridge downtime is given.

Column A contains the performance group number `PG_id`, and column B contains the location of the performance group. Each damage state takes the next two columns in order of ascending state severity. The first column contains the mean value and the second column the standard deviation of the downtime. Most of the downtime values are either 0 days, 1 day, or 60 days. The value of 60 days represents a major failure where standard repair methods are infeasible.

4 Testbed Bridge

The testbed bridge is from a series of bridge types presented in the PEER lifelines project report by Ketchum et al. (2004). Of the prevalent bridge designs in the California bridge inventory, post-tensioned concrete box girder and pre-tensioned, pre-cast concrete I-girder bridges are identified as the most common. A matrix of 11 common bridge configurations (types) was developed, including common geometry, deck width, deck depth, span arrangement, column height, and number of columns per bent. The straight, cast-in-place box girder bridges with five spans were selected for further study by the PEER testbed teams. Specifically, the two configurations with common deck sections and single column bents were selected for further study. The two configurations are designated as Type 1 and Type 11.

These bridge types are 39′ wide containing two 12′ lanes, a 4′ right shoulder, and an 8′ left shoulder and barrier rail on both sides. The Types 1 and 11 bridges are identical except for the column heights; the Type 1 has 22′ columns and the Type 11 has 50′ columns. The bridges have 3 internal spans of 150′ and 2 external spans of 120′ with a total length of 690′ and total deck area of 26,910 SF. The bridges are cast-in-place, pre-stressed (CIP/PS) 2-cell box girder bridges with the superstructure supported on neoprene bearing pads under each of the three box webs. While both Types 1 and 11 bridges were considered in this report, the complementary PEER testbed groups focused solely on Type 1. An elevation view, typical to both Types 1 and 11, is shown in Figure 4.1. The relative dimensions of the 22′ Type 1 columns and 50′ Type 11 columns are illustrated in Figure 4.2. Both Types 1 and 11 share a common pre-stressed deck cross section, show in Figure 4.3.

Each of these bridge types (1 and 11) has 12 different design realizations based on different column and foundation dimensions. The designs span a range of common column dimensions that

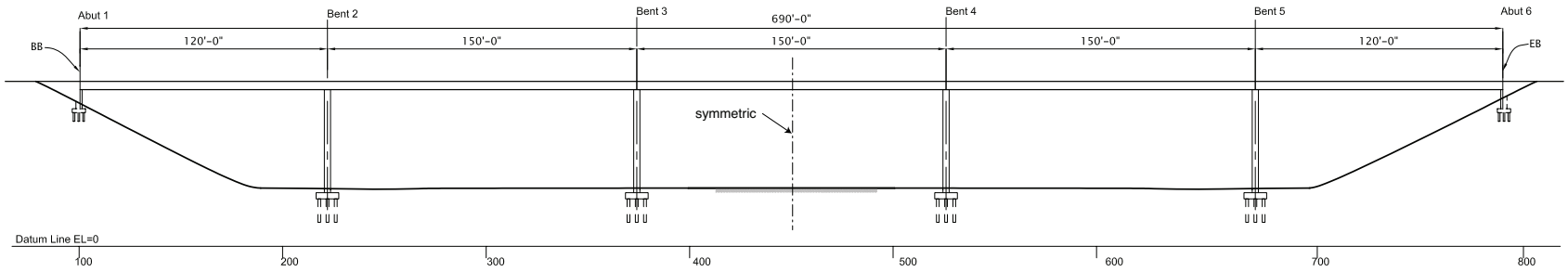

Fig. 4.1 Elevation of Type 1/11 (Ketchum et al., 2004).

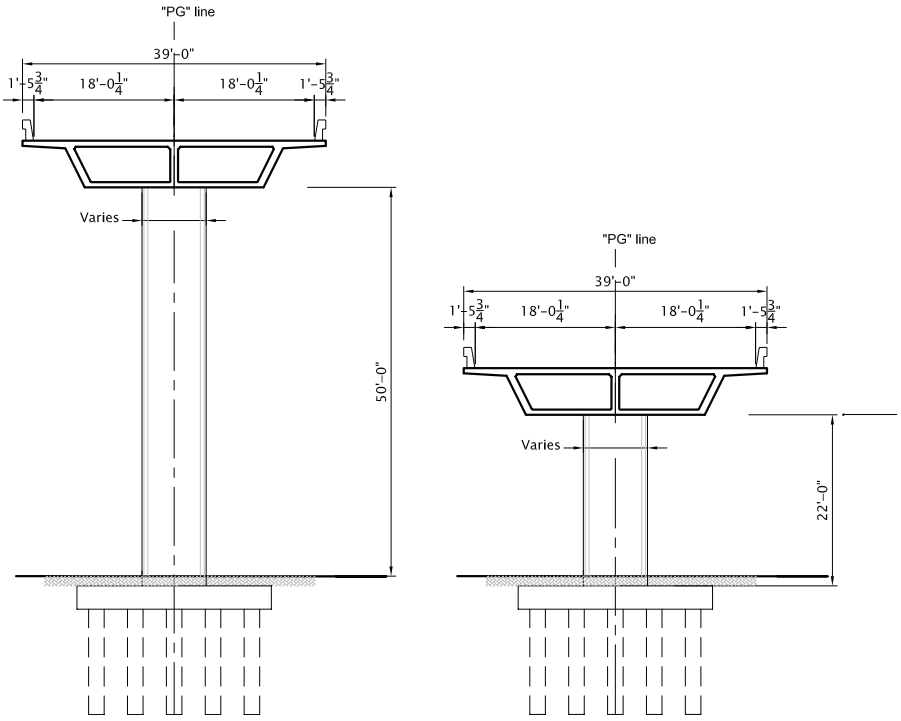

Fig. 4.2 Columns of Types 1 and 11 (Ketchum et al., 2004).

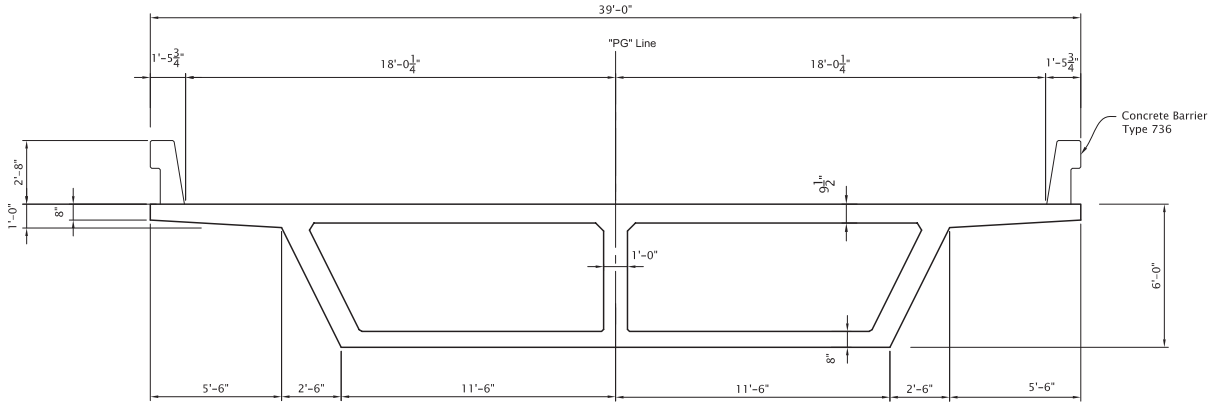

Fig. 4.3 Deck cross section (Ketchum et al., 2004).

were then evaluated for a corresponding maximum seismic intensity resistance level. Details of the 12 column configurations for Types 1 and 11 are shown in Tables 4.1 and 4.2, respectively. The Type 1 columns range from 1.2m (4 ft) diameter circular to 2.1 $\times$ 3.2m (7 $\times$ 10.5 ft) oblong configurations. The Type 11 columns range from 1.8m (6 ft) diameter circular to 2.1 $\times$ 3.2m (7 $\times$ 10.5 ft) oblong configurations. As mentioned, this report details analysis of several of the Types 1 and 11 configurations; however, the PEER testbed research groups selected the Type 1 bridge with column design option A as the testbed structure, designated Type 1A. This particular bridge design option has $4'$ diameter circular columns and $22'$ clear column heights measured from foundation to deck.

Based on the Caltrans comparative bridge costs (Division of Engineering Services—Cost Estimates Branch, 2007b), the new construction cost range for this type of bridge is \$150/SF to \$230/SF. Thus, the projected new cost of the bridge is between \$4.0M and \$6.2M including 10% mobilization costs. Without mobilization, these costs are \$3.7M and \$5.6M. The costs do not include quantities such as the approach slabs, slope paving, and retaining walls. More detailed (column and bridge type-specific) new cost estimates were made by escalating the 2003 costs developed in Ketchum et al. (2004) to a 2007 level.

4.1 BRIDGE DESIGN METHOD

Ketchum et al. (2004) describe a five-step process for designing the bridge configuration options:

1. A basic bridge design was developed, along with a suite of different column or bent designs that can potentially provide varying levels of seismic performance for that basic bridge design.
2. The seismic displacement capacity was evaluated for each column or bent design, using moment-curvature analysis and static push-over analysis.
3. The level of ground motion that would push the column to its displacement capacity was evaluated for each column design, by performing response spectrum analyses under various response spectra (ARS curves) that ranged from 0.1g to 1.0g PGA.
4. Capacity-protected items such as the foundation, bentcap, superstructure, etc., were designed by carrying out a plastic analysis of the bridge and applying SDC-required overstrength factors.

5. Cost estimates were determined by applying unit costs to quantity take-offs.

4.1.1 Superstructure Design

Ketchum et al. (2004) designed the bridges in compliance with Caltrans standards for "Ordinary Bridges" with weak-column strong-beam seismic behavior. The standards used for design included: Caltrans Bridge Design Specifications (BDS), April 2000 LRFD edition; Caltrans Memo to Designers (MTD); Caltrans Bridge Design Aids (BDA); Caltrans Bridge Design Details (BDD); and Caltrans Seismic Design Criteria (SDC), version 1.2, December 2001.

Structural analysis for the bridge designs were performed with SAP2000 3D models. The model used the cracked section properties for the column, uncracked properties for the superstructure, and foundation and abutment springs. The SDC acceleration response spectrum (ARS) curves assumed soil Type D for magnitudes (M_w) of 6.5, 7.25, and 8.0. Response spectrum analysis was performed using each ARS curve and peak ground accelerations (PGA) ranging from 0.1g to 1.0g in increments of 0.1g.

4.1.2 Column Design

The column designs considered circular and oblong columns. Columns are fixed at the base and top. The range of columns sizes for each bridge type were based on Equation 7.24 in the SDC

$$0.67 < \frac{D_c}{D_s} < 1.33$$

where D_c is the cross-sectional dimension of column in the direction of bending and D_s is the depth of superstructure at the bent cap. Type 1: Within the restrictions of those column dimensions and reinforcement limits of between 1–3% vertical steel, the bridge lateral force (Sa) resistance ranged from 0.44g to 2.4g. Type 11: Within the restrictions of those column dimensions and reinforcement limits of between 1–3% vertical steel, the bridge lateral force (Sa) resistance ranged from 0.43g to 2.3g.

The longitudinal reinforcement ratio (ρ) is limited by SDC Section 3.7 to a minimum of 0.01 and maximum of 0.04. However, based on previous experience, columns with $\rho > 0.03$ tend to be overly congested and difficult to construct. So, the columns used in the testbed are all designed in the range of $0.01 < \rho < 0.03$.

Table 4.1 Column design summary for Type 1 bridge.

Column type	Dimensions	Longitudinal Steel	Transverse Steel
1A	$4'$ circular	Bundled #10 total 28 (14 bundles)	#7 hoop @ $3.5''$
1B	$4'$ circular	Bundled #10 total 42 (21 bundles)	#8 hoop @ $3.5''$
1C	$5'$ circular	#11 total 18	#7 hoop @ $3.5''$
1D	$4' \times 6'$ oblong	#10 total 24	#6 hoop @ $5''$
1E	$4' \times 6'$ oblong	Bundled #10 total 48 (24 bundles)	#7 hoop @ $4.5''$
1F	$4' \times 6'$ oblong	Bundled #10 total 72 (36 bundles)	#7 hoop @ $3.25''$
1G	$5'$ circular	Bundled #11 total 36 (18 bundles)	#8 hoop @ $3''$
1H	$6'$ circular	#11 total 26	#8 hoop @ $3.5''$
1I	$7'$ circular	#11 total 36	#8 hoop @ $3''$
1J	$5'$-$6'' \times 8'$-$3''$ oblong	#11 total 36	#7 hoop @ $4''$
1K	$5'$-$6'' \times 8'$-$3''$ oblong	Bundled #11 total 72 (36 bundles)	#8 hoop @ $3.25''$
1L	$7' \times 10'$-$6''$ oblong	#11 total 58	#8 hoop @ $3.25''$

The lateral force of the column must be at least 10% of the tributary dead load P_{dl}. In past experience, Caltrans does not encounter spectral accelerations necessitating more than 20%. This provides a feasible range for lateral force resistance between $0.10P_{dl}$ and $0.20P_{dl}$

The displacement capacity of each column design option was evaluated using the SDC 4.1 three-part criteria. These criteria check the global displacements $\Delta_D < \Delta_C$, the target displacement demand ductility (μ_D), and the ductility capacity criteria $\mu_C > 3$ regardless of the actual demand ductility.

The column design options for the Type 1 and Type 11 bridge configurations are summarized in Tables 4.1 and 4.2.

4.1.3 Foundation Design

Ketchum et al. (2004) considered four foundation classes for the testbed bridge designs: H-piles, precast concrete piles, steel pipe piles, and cast-in-drilled hole (CIDH) shafts. For each class of piles, a typical configuration of the pile was selected (for example 24×0.5 in. steel pipe pile) along with a corresponding typical soil profile where such a pile may be employed. For example, the steel pipe piles were assumed to be founded on alternating layers of sand and clay with increasing density and bearing capacity.

However, for the purposes of the PEER testbed groups, a specific soil profile was developed for analysis. The profile was specifically chosen with a liquefaction-susceptible layer, and varying

Table 4.2 Column design summary for Type 11 bridge.

Column type	Dimensions	Longitudinal Steel	Transverse Steel
11A	$4' \times 6'$ oblong	Bundled #10 total 72 (36 bundles)	#7 hoop @ $5''$
11B	$6'$ circular	Bundled #11 total 52 (26 bundles)	#7 hoop @ $3.25''$
11C	$6'$ circular	Bundled #11 total 78 (39 bundles)	#8 hoop @ $3''$
11D	$7'$ circular	#11 total 36	#8 hoop @ $5.5''$
11E	$7'$ circular	Bundled #11 total 72 (36 bundles)	#8 hoop @ $2.75''$
11F	$8'$ circular	#14 total 32	#8 hoop @ $4.75''$
11G	$5'$-$6'' \times 8'$-$3''$ oblong	#11 total 36	#7 hoop @ $5.25''$
11H	$5'$-$6'' \times 8'$-$3''$ oblong	Bundled #11 total 72 (36 bundles)	#7 hoop @ $4.5''$
11I	$5'$-$6'' \times 8'$-$3''$ oblong	Bundled #11 total 108 (54 bundles)	#7 hoop @ $3.5''$
11J	$7' \times 10'$-$6''$ oblong	#14 total 40	#7 hoop @ $4.25''$
11K	$7' \times 10'$-$6''$ oblong	Bundled #14 total 80 (40 bundles)	#7 hoop @ $3.5''$
11L	$7' \times 10'$-$6''$ oblong	Bundled #14 total 120 (60 bundles)	#8 hoop @ $3.25''$

layer properties and depths between the left abutment and right abutment. The geotechnical testbed team at the University of Washington developed the profile and the details are contained in the corresponding testbed report (Kramer et al., 2008).

Given the site-specific profile developed for the testbed bridge (Type 1A), it was possible to design particular foundations for the piers and also the abutments. The 24×0.5 in. steel pipe piles were retained for both foundations; however, the analysis and ultimate dimensions and pile groups were based on the foundation analysis performed by the University of California, Berkeley, testbed team (Ledezma and Bray, 2008). In summary, the piles at the interior bents are $60'$ long, 60 ksi, 24×0.5 in. steel pipe piles in a 3×2 pile group. The piles at the abutments are $70'$ long, 60 ksi, 24×0.5 in. steel pipe piles in a 6×1 pile group.

4.2 PERFORMANCE GROUPS

The testbed bridge is broken down into performance groups (PGs) for each major bridge superstructure, substructure, and foundation component. Each performance group represents a collection of structural components that act as a global-level indicator of structural performance and that contribute significantly to repair-level decisions. Performance groups are not necessarily the same as load-resisting structural components. For example, non-structural components may also form a performance group, since they also suffer damage and contribute to repair costs.

The PGs generally correspond to things that are observable as a unit. Grouping bridge components into performance groups allows for more meaningful damage assessment than grouping by component. For example, knowing the relative displacement of a column might be more useful than knowing individual spiral deformation because the displacements better measure overall column performance. The notion of a performance group also allows grouping several components together for related repair work. For example, it is difficult to separate all of the individual structural components that comprise a seat-type abutment (shear key, back wall, bearings, approach slab, etc.) as they all interact during seismic excitation and their associated repair methods are coupled. Therefore, the "abutment" repair group incorporates the fact that repairs to the back wall require excavation of the approach slab. Relationships between the repair costs of multiple structural elements can be linked by bundling them into performance groups.

Performance groups also address the issue of potentially double counting related repair items. Some repair items require the same preparation work such as soil excavation. For example, both back wall repair and enlargement of an abutment foundation require at least 4 ft of excavation behind the back wall. If these repair items were in different performance groups, then double counting the excavation would be a problem. But, since these repairs are inside a single performance group, the repair quantities can be defined without overlap. Bundling these related repair methods within a performance group allows for independent consideration of each performance group.

The correlation between repair items from the performance groups can be handled at the demand model level in the PEER methodology. This allows for independent development of the decision models used in calculating repair cost. The spatial correlation of structural response measured during simulation will capture the correlation between damage and repair. Correlation effects enter only when summing repair quantities between different performance groups. Once the total material quantity moments (first and second probabilistic moments) are obtained, the repair quantities can be related through a unit cost function to the total cost of repair for the bridge. It should therefore be noted, that only spatially correlated demand is treated in this testbed; no additional correlation between discrete damage states is introduced.

The performance groups considered for the testbed bridge are:

1. Columns based on maximum displacement — 1 performance group per column

2. Columns based on residual displacement — 1 performance group per column
3. Deck/Superstructure — 1 performance group per bridge span
4. Abutment — 1 performance group per abutment
5. Bearings — 1 performance group per abutment including all bearings
6. Shear keys — 1 performance group per abutment including both external shear keys
7. Approach — 1 performance group per approach
8. Abutment piles — 1 performance group per abutment
9. Pile groups — 1 performance group per column

Therefore, a total of N_{PG} = 27 performance groups are utilized in this study.

4.3 STRUCTURAL MODEL

A modular three-dimensional nonlinear finite element bridge model was developed for all of the permutations of bridge Types 1 and 11. The PEER Center finite element platform OpenSees (*http://opensees.berkeley.edu*) was utilized. The model was created in a modular fashion to seamlessly allow the future addition of new structural elements and finite element models for soil and foundations. The baseline model and modules described in this report define a benchmark for comparisons to models that incorporate ground deformation (Kramer et al., 2008; Ledezma and Bray, 2008) or models with enhanced structural elements (Lee and Billington, 2008).

Different modules were developed for each of four different bridge components: deck, column, foundation, and abutment. Each module was designed to be interchangeable and independent of the other modules. Such a modular design of the bridge finite element model is reminiscent of class design in object-oriented programming. A diagram of the modules utilized for the bridges in this study is shown in Figure 4.4. The modular design depends on a central core file that describes the basic bridge geometry in terms of column-top and -bottom and deck-end nodes. Beyond this, each component initializes itself and creates instantiations of itself given the constraints of the core geometry. The element centerlines and lumped masses were placed at the center of mass of the deck cross section. Rigid offsets prevent the columns from deforming inside the deck.

For the purposes of this baseline study, several modules were created: a single deck module (Deck_PT_39), two column modules (CircularColumn and OblongColumn), four abutment modules (RollerAbutment, SimplifiedAbutment, SpringAbutment, and BreakOffAbutment), and three

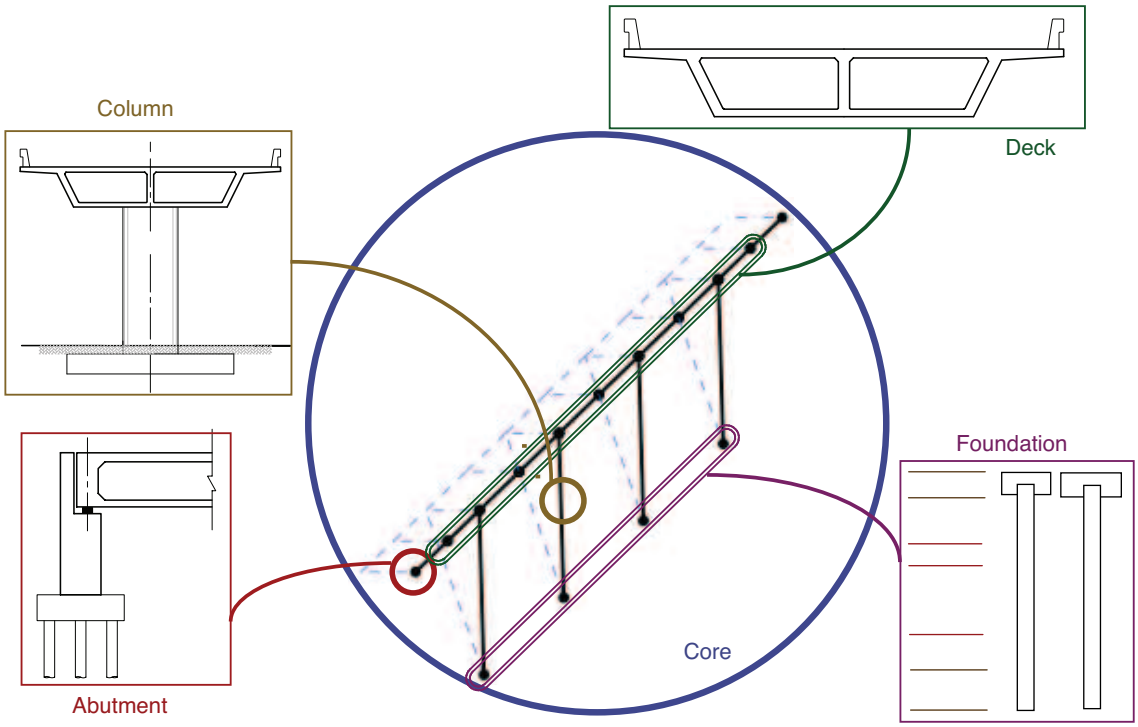

Fig. 4.4 Modular bridge analysis model.

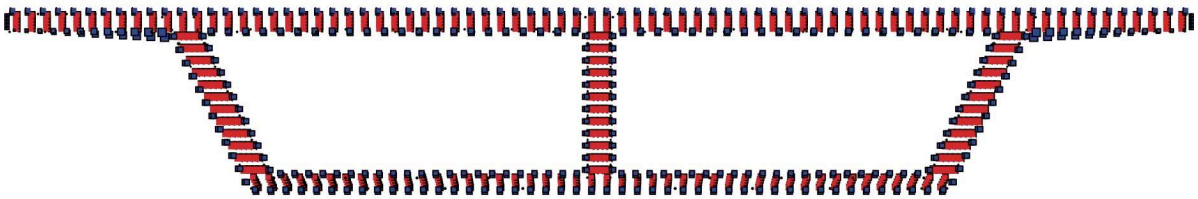

Fig. 4.5 Deck_PT_39 fiber cross section.

foundation modules (Fndn_fixed, Fndn_spring, and Fndn_UWsoil). All the results in this report are based on the fixed- and spring-foundation modules. The fixed-foundation module has all degrees of freedom at the column base restrained, while the spring foundation module allows for the assignment of any uniaxial constitutive model for each degree of freedom at the column base. Extension of the model to include full soil-structure-foundation interaction is detailed in the University of Washington report (Kramer et al., 2008).

4.3.1 Deck

The deck cross section is the same in both bridge Types 1 and 11. Therefore, only one deck module was necessary for this study. The post-tensioned two-cell box dimensions and reinforcement are detailed in Ketchum et al. (2004). In summary, the superstructure contains two layers of longitudinal reinforcing bars in the deck, soffit, and girders, additional mild steel in the deck and soffit over the bents, post-tensioned steel to provide a 31,100 kN (7,000k) pre-stressing force, and 34,475 kPa (5 ksi) concrete. A fiber cross section was generated to explicitly account for longitudinal reinforcing bar placement and unconfined and confined concrete effects (Fig. 4.5). A cover depth of 3.8 cm (1.5 in.) was used. The reinforcing steel was modeled by a Giuffre-Menegotto-Pinto strain-hardening model. It includes the Bauschinger effect as well as a strain-softening backbone beyond the ultimate steel stress. The concrete constitutive models used are based on the Kent-Scott-Park model for unconfined and confined concrete. Peak confined concrete strength values were determined according to the Caltrans SDC. Distributed loads to model the structural self weight were applied to the flexibility-formulated elements representing the deck. Axial pre-stressing forces were added to the deck ends. The deck torsional response about its longitudinal axis was assumed to be elasto-plastic with an initial elastic stiffness of $0.5GJ/L$.

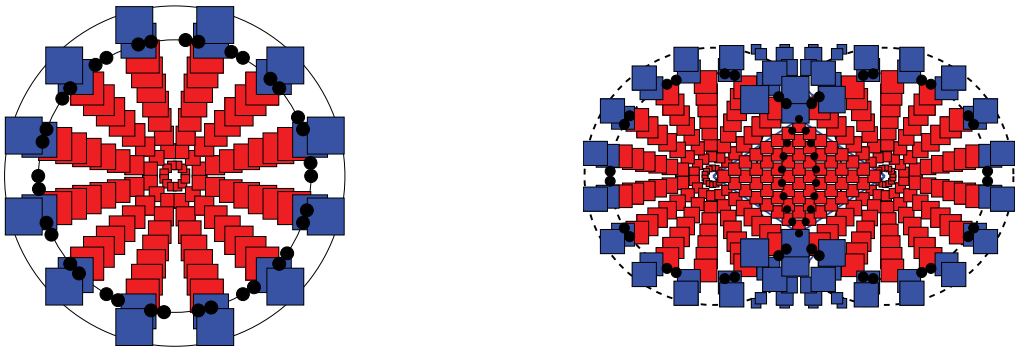

(a) (b)

Fig. 4.6 Cross sections for (a) CircularColumn and (b) OblongColumn.

4.3.2 Columns

Twelve different column configurations with transverse spiral reinforcement were designed for each of the Type 1 and Type 11 bridges, as shown in Tables 4.1 and 4.2. Both the circular and oblong configurations feature either evenly spaced perimeter longitudinal reinforcing bars or evenly spaced bundles of two longitudinal bars. The oblong columns also have additional mild longitudinal reinforcement in the interlocking spiral region. The fiber cross sections used in this study are shown in Figure 4.6 for the circular (CircularColumn module) and oblong (OblongColumn module) configurations, respectively.

The constitutive models used in the columns are the same as those used for the deck. However, the peak confined concrete compressive strength was obtained from the Mander concrete model. Shear stress versus shear strain relationships were aggregated with the column sections at all five integration points of the single flexibility-based beam-column element used to model the column. The values for the shear strength were obtained from the steel (V_s) and concrete (V_c) shear strength equations in the Caltrans SDC. Demand models and damage fragilities for the smallest circular column cross section for each of the two bridge types with a 2% longitudinal steel reinforcing ratio are presented in Chapter 7. This corresponds to column type A for bridge Type 1 and column type B for bridge Type 11. Fragilities for other column cross-sectional types were also computed. These other results are not discussed, however, since the major trends among all the columns were found to be well-represented by the Types 1A and 11B columns chosen here.

4.3.3 Abutments and Expansion Joints

The choice of abutment models has a profound effect on the response of the bridge, especially the end spans closest to the abutments. Therefore, four benchmark abutment modules were developed for the testbed bridge. The first is a simple boundary condition module (RollerAbutment) that applies single point constraints against displacement in the vertical direction and rotation about the deck longitudinal axis. The SimplifiedAbutment module is an implementation of the backbone longitudinal abutment force-displacement response of the Caltrans SDC Section 7.8. The transverse force-displacement response is based on a modification of this curve that includes no initial gap, plus wing wall effectiveness (C_L) and participation coefficients (C_w) of 2/3 and 4/3 obtained from Maroney and Chai (1994).

The remaining two modules (SpringAbutment and BreakOffAbutment) provide a more complex array of elements and materials that model abutment response in both the longitudinal and transverse directions. The longitudinal response is based on the system response of the elastomeric bearing pads, abutment back wall, abutment piles, and soil backfill material. The transverse response is based on the system response of the elastomeric bearing pads, exterior concrete shear keys, abutment piles, wing walls, and backfill material. The SpringAbutment can be used for any stand-alone analysis; however, the longitudinal-only implementation of this module that must accompany the soil-foundation mesh from the University of Washington (Kramer et al., 2008) is the BreakOffAbutment. A more detailed description of the components of the SpringAbutment module follows (the BreakOffAbutment has only the elements with a longitudinal component).

In the longitudinal direction, prior to impact (gap closure), the deck forces are transmitted through the elastomeric bearing pads to the stem wall, and subsequently the piles and backfill, in a series system. After gap closure, the superstructure bears directly on the abutment back wall and mobilizes the full passive back fill pressure. For this study, the gap was considered to be 10 cm (4 in.) and the abutment stiffness (K_{abut}) and ultimate strength (P_{bw}) were based on the same Caltrans SDC Section 7.8 backbone as the SimplifiedAbutment. Three bearing pads (one beneath each of the girders in the box) were used with assumed dimensions of 51 cm (20 in.) square and 5 cm (2 in.) thickness. The yield displacement and ultimate displacement of the bearings were assumed to be at 150% and 300% shear strain, respectively. For the dynamic coefficient of

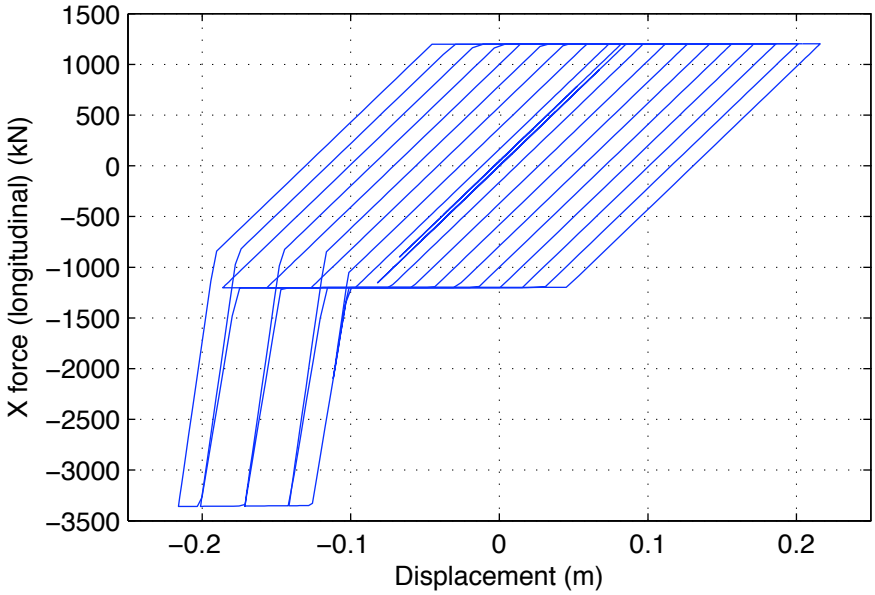

Fig. 4.7 SpringAbutment longitudinal response.

friction of 0.40 for neoprene on concrete, the bearing pads will fail in shear before sliding. The abutment stiffness and strength materials were placed in series with the bearing pads at each of the two extreme (transversely) bearing pad locations to account for rotation of the deck about the vertical bridge axis. The resultant force-displacement response of the abutment in the longitudinal direction (tension and compression) is shown in Figure 4.7.

In the transverse direction, the same (uncoupled with longitudinal direction) bearing pad models were used. The constitutive model of the exterior shear keys was derived from experimental tests (Megally et al., 2002). The ultimate shear key strength was assumed to be 30% of the deck dead load (according to SDC requirements). A hysteretic material with tri-linear response backbone curve (two hardening and one softening stiffness values) was used. The initial stiffness was a series-system stiffness of the shear and flexural response of a concrete cantilever with shear key dimensions. The hardening and softening branches each are assumed to have magnitudes of 2.5% of the initial stiffness. The transverse stiffness and strength of the back fill, wing wall and pile system was calculated using a modification of the SDC procedure for the longitudinal direction. Wing wall effectiveness (C_L) and participation coefficients (C_w) of 2/3 and 4/3 were obtained from Maroney and Chai (1994). These were used to modify the abutment stiffness (K_{abut}) and back wall

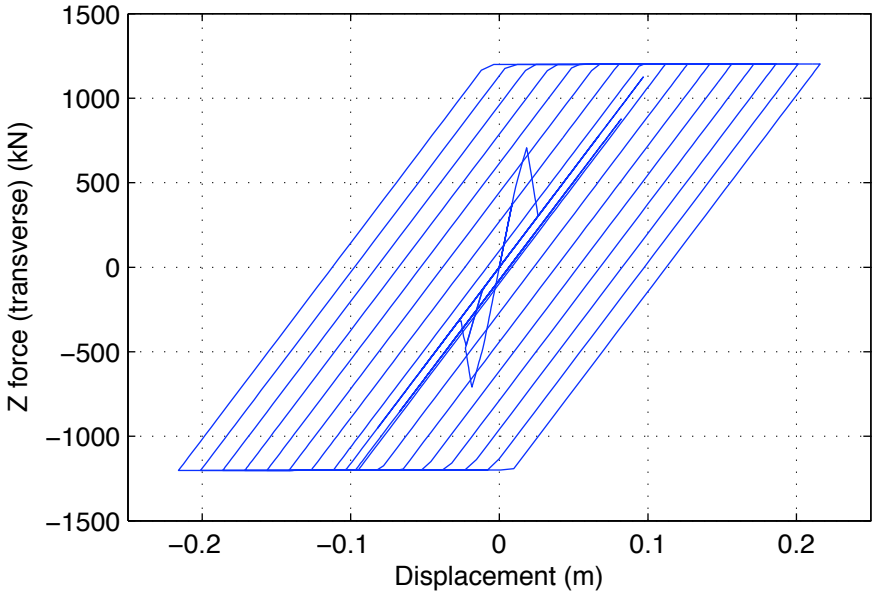

Fig. 4.8 SpringAbutment transverse response.

strength (P_{bw}) equations in conjunction with a wing wall length of half the back wall length (back wall usually 2–3 times wing wall dimension). The bearing pads and shear keys act in parallel. The combined bearing pad, shear key system acts in series with the transverse abutment stiffness and strength. The resultant force-displacement response of the abutment in the transverse direction is shown in Figure 4.8.

Vertical stiffness of the abutment was also included in the abutment model as the vertical stiffness of the bearing pads in series with the vertical stiffness of the trapezoidal embankment obtained from Zhang and Makris (2001). The abutment was assumed to have a nominal mass proportional to the superstructure dead load at the abutment. The response of the structure is sensitive to the magnitude of the abutment mass chosen; therefore, while the models used here are quite advanced, more research is needed to standardize modeling recommendations for Caltrans bridges.

4.3.4 Modal Analysis

Four separate fixed-foundation benchmark bridge models were generated in this report for each of the two bridge types. The abutment module and column type used in each of the four models is listed in Table 4.3. The initial elastic natural periods of the first two vibration modes are also listed

in the table. The fundamental mode shape (1st mode) is a transverse translation of the deck. The second mode shape is a longitudinal translation of the deck. These two mode shapes for bridge Type 11A are illustrated in Figure 4.9.

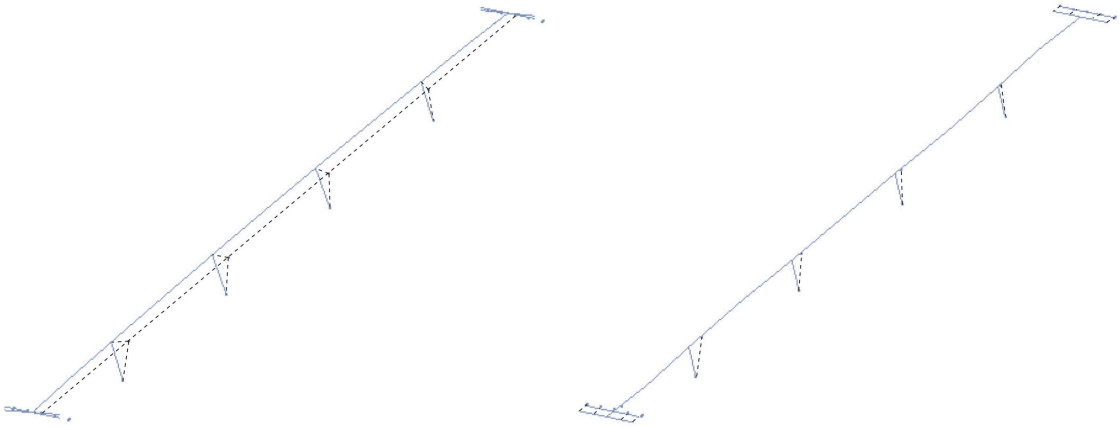

(a) (b)

Fig. 4.9 Bridge Type 11B mode shapes for (a) T_1 and (b) T_2.

Two additional bridge models were also generated in this study to investigate the effect of different foundation boundary conditions. Both foundation variants were made to bridge Type 1A only (smallest diameter circular column of bridge Type 1). The bridge model with translational and rotational springs located at the base of all the columns is listed as "Springs" in Table 4.3. The properties of the elastic springs were calibrated such that the displacement at the top of the column under the ultimate shear force in Ketchum et al. (2004) for the M_w=7.25 design event was equal to the footing displacement demand Δ_{foot} in the report. The final entry in Table 4.3 pertains to the complete soil-structure system created by the University of Washington group (Kramer et al., 2008). It is a 2D longitudinal-only implementation; therefore, both periods listed have mode shapes with longitudinal deformations. The natural periods were generated for the bridge-ground system; however, the soil nodes and pile-to-soil springs were constrained (no deformation).

Table 4.3 Bridge models and their vibration periods.

Bridge type	Column type	Abutment type	Foundation type	T_1 (sec)	T_2 (sec)
11	A (oblong)	Roller	Fixed	1.59	1.22
11	A (oblong)	Spring	Fixed	1.13	1.05
11	B (circular)	Roller	Fixed	1.53	0.85
11	B (circular)	Spring	Fixed	1.09	0.78
1	A (circular)	Roller	Fixed	1.09	0.55
1	A (circular)	Spring	Fixed	0.95	0.53
1	B (circular)	Roller	Fixed	1.06	0.53
1	B (circular)	Spring	Fixed	0.93	0.51
1	A (circular)	Spring	Springs	1.46	0.77
1	A (circular)	BreakOff	Soil mesh	1.92	1.51

5 Repair Methods

Selection of repair methods is a crucial step in computing the repair-related decision variable, repair cost ratios and repair time. Unfortunately, the selection of repair methods depends on the specific structure under investigation: even though many structures are similar, it is quite difficult to generalize across an array of such structures if for no other reason than because in a real-life situation different contractors would bid and execute the same job in different ways.

A selection of repair methods specific for the damage states of the benchmark bridges is presented in this chapter. This selection is made with the help of Caltrans maintenance engineers using a Caltrans database of typical repair techniques, unit costs, and unit quantities of work effort. While such data are specific for the benchmark bridges, the method for collection, organization, and use of repair-related decision data presented in this chapter can be generalized and used for performance-based evaluation of other structures.

5.1 DAMAGE STATES

Each performance group contains a number of discrete damage states (DS) corresponding to repair quantities needed for restoring the bridge. The damage states are numbered DS0, DS1, DS2, etc. with higher numbers indicating more severe damage. The DS0 damage state corresponds to the onset of damage when repair costs begin to accumulate. For analysis, the repair cost of the bridge is treated as $0 below the DS0 level of damage. Damage beyond DS0 is where repairs are needed and costs begin to accumulate. Slight damage less than DS0 is assumed to be insignificant and not needing repair.

Even though the defined damage states are discrete, the moment-based computation method assumes that a continuous range of damage exists between the discrete states. This assumption

allows for the closed-form computation of the PEER integral using the Fourway method. This computation method requires the definition of maximum possible repair quantities to define an upper limit to the quantities and costs. The upper limit is called DS∞, since it corresponds to the most severe possible damage state for the elements in a performance group. DS∞ usually corresponds to complete failure and replacement of all the elements in the entire performance group.

5.2 BRIDGE STRUCTURE

The components of the bridge structure considered are the columns, superstructure with deck, and bearings. In this report, the superstructure supported by the columns and the deck containing the roadway surface atop the superstructure are considered one structural element. The term "deck" is used interchangeably with "superstructure" to refer to this single structural element comprising the roadway surface plus superstructure.

5.2.1 Columns

The performance of the bridge columns is represented by two different types of performance groups tracking different engineering demand parameters (EDPs). The performance groups for the columns themselves are quantified in terms of maximum displacement and residual displacement. Specifically, the displacements are measured as the maximum square-root-sum-of-squares (SRSS) drift ratio and the residual SRSS drift ratio. The damage states for the maximum displacement performance groups are spalling, bar buckling, and column failure. The column damage and repair due to residual structure displacement are categorized in separate performance groups based on the EDP of residual SRSS column drift. The geotechnical limit states for the foundations under the columns are based on residual displacement of the pile cap and are detailed in the foundation section.

Maximum column drift

The columns are typical, spiral reinforced, concrete columns, with either single hoop circular or double hoop oblong cross sections. Much analytical and experimental data are available on the performance of these bridge columns. The availability of the data allows the use of not only EDP

Table 5.1 Maximum column drift damage states.

	Damage state limit description	Median drift ratio for limit state	λ	β
DS0	Negligible damage with initial cracking	Drift ratio associated with cracking moment M_{cr}	0.23	0.30
DS1	Cover concrete spalling	Δ_{sp} equation from Berry and Eberhard (2003)	1.64	0.33
DS2	Longitudinal reinforcing bar buckling	Δ_{bb} equation from Berry and Eberhard (2003)	6.09	0.25
DS3	Column failure	Δ_{ff} equation from Mackie and Stojadinović (2007b)	6.72	0.35

Table 5.2 Bar reinforcement estimates.

Element description	Steel weight per unit volume
Deck slab on prestressed or steel girders	134 kg/m^3
Bent caps	90 kg/m3
Single column bents	268 kg/m^3 (170–324 variation)
Piers and walls of simulated closed end abutments	48 kg/m^3
Footings	90–119 kg/m^3
End diaphragm abutments	48 kg/m^3

information, but also the addition of specific performance levels on the DM level. Four damage states and their median drift ratios are defined for the column in Table 5.1. The repair quantities and repair method descriptions for these damage states are summarized in Table 5.3.

Quantities for bar reinforcement are estimated based on the gross volume of concrete and the estimated rebar density data from BDA 11-5 (Table 5.2). For the columns, this density estimate is 268 kg/m^3. This value accounts for both the longitudinal and transverse steel in the column.

It is expected that the repair cost will increase slightly with column repair and then jump as soon as a column needs replacement. For replacement of a single column for bridge Type 1A, the estimated repair cost is about \$807,300, which is between 23% and 33% of the total construction cost.

For DS1 with the onset of spalling, the amount of cracks to repair is estimated at 44 LF, which is equal to 2 times the height of the Type 1A column. The volume of concrete to be removed and patched is obtained from the cover depth plus 1″ additional depth times 10% of the column height. For DS2, repeat with 4 times the height for 88 LF of cracks and 25% of height for removing and

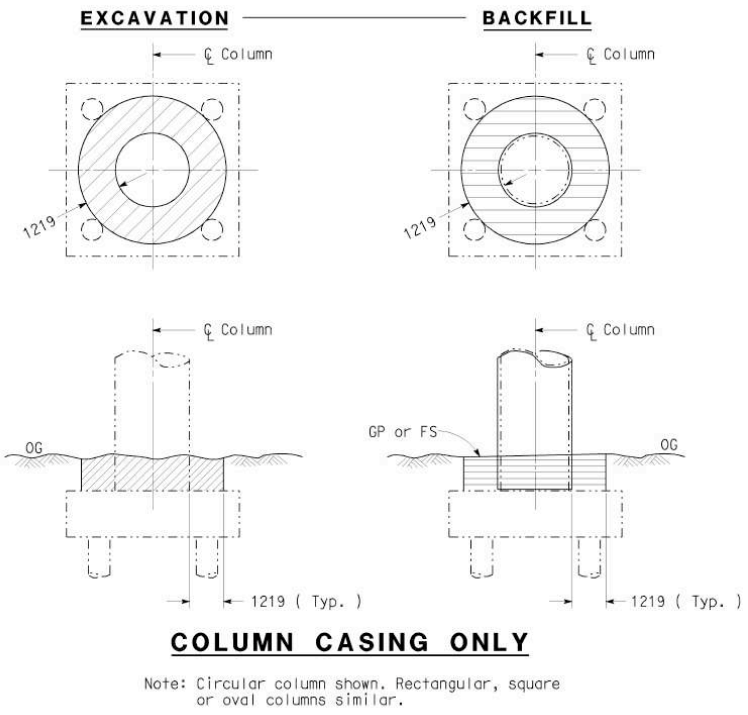

Fig. 5.1 Pay limits for steel column casing excavation and fill (Caltrans detail sheet XS7-310).

patching concrete.

For DS3, the repair action is column replacement. Since the entire column is replaced, there are no concrete or steel patch repairs for this damage state. The replacement column has the same amount of structural concrete and reinforcing steel as the original column. To replace the column, temporary superstructure support needs to be provided. The amount of temporary support is estimated based on the deck area requiring support. The deck area requiring support is estimated by the tributary area from the span on each side of the column. This quantity is different for the columns at the ends and in the middle. The portion of the column embedded below grade is excavated and backfilled. The depth of embedment was taken as $3'$ and the plan area was estimated based on a $4'$ concentric circle surrounding the column diameter, as shown in Figure 5.1.

Residual column drift

The column damage states based on residual column drift Δ_{res} are summarized in Table 5.4. When the residual displacement of the column is large enough to produce a significant visual or struc-

Table 5.3 Repair items: maximum column drift damage states.

Damage State	Repair Item	Unit Computation
DS1	*Seal cracks and minor removal and patching of concrete*	
	Epoxy inject cracks (LF)	2 × column height
	Repair minor spalls (CY)	10% × (surface area) × (cover + 1″)
DS2	*Seal cracks, major patching*	
	Epoxy inject cracks (LF)	4 × (column height)
	Repair minor spalls (CY)	25% × (surface area) × (cover + 1″)
DS3	*Replace column*	
	Structural concrete, bridge (CY)	Gross column volume = (column height × (column diameter)
	Bar reinforcing steel, bridge (LB)	(column gross volume) × (rebar weight estimate based on BDA 11-5)
	Temporary support, bridge (SF)	Tributary length × (deck width)
	Structure excavation (CY)	3′ embedment plus 4′ concentric circle around column
	Structure backfill (CY)	Same as structure excavation

tural effect, then the typical repair is to enlarge the column so that it appears straight. Often, visual appearance is very important for public perception of bridge safety, so repairs are often executed even when there is no serious structural deficiency. Column enlargement is usually done by doweling into the existing column and casting reinforced concrete around it, or providing an enlarged cross section by adding a steel column jacket. The cost of doweling can be significant for large numbers of dowels. It is assumed that all column enlargements are accompanied by a steel jacket in this study. It is assumed that a certain amount of rebar will added to replace buckled bars before installing a jacket. A weight of 5% of the total column rebar weight was assumed.

The column casing item is for steel jacketing of the column. The different classes of steel jackets are described in Caltrans Bridge Standard Detail Sheet XS7-010e. For the Type 1A bridge, a casing thickness of 1/4″ is used corresponding to the column diameter being less than 4′-4″. The jacket is full-length and assumed as class P/F column. The outside diameter of jacket is 4″ greater than nominal outside diameter of column. To install the jacket, the amount of column embedded below grade needs to be excavated and subsequently backfilled. The depth of embedment was taken as 2′ and the plan area was estimated based on a 4′ concentric circle surrounding the column diameter, as shown in Figure 5.1.

Table 5.4 Residual column drift damage states.

	Damage State Description	λ	β
DS0	Onset of significant damage	0.50	0.30
DS1	Thicken pier and install jacket	1.25	0.40
DS2	Re-center column	2.00	0.40
DS3	Column failure (same as for max drift)	6.72	0.35

Table 5.5 Repair items: residual column drift damage states.

Damage State	Repair Item	Unit Computation
DS1	*Replace buckled reinforcement, install steel column casing, excavate and backfill where necessary*	
	Column steel casing (LB)	Steel casing volume calculated using: Outside diameter = (column diameter) + 4″, and thickness = 0.25″
	Bar reinforcing steel, bridge (LB)	5% × (total rebar weight)
	Temporary support (SF)	1/2 Tributary length × (deck width)
	Structure excavation (CY)	2′ embedment plus 4′ concentric circle around column
	Structure backfill (CY)	Same as structure excavation
DS2	*Re-center column(s)*	
	Re-center column (EA)	Per column. No cost associated with this item yet.
DS3	*Column replacement (coincides with the DS from Table 5.3)*	

The addition of column flexural strength due to the jacket leads to the necessity of a footing enlargement to prevent the failure mode moving into the foundation. Therefore, temporary shoring is required for most work performed on the column and foundations. When shoring is done, it is usually over a whole segment instead of just over a small localized portion of the bridge. However, the foundation repairs are separated into the column foundation performance groups, and are discussed there. Correlation between performance groups is maintained in the overall analysis; therefore, the foundation and column repairs do not occur independently.

There is an additional damage state (DS2) in Table 5.4 for re-centering the column. This is a placeholder value in this simulation and is not used. However, it allows for further studies on the effect of mitigating residual displacement through enhanced technologies if an accurate repair method and unit cost/production rate are paired with this DS.

Table 5.6 Deck damage states.

	Damage State Description	λ	β
DS0	2% of spalling strain	0.00402	0.40
DS1	25% of spalling strain	0.00425	0.40
DS2	50% of spalling strain	0.00450	0.40

Table 5.7 Deck surface areas by segment.

	Whole deck	25% deck	50% deck
Interior	5850 SF	1462.5 SF	2925 SF
Exterior	4680 SF	1170 SF	2340 SF

5.2.2 Deck and Superstructure

The link between EDPs and damage is currently an arbitrary linear relationship between the maximum concrete strain in the deck and the percentage of deck area that needs to be refinished. The damage states are defined in terms of percentages of the concrete spalling strain. None of the current simulations has produced spalling at any depth in the deck. Recorders are placed at both the deck and soffit flanges of the deck, at both extreme transverse locations. A linear strain profile is calculated for each flange location and extrapolated to a location 6″ above the actual structural surface to account for roadway and/or overlay. The damage states are summarized in Table 5.6.

The repair methods for the deck damage states are defined as the percentage of the deck surface that needs refinishing for crack repairs. DS1 calls for refinishing 25% of the deck with methacrylate, and DS2 calls for 50% of the deck. Deck surface areas for repair are given in Table 5.7.

The methacrylate overlay method is chosen to repair the deck cracks because small cracks are more probable than large cracks for strains less than the spalling strain. Repairing small deck cracks with methacrylate involves three stages and different cost items: (1) Cleaning is priced per SF of deck; (2) Furnishing methacrylate is priced per GAL estimating deck area coverage at 90 SF/GAL; (3) Treating the deck with methacrylate is priced per SF of deck. Large deck cracks would still be repaired using epoxy injection. The deck repair amounts are given in Table 5.8.

Table 5.8 Deck repair items.

Damage state	Repair Item	Unit computation
DS1	Clean deck for methacrylate (SF)	25% $\times$ (deck area)
	Furnish methacrylate (GAL)	25% $\times$ (deck area) / (90 SF/GAL)
	Apply methacrylate (SF)	25% $\times$ (deck area)
DS2	Epoxy inject cracks (LF)	50% $\times$ (deck length)
	Clean deck for methacrylate (SF)	50% $\times$ (deck area)
	Furnish methacrylate (GAL)	50% $\times$ (deck area) / (90 SF/GAL)
	Apply methacrylate (SF)	50% $\times$ (deck area)

Table 5.9 Bearing damage states.

	Damage State Description	λ	β
DS0	Bearing yield	0.076	0.25
DS1	Bearing failure	0.152	0.25

5.2.3 Bearings

The bearing is what the deck rests on in a seat-type abutment or an in-span hinge; however, there are no intermediate hinges in the bridges considered in this study. The bearing is typically made of elastomeric material (PTFE) according to the Caltrans standard specifications. The bearings are manufactured to undergo large displacement demands without degrading strength. Therefore, it was decided to provide only a single damage state that corresponds to the shear failure of the bearing (Table 5.9). The EDP used is the maximum absolute bearing displacement (maximum of either the longitudinal or transverse displacement).

The typical displacement limit on shear failure for a bearing can be as high as 350% shear strain for the final tearing limit. From discussions with Ketchum, the bearings are mostly tested to at least 200% strain, but as soon as there is any indication of problems, Caltrans will likely recommend complete replacement. The median displacement at failure was set to 300% shear strain.

There is one bearing underneath each of the girders at the right and left abutment. For the Types 1 and 11 testbed bridges both with a 2-cell box, there are a total three bearings on each abutment. There is no intermediate damage state between bearing failure and functional bearings. Since the cost of bearings is small compared to the mobilization work, it is almost always better to replace all the bearings at once. Note, however, that the simulation model does not take into account any

sliding friction effects after bearing failure if the bearings are damaged and repaired independently.

5.3 FOUNDATIONS, ABUTMENTS, AND APPROACHES

This section covers the foundations for both the columns and abutments (piles and pile caps). In addition, deformations and consequences derived from the embankments are addressed. The performance groups considered here are: Column Foundation, Abutment Foundation, Shear Key, Abutment, and Approach.

5.3.1 Column Foundations

Each column foundation consists of the piles and pile cap. Both of these components comprise the performance group for column foundations. The EDP for this performance group is the residual pile cap displacement. Only DS0 and DS1 are defined for this performance group with DS1 corresponding to enlarging the foundation and adding additional piles around the perimeter (Table 5.10). The damage state λ values are not the same at each column due to differences in the soil layer properties along the bridge and the expected depths of the liquefiable layers (Ledezma and Bray, 2008). The values of displacement in the table were calculated based on the addition of the elastic and plastic pile displacements between two fixed-fixed end conditions separated by a distance detailed further in Ledezma and Bray (2008). The add pile threshold was selected to have a target displacement ductility of 3 while a displacement ductility of 5 was selected for enlarging the pile cap and adding piles.

The repair method associated with DS1 is to enlarge the pile cap and add additional piles surrounding the existing ones. When the pile groups are expanded, they are typically expanded by going completely around in both dimensions. So, the column piles would be expanded from a 3×2 group into a 5×4 group. The enlarged pile cap is tied to the existing cap by drilling into the existing cap and placing dowels.

The columns for bridge Type 1A specifically are supported by pile caps on groups of 3×2 steel pipe piles. The piles were designed for the bridge loads by Ledezma and Bray. Pile dimensions are a 3×2 pile group, $60'$ length, $24''$ diameter, $1/2''$ thick, spaced at three diameters on center. The pile cap dimensions were obtained from the original Ketchum report for a 3×2 pile group under a 4 ft column. The long and short pile cap dimensions are $15'$ and $10'$, respectively. The pile cap

Table 5.10 Column foundation damage states.

	Damage State Description	λ	β
DS0	Add pile threshold	0.29 (col1)	0.40
		0.41 (col2)	0.40
		0.68 (col3)	0.40
		0.83 (col4)	0.40
DS1	Enlarge pile cap and add piles	0.49 (col1)	0.40
		0.68 (col2)	0.40
		1.15 (col3)	0.40
		1.41 (col4)	0.40

Table 5.11 Column foundation repair items.

Damage state	Repair Item	Unit computation
DS1	Structure excavation (CY)	Volume = existing dimensions + 2 $\times$ spacing + 2′ clearance
	Structure backfill (CY)	Volume = new dimensions + 2′ clearance
	Temporary support, bridge (SF)	Tributary area of deck on both sides of column
	Structural concrete, footing (CY)	Volume of enlargement increased by (2 $\times$ spacing) in each dimension
	Bar reinforcing steel (CY)	105 kg/m^3 $\times$ additional concrete volume
	Drill and bond dowel (LF)	(area of existing pile cap) / (4 dowels/SF) $\times$ (16″ per dowel)
	Furnish steel pipe pile (LF)	(No. piles) $\times$ (pile length)
	Drive steel pipe pile (EA)	(No. piles)

thickness is 3.25′ and the steel reinforcing ratio is 3.65%.

The amount of steel required in the pile cap can be estimated based on the range of 90–119 kg/m^3 (Table 5.2). The middle of this range is about 105 kg/m^3 and this number is used to estimate the amount of reinforcing steel used in repairs.

5.3.2 Abutment Foundations

The abutments designs are documented in Ledezma and Bray (2008). The abutment pile group dimensions are a 6×1 pile group, 70′ in length, with the same nominal steel pipe pile sections (24″×0.5″). Center-to-center spacing at the abutment is 4 pile diameters (8′). Based on the design for earth pressure loads the thickness is taken to be 3′ and nominal dimensions of 36′ by 10′ selected

Table 5.12 Abutment foundation damage states.

	Damage State Description	λ	β
DS0	Add pile threshold	0.29 (left)	0.40
		0.83 (right)	0.40
DS1	Enlarge foundation and add piles	0.49 (left)	0.40
		1.41 (right)	0.40

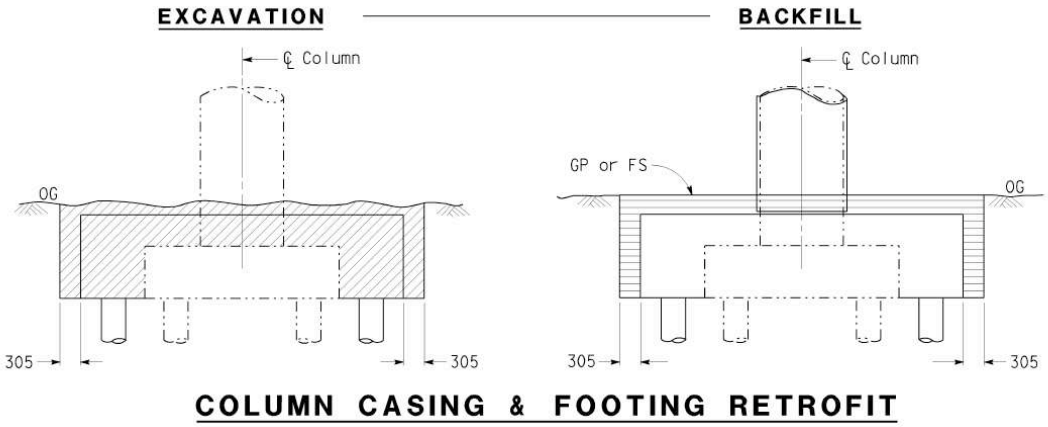

Fig. 5.2 Caltrans XS7-310 excavation and backfill for footing retrofit.

based on the size of a 6×2 pile group in Ketchum et al. (2004).

The abutment foundations consist of the piles, pile cap, and attached wing walls. These components comprise the performance group for abutment foundations. The EDP for this performance group is the residual pile cap displacement. As with the column foundation PG, the EDP limits for the abutment piles were determined from the elastic and plastic displacement of the piles over an expected depth of the liquefibale layer. Only DS0 and DS1 are defined for this performance group with DS1 corresponding to excavation and backfilling, enlarging the foundation, adding additional piles around the perimeter, and replacing the wing wall (Fig. 5.2, Table 5.12). The damage state λ values are not the same at the right and left abutment due to differences in the soil layer properties and depths along the bridge (Kramer et al., 2008; Ledezma and Bray, 2008).

The enlarged pile cap is attached to the existing pile cap through bonded dowels. Holes are drilled about 16″ deep and rebar dowels are inserted and bonded. Based on previous Caltrans repair plans, dowels are assumed to be distributed one for every 4 SF of horizontal contact area.

Table 5.13 Abutment foundation repair items.

Damage state	Item	Unit computation
DS1	Structure excavation (CY)	Volume based on (existing dimensions) + 2 × spacing + 2′ clearance
	Structure backfill (CY)	Volume based on (new dimensions) + 2′ clearance
	Temporary support, bridge (SF)	Tributary area on either side (int/ext span, or int/int span)
	Structural concrete, bridge (CY)	Wing wall volume
	Structural concrete, footing (CY)	Volume of enlarged foundation increased by (2 × spacing) in each dimension
	Bar reinforcing steel, bridge (CY)	54 kg/m^3 × (additional bridge concrete volume)
	Bar reinforcing steel, footing (CY)	105 kg/m^3 × (additional footing concrete volume)
	Drill and bond dowel (LF)	(area of existing pile cap) / (4 dowels/SF) × (16″ per dowel)
	Furnish steel pipe pile (LF)	(No. piles) × (pile length)
	Drive steel pipe pile (EA)	(No. piles)

Table 5.14 Abutment damage states.

	Damage State Description	λ	β
DS0	Onset of repairable damage	0.051	0.25
DS1	Replace joint seal assembly	0.102	0.25
DS2	Replace joint seal assembly, repair back wall	0.111	0.30
DS3	Replace joint seal assembly, replace back wall, replace approach slab	0.138	0.30

5.3.3 Abutments

The abutment performance groups include several components: expansion joints, back walls, and the approach slabs. All of these components are lumped together in a single performance group because they are all connected and have related repair methods. The damage states defined for the abutment performance group are given in Table 5.14. The EDP for this performance group is the maximum longitudinal relative displacement between the abutment and deck end. The use of a purely longitudinal EDP separates the transverse abutment components into a separate PG. The repair items are described in Table 5.15.

Table 5.15 Abutment repair items.

Damage State	Repair Item	Quantity
DS1	*Replace joint seal assembly*	
	Joint seal assembly (LF)	(deck width)
	Structural concrete, bridge (CY)	(blockout volume) = 2 × (H × B × deck width)
	Bar reinforcing steel, bridge (LB)	(blockout volume) × 48 kg/m^3
	Bridge removal, portion (CY)	(blockout volume)
DS2	*Replace joint seal assembly*	
	Joint seal assembly (LF)	(deck width)
	Structural concrete, bridge (CY)	(blockout volume) = 2 × (H × B × deck width)
	Bar reinforcing steel, bridge (LB)	(blockout volume) × 48 kg/m^3
	Bridge removal, portion (CY)	(blockout volume)
	Repair back wall	
	Epoxy inject cracks (LF)	2 × (backwall height)
	Repair minor spalls (SF)	10% × (back wall height) × (deck width)
	Structure excavation (CY)	(deck width) × (deck depth) × 1′
	Structure backfill (CY)	(deck width) × (deck depth) × 1′
DS3	*Replace joint seal assembly*	
	Joint seal assembly (LF)	(deck width)
	Structural concrete, bridge (CY)	(blockout volume) = 2 × (H × B × deck width)
	Bar reinforcing steel, bridge (LB)	(blockout volume) × 48 kg/m^3
	Bridge removal, portion (CY)	(blockout volume)
	Replace back wall	
	Structural concrete, bridge (CY)	(back wall volume) × 54 kg/m^3
	Bar reinforcing steel, bridge (LB)	
	Structure excavation (CY)	(deck width) × (deck depth) × 4′
	Structure backfill (CY)	(deck width) × (deck depth) × 4′
	Bridge removal, portion (CY)	(back wall volume)
	Replace approach slab	
	Structural concrete, approach slab (CY)	(approach slab volume)
	Aggregate base, approach slab (CY)	1/2 × (settlement due to 1/62.5 gradient) × (approach slab area)
	Approach slab removal (CY)	(approach slab volume)

Expansion joint

The expansion joint is the longitudinal gap separating the bridge deck from the back wall of the abutment. The joints are typically sealed with some kind of rubber-like material. The size of the joint gap is based on the movement rating of the bridge and typically ranges between 1/2″ and 4″. The movement rating of the bridge can be calculated based on the worksheet in MTD 7-10. A joint seal is used for movement ratings (MR) less than 2″, and a joint seal assembly is used when MR $>$ 2″. For the Type 1A bridge, it is assumed that we have MR = 4″ with a joint seal assembly.

The calculation of the expansion joint performance is complicated by the fact that joint damage is highly correlated with damage elsewhere in the abutment and back wall. So, it makes sense to include the expansion joint in a single performance group with the other related elements.

A joint seal assembly repair is more than the joint seal alone because the assembly requires a concrete blockout on both sides of the expansion joint. One blockout is in the approach slab-back wall connection and the other is in the deck. From the MTD 10-7, a 4″ MR has a concrete blockout with dimensions H = 12″ and B = 10″ (Fig. 5.3). The reinforcing steel quantity does not include the possibility of reusing existing steel. The required steel quantity is estimated using the blockout volume and the BDA estimate of 48 kg/m^3 steel per volume of concrete abutment wall.

No separate item is needed for cleaning the expansion joint, because the quantities needed for replacement include the cost of cleaning. There is also no separate item for removing damaged concrete, since the cost for removal is included by contractors in the other repair quantities.

Back wall

For newer Caltrans abutments and according to large-scale tests at San Diego, the abutment back wall will be designed to break/shear off. It is assumed that no damage occurs to the stem wall other than the portions of concrete that need to be chipped out when repairing the back wall and other related elements (see Fig. 5.4).

The back wall is on the back face of the abutment, atop the stem wall. The gap between the back wall and the bridge deck is filled with the joint material. The back wall is engaged only once the gap closes. If the back wall is broken, it needs to be replaced with concrete and reinforcement as with the shear key, and it also requires some earthwork. For the time being, it is assumed there is a minor damage state for the back wall as well that corresponds to a 0.5% drift ratio (measured

Movement Rating	Blockout Width (*B*)	Depth (*H*)
2½" to 4"	1'-0"	10"
6" (2 cells)	1'-6"	14"
9" (3 cells)	2'-0"	15"
12" (4 cells)	2'-6"	16"
15" (5 cells)	2'-6"	16"

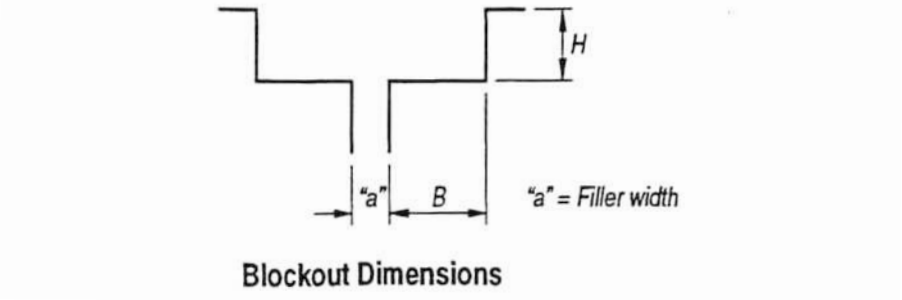

Blockout Dimensions

Fig. 5.3 Blockout dimensions (Caltrans MTD 7-10 1994, p. 10).

at the top of the back wall). NCHRP gives a limit state of 2% of the deck height for longitudinal movement into the abutment fill. The suggested design improvements are to increase the gap between the superstructure and abutment back wall, stiffen the interior supports, and increase the amount of fill that is engaged.

The back wall is designed to act as a fuse that prevents damage to the rest of the abutment. So, the capacity of the back wall should be less than that of the rest of the abutment it is attached to. The NCHRP LRFD draft specifications give an illustration of this design. Some tests on back walls were run at UCSD; however, specific results from these tests have not yet been incorporated into the analytical bridge model.

As with the shear keys, the amount of concrete required for patching was assumed to be 10% of the volume of concrete required to replace the back wall. The length of the wall was taken as the width of the deck plus about 6′, since the back wall is probably a little wider than the box. The height is assumed to be the same as the deck height, although this is not strictly correct because of the bearing height (see Fig. 5.4). The thickness is assumed to be 1′. The volume of earthwork required for excavation and backfill were obtained from the same surface area of the wall, but considering a 1′ extension into the back fill.

Approach slab

The approach slab lies over the top of the soil behind the back wall. Its purpose is to ensure a smooth approach to the bridge deck. Problems with soil settlement, displacement, etc., could cause the approach to become uneven. The approach slab is tied to the bridge using rebar dowels and has a special detail at the expansion joint to accommodate the joint assembly blockout. The failure of the slab will be tied to the failure of the back wall and other components in the abutment.

Hoppe (1999) gives some insight into the approach slabs. Particularly, there is some California-specific information from a survey on approach slab practices among the states. In California, the typical slab dimensions are 30′ long and 12″ thick with a width that runs curb-to-curb. Slabs are doweled or tied to the back wall. Drainage of the backfill is provided by plastic pipes and filter fabric with geocomposites. The design purpose for the slab is for smooth ride only.

In the approach performance group, it is assumed that when the back wall is impacted then there will be some slope settlement due to the active earth pressure from the transverse displacement of

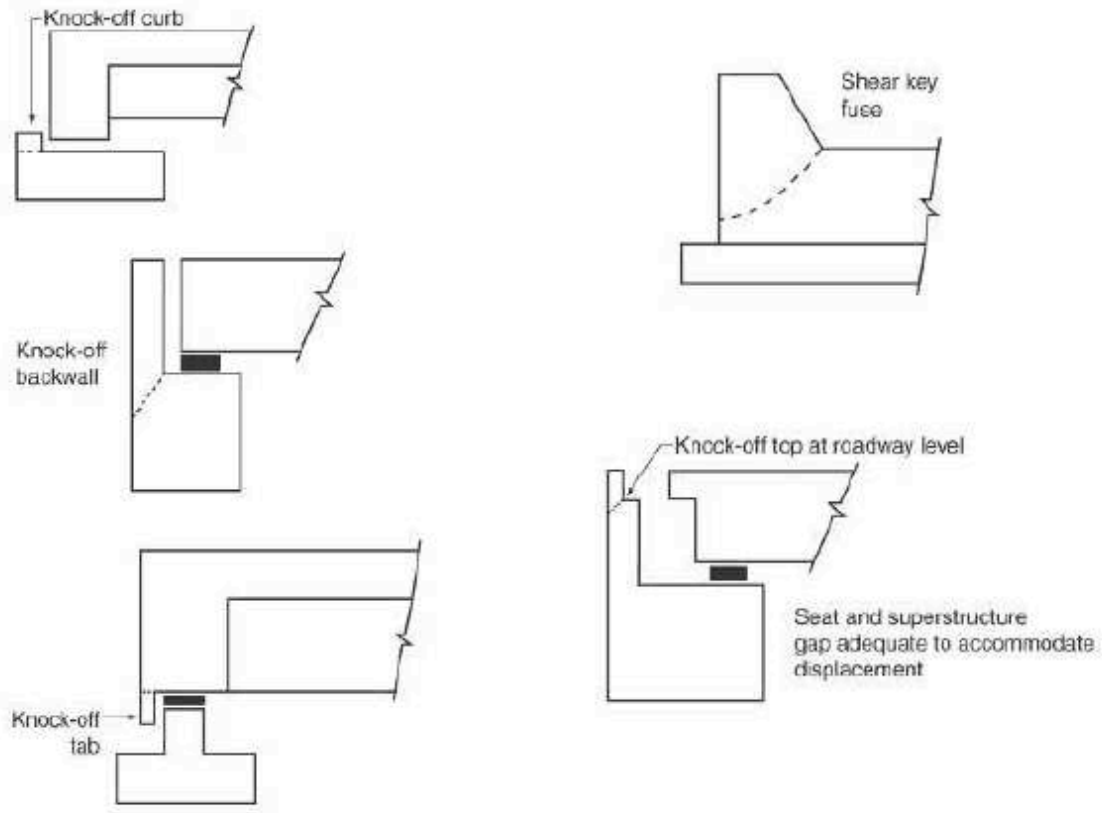

Figure C2.5.6-4Methods of Minimizing Damage to Abutment Foundation

Fig. 5.4 Back wall design (ATC/MCEER Joint Venture, 2002).

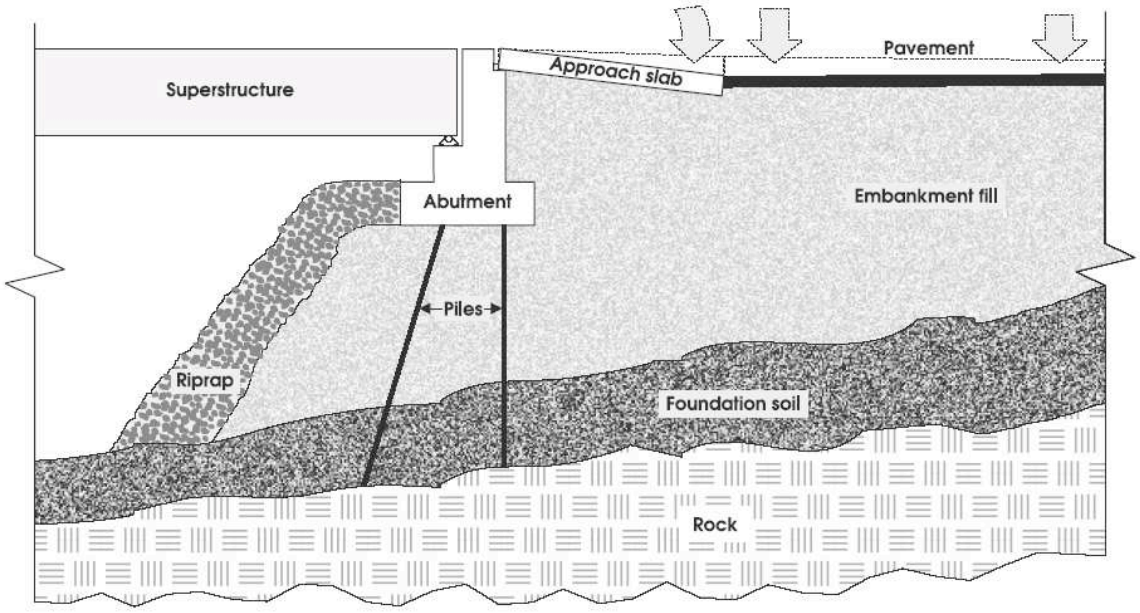

Fig. 5.5 Bridge approach settlement (Hoppe, 1999).

the bridge superstructure. The slab is a standard 30′ long and 39′ wide across the entire deck width having an area of 1170 SF. The replacement requires structural concrete particular to the approach slab in addition to an aggregate base beneath the slab to create a proper grade.

5.3.4 Shear Keys

The shear keys prevent transverse displacement under low to moderate demand levels. On the abutment, the bridge sits on the bearings which are positioned atop the stem wall. In the transverse direction there are exterior shear keys that limit both service-level and excessive transverse displacements. However, the shear keys are designed in a way that they will also shear (break) off, similar to the back wall. Since the shear keys engage under all transverse demands, they are designed as fuses. There are no internal shear keys in the testbed bridge. Interior shear keys are typically seen only in older bridges, and are uncommon in new construction.

The EDP used for the shear key performance groups is maximum force in the shear keys (Table 5.16) . The damage state DS1 is defined by the first yield of the shear key. DS2 is defined by the ultimate strength/failure of the shear key. The hysteretic properties of the shear keys were taken from tests at UC San Diego (Bozorgzadeh et al., 2005).

Table 5.16 Shear key damage states.

	Damage State Description	λ	β
DS0	Elastic limit	370	0.30
DS1	Concrete spalling	493	0.30
DS2	Shear key failure	740	0.30

Table 5.17 Shear key repair items.

Damage State	Repair Item	Quantity
DS1	Repair minor spalls (CY)	10% × (shear key volume)
	Epoxy inject cracks (LF)	2 × (shear key height) × (number of shear keys)
DS2	*Replace shear keys*	
	Structural concrete, bridge (CY)	Concrete volume = (shear key height) × (shear key depth) × (top width - bottom width) / 2
	Bar reinforcing steel, bridge (LB)	48 kg/m^3 × (concrete volume)
	Bridge removal, portion (CY)	Concrete volume

The repair amounts for the shear keys are in Table 5.17. The volume of concrete required to replace the shear key was estimated based on the shear key thickness at the top and an equivalent square area obtained from the shear key height and average width at the top of deck and bottom of superstructure. For the minor damage state, it was assumed that 10% of the concrete would need to be removed and patched. The weight of reinforcing steel required to replace the shear key was obtained from the BDA estimate of 48 kg/m^3 for abutments.

5.3.5 Approaches

The bridge approach performance groups represent the roadway that leads up to the beginning and end of the bridge. Large vertical offsets due to embankment and abutment settlements could make the bridge approach too dangerous to travel over at high speeds. The EDP for this performance group is the residual vertical displacement at each abutment. This is related to the approach slab; however, the repair methods for this performance group do not involve modifications to the approach slab itself.

The approach settlement is repaired by either a simple repair with one thick placement of asphalt concrete (AC) to quickly restore the grade, or by a more extensive repair involving larger

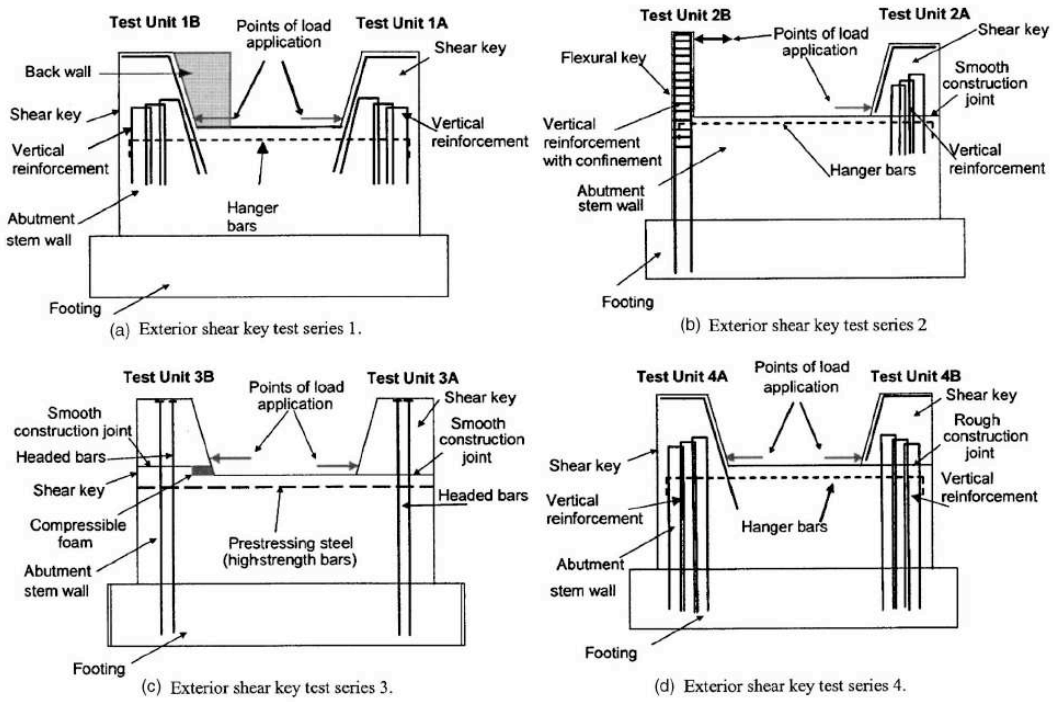

Fig. 5.6 Shear key diagrams (Bozorgzadeh et al., 2005).

amounts of AC in addition to mudjacking under the approach slab. Regrading the embankment and abutment would be done only if the settled section has a relatively long length on the order of 100′, but this is unlikely for the testbed bridge. Thick AC placement is usually the better option for shorter settled sections like the testbed bridge because it can be completed relatively quickly with minimal traffic disruption. This speed factor often makes AC alone a better choice than a total approach rehabilitation with regrading and approach slab replacement, even if a very large amount of AC is needed up to about 36″ thick. High bridge traffic demand necessitates that speed often dominates upfront cost in making repair decisions.

Vertical settlements underneath a Portland cement concrete (PCC) approach slab could be permanently repaired with mudjacking. This procedure is effective when the slab remains in good condition. Mudjacking works especially well when the connecting road is also PCC. In that case, both the slab and roadway can be mudjacked to restore grade. A small quantity of AC is often used to cover any gap between the approach slab end and the road surface.

The damage states for the bridge approach are tied to the limits in Hoppe (1999) regarding the

Table 5.18 Approach damage states.

	Damage State Description	λ	β
DS0	Onset of pavement problems	0.073	0.40
DS1	AC regrade	0.146	0.40
DS2	AC regrade and mudjacking	0.305	0.40

Table 5.19 Approach repair items.

Damage State	Repair Item	Repair Quantity
DS1	Asphalt concrete (TON)	(vertical settlement) $\times$ (approach slab area)
DS2	Asphalt concrete (TON)	(vertical settlement) $\times$ (approach slab area)
	Excavation and backfill (CY)	(deck width + $6'$) $\times$ deck depth $\times$ (thickness + $1'$)

point where remedial measures are needed. A gradient of 1/200 is the limit for rider comfort, and 1/125 is the point where remedial measures are needed. This 1/125 gradient is selected as DS0 and the increasing damage states are incrementally worse. The damage state parameters are given in Table 5.18 and the repair methods in Table 5.19.

5.4 NON-STRUCTURAL COMPONENTS

Non-structural elements can also be included in the repair cost methodology in the same way as structural elements. In this study, they were not incorporated into a performance group but could be if cost and performance data for non-structural elements were available. This section describes possible definitions for non-structural performance groups for barrier rail and lighting poles. Other non-structural components, such as utility conduits, were not considered in this study.

5.4.1 Barrier Rail

A portion of the barrier rail is often replaced when there is anything more than a $2''$ offset anywhere along the length. Although offsets this small are not indicative of structural deficiency, the barrier rail is often replaced at this level anyway because of public perception. This performance group is expected to correlate well with the residual column displacement EDP.

The bridge has two sets of barrier rail on each side for a total of 1380 LF of railing. Ketchum et al. (2004) specifies a Caltrans Type 732 concrete barrier rail (Fig. 5.7). The barrier is cast-in-

Table 5.20 Barrier rail repair items.

Damage State	Repair Item	Repair Quantity
DS1	Barrier rail, replace (LF)	10% × (deck segment length)
DS2	Barrier rail, replace (LF)	25% × (deck segment length)

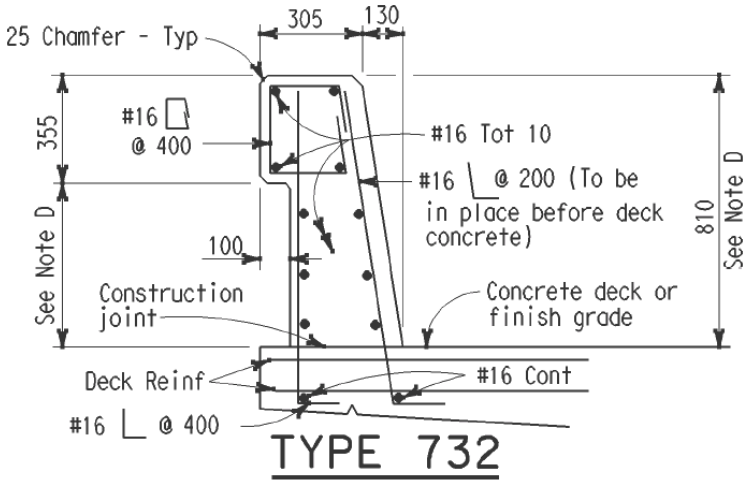

Fig. 5.7 Barrier rail (Standard Plan ES-6A).

place reinforced concrete and has a construction joint between the barrier and the bridge deck. The barrier rail is connected to the deck via #16 bars placed at 200 mm (8″) spacing. The damage states are defined in terms of the length of barrier rail requiring replacement as a percentage of the bridge span segment (Table 5.20).

5.4.2 Lighting Poles

Lighting poles are also significant non-structural elements. Lighting poles can undergo significant seismic excitation and may be damaged. The testbed bridge design does not specifically call for lighting poles. However, given a nominal spacing of about 50′ on both sides, this would suggest approximately 25 lighting poles over the entire bridge. They are usually mounted on top of the barrier rail. The damage states are defined by the number of lighting poles requiring replacement (Table 5.21).

Table 5.21 Lighting pole repair items.

Damage State	Repair Item	Repair Quantity
DS1	Light pole, 35′ height (EA)	10% × (no. lights)
	High pressure sodium luminare (EA)	10% × (no. lights)
DS2	Light pole, 35′ height (EA)	25% × (no. lights)
	High pressure sodium luminare (EA)	25% × (no. lights)
DS3	Light pole, 35′ height (EA)	50% × (no. lights)
	High pressure sodium luminare (EA)	50% × (no. lights)

6 Repair Cost and Time

Data for repair cost and repair time were obtained using a variety of sources, including published Caltrans construction estimation data, case studies from previous earthquakes, and hypothetical damage scenarios based on the Type 1A testbed bridge model developed specifically for this report.

6.1 COST INDEX

Cost index data from Caltrans are used to adjust for inflation. Beginning around 2002, the cost of bridge construction began increasing rapidly. Data collected from meetings with Caltrans are based on the most current values and older values are adjusted using the Caltrans cost index data. The original Ketchum et al. (2004) report used cost data from 2004, which need to be inflation adjusted to current values in order to make equivalent comparisons.

Price Index for Selected Highway Construction Items (Division of Engineering Services, 2007) provides cost index data for the current quarter, last 12 months, and the number of average bidders per project. Short summaries of contracts over $5M are provided. The prices of seven construction items are tracked in English and metric units since 1972: roadway excavation, aggregate base, asphalt concrete pavement, Portland cement concrete (pavement), Portland cement concrete (structure), bar reinforcing steel, and structural steel. The base year in this publication is 1987.

Bridge Construction Cost Index (Division of Engineering Services—Cost Estimates Branch, 2007a) is specific for bridges alone instead of including all contracts. The cost index is given for 1940 and 1966–current for the base years 1940, 1967, and 1977. Structure Cost Index provides cost indexes for 1984–current for every quarter and the four-quarter moving average.

6.2 BRIDGE CLOSURE DOWNTIME

Downtime is the amount of time that a bridge is closed to all traffic after an earthquake. The downtime is usually very short, typically only one day at the most, because many bridge repairs can be performed without completely closing the bridge. For repairs that require shoring, the only required downtime is the time it takes to shore the bridge.

When materials are available, shoring for each bent can be completed within 6–8 hours. The type of shoring is usually lumber or steel pipe. The most common height of shoring is 20′, which corresponds to the above-grade height of the Type 1 testbed model bridge. Even for repairs on the bridge columns, the required downtime is minimal. For example, installing a steel column casing takes several working days, but only one day of downtime for shoring installation. Similarly for column replacement, demolishing the damaged column and building a replacement column takes many days, but only one day of downtime is needed for shoring installation. Temporary emergency repairs can be performed in order to restore traffic onto a damaged bridge as soon as possible. For example, asphalt concrete (AC) and steel plates can be placed in order to restore roadway grades. Even extensive repairs to bridge approaches can be performed in segments requiring only partial closures with no complete downtime. This type of work can be completed at night with minimal disruption to traffic flow.

Because of these factors, downtime can be considered as a binary decision: either 1 day or none. If a bridge experiences substantial superstructure failure to the extent that it cannot carry traffic, then the downtime can be assumed to be 60 days.

6.3 REPAIR COST RATIO

Normalized costs of repair are obtained by using the repair cost ratio (RCR) between the cost of repair and the cost of original new construction. This ratio is useful for comparing the performance of different bridge design options for new construction. For the evaluation of existing structures, the RCR including demolition costs might be more useful. Constructing a new bridge on the same site after an earthquake would require both demolition of the damaged bridge and construction of its replacement.

The cost of new construction can be obtained using different methods. Ketchum et al. (2004)

Table 6.1 Cost of new construction.

Bridge type	2003 prices in Ketchum et al. (2004)	Adjusted to 2007Q2
1A	$2,028,895	$3,798,457
1B	$2,468,517	$4,621,509
11A	$2,327,278	$4,357,084
11B	$2,479,591	$4,642,241

computed construction costs based on quantity estimates for each of the testbed bridge models. Also, Caltrans bridge cost estimates for planning purposes are based on the deck and type of construction. These estimates provide a range of cost/SF of deck area.

The cost of new construction must be adjusted by the price index to make comparisons between current 2007 cost data and the new construction costs reported in Ketchum et al. (2004) that were based on 2003 cost estimates. The quarterly cost index four-quarter moving average is used for comparison (see *http://www.dot.ca.gov/hq/esc/estimates/*). In 2003Q4 the moving average cost index was 266 and the cost index for 2007Q2 is 498. So, the construction costs in Ketchum et al. (2004) can be corrected to 2007 dollars by the equation

$$\text{Cost}_{2007} = \text{Cost}_{2003} \frac{\text{Index}_{2007}}{\text{Index}_{2003}}$$

Based on these cost index values, the adjusted costs in Table 6.1 can be used for computing repair cost ratios. If the cost of demolition is considered in the repair cost ratio, then an additional cost for bridge removal must be added. The January 2007 Caltrans comparative bridge costs sheet estimates $15–$20/SF for removal of a box girder structure, which is $403,650–$538,200 for the Types 1 and 11 bridge models.

6.4 REPAIR ITEM UNIT COSTS

The unit costs for the repair items are given in Table 6.2. Most unit costs are insensitive to the quantity. However, some of the repair items have higher unit costs with small quantities and lower unit costs with larger quantities. These changes in unit price are indicated in the notes of Table 6.2. Unit cost uncertainty can be computed from the available data on previous bridge contracts. Or, a simple estimate of the coefficient of variation of the unit costs can be used, as was assumed in this report. A coefficient of variation of 20% was used for all repair items. A final approach to

Table 6.2 Repair item unit cost.

Item name	Unit	Mean unit cost	Notes
Structure excavation	CY	$165.00	$250 for $<$ 50 CY
Structure backfill	CY	$220.00	$335 for $<$ 14 CY, $115 for $>$ 250 CY
Temporary support (superstructure)	SF	$38.00	
Structural concrete (bridge)	CY	$2,225.00	$2,000 for $>$ 10 CY
Structural concrete (footing)	CY	$520.00	
Structural concrete (approach slab)	CY	$1,625.00	
Aggregate base (approach slab)	CY	$325.00	
Bar reinforcing steel (bridge)	LB	$1.35	$6.50 for $<$ 400 LB
Epoxy inject cracks	LF	$215.00	
Repair minor spalls	SF	$300.00	
Column steel casing	LB	$10.00	
Joint seal assembly	LF	$275.00	
Elastomeric bearings	EA	$1,500.00	
Drill and bond dowel	LF	$55.00	
Furnish steel pipe pile	LF	$55.00	
Drive steel pipe pile	EA	$2,050.00	$9,000 for low clearance and splicing
Asphalt concrete	TON	$265.00	
Mud jacking	CY	$380.00	
Bridge removal (portion)	CY	$2,355.00	$3,405 for column removal, $1,000 for other removal
Clean deck for methacrylate	SF	$0.40	
Furnish methacrylate	GAL	$85.00	
Treat bridge deck	SF	$0.55	

capture the total repair cost (TC) uncertainty due to possible fluctuations in unit cost is to add an additional uncertainty term as discussed in the Methodology chapter.

6.5 REPAIR DURATION AND EFFORT ESTIMATES

The repair time for the bridge can be expressed either as an approximation of the repair duration or the repair effort.

The repair effort represents the total number of crew-workdays required to complete the repair task. This is different from repair duration which counts the actual total duration of the entire repair project. The repair duration includes the effect of scheduling concurrent on-site construction processes, while the repair effort does not. The repair duration can vary based on the amount

Table 6.3 Repair time for damage scenarios.

Scenario	Repair Duration	Repair Effort
Minor	72 days	112 crew-days
Major	78 days	254 crew-days
Abutment	82 days	107 crew-days

and type of concurrent construction processes, schedule dependencies, availability of labor, and whether or not contract incentives are provided in order to decrease duration. However, the repair effort is independent of these items.

The use of a repair effort provides a normalized metric that is independent of labor resources, use of incentives on the job, or other constraints that control the project schedule. For example, the repair effort for two columns with the same damage and repair methods will have twice the repair effort of a similar single column. However, the repair time for one column or two columns could be the same if the repair work can be carried out concurrently.

This difference between repair effort and repair duration can be seen in the number of working days required for each damage scenario (Table 6.3). Here, the repair time is measured in working days. For comparison, a repair effort can be measured by the quantities of repair items required. The repair times for the minor and major scenarios is almost the same, differing only by 6 working days. In this example, the repair effort was computed by summing the amount of days required for each task including tasks that were scheduled concurrently. The difference between the two is substantial, which indicates the sensitivity to the method chosen for expressing repair time.

Mobilization also makes a significant contribution to the overall repair time. The mobilization time could be a fixed amount regardless of the amount or scope of work needed for the repairs.

6.6 DAMAGE SCENARIOS

Cost and repair time data were collected using three damage scenarios representing a range of different damage states for each performance group in the testbed bridge (Type 1A). The damage scenarios do not correspond to a particular earthquake ground motion. Rather, they are designed to cover the range of damage state possibilities in order to refine the unit cost and repair time estimates used in the analytical decision model. A minor and major damage scenario represent prin-

cipal damage to the bridge structure and column foundations, while the abutment damage scenario represents significant damage to the bridge abutments. Damage scenario drawings were prepared that include the repair methods and repair quantities corresponding to the different performance group damage states. A Caltrans bridge estimator evaluated the damage scenarios and provided a set of cost and scheduling estimates for each scenario. These estimates were used to refine the input data for repair cost analysis.

The damage states for the minor damage scenario are summarized in Table 6.4, the major damage scenario in Table 6.5, and the abutment damage scenario in Table 6.6. The major damage scenario contains extensive damage to all the major bridge components and high levels of damage states in every performance group. The abutment damage scenario is an uncommonly used repair sequence for Caltrans. Past instances of severe abutment damage were strongly correlated with extreme structure and superstructure damage. Because of this, bridges with high levels of abutment damage were usually completely replaced instead of repaired. However, there are examples of extensive abutment repairs completed in the past.

Construction constraints for abutment work make extensive abutment repairs costly and time consuming. Clearance on the bridge side of the abutment is impeded by the superstructure. No additional pipe piles are added on the bridge side because there is insufficient clearance for pile driving equipment. Temporary shoring would be needed to support the superstructure which might cause additional space constraints for abutment expansion. The quantities of steel and concrete required for the expansion are very large.

6.7 DAMAGE SCENARIO REPAIR ESTIMATES

The cost estimates for the minor damage scenario are given in Table 6.7, major damage scenario in Table 6.8, and abutment damage scenario in Table 6.9.

The mobilization required for several of the items dominated the repair time. For example, preparing the material and safety plan for methacrylate deck overlay takes 20 working days, while the actual cleaning and treating of the bridge deck takes only 2 working days. Also, submitting and reviewing shop plans for a steel column casing takes 32 working days and procurement for the column casing is estimated at 30 days, while actual on-site work for casing installation is only 10 days.

Table 6.4 Minor damage scenario.

Performance group	Damage State	Description
PG1 col1 max	DS1	minor repair
PG2 col2 max	DS1	minor repair
PG3 col3 max	DS1	minor repair
PG4 col4 max	DS0	
PG5 col1 residual	DS0	
PG6 col2 residual	DS0	
PG7 col3 residual	DS0	
PG8 col4 residual	DS1	steel column casing
PG9 BB abutment	DS0	
PG10 EB abutment	DS0	
PG11 BB bearing	DS0	
PG12 EB bearing	DS0	
PG13 BB shear key	DS1	minor repair
PG14 EB shear key	DS1	minor repair
PG15 BB approach	DS1	AC overlay
PG16 EB approach	DS2	AC overlay and mudjacking
PG17 span1	DS3	50% deck resurface
PG18 span2	DS3	50% deck resurface
PG19 span3	DS3	50% deck resurface
PG20 span4	DS3	50% deck resurface
PG21 span5	DS3	50% deck resurface
PG22 BB abutment foundation	DS0	
PG23 EB abutment foundation	DS0	
PG24 col1 foundation	DS0	
PG25 col2 foundation	DS0	
PG26 col3 foundation	DS0	
PG27 col4 foundation	DS0	

Table 6.5 Major damage scenario.

Performance group	Damage State	Description
PG1 col1 max	DS0	
PG2 col2 max	DS0	
PG3 col3 max	DS0	
PG4 col4 max	DS3	replace column
PG5 col1 residual	DS2	enlarged steel column casing
PG6 col2 residual	DS1	steel column casing
PG7 col3 residual	DS1	steel column casing
PG8 col4 residual	DS0	
PG9 BB abutment	DS2	repair back wall, replace expansion joint
PG10 EB abutment	DS3	repair back wall, replace expansion joint, approach slab, back wall
PG11 BB bearing	DS1	replace bearings
PG12 EB bearing	DS0	
PG13 BB shear key	DS2	replace shear keys
PG14 EB shear key	DS0	
PG15 BB approach	DS0	
PG16 EB approach	DS0	
PG17 span1	DS3	100% deck resurface
PG18 span2	DS3	100% deck resurface
PG19 span3	DS3	100% deck resurface
PG20 span4	DS3	100% deck resurface
PG21 span5	DS3	100% deck resurface
PG22 BB abutment foundation	DS0	
PG23 EB abutment foundation	DS0	
PG24 col1 foundation	DS1	enlarge column foundation
PG25 col2 foundation	DS0	
PG26 col3 foundation	DS0	
PG27 col4 foundation	DS0	

Table 6.6 Abutment damage scenario.

Performance group	Damage State	Description
PG1 col1 max	DS0	
PG2 col2 max	DS0	
PG3 col3 max	DS0	
PG4 col4 max	DS0	
PG5 col1 residual	DS0	
PG6 col2 residual	DS0	
PG7 col3 residual	DS0	
PG8 col4 residual	DS0	
PG9 BB abutment	DS0	
PG10 EB abutment	DS0	
PG11 BB bearing	DS0	
PG12 EB bearing	DS0	
PG13 BB shear key	DS2	replace shear keys
PG14 EB shear key	DS0	
PG15 BB approach	DS0	
PG16 EB approach	DS0	
PG17 span1	DS0	
PG18 span2	DS0	
PG19 span3	DS0	
PG20 span4	DS0	
PG21 span5	DS0	
PG22 BB abutment foundation	DS1	enlarge abutment foundation, excavation and backfill, drive piles, replace wing walls
PG23 EB abutment foundation	DS0	
PG24 col1 foundation	DS0	
PG25 col2 foundation	DS0	
PG26 col3 foundation	DS0	
PG27 col4 foundation	DS0	

Table 6.7 Minor scenario repair cost estimate.

Contract Item	Unit	Quantity	Price	Amount
Inject Crack (Epoxy)	LF	132	$215.00	$28,380.00
Repair Spalled Surface Areas	SF	84	$300.00	$25,200.00
Structure Excavation (Bridge)	CY	8	$250.00	$2,000.00
Structure Backfill (Bridge)	CY	8	$335.00	$2,680.00
Column Casing	LB	2,925	$10.00	$29,250.00
Bar Reinforcing Steel	LB	231	$6.25	$1,443.75
Clean Bridge Deck	LF	13,455	$0.40	$5,382.00
Furnish Bridge Deck Treatment Material	GAL	150	$85.00	$12,750.00
Treat Bridge Deck	SF	13,455	$0.55	$7,400.25
Repair Spalled Surface Areas	SF	6	$300.00	$1,800.00
Inject Crack (Epoxy)	LF	40	$215.00	$8,600.00
Asphalt Concrete	TON	31	$265.00	$8,215.00
Mudjacking	CY	122	$280.00	$46,360.00
			Subtotal	$179,461.00

The amount of time needed to repair each damage state in each performance group are summarized in Tables 6.10–6.17. The totals under each damage state reflect the combination of concurrent work within a damage state. Driving abutment piles is more costly and takes longer than driving column foundation piles because of limited access and overhead clearance. The limited access and overhead clearance requires the piles to be driven in sections and welded in the field.

6.8 REPAIR TIMES BASED ON QUANTITY

Repair times are also computed on the basis of each repair quantity Q (Table 6.18). This allows the methodology for computing repair cost to be applied for computing repair times as well. For any repair item n a value for $Q_n > 0$ (note, the criteria is actually based on a probability, as detailed in Chapter 2) indicates that the associated repair time should be added to the total repair time for the project. Repair tasks that use the same repair items are assumed to occur simultaneously. So, when the repair times are added up, this estimate more closely approximates repair duration instead of repair effort.

Table 6.8 Major scenario repair cost estimate.

Contract Item	Unit	Quantity	Price	Amount
Temporary Support	SF	7,605	$38.00	$288,999.00
Clean Bridge Deck	SF	26,910	$0.40	$10,764.00
Bridge Removal (Portion)	CY	30.3	$2,355.00	$71,238.75
Structure Excavation (Bridge)	CY	189	$165.00	$31,185.00
Structure Backfill (Bridge)	CY	114	$220.00	$25,080.00
Aggregate Base (Approach Slab)	CY	10	$325.00	$3,250.00
Furnish Piling (Class 140) (Alternative W)	LF	840	$55.00	$46,200
Drive Pile (Class 140) (Alternative W)	EA	14	$9,000	$126,000.00
Structural Concrete (Bridge Footing)	CY	75	$520.00	$39,000.00
Structural Concrete (Bridge)	CY	30.3	$2,225.00	$67,306.25
Structural Concrete, Approach Slab	CY	43	$2,625.00	$69,875.00
Bar Reinforcing Steel (Bridge)	LB	20,186	$1.35	$27,251.10
Column Casing	LB	10,540	$10.00	$105,400.00
Furnish Bridge Deck Treatment Material	GAL	299	$85.00	$25,415.00
Treat Bridge Deck	SF	26,910	$0.55	$14,800.50
Replace Bearing	EA	3	$1,500.00	$4,500.00
Inject Crack (Epoxy)	LF	12	$215.00	$2,580.00
Repair Spalled Surface Areas	SF	23	$300.00	$6,900.00
Joint Seal Assembly (MR 4″)	LF	78	$275.00	$21,450.00
Drill and Bond Dowel	LF	50	$55.00	$2,750.00
			Subtotal	$989,936.00

Table 6.9 Abutment scenario repair cost estimate.

Contract Item	Unit	Quantity	Price	Amount
Structure Excavation (Bridge)	CY	490	$165.00	$80,850.00
Structure Backfill (Bridge)	CY	365	$115.00	$41,975.00
Furnish Piling	LF	700	$55.00	$38,500.00
Drive Pile (Class 140) Alternative W	EA	10	$2,050.00	$20,500.00
Structural Concrete (Bridge Footing)	CY	125	$520.00	$65,000.00
Bar Reinforcing Steel (Bridge)	LB	11,868	$1.35	$16,024.80
Drill and Bond Dowel	LF	150	$55.00	$8,250.00
Structural Concrete (Bridge)	CY	21	$2,000.00	$41,800.00
Bridge Removal (Portion)	CY	21	$1,000.00	$20,900.00
			Subtotal	$333,797.00

Table 6.10 Column repair time.

DS	Description	Work Item	Working Days
DS1 max	Minor patching	Repair minor spalls	3
		Repair cracks with epoxy	3
		Total	3
DS2 max	Major patching	Repair minor spalls	3
		Repair cracks with epoxy	3
		Total	3
DS3 max	Replace column	Submit/review bridge removal plan	15
		Submit/review temporary support	30
		Install temporary support	3
		Remove existing column	1
		Place reinforcement	2
		Place column forms	1
		Pour concrete	1
		Cure	10
		Remove forms	1
		Remove temporary support	1
		Total	50
DS1 residual	Column steel casing	Submit shop plans	2
		Review shop plans	30
		Fabricate/procure column casing	30
		Mobilize	5
		Excavate	1
		Set column casing and weld	2
		Grout and paint	6
		Backfill	1
		Total	72
DS2 residual	Enlarged column steel casing	*Time estimates same as regular casing*	

Table 6.11 Abutment repair time.

DS	Description	Work Item	Working Days
DS1	Replace joint seal assembly	Install joint seal assembly	2
		Total	2
DS2	DS1 + repair back wall	Install joint seal assembly	2
		Excavate	1
		Repair cracks with epoxy	1
		Repair spalls	1
		Backfill	2
		Total	7
DS3	DS2 + replace approach slab and back wall	Install joint seal assembly	2
		Repair cracks with epoxy	1
		Repair spalls	1
		Excavate	1
		Remove 1/2 back wall and approach slab	2
		Construct 1/2 back wall	2
		Backfill	2
		Construct 1/2 approach slab	1
		Construct 1/2 back wall and approach slab	7
		Total	19

Table 6.12 Bearing repair time.

DS	Description	Work Item	Working Days
DS1	Replace bearing	Submit/review temporary support	30
		Install temporary support	2
		Install replacement bearing	1
		Remove temporary support	1
		Total	34

Table 6.13 Shear key repair time.

DS	Description	Work Item	Working Days
DS1	Minor patching	Repair cracks with epoxy	1
		Repair spalls	1
		Total	2
DS2	Replace shear keys	Demo existing shear key	1
		Install reinforcement	1
		Install forms	1
		Pour concrete	1
		Cure concrete	7
		Strip forms	1
		Total	12

Table 6.14 Approach repair time.

DS	Description	Work Item	Working Days
DS1	AC Overlay	Asphalt Concrete	2
		Total	2
DS2	AC Overlay and mudjacking	Asphalt Concrete	2
		Mudjacking	2
		Total	4

Table 6.15 Deck repair time.

DS	Description	Work Item	Working Days
DS1	50% deck resurface	Material Sampling	10
		Methacrylate safety plan	10
		Clean & treat bridge deck	2
		Total	22
DS2	100% deck resurface	Material Sampling	10
		Methacrylate safety plan	10
		Clean & treat bridge deck	2
		Total	22

Table 6.16 Abutment foundation repair time.

DS	Description	Work Item	Working Days
DS1	Enlarge abutment foundation	Submit/review demo plan	20
		Procure piling	40
		Excavate abutment/demo wing walls	3
		Drive piles	3
		Drill and bond dowels	1
		Place reinforcement and formwork	1
		Pour footing	1
		Cure footing	7
		Construct wing walls	4
		Cure wing walls	7
		Backfill	4
		Total	71

Table 6.17 Column foundation repair time.

DS	Description	Work Item	Working Days
DS1	Enlarge column foundation	Fabricate/procure pipe piles	30
		Excavate bent	1
		Drive piles	2
		Place forms	1
		Place reinforcement	2
		Pour concrete	1
		Cure	7
		Backfill bent	1
		Total	45

Table 6.18 Repair times for each repair quantity Q.

Repair Item (Q)	Days	Description
Structure excavation	1.0	Excavation (1)
Structure backfill	2.0	Backfill (1–4)
Temporary support (superstructure)	34.0	Submit/review temporary support (30), Install (3), Remove (1)
Temporary support (abutment)	33.0	Submit/review temporary support (30), Install (2), Remove (1)
Structural concrete (bridge)	10.0	Place forms (0–1), Cure (7–10), Strip forms (1)
Structural concrete (footing)	10.0	Place forms (0–1), Cure (7–10), Strip forms (1)
Structural concrete (approach slab)	2.0	Construct approach slab (1 + 1, in half-width strips)
Aggregate base (approach slab)	1.0	
Bar reinforcing steel (bridge)	2.0	Place reinforcement (1–2)
Bar reinforcing steel (footing, retaining wall)	2.0	Place reinforcement (1–2)
Epoxy inject cracks	2.0	Repair cracks with epoxy (1–3)
Repair minor spalls	2.0	Repair spalls (1–3)
Column steel casing	70.0	Submit shop plans (2), Review shop plans (30), Procure column casing (30), Set and weld (2), Grout and paint (6)
Joint seal assembly	2.0	Install joint seal assembly (2)
Elastomeric bearings	1.0	Install bearings (1)
Drill and bond dowel	1.0	Drill and bond dowels (1)
Furnish steel pipe pile	35.0	Procure piling (30–40)
Drive steel pipe pile	2.0	Drive piles (2)
Drive abutment pipe pile	3.0	Drive piles (3)
Asphalt concrete	2.0	Asphalt concrete (2)
Mud jacking	2.0	Mudjacking (2)
Bridge removal (column)	16.0	Submit/review bridge removal plan (15), Remove existing column (1)
Bridge removal (portion)	2.0	Demo existing / Remove (1–3); Use for miscellaneous removal, e.g., shear keys
Approach slab removal	4.0	Remove approach slab (2 + 2, in half-width strips)
Clean deck for methacrylate	1.0	Clean bridge deck (1)
Furnish methacrylate	20.0	Material sampling (10), Methacrylate safety plan (10)
Treat bridge deck	1.0	Treat bridge deck (1)

7 Outcomes

This chapter presents an array of results obtained by applying the methodology and repair chapters to the baseline testbed bridges. While the repair cost and repair time scenarios were generated exclusively for bridge Type 1A, the demand and damage analysis was performed for all of the Types 1 and 11 bridges mentioned in Chapter 4. The scope of this study is limited to development of a data structure and methodology to support the vulnerability assessment of highway bridges in terms of repair costs and repair times. To this end, performance, damage, and repair data were obtained for the specific testbed bridges. It was not the intent of this study to perform a parametric or sensitivity study on all of the bridges that may be found in a given transportation network. The parameterization or tabulation of fragility curve parameters for different bridges is a topic for future studies.

7.1 PROBABILISTIC SEISMIC DEMAND MODELS

Each bridge configuration was subjected to suites of recorded ground motions. A total of 7 bins of 20 records each were utilized. Each ground motion record has two orthogonal horizontal components and a vertical acceleration component. For this benchmark study, the motions were applied uniformly at the base of the structure. The first four bins are identical to those used in previous bridge studies (Mackie and Stojadinović, 2005) and correspond to typical non-near-fault California recordings. Two additional bins were created from the ground motions selected for the I-880 PEER testbed study (Kunnath, 2006). This site is located near the Hayward fault: thus, the motions are anticipated to exhibit distinct directivity effects. The I-880p bin contains all the motions from the I-880 PEER testbed project with the original fault parallel motions aligned with the bridge transverse direction. Similarly, the I-880n bin contains all the original fault normal motions aligned

with the transverse bridge direction. The final, seventh, bin (VN) was obtained from the unscaled PEER Van Nuys testbed (Krawinkler, 2005) motions. These motions were already identified as longitudinal and transverse; therefore, they were applied to the bridge as is. The cloud method of probabilistic seismic demand analysis was used (Mackie and Stojadinović, 2005) to generate (continuous) relationships between IMs and EDPs, known as probabilistic seismic demand models (PSDMs). A total of 192 EDPs and 120 IMs were tracked during each analysis.

The resultant number of possible PSDMs is 2560 in each direction (longitudinal, transverse, vertical) for a total of 7680 PSDMs. Only the PSDMs utilizing the maximum tangential column drift ratio, residual tangential column drift ratio, longitudinal deck-end displacement relative to the backwall, bearing absolute displacement, shear key force, vertical abutment displacement, and strain at roadway surface are considered in this report. This includes all the PGs except the residual displacement of the pile caps. The maximum tangential drift ratio is defined as the larger of the column displacements above and below the column inflection point, normalized by the respective distances of the locations of maximum displacement to the inflection point. The location of the inflection point moves during transient analysis; therefore, the drift ratio was calculated at each time step. The drifts were measured for each of the four bridge columns, in each direction (longitudinal and transverse); a square-root-sum-of-squares (SRSS) drift magnitude was also reported. The abutment-specific EDPs are limited to the bridge models containing the SpringAbutment module.

The choice of IM for use with EDPs listed above is limited to several spectral quantities in this study. Previous research has indicated that the optimal (not necessarily the most efficient) IMs for use in bridge PSDMs involving global response measures such as drift are spectral acceleration $Sa(T_1)$ or spectral displacement $Sd(T_1)$. However, it is difficult to draw direct comparisons between PSDMs from different bridge configurations due to the period dependence of the IM. Therefore, two classes of PSDMs are presented here. The first utilizes the spectral acceleration at the second mode period for the longitudinal direction, $Sa(T_2)$, and the first-mode period, $Sa(T_1)$, for the transverse direction (see Table 4.3). The second utilizes the spectral displacement at a fixed period of T = 1 sec, $Sd(T = 1)$, for all directions. While the PSDMs formulated with the correct structural period yield more efficient results, the T = 1 sec PSDMs are also moderately efficient due to the period range of the bridges under consideration (Table 4.3).

The peak magnitude (SRSS of longitudinal and transverse directions) of intensity and response

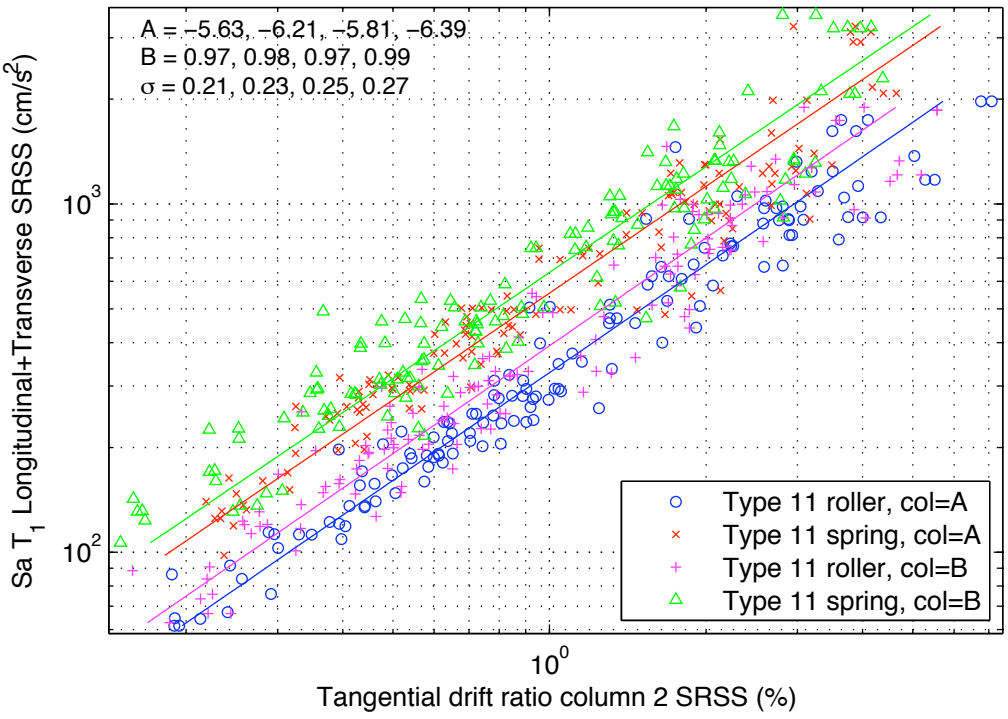

Fig. 7.1 PSDM for four Type 11 configurations using $Sa(T_1)$ and drift ratio SRSS.

are plotted for four permutations of bridge Type 11 in Figure 7.1. Column types A and B and two abutment modules are considered (RollerAbutment and SpringAbutment). The maximum tangential drift ratio monitored for the PSDMs shown in the figure was for the second column, labeled bent 3 in Figure 4.1. The coefficients of the linear fit in log space are shown in the upper-left of the figure and correspond to those used in Equation (2.6). The dispersion σ (shown in the figure) corresponds to $\sigma_{EDP|IM}$.

A similar set of PSDMs is shown in Figure 7.2 for two column types and abutment conditions (RollerAbutment and SpringAbutment) of Type 1. However, the structure-independent IM $Sd(T = 1)$ is used for the intensity. The maximum tangential drift ratio shown in the figure is for the first column, labeled bent 2 in Figure 4.1. It is evident from Figure 7.2 that the different bridge Type 1 configurations yield similar performance; however, column type B is stiffer and the use of the SpringAbutment module results in decreased peak drift demands. For a single earthquake event with known magnitude, the different bridge configurations can be compared directly by drawing a line of constant intensity horizontally across Figure 7.2.

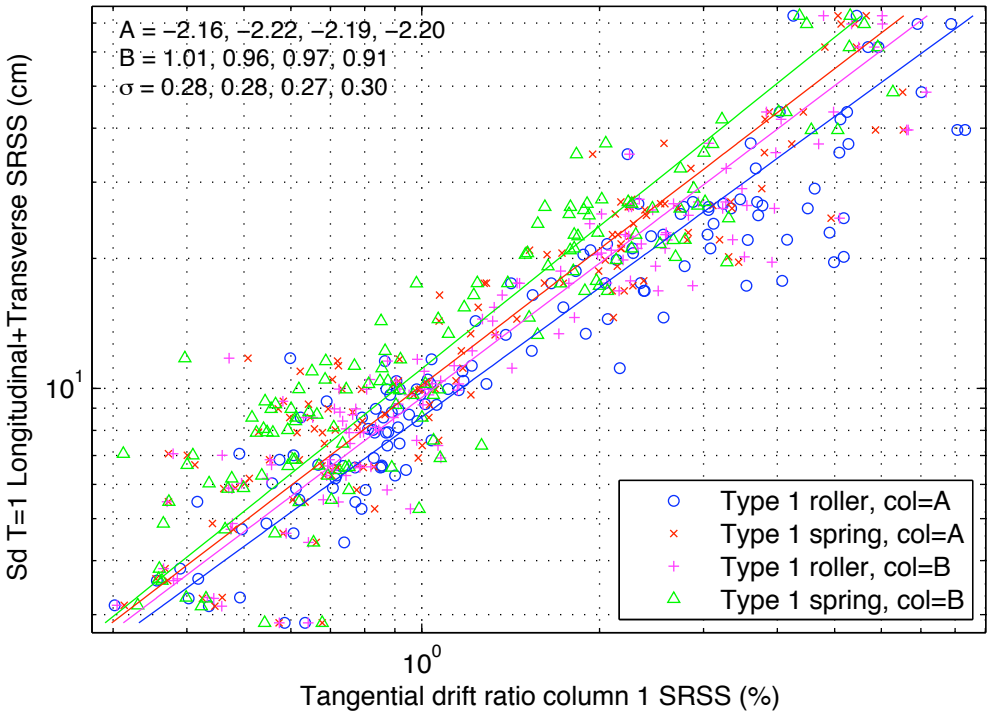

Fig. 7.2 PSDM for four Type 1 configurations using $Sd(T = 1)$ and drift ratio SRSS.

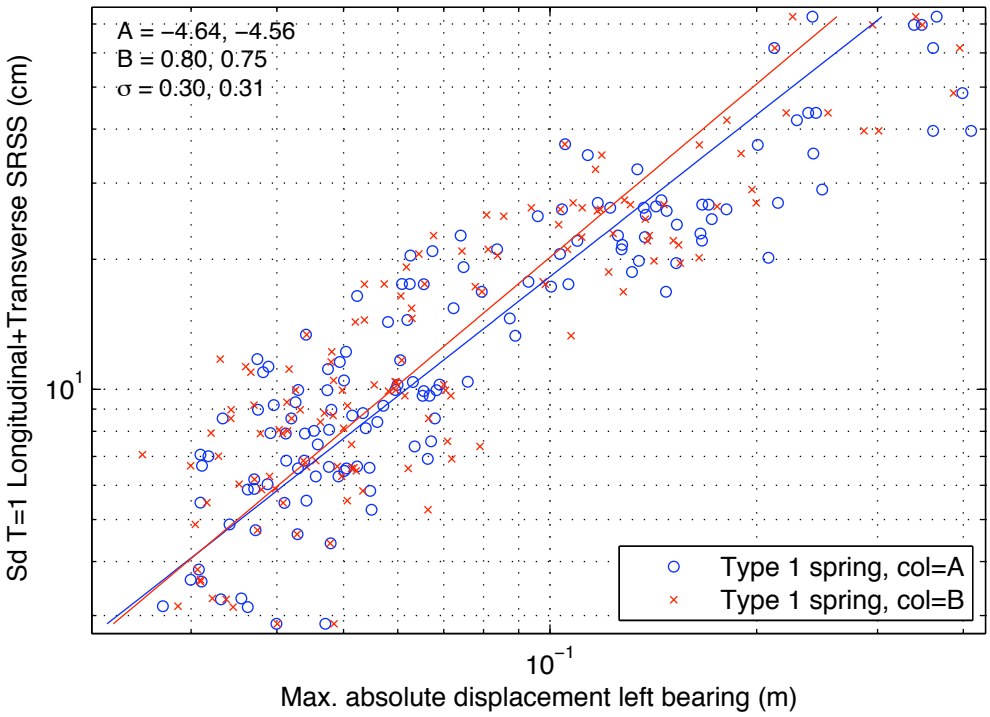

Fig. 7.3 PSDMs for Type 1A and Type 1B using $Sd(T = 1)$ and maximum absolute bearing displacement.

Space limitations prevent the illustration of PSDMs for all of the performance groups and their corresponding EDPs. However, an example of one of the PSDMs not pertaining to column damage is provided in Figure 7.3. The structure-independent IM $Sd(T = 1)$ is maintained in this PSDM; however, the EDP under consideration is the maximum absolute displacement of the bearing at the left abutment (labeled abut 1 in Fig. 4.1). Only a comparison between bridge Type 1 column configurations is shown, both with the SpringAbutment module. The maximum absolute bearing displacement is considered because the abutment models are not coupled in the longitudinal and transverse direction. As with Figure 7.2, Type 1B shows a slight reduction in demand due to the increased percentage of steel in the column, an effect that increases with earthquake intensity.

Of additional interest is the effect of the selection of ground motions on the resultant PSDM, especially in the case of near-fault records. To investigate the range of intensities covered by each bin, as well as the likely trends followed, a single PSDM (for Type 11B) is separated into a seismicity plot. This is of particular relevance with the I-880 records as they are expected to exhibit

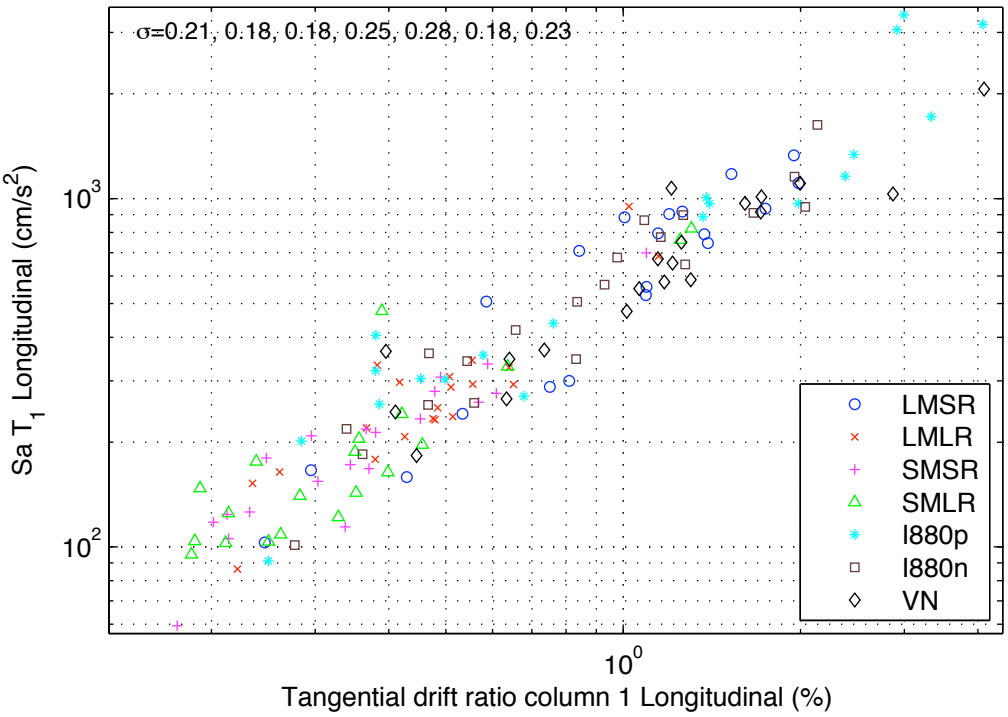

Fig. 7.4 Longitudinal seismicity plot for Type 11B, RollerAbutment.

some near-field/directivity effects. To isolate the fault-normal and fault-parallel effects, nominal PSDMs are generated in the bridge longitudinal and transverse directions separately. The response in both directions is dominated in the high-intensity region by the I-880p bin for longitudinal (Fig. 7.4) and I-880n bin for transverse response (Fig. 7.5). This indicates that the fault-normal component causes greater response for each case. The near-fault records do not bias the slope of the demand models (particularly for the periods under consideration).

7.2 PROBABILISTIC DAMAGE MODELS

The damage model considered for the performance groups in the bridge provides the relationship between the DMs and the EDPs from the demand model. The damage models developed for each bridge component type are taken from component-level limit state median values and dispersions. For the first (scalar) approach, only a single damage model is developed for the reinforced concrete columns. In this scenario, all of the columns are lumped together into a single performance group. A total of seven and nine damage models are developed for the second and third (vector)

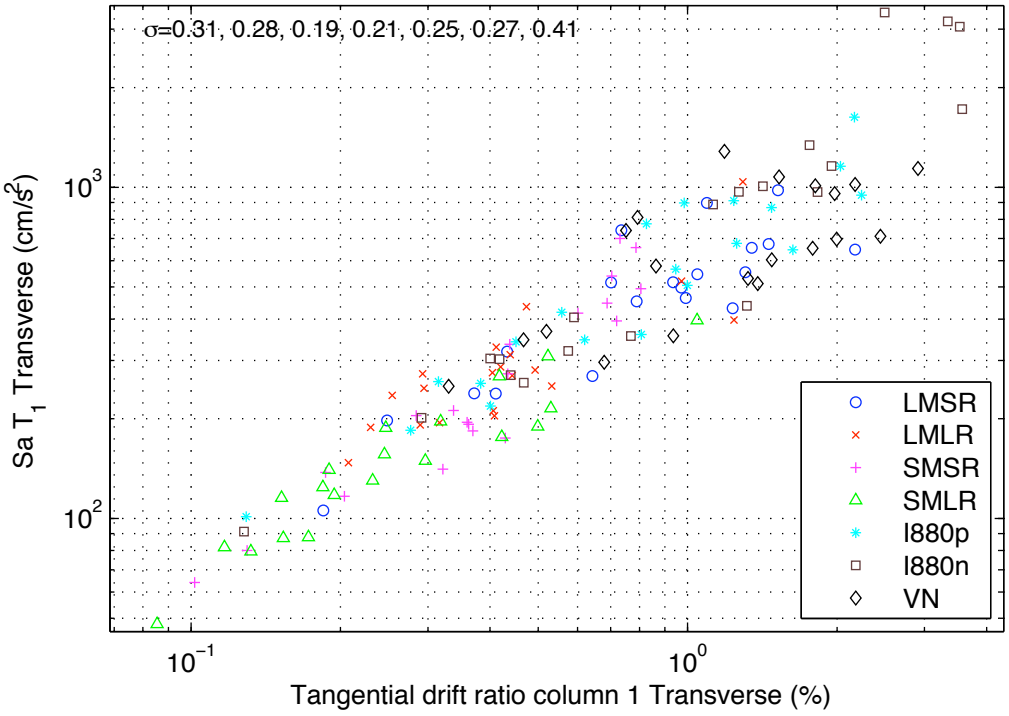

Fig. 7.5 Transverse seismicity plot for Type 11B, RollerAbutment.

approaches, respectively. For the vector approaches, the number of damage models is not equal to the number of performance groups, since the performance groups that deal with the same type of component (e.g., 4 columns) use the same damage model. Each performance group has discrete damage states that are each associated with repair methods and quantities. Some performance groups have many intermediate damage states when several repair methods are possible. Other performance groups have only two damage states when element replacement is considered the only option. Each performance group also has a "no damage" damage state designated DS0, with all repair quantities equal to zero, as well as a repair quantity cap damage state designated DS∞. Additional details pertaining to the damage state limit values, repair methods, and unit repair costs are provided in Chapters 4, 5, and 6.

Approach 1 damage fragilities are generated using the reinforced concrete column structural performance database (*http://nisee.berkeley.edu/spd/*). The discrete damage states of concrete cover spalling, buckling of longitudinal reinforcing bars, and column failure from the database are utilized in this report. Failure is defined as the first occurrence of any of the alternate damage states in the database (bar buckling, longitudinal bar fracture, spiral fracture, concrete crushing, and loss of axial-load-carrying capacity). An additional lower-level damage state is defined for the onset of cracking. Damage models were developed (Berry and Eberhard, 2003, 2005) from the database that relate the probability of exceeding the damage state at varying levels of demand, defined in terms of the tangential drift ratio. Damage fragility curves are shown in Figure 7.6 for the Type 11B bridge and Figure 7.7 for Type 1 bridges. Note that motions with large IMs are required to cause significant probabilities of both bar buckling and column failure.

Damage fragilities can similarly be generated for the other PGs utilized in Approaches 2 and 3; however, these PGs are not illustrated individually here. The parameters of the lognormal distribution that define the probability of exceeding each discrete damage state conditioned on EDP for each PG in this study are contained in Chapter 5.

7.3 PROBABILISTIC LOSS MODELS

The loss model generation phase also differs depending on the approach taken. For the simplified (scalar) approach, the standard PEER method of relating IM-EDP-DM-DV is followed. A loss model is developed that directly relates the bridge-level damage states to repair costs. The repair

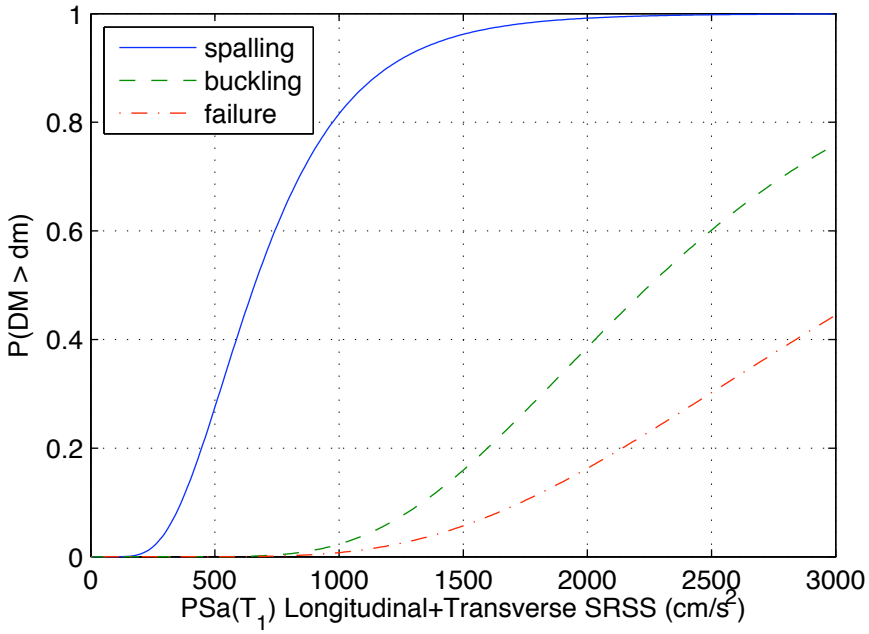

Fig. 7.6 Damage fragilities for Type 11B, RollerAbutment.

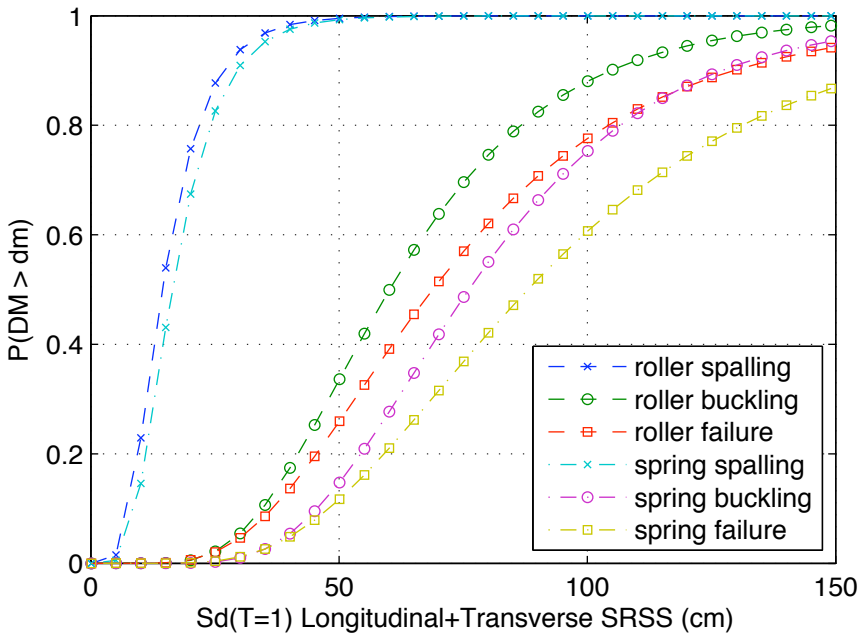

Fig. 7.7 Damage fragilities for Type 1A, SpringAbutment and RollerAbutment.

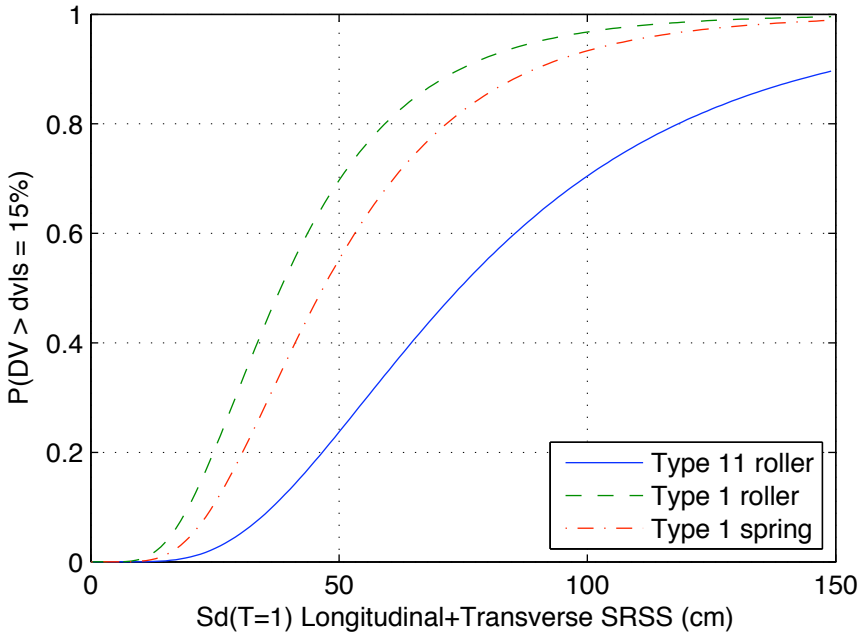

Fig. 7.8 Repair cost ratio fragility for three bridge configurations using HAZUS RCR data and Approach 1.

cost ratio (RCR) data in HAZUS (Basöz and Mander, 1999) were used to define the losses. The damage states of spalling, bar buckling, and failure were matched to the HAZUS damage states of slight, extensive, and complete, respectively to accomplish this. This matching provided a mapping of the component-level damage of the column to the observed bridge level damage that impacted the total repair cost. The resultant loss fragility curves for Types 1 and 11 bridges are shown in Figure 7.8. The loss fragilities also require a limit state for calculation; a value of 15% of the replacement cost is selected here for illustration. It is evident that, for example, even a 60% probability of spalling (from Fig. 7.7) does not incur a significant repair cost. However, the design choices (Type 1 versus Type 11) and modeling choices (Roller versus SpringAbutment) have a significant impact on the probability of exceeding the limiting RCR. These differences can be determined directly from Figure 7.8 because $Sd(T = 1)$ is a structure-independent IM.

To facilitate comparison between the first two approaches taken in this study, the total repair costs obtained using the second approach were normalized by the estimated construction cost of each bridge (Ketchum et al., 2004). The mobilization and contingency costs were removed from the construction cost as they are not included in the repair cost analysis either. This allows a

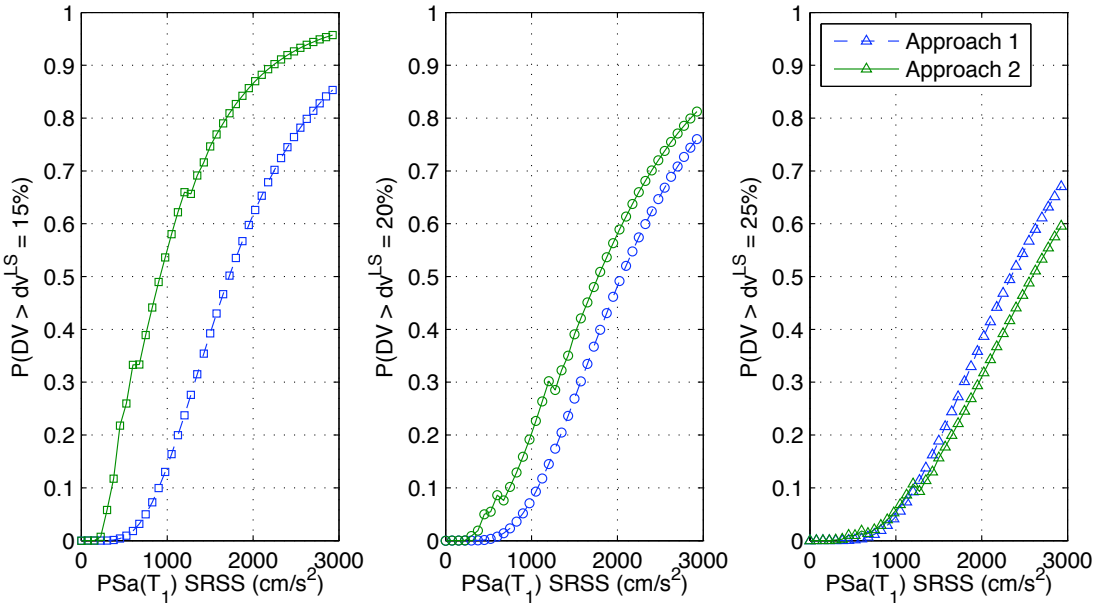

Fig. 7.9 Comparison of repair cost fragilities for Type 11B, RollerAbutment, from Approaches 1 and 2.

comparison of costs without local site considerations. The same RCR limit state (15%) is used for comparison, as well as two additional limit states (20% and 25%). All three RCR limit state fragility comparisons are shown in Figure 7.9. While the formulation of each approach is vastly different, as is the source of cost data, the two methods compare favorably, especially at larger RCR values. For small RCR limit states, the vector approach is conservative (higher probability of exceedance at the same intensity), whereas the opposite is true for larger RCR limit states. This is not a linear trend; however, as the vector approach considers the intensity-dependent behavior of each bridge component. Therefore, at higher intensities, the column replacement repair method will control the repair costs, resulting in a sharp increase in the RCR-IM relationship (Mackie et al., 2006, 2007a).

7.4 DEMAND METHOD COMPARISON

Numerous approaches exist for generating the seismic demands on structures other than the probabilistic seismic demand approach taken in this study. Of particular interest are the different methods of simulation, artificial ground motion record generation, earthquake binning strategies, and

methods of scaling recorded ground motion records. The ATC-58 Project describes some alternative methods for selecting, organizing, and scaling ground motions for use with seismic demand analysis. Other PEER researchers have relied primarily on different forms of stripe or incremental dynamic analyses (IDA).

The modular bridge framework developed in this study is ideal for ground motion studies and comparison of common results. For example, a subset of ground motion records (18 total) was taken from each of the 7 bins used in this study. The I-880 records selected for the testbed project were intended to be scaled, hence 13 of the records were taken from the I-880 bin. All the selected motions were scaled to a constant intensity (longitudinal spectral acceleration at the first-mode period). The process was repeated for 10 intensity levels and the results presented in the same PSDM format used above. The resulting PSDA/IDA comparison is shown in Figure 7.10 for bridge Type 11A with roller abutment. The figure illustrates that the scaling of records within the range of intensities covered by the original cloud study (scaling with, on average, epsilon-neutral records) does not bias the trend of this PSDM. However, it does confirm that the dispersions at higher intensities are larger than lower intensities, a feature not captured by the cloud approach.

7.5 REPAIR COST RATIO RESULTS

This section illustrates in more detail the application of Approach 3 to the baseline bridge (Type 1A) for calculating repair costs. Approach 3 makes use of all of the data presented in Chapters 5 and 6. For comparison, the repair cost ratio models generated in the previous section using Approach 2 are also included in several of the plots. As mentioned in Chapter 2, the data used in Approach 2 were not modified from the original values presented in Mackie et al. (2006, 2007a); therefore, care was taken to normalize the calculated repair costs using the replacement cost corresponding to the 2004 bridges for Approach 2 and 2007 bridges for Approach 3. The normalized quantities (RCR) are thus comparable between the two approaches.

An immediate benefit of the methodology employed in this report is that the intensity-dependent variation in repair cost ratios can be assessed. Both the first and second probabilistic moments of repair cost ratio are calculated for each intensity level, and are shown in Figure 7.11 for three scenarios. It was assumed that after the summing of all of the costs from each repair quantity, the final RCR model followed a normal distribution. The first scenario, labeled “Fixed mean”

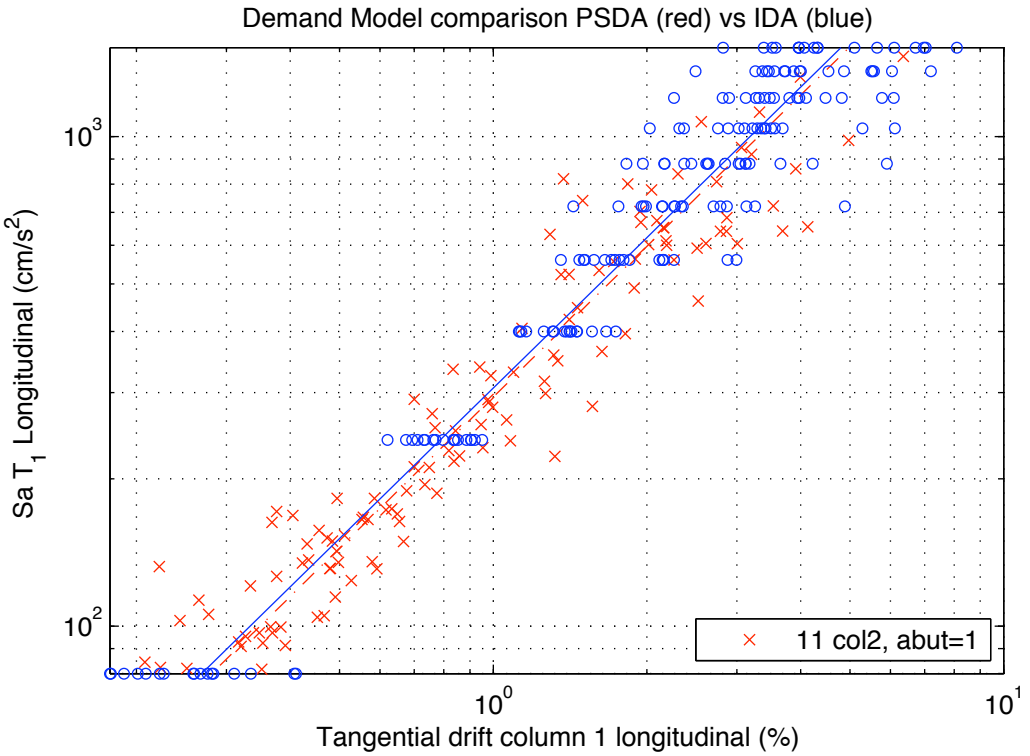

Fig. 7.10 Comparison of tangential drift ratio PSDM for Type 11B, RollerAbutment, using PSDA (red) and IDA (blue).

and "Fixed $\pm 1\sigma$," shows the loss model generated using Approach 3 (RCR versus IM) for testbed bridge Type 1A using SpringAbutment and fixed foundations. For comparison, the same model is analyzed; however, some flexibility is introduced at the base of the columns (Section 4.3). This scenario is labeled as "Springs mean" and "Springs $\pm 1\sigma$." Finally, the previous data set and results generated for the fixed column base case using Approach 2 are included as the scenario labeled "Fourway mean" and "Fourway $\pm 1\sigma$."

Several important observations can be drawn from Figure 7.11. The repair cost ratios are intensity dependent and in this case a structure-independent IM was selected (PGV). This allows direction comparison between all three scenarios shown in the plot by simply selecting a target hazard level on the horizontal axis. Note that while the same structure is employed in all three scenarios, the fundamental periods are different based on modeling assumptions (Table 4.3). In addition, it is apparent that while Approaches 2 and 3 yield similar overall results, Approach 3 provides a higher fidelity on not only the intensity-dependent mean, but also the intensity-dependent uncertainty. Of particular note is the inclusion of DS0 that allows zero (or small) repair cost ratios for small earthquake events, but a rapid growth in the RCR after triggering of damage, whereas Approach 2 shows (unrealistically) an immediate accumulation of RCR. Finally, by introducing some flexibility into the foundation model, some of the non-column damage states are triggered at smaller intensities, leading to higher initial RCRs. However, due to the well-behaved Q-DM models (that include plateaus, for example) using Approach 3, both variants of the same structural model eventually converge to exactly the same RCR.

As is commonly done in seismic risk assessment, it is of interest to plot the repair cost ratio fragility curves for several different discrete hazard levels. For example, for a site in Berkeley, California, the 2%-, 10%-, and 50%-probabilities of exceeding a certain PGA value in 50 years were determined from USGS hazard maps. These PGA values were converted to PGV values using the firm ground conversion of 48 in./sec/g. The resulting PGV values are 149, 89, and 51 cm/s, respectively. The probabilistic moments at each intensity from Figure 7.11 were determined for each of the three hazard scenarios and plotted as complete CDFs in Figure 7.12. The individual curves are labeled as CDFs rather than RCR fragilities because they do not show the probability of a single loss limit state at different earthquake intensity levels. The dotted lines mirroring each curve in the figure are the CDFs obtained by assuming that the resulting repair cost distribution is

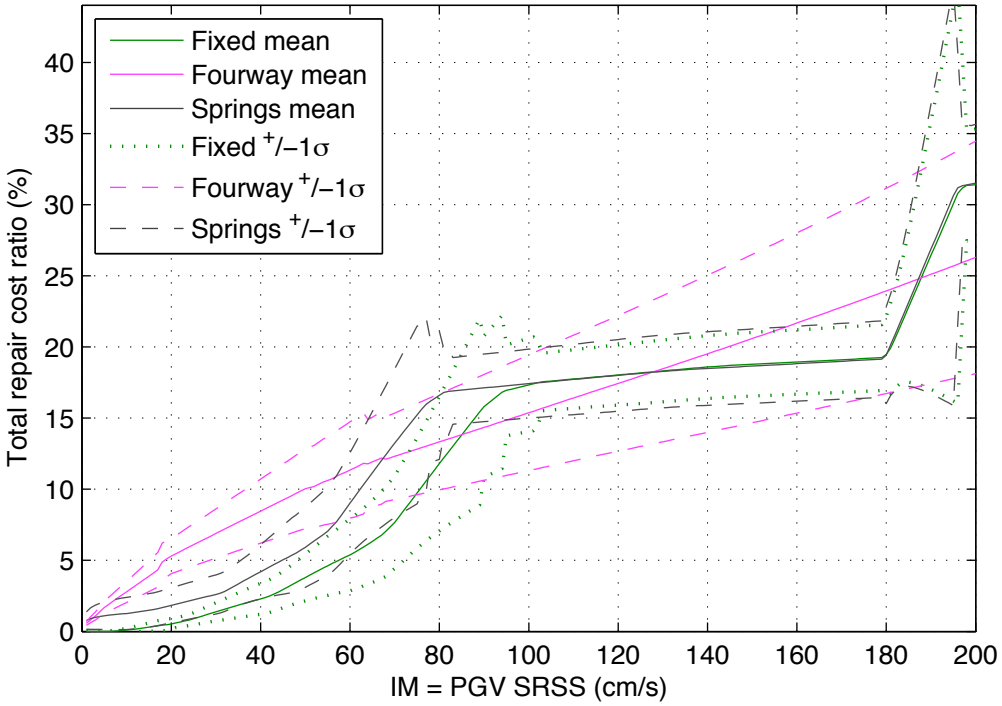

Fig. 7.11 Repair cost ratio loss model as a function of intensity.

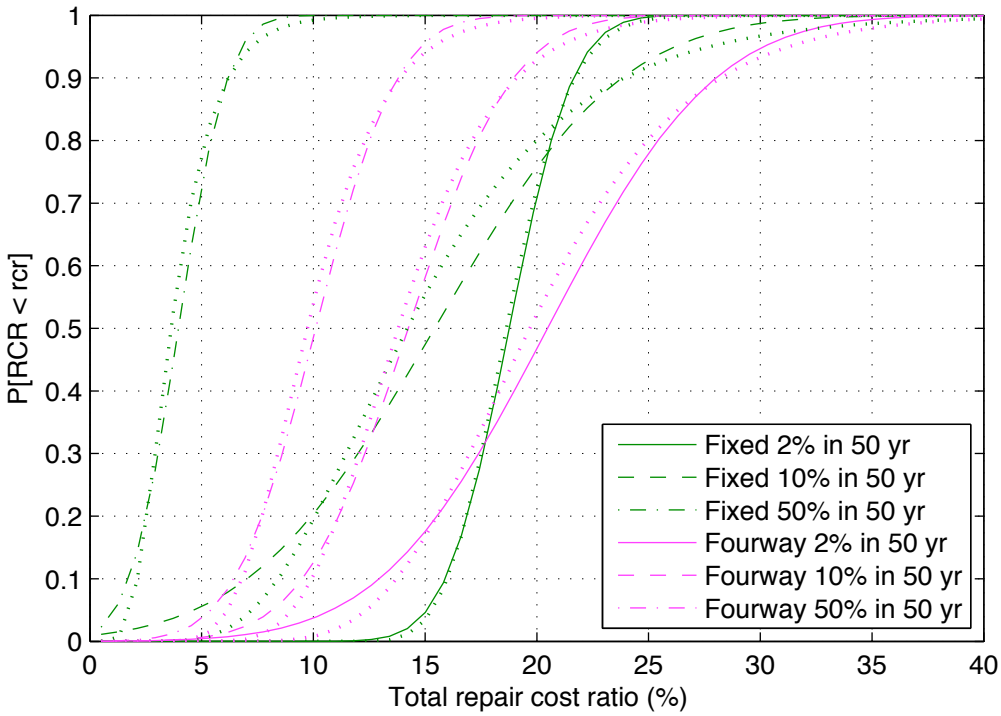

Fig. 7.12 Repair cost ratio CDF for three hazard intensity levels.

lognormal rather than normal.

Rather than generating CDFs for discrete hazard levels, it is also possible to generate standard loss fragility curves that illustrate $P[RCR > rcr|IM = im]$. The resulting fragility curves for three repair cost ratios are shown in Figure 7.13 for the same three limit states used to compare Approaches 1 and 2. As in the previous figure, the curves were computed assuming that the repair cost probability distribution is normal; the curves from a lognormal distribution are shown in dotted lines. However, the major difference is that both the mean and standard deviation for each data point on the fragility curves is intensity dependent. Therefore, for the range of intensities where the repair cost ratios remain essentially constant, so does the probability of exceeding that RCR. The resulting fragility curves are therefore stepwise CDFs and do not necessarily appear like the CDF of a normal distribution. The fragility curves, as plotted, were smoothed using a running average window of one tenth the data length. The agreement between Approaches 1 and 2 is more apparent when considering fixed RCR limit states, rather than the fixed intensities as in Figure 7.12. However, Approach 2 fails to capture the local behavior of the repair cost estimates in intensity

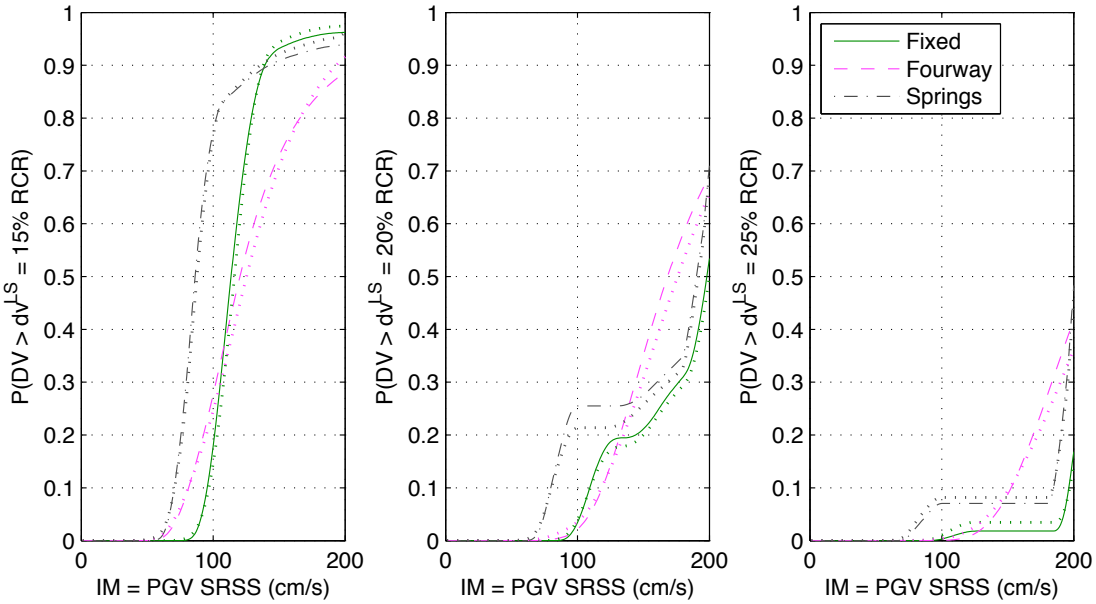

Fig. 7.13 Repair cost ratio fragilities.

windows where repair quantities have plateaued or are not consistently increasing with intensity.

7.5.1 Disaggregation by Repair Quantity

Due to the assembly-based (vector) nature of Approach 3, it is also possible to disaggregate the final repair costs into individual contributions from each repair quantity. Retaining an intensity-dependent format similar to Figure 7.11, the total expected cost from each repair quantity (Q) is shown in Figure 7.14. The ordinate is plotted in units of cost (not normalized as a RCR), and shows only the expected (mean) cost. The peak contribution at the range of intensities between 2%- and 50%- (in-50-years) exceedance probabilities is from temporary support at the abutments. However, this repair quantity is not the chief contributor at all intensities. For example, for PGV less than 50 cm/s, it is a low-level damage repair item (epoxy inject cracks) that controls. Conversely, at PGV of approximately 175 cm/s, serious damage leads to the need to replace a column and hence temporary support of the superstructure begins to rise rapidly as a contributing cost.

A similar disaggregation can be shown for the contribution of each repair quantity to the total cost standard deviation, as in Figure 7.15. Due to the formulation, and intuitively as well, when individual repair quantities are rising rapidly, there is greater uncertainty in the prediction of the

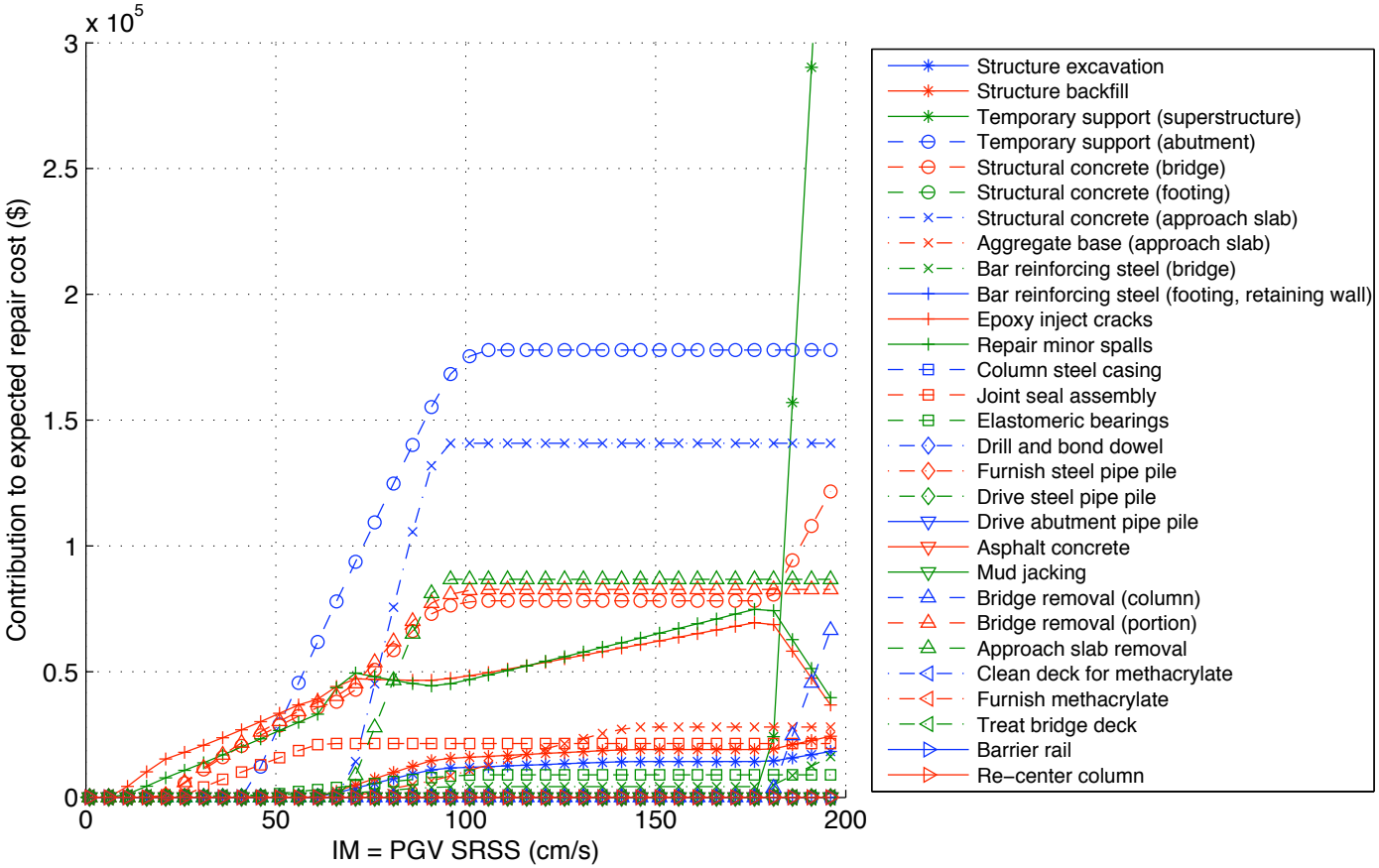

Fig. 7.14 Disaggregation of expected repair cost by repair quantity as a function of intensity.

total cost due to that repair quantity. On the contrary, once repair quantities have stabilized (for example, a certain repair quantity has reached the maximum permissable value DS∞), there is relatively small uncertainty surrounding the total cost due to that repair quantity. These trends are reflected clearly in Figure 7.15. Once the abutment temporary support repair quantity stabilizes, the standard deviation drops to a constant level, whereas the standard deviation of the superstructure temporary support climbs steeply with the increase in the expected value of the quantity.

A similar presentation of the disaggregation of expected repair cost by repair quantity can be made by selecting discrete hazard levels of interest and plotting repair quantity contributions in the form of a pie chart. The disaggregation of expected costs at the four hazard levels of 2%-, 10%-, 50%-, and 86%-in-50-years exceedance probabilities is shown in Figure 7.16. The charts have been calibrated such that the remaining repair quantities that contribute a total of 10% or less of the total expected cost are lumped together in a group named "Other." The relative contribution of, for example, epoxy injecting cracks at the 86% probability of exceedance in 50 years is evident, whereas, the largest contribution is from abutment temporary support for the 2%-in-50-years hazard level.

7.5.2 Disaggregation by Performance Group

While disaggregation by repair quantity is helpful, it does not describe specifically what component or performance group contributes most to the ultimate repair cost. It is also possible for one repair quantity to dominate because several performance groups require that item in the associated repair methods for that group. Therefore, the total expected cost was also disaggregated by performance group, as shown in Figure 7.17. This disaggregation is possible for the expected cost; however, it is not as straightforward to obtain the contribution of each performance group to the repair cost standard deviation due to the correlations introduced between performance groups (Eq. 2.19). Figure 7.17 provides more insight into why a repair quantity employed in several performance group repair methods features in the expected cost.

For example, bridge structural concrete contributes to a significant portion of the overall expected cost at all intensities in Figure 7.14. The reason for this is more readily apparent in Figure 7.17 as both the abutment PGs (BB and EB in Fig. 4.1), with damage states defined in terms of the maximum longitudinal relative deck-end/abutment displacement EDPs, have the largest con-

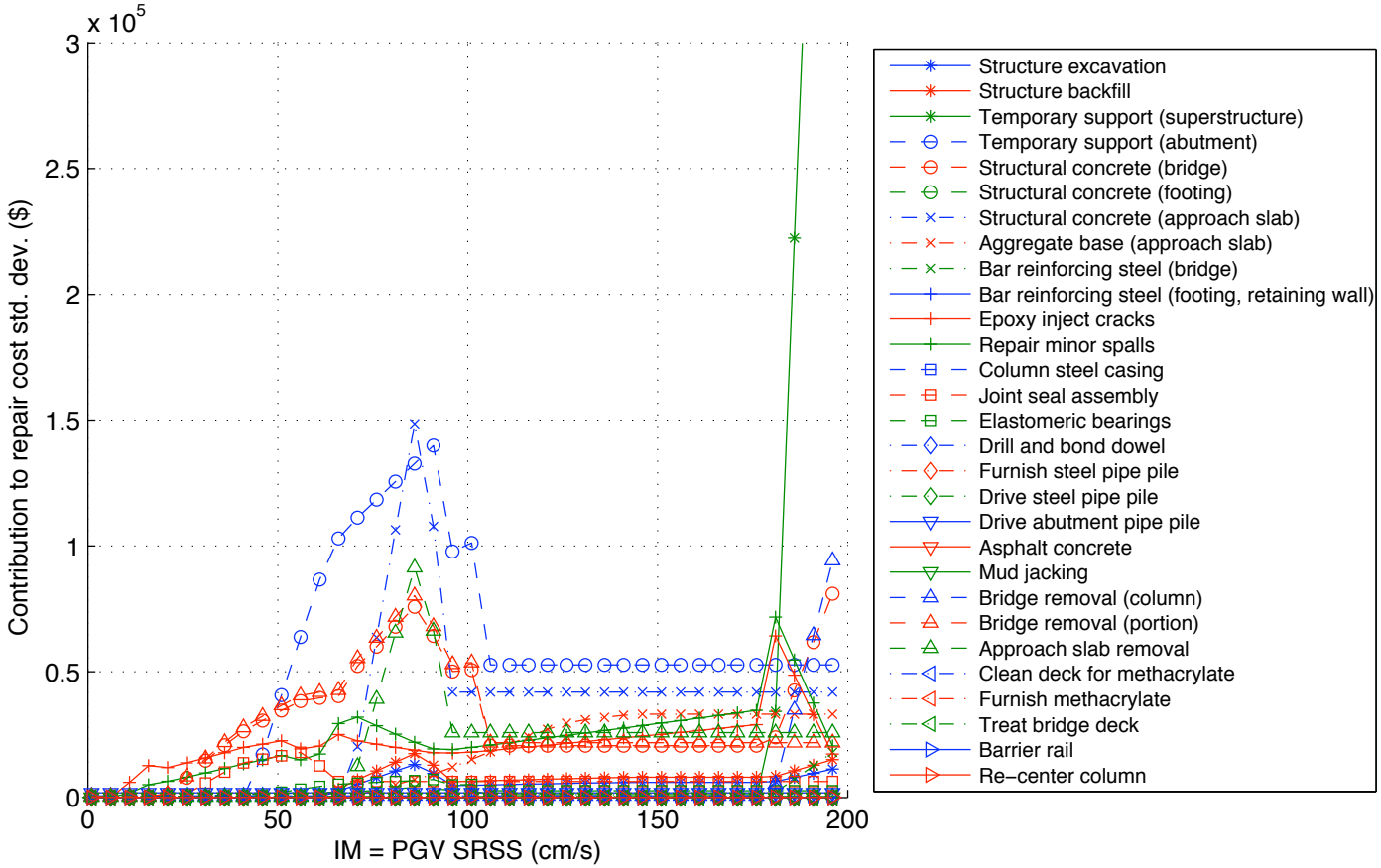

Fig. 7.15 Disaggregation of repair cost standard deviation by repair quantity as a function of intensity.

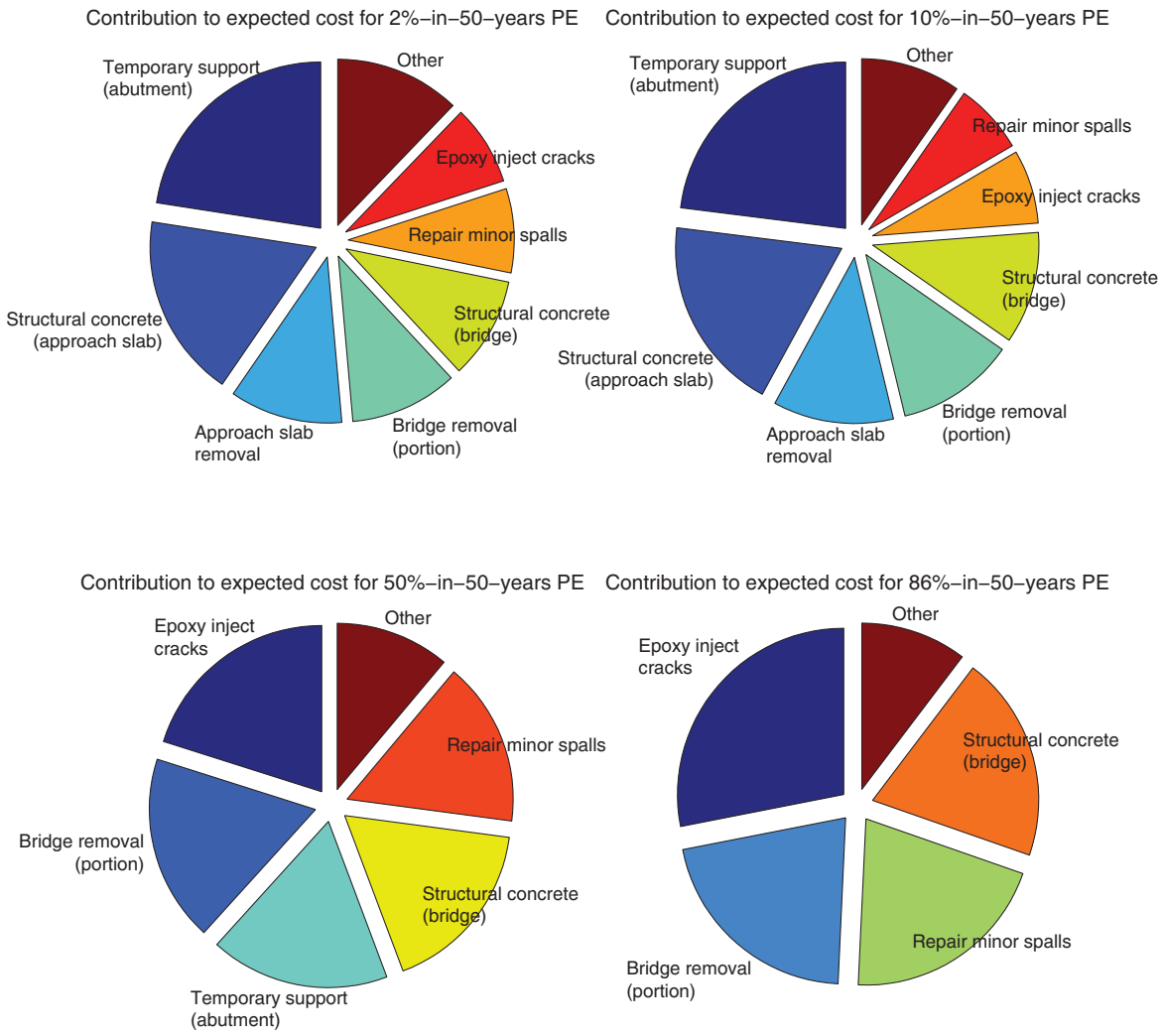

Fig. 7.16 Disaggregation of repair cost by repair quantity for 4 discrete hazard levels.

tribution in the range of intensities between 2%- and 50%- (in-50-years) exceedance probabilities. This indicates that the concrete is necessary to repair the back wall. The overall repair to the abutment PGs are more costly than the bearing repairs that require temporary abutment support, as would be surmised from looking at Figure 7.14 alone. Another illustration of information gained from Figure 7.17 is the sharp increase in costs at an intensity of approximately 175 cm/s. Figure 7.14 indicates only that this is due to the need for temporary support of the superstructure. However, from Figure 7.17, one is able to discern that the increase is due to the excessive maximum tangential drift ratios of columns 2 and 3 requiring support to replace the column.

7.6 REPAIR TIME RESULTS

The following plots show repair time results for the baseline bridge (Type 1A) using Approach 3. As with the results for repair cost ratio, the two different foundation modeling scenarios were considered. Figure 7.18 shows the first two probabilistic moments of the intensity-dependent total repair time loss model (in terms of CWD). The uncertainty arises from the PERT criteria for each of the repair quantities, not from the uncertainty in the repair quantities themselves. The fixed-base column scenario is labeled "Fixed mean" and "Fixed $\pm 1\sigma$," while the column bases with flexibilities scenario is labeled "Springs mean" and "Springs $\pm 1\sigma$." As with the RCR estimates, repair time estimates from both foundation models converge to the same values at intensities greater than about 70 cm/s. It is reiterated here that the repair time estimates are based on the numerous simplifying assumptions for repair effort (not repair duration) described in Chapter 6. They are not intended to be complex estimates that take into account work crew dependencies, furnishing and installation times, and critical paths.

The fixed-base scenario demonstrates the probabilistic accumulation of repair effort (in terms of CWD) required as the earthquake intensity increases. As with the repair cost plots, at intensities greater than 175 cm/s, the column replacement repair is triggered and both the required repair effort and report cost increase substantially. The scenario with foundation flexibility yields similar results. However, as a byproduct of the methodology, this scenario also yields a small estimated number of CWD for zero intensity events. This is due to the larger initial transverse forces on the abutment shear keys that trigger the shear key repair methods immediately. Once again, this information is more easily obtained by disaggregating the total expected repair time by repair

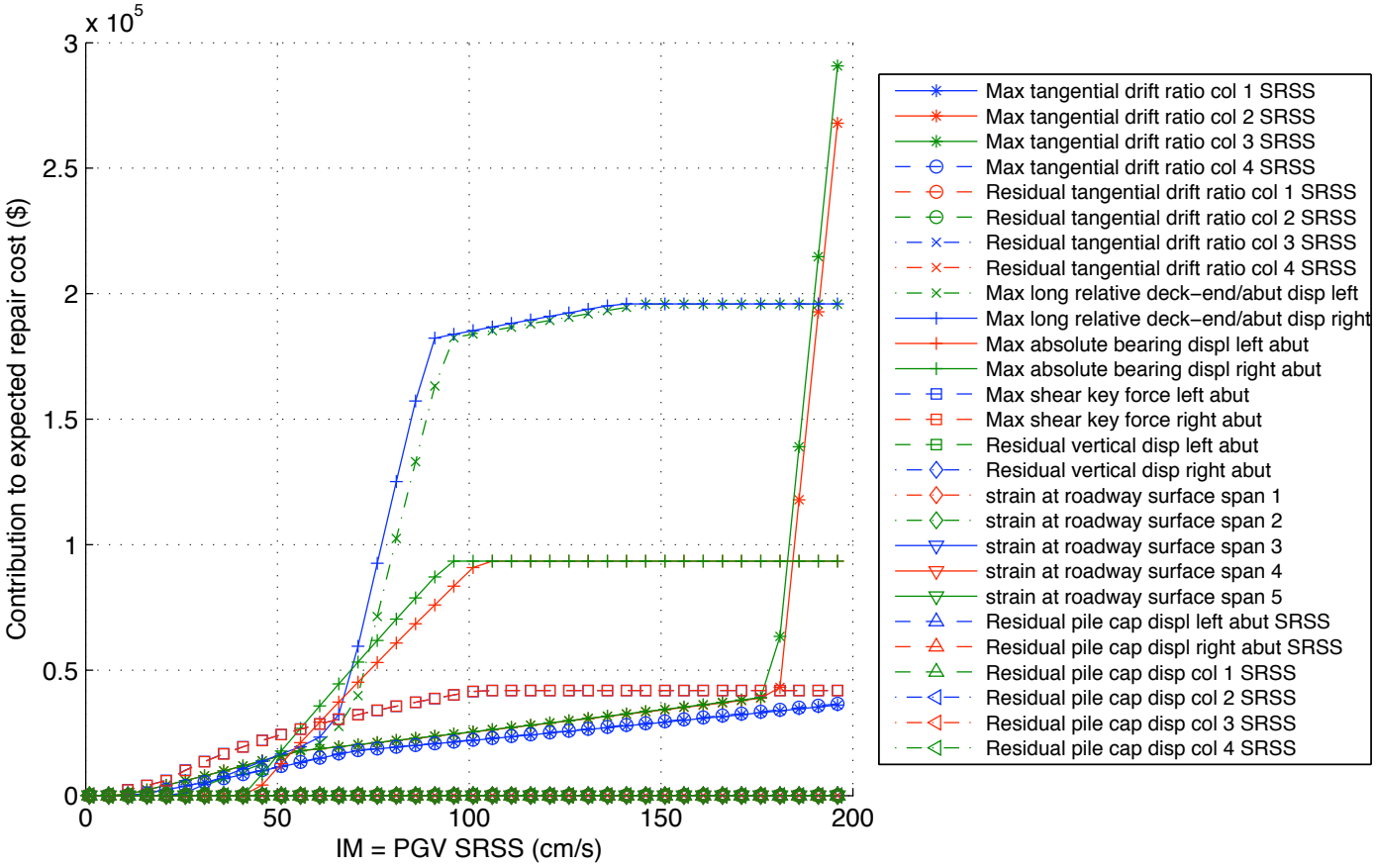

Fig. 7.17 Disaggregation of repair cost by performance groups as a function of intensity.

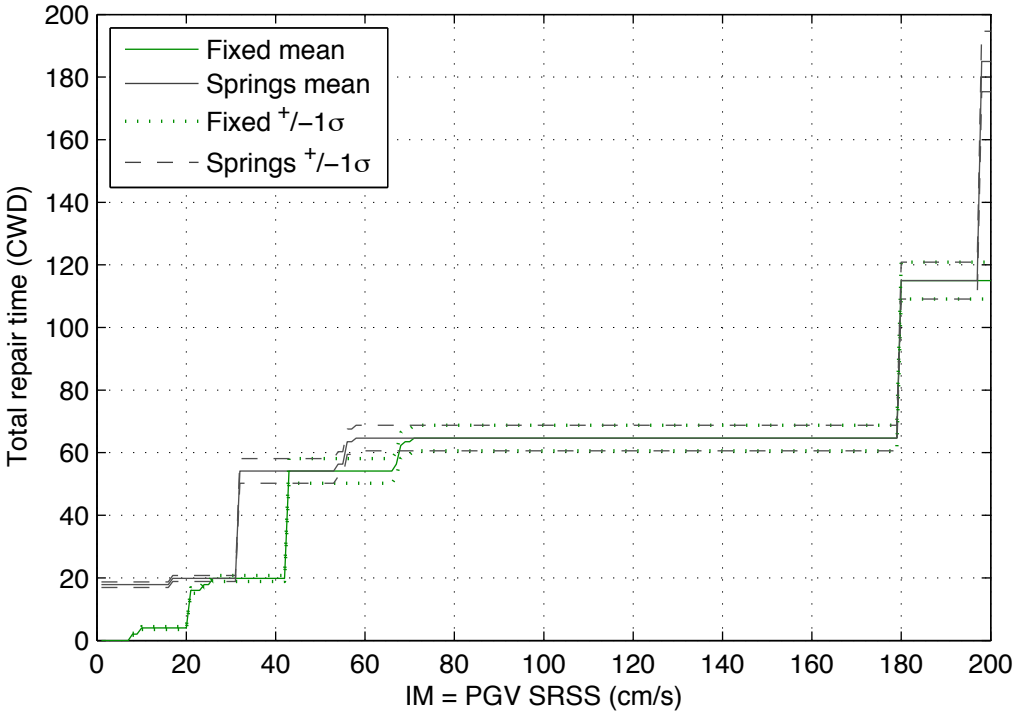

Fig. 7.18 Repair time loss model as a function of intensity.

quantity, as illustrated for the fixed-base scenario in Figure 7.19.

However, such a disaggregation plot does not provide as much information at the disaggregation of repair cost by repair quantity because the plot shows only when each repair quantity triggers a contribution to the total repair effort. Therefore, the maximum values in Figure 7.19 are merely the mean values from the production spreadsheet. Along similar lines, it is nonsensical to disaggregate the expected repair time by performance group as was done for repair cost because multiple performance groups may cause an increase in repair quantity that would trigger the repair effort increase.

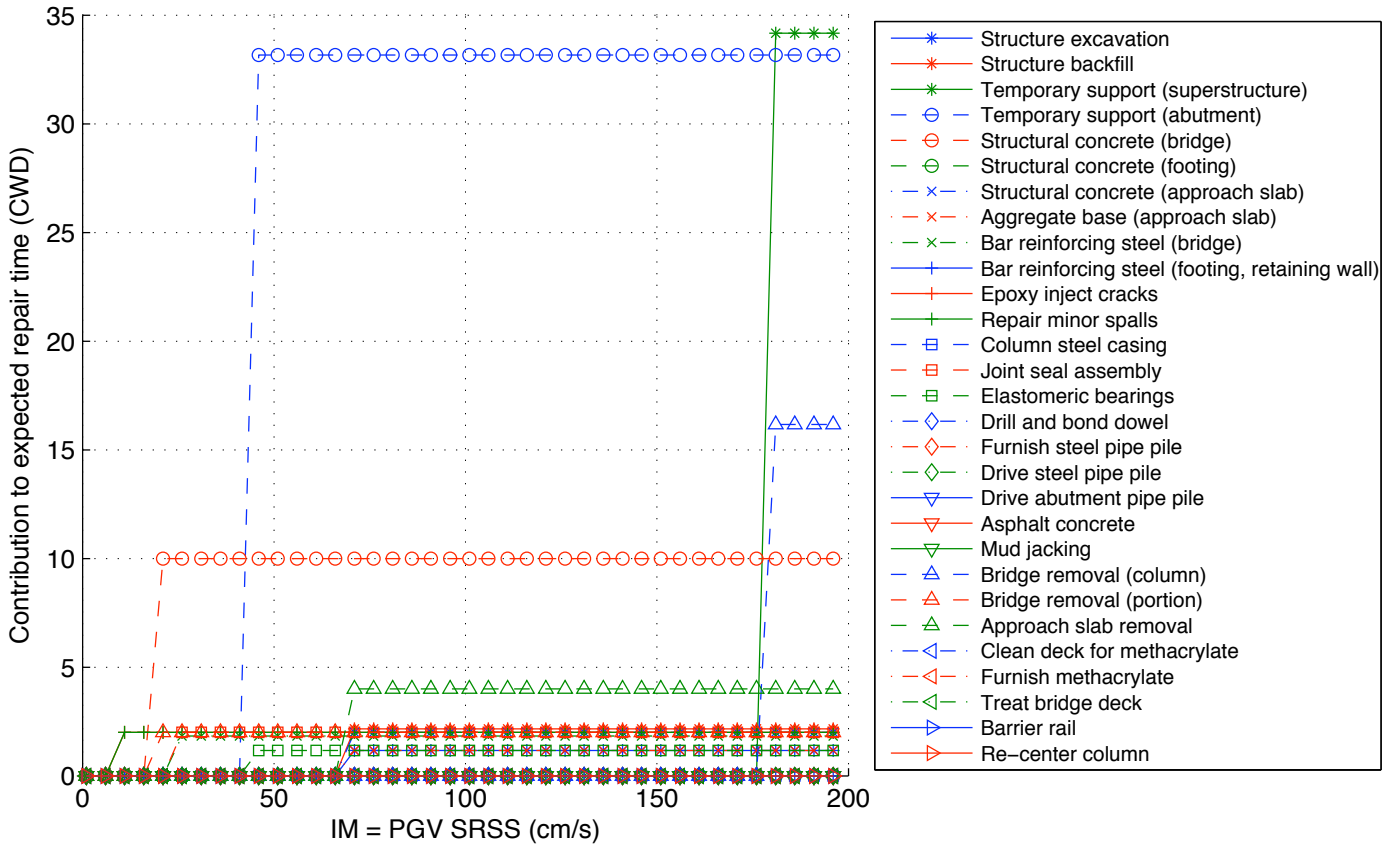

Fig. 7.19 Disaggregation of expected repair cost by repair quantity as a function of intensity.

8 Conclusions

Performance-based earthquake engineering aims to quantify the seismic performance of engineered facilities using metrics that are of immediate use to both engineers and stakeholders. Such an engineering approach directly addresses the need to increase the earthquake safety and reduce the earthquake risk exposure of our society. Practicing performance-based earthquake engineering requires abandoning the prescriptive safety specifications and embracing a design for performance objectives defined in terms of quantities familiar to engineers, owners, managers, and stakeholders alike. The main goals of the multi-disciplinary research teams that constitute the PEER Center have been to develop a performance-based earthquake engineering (PBEE) methodology and probabilistic framework, and to facilitate their adoption in engineering practice.

Performance-based seismic evaluation and design of bridges is an important component of the PEER Center effort. Bridges are expensive infrastructure components, requiring significant investments for both new construction and repair. They are also essential elements of regional transportation networks, vital for post-earthquake recovery and resumption of normal life. A coordinated group of PEER research teams addressed performance-based earthquake engineering of bridges. A central component of the PEER bridge work, an integrated probability-based evaluation of seismic performance of typical reinforced concrete bridges in California, is presented in this report.

Two classes of benchmark reinforced concrete bridge types typical of new construction in California are evaluated. Models of these structures are created that account for nonlinear behavior of the columns, deck, abutments, and expansion joints at the abutments. The performance-based evaluation procedure is then followed: seismic demand models are then developed using nonlinear time history analysis, damage to vital bridge components classified into performance groups is

determined using experimental and empirical databases, repair methods are associated with each performance group and damage state, and repair cost ratios and repair durations are estimated. Three realistic damage scenarios are developed to calibrate repair cost and repair working days estimate data.

The results are presented as repair cost ratio and repair time loss models and fragilities. Three separate approaches were employed to estimate the resultant fragilities: one scalar approach based on discrete bridge-level damage states, and two vector approaches that use an assembly of discrete damage states over all the performance groups. The performance of the benchmark bridges, particularly bridge Type 1A, is intended to serve as a baseline for other PEER researchers to measure the change of bridge seismic performance due to use of new, experimentally calibrated models of column, abutment, and foundation components; due to use of new enhanced-performance structural elements and response modification devices; and due to explicit consideration of liquefaction and lateral spreading. The benchmark bridges performance research can also serve as a baseline for transportation network studies by other PEER researchers.

Two valuable contributions are presented in this report:

- The first contribution is a method to generate decision-level repair cost and repair time bridge fragility curves directly, using a fully consistent probabilistic implementation of the PEER PBEE framework. This method is based on a closed-form integration of the total probability framing equation and on analytical representation of the intermediate demand, damage, and decision models. Guidelines for developing these models are also presented and illustrated using the benchmark bridges. The particular fragility curves computed for the selected benchmark bridges presented in this report are valid and can be used as input for traffic network evaluation or other studies. However, a wider use of the fragility curves presented in this report is limited by the selection of the benchmark bridges. The presented method enables engineers to generate the relevant fragility curves for the particular bridge with the fidelity required for the particular practical application.
- The second contribution is an implementation of the PEER PBEE framework. This implementation, developed for the testbed bridges, is modular to allow plug-and-play incorporation of emerging structural components, response modification technologies, analysis methods and repair techniques instead of the ones used in this report. The implementation

is based on a general closed-form solution of the PEER framework total probability integral based on demand, damage, and loss models developed in this report for the benchmark bridges. A method for developing such models for other structures is presented. A Matlab-based tool is developed to facilitate the integration of the PEER framework total probability integral. Finally, a data structure designed to efficiently organize and store the data and interim results, is presented. Together, the implemented tools and data structures form a solid basis for conducting probabilistic performance-based seismic evaluations of any structure using the PEER Center framework.

The findings presented in this report, as well as the work of other PEER researchers, are already impacting the practice of structural engineering. Fragilities of the benchmark bridges are, also, used in several followup ongoing research projects. The goals of these projects are to directly affect the way Caltrans engineers design bridges by providing modeling guidelines and formulating changes in the Caltrans Seismic Design Criteria document.

Nevertheless, many opportunities for further work remain. Much work is needed to better understand bridge components other than columns. Abutment structures, joints, approaches, and foundations are important contributors to repair-related decisions. Improving their finite element models, cataloguing their damage states, and examining their repair methods is essential for completing the bridge work started in this report. Another important area where focused research may yield a significant payoff is the investigation of decision-level fragility curve sensitivity to the accuracy and associated complexity of the finite element model of the bridge used to formulate the demand model. Some of the results presented in this report suggest that a significantly simpler bridge model may be used to evaluate seismic demand without a significant loss of accuracy of the resulting repair-related fragility curves. This conclusion is based on the current discrete definition of bridge component damage states. This is the most important research area related to the individual element of the PEER PBEE framework. A significant reduction in the dispersion (uncertainty) of the resulting fragility curves can be achieved by redefining damage as continuous rather than a discrete-valued quantity. The impact of such fundamental change on reducing uncertainty may justify the significant effort needed to redefine practically all damage models developed to date.

Performance evaluation of bridge systems is another widely open research field. Using the implementation of the PEER framework presented in this study, researchers can easily accom-

plish evaluations of other typical bridge types. These bridges should include multi-column bents, skew at abutments, expansion joints, different column heights, and curved deck geometries. Completion of benchmark fragility curves for such bridges would practically cover the entire Caltrans bridge portfolio, providing excellent data for traffic network studies. Another area of bridge system investigations opened by this report is a rational evaluation of the benefits and costs of enhanced-performance bridge structural elements and response modification devices. Rigorous application of the PBEE framework and the benchmark bridge data would enable a direct comparison of the total life-cycle costs of such new bridge designs to the conventional bridges. Such comparisons may identify the new technologies which would not only improve bridge performance but also reduce their costs.

Finally, two important aspects of engineering design methodology should be investigated further. First, the implementation of the PEER PBEE framework presented in this report is focused on the problem of evaluation. However, it can be used as a basis to develop direct performance-based design methods. Second, the synergy among engineering specialties required to produce demand, damage and decision models presented in this report (namely, structural, geotechnical and construction engineering) points to the need to reconsider the merits of modern division between these specialities. An integrated approach to design, such as set-based performance-centric design, may yield such significant economies to mandate a change of the current engineering design model and strengthen the need for a holistic approach to design. This may, in turn, trigger a change from training highly specialized experts back to educating engineers capable of understanding the entire design problem. A performance-based paradigm may, indeed, permeate civil engineering in ways we have not imagined to date.

REFERENCES

Alavi, B. and Krawinkler, H. (2004). Behavior of moment-resisting frame structures subjected to near-fault ground motions. *Earthquake Engineering and Structural Dynamics* 33(6): 687–706.

ATC (1996). *Seismic evaluation and retrofit of concrete buildings*, volume 1. Applied Technology Council, Redwood City, CA.

ATC/MCEER Joint Venture (2002). *Comprehensive Specification for the Seismic Design of Bridges*. Report No. NCHRP Report 472, National Cooperative Highway Research Program, Transportation Research Board, Washington DC. URL `http://onlinepubs.trb.org/onlinepubs/nchrp/nchrp_rpt_472.pdf`.

Baker, J. W. and Cornell, C. A. (2003). *Uncertainty specification and propagation for loss estimation using FOSM methods*. Report No. 2003/07, University of California, Pacific Earthquake Engineering Research Center, Berkeley CA.

Baker, J. W. and Cornell, C. A. (2005). A vector-valued ground motion intensity measure consisting of spectral acceleration and epsilon. *Earthquake Engineering and Structural Dynamics* 34(10): 1193–1217.

Basöz, N. and Kiremidjian, A. S. (1996). *Risk assessment for highway transportation systems*. Report No. 118, Stanford University, John A Blume Earthquake Engineering Center, Stanford CA.

Basöz, N., Kiremidjian, A. S., Hortacsu, A., and Williams, M. (1997). *Evaluation of bridge damage data from the Loma Prieta and Northridge, CA earthquakes*. Report No. 127, Stanford University, John A Blume Earthquake Engineering Center, Stanford CA.

Basöz, N., Kiremidjian, A. S., and King, S. A. (1999). Statistical analysis of bridge damage data from the 1994 northridge, CA, earthquake. *Earthquake Spectra* 15(1): 25–54.

Basöz, N. and Mander, J. (1999). *Enhancement of the highway transportation lifeline module in HAZUS*. National Institute of Building Sciences, Washington DC.

Beaulieu, N. C., Abu-Dayya, A. A., and McLane, P. J. (1995). Estimating the distribution of a sum of independent lognormal random variables. *IEEE Transactions on Communications* 43(12): 2869–2873.

Berry, M. P. and Eberhard, M. O. (2003). *Performance models for flexural damage in reinforced concrete columns*. Report No. 2003/18, University of California, Pacific Earthquake Engineering Research Center, Berkeley CA.

Berry, M. P. and Eberhard, M. O. (2004). *PEER structural performance database user's manual*. Report no., University of California, Pacific Earthquake Engineering Research Center, Berkeley CA.

Berry, M. P. and Eberhard, M. O. (2005). Practical performance model for bar buckling. *Journal of Structural Engineering* 131(7): 1060–1070.

Bozorgzadeh, A., Megally, S., Restrepo, J. I., and Ashford, S. A. (2005). Capacity evaluation of exterior sacrificial shear keys of bridge abutments. *Journal of Bridge Engineering* 11(5): 555–565.

Branco, F. A. and de Brito, J. (2004). *Handbook of concrete bridge management*. American Society of Civil Engineers, Reston, VA, 227–266 pp.

Caltrans (1999a). *Seismic Design Criteria 1.1*. California Department of Transportation, Sacramento, CA.

Caltrans (1999b). *Standard Specifications*. California Department of Transportation, Sacramento, CA, July.

Caltrans (2004). *Seismic Design Criteria 1.3*. California Department of Transportation, Sacramento, CA.

Choi, E., DesRoches, R., and Nielson, B. (2004). Seismic fragility of typical bridges in moderate seismic zones. *Engineering Structures* 26(2): 187–199.

Conte, J. P. (2003). Ground motion intensity measures for performance-based earthquake engineering. In *Proc., 9th International Conference on Application of Statistics and Probability in Civil Engineering*, San Francisco, CA, July 6-9.

Cornell, C. A., Jalayer, F., Hamburger, R. O., and Foutch, D. A. (2002). Probabilistic basis for 2000 SAC/FEMA steel moment frame guidelines. *Journal of Structural Engineering* 128(4): 526–533.

Cornell, C. A. and Krawinkler, H. (2000). Progress and challenges in seismic performance assessment. *PEER Center News* 3(2): 1–2.

Der Kiureghian, A. (2005). Non-ergodicity and PEER's framework formula. *Earthquake Engineering and Structural Dynamics* 34(13): 1643–1652.

Division of Engineering Services (1994). *Bridge Design Details*. Report no., California Department of Transportation. URL `http://www.dot.ca.gov/hq/esc/techpubs/manual/bridgemanuals/bridge-design-details/bdd.html`.

Division of Engineering Services (2004). *Bridge Memo to Designers*. Report no., California Department of Transportation. URL `http://www.dot.ca.gov/hq/esc/techpubs/manual/bridgemanuals/bridge-memo-to-designer/bmd.html`.

Division of Engineering Services (2005). *Bridge Design Aids*. Report no., California Department of Transportation. URL `http://www.dot.ca.gov/hq/esc/techpubs/manual/bridgemanuals/bridge-design-aids/bda.html`.

Division of Engineering Services (2007). *Price Index for Selected Highway Construction Items*. Report no., California Department of Transportation. URL `http://www.dot.ca.gov/hq/esc/oe/contract_progress/cost-index-summary.pdf`.

Division of Engineering Services—Cost Estimates Branch (2007a). *Bridge Construction Cost Index, 1970–2006*. Report no., California Department of Transportation. URL `http://www.dot.ca.gov/hq/esc/estimates/Bridge_Construct_Cost_Index_1970_2006.xls`.

Division of Engineering Services—Cost Estimates Branch (2007b). *Comparative Bridge Costs, 2006*. Report no., California Department of Transportation. URL `http://www.dot.ca.gov/hq/esc/estimates/COMP_BR_COSTS_2006-eng.xls`.

Division of Engineering Services—Cost Estimates Branch (2007c). *Structure Cost Index*. Report no., California Department of Transportation. URL `http://www.dot.ca.gov/hq/esc/estimates/quarterlycostindex.xls`.

Division of Engineering Services—Office Engineer (2004). *Standard Plans*. California Department of Transportation, Sacramento, CA, July.

Division of Structure Maintenance and Investigations (2000). *Element Level Inspection Manual*. California Department of Transportation, Sacramento, CA, September.

Elnashai, A. S., Borzit, B., and Vlachos, S. (2004). Deformation-based vulnerability functions for RC bridges. *Struct. Engng. and Mech.* 17(2): 215–244.

Fajfar, P., Gašperšiš, P., and Drobnič, D. (1997). A simplified nonlinear method for seismic damage analysis of structures. In *Seismic design methodologies for the next generation of codes*, *Eds.* Fajfar, P. and Krawinkler, H., Balkema, Rotterdam, pp. 183–194.

Federal Highway Administration (2003). National bridge inventory. URL `http://www.fhwa.dot.gov/bridge/nbi.htm`.

Gardoni, P., Der Kiureghian, A., and Mosalam, K. M. (2002). *Probabilistic models and fragility estimates for bridge components and systems*. Report No. 2002/13, University of California, Pacific Earthquake Engineering Research Center, Berkeley CA.

Harris, R. B. (1978). *Precedence and arrow networking techniques for construction*. Wiley, New York, NY, 326–329 pp.

Hoppe, E. J. (1999). *Guidelines for the use, design, and construction of bridge approach slabs*. Report No. VTRC 00-R4, Virginia Transportation Research Council, Virginia Transportation Research Council, Charlottesville, VA. URL `http://ntl.bts.gov/lib/9000/9800/9852/00-r4.pdf`.

Hose, Y., Silva, P., and Seible, F. (2000). Development of a performance evaluation database for concrete bridge components and systems under simulated seismic loads. *Earthquake Spectra* 16(2): 413–442.

Iervolino, I. and Cornell, C. A. (2005). Record selection for nonlinear seismic analysis of structures. *Earthquake Spectra* 21(3): 685–713.

Jalayer, F. (2003). *Direct probabilistic seismic analysis: Implementing nonlinear dynamic assessments*. Ph.D. thesis, Stanford University.

Jeong, H., Sakai, J., and Mahin, S. A. (2008). *Shaking table tests of self-centering reinforced concrete columns*. Report No. 2008/xx, forthcoming, University of California Berkeley, Pacific Earthquake Engineering Research Center, Berkeley CA.

Karim, K. R. and Yamazaki, F. (2001). Effect of earthquake ground motions on fragility curves of highway bridge piers based on numerical simulation. *Earthquake Engng. Struct. Dyn.* 30(12): 1839–1856.

Ketchum, M., Chang, V., and Shantz, T. (2004). *Influence of Design Ground Motion Level on Highway Bridge Costs*. Report No. Lifelines 6D01, University of California, Pacific Earthquake Engineering Research Center, Berkeley CA.

Kiremidjian, A. S., Hortacsu, A., and Williams, M. (2002). Implications of different site hazards on the highway network loss estimation. In *Proceedings of the Fourth China-Japan-USA Trilateral Symposium on Lifeline Earthquake Engineering*, Qindao, China, October 28-31.

Kramer, S. L., Arduino, P., and Shin, H. (2008). *Performance-based evaluation of bridges on liquefiable soils using OpenSees*. Report No. 2008/xx, forthcoming, University of California Berkeley, Pacific Earthquake Engineering Research Center, Berkeley CA.

Krawinkler, H., *Ed.* (2005). *Van Nuys hotel building: Exercising seismic performance assessment*. Report No. 2005/11, University of California Berkeley, Pacific Earthquake Engineering Research Center, Berkeley CA.

Krawinkler, H. and Ibarra, L. (2003). Collapse probability of frame structures with deteriorating properties. In *Performance-based engineering for earthquake resistant reinforced concrete structures: A volume honoring Shunsuke Otani, Eds*. T.Kabeyasawa and Shiohara, H., pp. 325–338.

Kunnath, S. K., *Ed*. (2006). *Application of the PEER PBEE Methodology to the I-880 Viaduct*. Report No. 2006/10, University of California Berkeley, Pacific Earthquake Engineering Research Center, Berkeley CA.

Ledezma, C. A. and Bray, J. D. (2008). *Performance-based earthquake engineering design evaluation procedure for bridge foundations undergoing liquefaction-induced lateral spreading*. Report No. 2007/xx, forthcoming, University of California Berkeley, Pacific Earthquake Engineering Research Center, Berkeley CA.

Lee, W. K. and Billington, S. L. (2008). *Performance-based earthquake engineering assessment of self-centering post-tensioned concrete bridge systems*. Report No. 2008/xx, forthcoming, University of California Berkeley, Pacific Earthquake Engineering Research Center, Berkeley CA.

Luco, N. and Cornell, C. A. (2003). Structure-specific scalar intensity measures for near-source and ordinary earthquake ground motions. *Earthquake Spectra* in press.

Luna, R., Robison, J. L., and Wilding, A. (2003). *Evaluation of bridge approach slabs, performance and design*. Report No. University Transportation Center Report R80, University of Missouri–Rolla, Center for Infrastructure Engineering Studies. URL `http://campus.umr.edu/utc/research/r080/cr/cr.pdf`.

Mackie, K. (2004). *Fragility-based Seismic Decision Making for Highway Overpass Bridges*. Ph.D. thesis, University of California, Berkeley, CA.

Mackie, K. and Stojadinović, B. (2001). Probabilistic seismic demand model for california highway bridges. *Journal of Bridge Engineering* 6(6): 468–481.

Mackie, K. and Stojadinović, B. (2003). *Seismic demands for performance-based design of bridges*. Report No. 2003/16, University of California, Pacific Earthquake Engineering Research Center, Berkeley CA.

Mackie, K. and Stojadinović, B. (2004a). Improving probabilistic seismic demand models through refined intensity measures. In *Proc., 13th World Conference on Earthquake Engineering*, Vancouver, Canada, August 1-6.

Mackie, K. and Stojadinović, B. (2004b). Residual displacement and post earthquake capacity of highway bridges. In *Proc., 13th World Conference on Earthquake Engineering*, Vancouver, Canada, August 1-6.

Mackie, K. and Stojadinović, B. (2006a). Seismic vulnerability of typical multi-span california highway bridges. In *Proc., 5th National Seismic Conference on Bridges and Highways*, San Francisco, CA, September 18-20.

Mackie, K. R. (2007a). Matlab closed-form PBEE tool. Matlab file PEER_PBEE.m. URL `http://www.ce.berkeley.edu/~boza/PEER-PBEE`.

Mackie, K. R. (2007b). Matlab generalized PBEE tool. Matlab file PEER_PBEE_general.m. URL `http://www.ce.berkeley.edu/~boza/PEER-PBEE`.

Mackie, K. R. and Stojadinović, B. (2005). *Fragility basis for California highway overpass bridge seismic decision making*. Report No. 2005/02, University of California Berkeley, Pacific Earthquake Engineering Research Center, Berkeley CA.

Mackie, K. R. and Stojadinović, B. (2006b). Fourway: a graphical tool for performance-based earthquake engineering. *Journal of Structural Engineering* 132(8): 1274–1283.

Mackie, K. R. and Stojadinović, B. (2006c). Fragilities of peer center testbed bridges. In *Proc., 1st European Conference on Earthquake Engineering and Seismology*, Geneva, Switzerland, September 3-8.

Mackie, K. R. and Stojadinović, B. (2006d). Probabilistic repair cost evaluation for the uc berkeley seismic replacement building using the fourway graphical method. In *Proc., 8th National Conference on Earthquake Engineering*, San Francisco, April 18-22.

Mackie, K. R. and Stojadinović, B. (2007a). Performance of benchmark bridge structures. In *Proc., ASCE Structures Congress*, Long Beach, CA, May 16-19.

Mackie, K. R. and Stojadinović, B. (2007b). R-factor parameterized bridge damage fragility curves. *Journal of Bridge Engineering* 12(4): 500–510.

Mackie, K. R., Wong, J., and Stojadinović, B. (2006). Method for post-earthquake bridge repair cost estimation. In *Proc., 5th National Seismic Conference on Bridges and Highways*, San Francisco, CA, September 18-20.

Mackie, K. R., Wong, J., and Stojadinović, B. (2007a). Comparison of post-earthquake highway bridge repair costs. In *Proc., ASCE Structures Congress*, Long Beach, CA, May 16-19.

Mackie, K. R., Wong, J., and Stojadinović, B. (2007b). Post-earthquake bridge repair cost sensitivity to ground motion scaling. In *Proc., 3rd International Conference on Structural Engineering, Mechanics, and Computation*, Cape Town, South Africa, September 10-12.

Maroney, B. H. and Chai, Y. H. (1994). Bridge abutment stiffness and strength under earthquake forces. In *Proc., 2nd International Workshop on Seismic Design and Retrofitting of Reinforced Concrete Bridges*, Queenstown, New Zealand, August 9-12.

Medina, R. and Krawinkler, H. (2003). *Seismic demands for non-deteriorating frame structures and their dependence on ground motions*. Report No. 2003/15, University of California Berkeley, Pacific Earthquake Engineering Research Center, Berkeley CA.

Medina, R., Krawinkler, H., and Alavi, B. (2001). Seismic drift and ductility demands and their dependence on ground motions. In *Proc., US-Japan Seminar on Advanced Stability and Seismicity Concepts for Performance-Based Design of Steel and Composite Structures*, Kyoto, Japan, July 23-27.

Megally, S. H., Silva, P. F., and Seible, F. (2002). *Seismic response of sacrificial shear keys in bridge abutments*. Report No. SSRP-2001/23, University of California San Diego, Department of Structural Engineering, San Diego CA.

Miranda, E. and Aslani, H. (2003). *Probabilistic response assessment for building-specific loss estimation*. Report No. 2003/03, University of California Berkeley, Pacific Earthquake Engineering Research Center, Berkeley CA.

Naus, J. I. (1969). The distribution of the logarithm of the sum of two log-normal variates. *Journal of the American Statistical Society* 64(326): 655–659.

Padgett, J. E. (2007). *Seismic vulnerability assessment of retrofitted bridges using probabilistic methods*. Ph.D. thesis, Georgia Institute of Technology, Atlanta, GA.

Panagiotakos, T. B. and Fardis, M. N. (2001). Deformations of reinforced concrete members at yielding and ultimate. *ACI Structural Journal* 98(2): 135–148.

Perry, C. and Grieg, I. D. (1975). Estimating the mean and variance of subjective distributions in pert and decision analysis. *Management Science* 21(12): 1477–1480.

Porter, K. A. (2004). *A survey of bridge practitioners to relate damage to closure*. Report No. EERL 2004-07, California Institute of Technology, Pasadena, CA.

Porter, K. A. and Kiremidjian, A. S. (2001). Verifying performance-based design objectives using assembly-based vulnerability. In *Proc., Structural Safety and Reliability: ICOSSAR 2001*, Newport Beach, CA, June 17-22.

RSMeans Engineering Staff, *Ed*. (2004). *Means heavy construction cost data 2004 book*. RS Means, New York, NY, 18 edition.

Shinozuka, M., Feng, M. Q., Lee, J., and Naganuma, T. (2000). Statistical analysis of fragility curves. *Journal of Engineering Mechanics* 126(12): 1224–1231.

Shome, N. and Cornell, C. A. (1999). *Probabilistic seismic demand analysis of nonlinear structures*. Report No. RMS 35, Stanford University, Department of Civil and Environmental Engineering, Stanford, CA.

Stewart, J. P., Chiou, S., Bray, J. D., Graves, R. W., Somerville, P. G., and Abrahamson, N. A. (2001). *Ground motion evaluation procedures for performance-based design*. Report No. 2001/09, University of California Berkeley, Pacific Earthquake Engineering Research Center, Berkeley CA.

HAZUS (1999). *Earthquake loss estimation methodology, Technical Manual*. National Institute of Building Sciences for Federal Emergency Management Agency, Washington, DC, SR2 edition.

USGS (2002). National seismic hazard maps. URL `http://earthquake.usgs.gov/hazmaps/`.

Vamvatsikos, D. and Cornell, C. A. (2002). Incremental dynamic analysis. *Earthquake Engineering and Structural Dynamics* 31(3): 491–512.

Werner, S. D., Taylor, C. E., Cho, S., Lavoie, J., Eitzel, C., Eguchi, R., and Moore, J. E. (2004). New developments in seismic risk analysis of highway systems. In *Proc., 13th World Conference on Earthquake Engineering*, Vancouver, Canada, August 1-6.

Werner, S. D., Taylor, C. E., Moore, J. E., and Walton, J. S. (2000). *A risk-based methodology for assessing the seismic performance of highway systems*. Report No. MCEER-00-0014, University at Buffalo, Multidisciplinary Center for Earthquake Engineering Research, Buffalo NY.

Yang, T. Y., Moehle, J., Stojadinović, B., and Der Kiureghian, A. (2006). An application of the peer performance-based earthquake engineering methodology. In *Proc., 8th National Conference on Earthquake Engineering*, San Francisco, April 18-22.

Zhang, J. and Makris, N. (2001). *Seismic response analysis of highway overcrossings including soil-structure interaction*. Report No. 2001/02, University of California Berkeley, Pacific Earthquake Engineering Research Center, Berkeley CA.

Appendix A: Spreadsheet Data

The following figures illustrate the spreadsheet implementation used in this report.

	A	B	C	D	E
1	Unit costs associated with each repair quantity				
2					
3	Item Name	Unit	Unit Cost mean	Unit Cost std dev	Notes
4	Structure excavation	CY	$ 165	$ 33	$250 for < 50 CY
5	Structure backfill	CY	$ 220	$ 44	$335 for < 14 CY, $115 > 250 CY
6	Temporary support (superstructure)	SF	$ 38	$ 8	
7	Temporary support (abutment)	SF	$ 38	$ 8	placeholder
8	Structural concrete (bridge)	CY	$ 2,225	$ 445	$2000 for > 10 CY
9	Structural concrete (footing)	CY	$ 520	$ 104	
10	Structural concrete (approach slab)	CY	$ 1,625	$ 325	
11	Aggregate base (approach slab)	CY	$ 325	$ 65	
12	Bar reinforcing steel (bridge)	LB	$ 1.35	$ 0.27	$6.50 < 400 LB
13	Bar reinforcing steel (footing, retaining wall)	LB	$ 1.20	$ 0.24	placeholder
14	Epoxy inject cracks	LF	$ 215	$ 43	
15	Repair minor spalls	SF	$ 300	$ 60	s1 has 100/sf
16	Column steel casing	LB	$ 10.00	$ 2	
17	Joint seal assembly	LF	$ 275	$ 55	MR101-160mm
18	Elastomeric bearings	EA	$ 1,500	$ 300	
19	Drill and bond dowel	LF	$ 55	$ 11	
20	Furnish steel pipe pile	LF	$ 55	$ 11	Class 625 (140)
21	Drive steel pipe pile	EA	$ 2,050	$ 410	610mm diameter. Class 625.
22	Drive abutment pipe pile	EA	$ 9,000	$ 1,800	610mm diameter. Class 70.
23	Asphalt concrete	TON	$ 265	$ 53	
24	Mud jacking	CY	$ 380	$ 76	
25	Bridge removal (column)	CY	$ 3,405	$ 681	
26	Bridge removal (portion)	CY	$ 2,355	$ 471	
27	Approach slab removal	CY	$ 1,000	$ 200	
28	Clean deck for methacrylate	SF	$ 0.40	$ 0.08	
29	Furnish methacrylate	GAL	$ 85	$ 17	
30	Treat bridge deck	SF	$ 0.55	$ 0.11	
31	Barrier rail	LF	$ 2	$ 0.40	placeholder
32	Re-center column	EA	$ 100	$ 20	placeholder

Fig. A.1 Cost spreadsheet.

	A	B	C	D	E	F	G	H	I	J	K	L
1	PG	location	DS0 trigger		DS1		DS2		DS3		DS4	
2			lambda	beta	lambda	beta	lambda	beta	lambda	beta		
3												
4	**Max col drift**		cracking		spalling		bar buckling		failure			
5	PG1	col1	0.23	0.30	1.64	0.33	6.09	0.25	6.72	0.35		
6	PG2	col2	0.23	0.30	1.64	0.33	6.09	0.25	6.72	0.35		
7	PG3	col3	0.23	0.30	1.64	0.33	6.09	0.25	6.72	0.35		
8	PG4	col4	0.23	0.30	1.64	0.33	6.09	0.25	6.72	0.35		
9												
10	**Residual col drift**		do nothing		thicken pier		re-center column?		failure (same as above)			
11	PG5	col1	0.50	0.30	1.25	0.40	2.00	0.40	6.72	0.35		
12	PG6	col2	0.50	0.30	1.25	0.40	2.00	0.40	6.72	0.35		
13	PG7	col3	0.50	0.30	1.25	0.40	2.00	0.40	6.72	0.35		
14	PG8	col4	0.50	0.30	1.25	0.40	2.00	0.40	6.72	0.35		
15												
16	**Abutment**		cleaning		assembly		back wall spalling		back wall failure			
17	PG9	left	0.051	0.25	0.102	0.25	0.111	0.30	0.138	0.30		
18	PG10	right	0.051	0.25	0.102	0.25	0.111	0.30	0.138	0.30		
19												
20	**Bearings**		yielding		failure							
21	PG11	left	0.076	0.25	0.152	0.25						
22	PG12	right	0.076	0.25	0.152	0.25						
23												
24	**Shear Key**		elastic		spalling		failure					
25	PG13	left	370	0.30	493	0.30	740	0.30				
26	PG14	right	370	0.30	493	0.30	740	0.30				
27												
28	**Approach**		pavement		AC regrade		Rebuilding					
29	PG15	left	0.073	0.40	0.146	0.40	0.305	0.40				
30	PG16	right	0.073	0.40	0.146	0.40	0.305	0.40				
31												
32	**Deck**		2% of spalling strain		25% of spalling strain		50% of spalling strain					
33	PG17	span1	4.02E-03	0.40	4.25E-03	0.40	4.50E-03	0.40				
34	PG18	span2	4.02E-03	0.40	4.25E-03	0.40	4.50E-03	0.40				
35	PG19	span3	4.02E-03	0.40	4.25E-03	0.40	4.50E-03	0.40				
36	PG20	span4	4.02E-03	0.40	4.25E-03	0.40	4.50E-03	0.40				
37	PG21	span5	4.02E-03	0.40	4.25E-03	0.40	4.50E-03	0.40				
38												
39	**Abutment foundation**		add pile threshold		enlarge and add piles							
40	PG22	left	0.29	0.40	0.49	0.40						
41	PG23	right	0.83	0.40	1.41	0.40						
42												
43	**Column foundation**		add pile threshold		enlarge and add piles							
44	PG24	col1	0.29	0.40	0.49	0.40						
45	PG25	col2	0.41	0.40	0.68	0.40						
46	PG26	col3	0.68	0.40	1.15	0.40						
47	PG27	col4	0.83	0.40	1.41	0.40						

Fig. A.2 Damage spreadsheet.

	A	B	C	D	E	F	G	H	I	J	K	L	M	N	O	P	Q	R	S	T	U	V	W	X	Y	Z	AA	AB
1	PGV Long + Trans SRSS (cm/s)	Max tangential drift ratio col 1 SRSS	Max tangential drift ratio col 2 SRSS	Max tangential drift ratio col 3 SRSS	Max tangential drift ratio col 4 SRSS	Residual tangential drift ratio col 1 SRSS	Residual tangential drift ratio col 2 SRSS	Residual tangential drift ratio col 3 SRSS	Residual tangential drift ratio col 4 SRSS	Max long relative deck-end/abut disp left	Max long relative deck-end/abut disp right	Max absolute bearing displ left abut	Max absolute bearing displ right abut	Max shear key force left abut	Max shear key force right abut	Residual vertical disp left abut	Residual vertical disp right abut	strain at roadway surface span 1	strain at roadway surface span 2	strain at roadway surface span 3	strain at roadway surface span 4	strain at roadway surface span 5	Residual pile cap displ left abut SRSS	Residual pile cap displ right abut SRSS	Residual pile cap disp col 1 SRSS	Residual pile cap disp col 2 SRSS	Residual pile cap disp col 3 SRSS	Residual pile cap disp col 4 SRSS
2	unit	%	%	%	%	%	%	%	%	m	m	m	m	kN	kN	m	m	m/m	m/m	m/m	m/m	m/m	m	m	m	m	m	m
3	PG	1	2	3	4	5	6	7	8	9	10	11	12	13	14	15	16	17	18	19	20	21	22	23	24	25	26	27
4	9.079	0.371	0.258	0.248	0.356	0.009	0.002	0.001	0.007	0.035	0.033	0.031	0.029	366.063	374.706	0.012	0.012	0.000	0.000	0.000	0.000	0.000	0.000	0.000	0.000	0.000	0.000	0.000
5	10.388	0.502	0.384	0.388	0.506	0.015	0.002	0.004	0.018	0.033	0.033	0.030	0.030	403.104	409.895	0.010	0.010	0.000	0.000	0.000	0.000	0.000	0.000	0.000	0.000	0.000	0.000	0.000
6	10.769	0.425	0.326	0.277	0.389	0.014	0.005	0.001	0.007	0.043	0.043	0.039	0.038	430.739	432.537	0.010	0.010	0.000	0.000	0.000	0.000	0.000	0.000	0.000	0.000	0.000	0.000	0.000
7	11.067	0.355	0.258	0.262	0.355	0.009	0.002	0.001	0.008	0.038	0.035	0.033	0.032	365.025	371.991	0.012	0.012	0.000	0.000	0.000	0.000	0.000	0.000	0.000	0.000	0.000	0.000	0.000
8	12.311	0.372	0.307	0.269	0.350	0.007	0.000	0.003	0.009	0.035	0.033	0.031	0.029	389.224	389.078	0.011	0.011	0.000	0.000	0.000	0.000	0.000	0.000	0.000	0.000	0.000	0.000	0.000
9	12.509	0.313	0.202	0.215	0.329	0.001	0.004	0.007	0.013	0.042	0.042	0.039	0.042	764.871	782.069	0.012	0.012	0.000	0.000	0.000	0.000	0.000	0.000	0.000	0.000	0.000	0.000	0.000
10	12.736	0.367	0.308	0.274	0.367	0.009	0.002	0.002	0.009	0.042	0.043	0.037	0.038	670.509	640.110	0.012	0.012	0.000	0.000	0.000	0.000	0.000	0.000	0.000	0.000	0.000	0.000	0.000
11	14.971	0.372	0.316	0.339	0.395	0.008	0.001	0.003	0.009	0.034	0.034	0.031	0.031	404.152	403.692	0.011	0.011	0.000	0.000	0.000	0.000	0.000	0.000	0.000	0.000	0.000	0.000	0.000
12	16.583	0.620	0.592	0.629	0.710	0.028	0.006	0.017	0.039	0.030	0.032	0.027	0.028	241.323	253.172	0.011	0.011	0.000	0.000	0.000	0.000	0.000	0.000	0.000	0.000	0.000	0.000	0.000
13	16.808	0.776	0.709	0.742	0.870	0.015	0.005	0.024	0.046	0.035	0.035	0.031	0.032	434.104	433.041	0.010	0.010	0.000	0.000	0.000	0.000	0.000	0.000	0.000	0.000	0.000	0.000	0.000
14	17.504	0.459	0.346	0.389	0.498	0.009	0.001	0.007	0.021	0.049	0.051	0.044	0.045	681.675	707.034	0.013	0.012	0.000	0.000	0.000	0.000	0.000	0.000	0.000	0.000	0.000	0.000	0.000
15	18.095	0.483	0.392	0.426	0.535	0.010	0.003	0.009	0.025	0.040	0.043	0.036	0.038	777.971	766.444	0.012	0.012	0.000	0.000	0.000	0.000	0.000	0.000	0.000	0.000	0.000	0.000	0.000
16	18.978	0.446	0.455	0.489	0.517	0.015	0.005	0.001	0.011	0.040	0.042	0.036	0.038	678.796	692.014	0.013	0.014	0.000	0.000	0.000	0.000	0.000	0.000	0.000	0.000	0.000	0.000	0.000
17	19.032	0.605	0.474	0.600	0.731	0.002	0.016	0.029	0.046	0.045	0.050	0.044	0.050	772.788	769.794	0.011	0.011	0.000	0.000	0.000	0.000	0.000	0.000	0.000	0.000	0.000	0.000	0.000
18	19.631	0.552	0.535	0.577	0.625	0.010	0.006	0.016	0.032	0.040	0.043	0.036	0.039	445.042	452.157	0.015	0.014	0.000	0.000	0.000	0.000	0.000	0.000	0.000	0.000	0.000	0.000	0.000
19	19.999	0.479	0.470	0.494	0.491	0.013	0.001	0.005	0.017	0.053	0.052	0.048	0.045	782.362	780.303	0.013	0.012	0.000	0.000	0.000	0.000	0.000	0.000	0.000	0.000	0.000	0.000	0.000
20	20.885	0.582	0.511	0.501	0.592	0.025	0.005	0.007	0.022	0.041	0.045	0.037	0.040	613.746	597.543	0.014	0.014	0.000	0.000	0.000	0.000	0.000	0.000	0.000	0.000	0.000	0.000	0.000
21	20.926	0.714	0.797	0.838	0.699	0.051	0.031	0.007	0.015	0.056	0.058	0.049	0.053	560.840	560.785	0.012	0.013	0.000	0.000	0.000	0.000	0.000	0.000	0.000	0.000	0.000	0.000	0.000
22	21.334	0.413	0.517	0.518	0.496	0.003	0.005	0.010	0.024	0.046	0.051	0.041	0.046	644.630	666.395	0.013	0.012	0.000	0.000	0.000	0.000	0.000	0.000	0.000	0.000	0.000	0.000	0.000
23	21.473	0.583	0.648	0.740	0.709	0.007	0.013	0.034	0.052	0.052	0.047	0.045	0.042	718.635	747.805	0.011	0.011	0.000	0.000	0.000	0.000	0.000	0.000	0.000	0.000	0.000	0.000	0.000
24	22.478	0.622	0.989	0.987	0.562	0.021	0.010	0.009	0.024	0.060	0.067	0.055	0.060	506.993	474.025	0.010	0.010	0.000	0.000	0.000	0.000	0.000	0.000	0.000	0.000	0.000	0.000	0.000
25	23.241	0.643	0.821	0.753	0.532	0.036	0.021	0.002	0.014	0.053	0.049	0.048	0.044	749.906	775.318	0.019	0.019	0.000	0.000	0.000	0.000	0.000	0.000	0.000	0.000	0.000	0.000	0.000
26	23.306	0.706	0.900	0.965	0.849	0.032	0.012	0.014	0.036	0.035	0.043	0.031	0.039	537.244	544.575	0.010	0.010	0.000	0.000	0.000	0.000	0.000	0.000	0.000	0.000	0.000	0.000	0.000
27	25.938	0.571	0.606	0.595	0.575	0.021	0.008	0.007	0.019	0.050	0.058	0.044	0.052	515.059	492.837	0.012	0.012	0.000	0.000	0.000	0.000	0.000	0.000	0.000	0.000	0.000	0.000	0.000
28	25.938	0.694	0.841	0.849	0.653	0.032	0.013	0.007	0.026	0.047	0.048	0.043	0.042	581.768	584.736	0.010	0.010	0.000	0.000	0.000	0.000	0.000	0.000	0.000	0.000	0.000	0.000	0.000
29	26.407	0.684	0.590	0.632	0.677	0.021	0.001	0.010	0.030	0.043	0.038	0.039	0.034	778.939	771.838	0.011	0.011	0.000	0.000	0.000	0.000	0.000	0.000	0.000	0.000	0.000	0.000	0.000
30	26.407	0.704	0.664	0.682	0.762	0.037	0.016	0.017	0.033	0.043	0.045	0.038	0.040	745.814	758.891	0.012	0.012	0.000	0.000	0.000	0.000	0.000	0.000	0.000	0.000	0.000	0.000	0.000
31	26.722	1.070	1.194	1.256	1.179	0.025	0.002	0.019	0.044	0.049	0.053	0.043	0.047	758.072	780.043	0.014	0.017	0.000	0.000	0.000	0.000	0.000	0.000	0.000	0.000	0.000	0.000	0.000
32	27.309	0.705	0.571	0.627	0.753	0.014	0.005	0.022	0.040	0.048	0.053	0.052	0.053	763.545	752.202	0.013	0.013	0.000	0.000	0.000	0.000	0.000	0.000	0.000	0.000	0.000	0.000	0.000
33	27.309	0.866	0.765	0.693	0.678	0.049	0.026	0.003	0.021	0.046	0.049	0.041	0.043	777.903	771.744	0.011	0.011	0.000	0.000	0.000	0.000	0.000	0.000	0.000	0.000	0.000	0.000	0.000
34	27.811	0.462	0.459	0.515	0.529	0.010	0.002	0.008	0.024	0.055	0.053	0.050	0.045	779.608	776.593	0.017	0.017	0.000	0.000	0.000	0.000	0.000	0.000	0.000	0.000	0.000	0.000	0.000
35	27.870	0.573	0.532	0.447	0.481	0.024	0.011	0.005	0.007	0.042	0.041	0.038	0.038	700.325	694.541	0.015	0.014	0.000	0.000	0.000	0.000	0.000	0.000	0.000	0.000	0.000	0.000	0.000
36	27.870	0.678	0.610	0.667	0.646	0.028	0.011	0.005	0.020	0.038	0.043	0.033	0.037	776.169	775.979	0.013	0.013	0.000	0.000	0.000	0.000	0.000	0.000	0.000	0.000	0.000	0.000	0.000
37	28.007	0.508	0.428	0.354	0.417	0.024	0.010	0.004	0.004	0.053	0.052	0.048	0.047	628.679	615.748	0.015	0.014	0.000	0.000	0.000	0.000	0.000	0.000	0.000	0.000	0.000	0.000	0.000
38	28.862	0.662	0.635	0.621	0.634	0.039	0.022	0.006	0.013	0.063	0.071	0.058	0.064	752.250	716.364	0.012	0.013	0.000	0.000	0.000	0.000	0.000	0.000	0.000	0.000	0.000	0.000	0.000
39	29.051	0.529	0.773	0.724	0.474	0.029	0.018	0.001	0.006	0.052	0.050	0.047	0.044	777.483	772.904	0.013	0.013	0.000	0.000	0.000	0.000	0.000	0.000	0.000	0.000	0.000	0.000	0.000
40	33.839	0.917	0.954	0.952	0.815	0.062	0.037	0.016	0.001	0.088	0.073	0.080	0.079	762.208	772.735	0.014	0.014	0.000	0.000	0.001	0.000	0.000	0.000	0.000	0.000	0.000	0.000	0.000
41	33.931	0.634	0.669	0.585	0.511	0.036	0.017	0.003	0.008	0.042	0.042	0.037	0.038	621.083	625.570	0.011	0.012	0.000	0.000	0.000	0.000	0.000	0.000	0.000	0.000	0.000	0.000	0.000
42	34.205	0.720	0.658	0.588	0.668	0.019	0.003	0.016	0.034	0.050	0.050	0.046	0.046	566.475	568.317	0.013	0.014	0.000	0.000	0.000	0.000	0.000	0.000	0.000	0.000	0.000	0.000	0.000
43	34.205	0.796	0.843	0.978	1.090	0.029	0.025	0.058	0.079	0.058	0.062	0.054	0.053	780.814	769.130	0.019	0.018	0.000	0.000	0.000	0.000	0.000	0.000	0.000	0.000	0.000	0.000	0.000
44	35.826	1.246	1.643	1.653	1.317	0.066	0.050	0.013	0.001	0.077	0.067	0.069	0.061	782.609	774.248	0.018	0.015	0.000	0.000	0.000	0.000	0.000	0.000	0.000	0.000	0.000	0.000	0.000
45	35.829	1.020	0.907	0.848	0.893	0.046	0.022	0.002	0.017	0.083	0.061	0.072	0.056	770.212	761.313	0.013	0.012	0.000	0.000	0.000	0.000	0.000	0.000	0.000	0.000	0.000	0.000	0.000
46	36.248	0.913	0.801	0.882	0.989	0.015	0.007	0.026	0.045	0.086	0.072	0.076	0.064	558.201	607.062	0.012	0.012	0.000	0.000	0.000	0.000	0.000	0.000	0.000	0.000	0.000	0.000	0.000
47	36.734	1.028	1.150	1.261	1.302	0.028	0.028	0.078	0.094	0.074	0.094	0.068	0.084	773.541	757.116	0.016	0.016	0.000	0.000	0.000	0.000	0.000	0.000	0.000	0.000	0.000	0.000	0.000
48	37.606	1.031	1.205	1.336	1.420	0.075	0.014	0.118	0.141	0.041	0.037	0.037	0.033	518.637	523.051	0.010	0.010	0.000	0.000	0.000	0.000	0.000	0.000	0.000	0.000	0.000	0.000	0.000
49	38.008	0.778	0.707	0.755	0.855	0.018	0.003	0.022	0.043	0.055	0.060	0.050	0.053	511.926	513.618	0.021	0.021	0.000	0.000	0.000	0.000	0.000	0.000	0.000	0.000	0.000	0.000	0.000
50	38.105	0.510	0.499	0.505	0.522	0.018	0.003	0.006	0.023	0.068	0.059	0.060	0.053	755.577	740.426	0.020	0.020	0.000	0.000	0.000	0.000	0.000	0.000	0.000	0.000	0.000	0.000	0.000
51	38.526	0.598	0.513	0.577	0.626	0.015	0.002	0.007	0.022	0.068	0.058	0.060	0.051	759.204	764.524	0.012	0.012	0.000	0.000	0.000	0.000	0.000	0.000	0.000	0.000	0.000	0.000	0.000
52	38.526	0.647	0.824	0.806	0.663	0.024	0.004	0.017	0.035	0.070	0.072	0.063	0.065	744.468	734.139	0.013	0.012	0.000	0.000	0.000	0.000	0.000	0.000	0.000	0.000	0.000	0.000	0.000
53	39.274	0.658	0.766	0.854	0.746	0.024	0.001	0.024	0.046	0.052	0.048	0.048	0.041	740.299	729.522	0.012	0.012	0.000	0.000	0.000	0.000	0.000	0.000	0.000	0.000	0.000	0.000	0.000
54	40.692	0.401	0.443	0.445	0.501	0.002	0.006	0.013	0.025	0.071	0.080	0.065	0.069	783.123	779.719	0.012	0.012	0.000	0.000	0.000	0.000	0.000	0.000	0.000	0.000	0.000	0.000	0.000
55	40.934	0.989	1.044	1.055	1.084	0.013	0.004	0.027	0.047	0.076	0.081	0.067	0.073	695.854	711.338	0.016	0.016	0.000	0.001	0.001	0.000	0.000	0.000	0.000	0.000	0.000	0.000	0.000
56	42.341	1.071	1.345	1.344	1.052	0.031	0.003	0.034	0.058	0.062	0.103	0.057	0.092	682.993	693.283	0.013	0.014	0.000	0.000	0.000	0.000	0.000	0.000	0.000	0.000	0.000	0.000	0.000
57	46.556	0.986	0.930	0.834	0.862	0.059	0.045	0.016	0.003	0.058	0.079	0.051	0.070	705.124	705.296	0.017	0.015	0.000	0.000	0.000	0.000	0.000	0.000	0.000	0.000	0.000	0.000	0.000
58	48.134	1.449	1.800	1.852	1.577	0.030	0.000	0.028	0.056	0.052	0.060	0.062	0.061	777.724	780.260	0.012	0.012	0.000	0.000	0.000	0.000	0.000	0.000	0.000	0.000	0.000	0.000	0.000
59	49.907	0.791	0.879	0.889	0.782	0.015	0.000	0.028	0.011	0.074	0.096	0.063	0.088	773.922	760.945	0.012	0.011	0.000	0.000	0.000	0.000	0.000	0.000	0.000	0.000	0.000	0.000	0.000
60	49.907	1.055	0.997	0.943	0.867	0.071	0.052	0.048	0.056	0.057	0.066	0.052	0.058	612.313	635.960	0.015	0.015	0.000	0.000	0.000	0.000	0.000	0.000	0.000	0.000	0.000	0.000	0.000
61	52.778	0.684	0.783	0.768	0.780	0.026	0.008	0.017	0.043	0.052	0.055	0.046	0.048	782.707	770.183	0.017	0.016	0.000	0.000	0.000	0.000	0.000	0.000	0.000	0.000	0.000	0.000	0.000
62	58.876	1.173	1.651	1.686	1.276	0.042	0.010	0.017	0.049	0.055	0.057	0.049	0.052	780.121	759.803	0.012	0.012	0.000	0.000	0.000	0.000	0.000	0.000	0.000	0.000	0.000	0.000	0.000
63	59.337	1.276	1.517	1.602	1.115	0.085	0.069	0.004	0.007	0.076	0.051	0.068	0.045	779.964	766.971	0.016	0.017	0.000	0.000	0.000	0.000	0.000	0.000	0.000	0.000	0.000	0.000	0.000
64	59.337	1.736	1.854	1.993	2.133	0.120	0.120	0.257	0.280	0.062	0.052	0.056	0.046	761.684	775.633	0.017	0.014	0.000	0.000	0.000	0.000	0.000	0.000	0.000	0.000	0.000	0.000	0.000
65	60.001	1.993	1.915	1.796	1.942	0.172	0.150	0.015	0.088	0.067	0.066	0.059	0.058	775.249	762.851	0.014	0.018	0.000	0.000	0.000	0.000	0.000	0.000	0.000	0.000	0.000	0.000	0.000
66	60.742	1.522	2.076	2.085	1.749	0.035	0.017	0.020	0.038	0.086	0.052	0.074	0.066	779.741	778.148	0.021	0.022	0.000	0.001	0.001	0.001	0.000	0.000	0.000	0.000	0.000	0.000	0.000
67	60.967	0.830	0.734	0.608	0.547	0.067	0.049	0.030	0.014	0.072	0.059	0.065	0.056	777.291	779.985	0.019	0.015	0.000	0.000	0.001	0.000	0.000	0.000	0.000	0.000	0.000	0.000	0.000
68	61.058	0.733	1.023	1.036	0.907	0.006	0.013	0.033	0.029	0.090	0.132	0.096	0.114	765.823	757.486	0.020	0.016	0.000	0.000	0.001	0.000	0.000	0.000	0.000	0.000	0.000	0.000	0.000
69	61.058	0.994	1.029	1.052	0.928	0.039	0.030	0.051	0.059	0.115	0.148	0.106	0.138	781.194	770.992	0.016	0.015	0.000	0.000	0.000	0.000	0.000	0.000	0.000	0.000	0.000	0.000	0.000
70	62.067	2.101	2.063	1.926	1.784	0.079	0.059	0.001	0.001	0.054	0.050	0.050	0.044	780.432	777.198	0.012	0.012	0.000	0.000	0.000	0.000	0.000	0.000	0.000	0.000	0.000	0.000	0.000
71	62.067	2.202	2.329	2.254	1.881	0.156	0.132	0.006	0.087	0.060	0.044	0.055	0.040	705.746	614.357	0.014	0.013	0.000	0.000	0.000	0.000	0.000	0.000	0.000	0.000	0.000	0.000	0.000
72	62.666	0.720	0.746	0.826	0.776	0.017	0.005	0.029	0.047	0.140	0.134	0.132	0.123	778.641	759.656	0.020	0.018	0.000	0.000	0.000	0.000	0.000	0.000	0.000	0.000	0.000	0.000	0.000

Fig. A.3 EDP spreadsheet.

	A	B	C	D	E	F	G	H	I	J	K	L	M	N	O	P	Q	R	S	T	U	V	W	X	Y	Z	AA	AB
1	PGV Long + Trans SRSS	Max tangentia l drift ratio col 1 SRSS	Max tangentia l drift ratio col 2 SRSS	Max tangentia l drift ratio col 3 SRSS	Max tangentia l drift ratio col 4 SRSS	Residual tangentia l drift ratio col 1 SRSS	Residual tangentia l drift ratio col 2 SRSS	Residual tangentia l drift ratio col 3 SRSS	Residual tangentia l drift ratio col 4 SRSS	Max long relative deck-end/abut disp left	Max long relative deck-end/abut disp right	Max absolute bearing displ left abut	Max absolute bearing displ right abut	Max shear key force left abut	Max shear key force right abut	Residual vertical disp left abut	Residual vertical disp right abut	strain at roadway surface span 1	strain at roadway surface span 2	strain at roadway surface span 3	strain at roadway surface span 4	strain at roadway surface span 5	Residual pile cap displ left abut SRSS	Residual pile cap displ right abut SRSS	Residual pile cap disp col 1 SRSS	Residual pile cap disp col 2 SRSS	Residual pile cap disp col 3 SRSS	Residual pile cap disp col 4 SRSS
2	unit	%	%	%	%	%	%	%	%	m	m	m	m	kN	kN	m	m	m/m	m/m	m/m	m/m	m/m	m	m	m	m	m	m
3	PG	1	2	3	4	5	6	7	8	9	10	11	12	13	14	15	16	17	18	19	20	21	22	23	24	25	26	27
73	63.223	1.630	2.001	2.116	1.993	0.007	0.031	0.054	0.079	0.045	0.057	0.043	0.052	775.931	779.246	0.015	0.017	0.000	0.000	0.000	0.000	0.000	0.000	0.000	0.000	0.000	0.000	0.000
74	64.685	1.727	2.220	2.363	2.033	0.047	0.031	0.014	0.037	0.071	0.110	0.061	0.101	777.983	779.849	0.019	0.021	0.000	0.000	0.000	0.000	0.000	0.000	0.000	0.000	0.000	0.000	0.000
75	65.098	1.946	2.481	2.426	2.103	0.068	0.044	0.018	0.007	0.108	0.096	0.100	0.079	745.830	770.488	0.024	0.021	0.001	0.001	0.001	0.001	0.000	0.000	0.000	0.000	0.000	0.000	0.000
76	66.081	2.127	2.081	2.180	2.048	0.127	0.103	0.027	0.054	0.102	0.144	0.110	0.130	770.418	769.693	0.025	0.024	0.001	0.001	0.001	0.001	0.000	0.000	0.000	0.000	0.000	0.000	0.000
77	67.685	2.045	1.930	1.801	1.632	0.137	0.113	0.021	0.065	0.074	0.094	0.067	0.085	773.031	771.236	0.023	0.018	0.000	0.000	0.000	0.000	0.000	0.000	0.000	0.000	0.000	0.000	0.000
78	70.326	2.276	3.252	3.305	2.466	0.063	0.042	0.004	0.027	0.098	0.111	0.089	0.102	757.108	759.572	0.020	0.019	0.000	0.000	0.000	0.000	0.000	0.000	0.000	0.000	0.000	0.000	0.000
79	70.409	2.250	2.403	2.520	2.651	0.014	0.231	0.361	0.388	0.150	0.127	0.138	0.122	777.083	773.775	0.016	0.016	0.000	0.000	0.000	0.000	0.000	0.000	0.000	0.000	0.000	0.000	0.000
80	70.816	2.254	2.615	2.758	2.677	0.097	0.352	0.494	0.513	0.072	0.079	0.065	0.069	763.449	767.102	0.023	0.019	0.000	0.000	0.000	0.000	0.000	0.000	0.000	0.000	0.000	0.000	0.000
81	75.961	0.969	1.263	1.353	1.101	0.020	0.002	0.029	0.045	0.112	0.123	0.172	0.172	708.908	703.236	0.026	0.024	0.001	0.001	0.001	0.001	0.001	0.000	0.000	0.000	0.000	0.000	0.000
82	75.961	1.211	1.533	1.496	1.396	0.027	0.029	0.072	0.094	0.131	0.171	0.122	0.161	746.493	764.612	0.026	0.024	0.001	0.001	0.001	0.001	0.001	0.000	0.000	0.000	0.000	0.000	0.000
83	77.751	2.580	2.471	2.335	2.353	0.193	0.167	0.033	0.113	0.145	0.182	0.137	0.172	753.722	772.362	0.023	0.029	0.000	0.000	0.001	0.001	0.001	0.000	0.000	0.000	0.000	0.000	0.000
84	78.015	2.386	2.295	2.182	2.023	0.056	0.041	0.016	0.029	0.156	0.113	0.148	0.104	775.980	781.239	0.014	0.013	0.000	0.000	0.000	0.000	0.000	0.000	0.000	0.000	0.000	0.000	0.000
85	91.344	2.283	2.143	2.009	1.886	0.193	0.168	0.038	0.117	0.103	0.118	0.093	0.107	681.150	769.789	0.027	0.030	0.001	0.001	0.001	0.001	0.001	0.000	0.000	0.000	0.000	0.000	0.000
86	92.477	2.174	3.148	3.184	2.498	0.079	0.307	0.394	0.145	0.099	0.141	0.084	0.139	782.878	780.644	0.016	0.016	0.000	0.001	0.001	0.001	0.000	0.000	0.000	0.000	0.000	0.000	0.000
87	92.477	3.337	3.319	3.222	2.909	0.572	0.538	0.448	0.482	0.095	0.133	0.212	0.192	987.791	799.716	0.015	0.017	0.000	0.001	0.001	0.001	0.000	0.000	0.000	0.000	0.000	0.000	0.000
88	95.051	2.571	3.517	3.502	2.526	0.065	0.081	0.048	0.053	0.156	0.159	0.145	0.149	780.064	771.243	0.018	0.018	0.000	0.000	0.000	0.000	0.000	0.000	0.000	0.000	0.000	0.000	0.000
89	97.146	3.307	3.512	3.661	3.773	0.120	0.365	0.504	0.536	0.221	0.177	0.215	0.164	782.662	781.987	0.032	0.034	0.001	0.001	0.001	0.001	0.001	0.000	0.000	0.000	0.000	0.000	0.000
90	105.694	2.177	2.945	3.040	2.579	0.126	0.126	0.277	0.282	0.177	0.134	0.166	0.125	736.428	736.305	0.017	0.019	0.000	0.001	0.001	0.001	0.000	0.000	0.000	0.000	0.000	0.000	0.000
91	106.598	2.815	3.302	3.354	2.964	0.004	0.179	0.310	0.332	0.139	0.183	0.127	0.176	778.140	757.114	0.024	0.023	0.000	0.000	0.000	0.000	0.000	0.000	0.000	0.000	0.000	0.000	0.000
92	107.014	2.376	3.009	3.036	2.531	0.060	0.022	0.077	0.134	0.249	0.282	0.242	0.271	777.510	752.899	0.029	0.033	0.001	0.001	0.001	0.001	0.001	0.000	0.000	0.000	0.000	0.000	0.000
93	108.132	3.191	3.533	3.601	2.920	0.261	0.119	0.183	0.161	0.134	0.175	0.126	0.163	767.355	761.364	0.015	0.017	0.000	0.000	0.000	0.000	0.000	0.000	0.000	0.000	0.000	0.000	0.000
94	109.574	4.934	6.835	6.708	4.794	0.727	0.584	0.537	0.638	0.087	0.127	0.104	0.115	780.631	772.263	0.030	0.028	0.000	0.001	0.001	0.001	0.000	0.000	0.000	0.000	0.000	0.000	0.000
95	112.918	2.855	4.029	4.018	2.979	0.195	0.313	0.459	0.536	0.136	0.178	0.241	0.273	727.433	677.881	0.049	0.037	0.001	0.001	0.001	0.001	0.001	0.000	0.000	0.000	0.000	0.000	0.000
96	114.574	2.826	2.721	2.620	2.455	0.432	0.418	0.298	0.044	0.173	0.179	0.167	0.165	776.647	733.514	0.032	0.031	0.001	0.001	0.001	0.001	0.001	0.000	0.000	0.000	0.000	0.000	0.000
97	118.406	3.812	4.258	4.157	4.132	0.028	0.009	0.141	0.166	0.144	0.102	0.153	0.162	768.899	781.612	0.017	0.018	0.000	0.001	0.001	0.001	0.000	0.000	0.000	0.000	0.000	0.000	0.000
98	123.561	3.441	4.600	4.605	3.396	0.599	0.524	0.459	0.471	0.138	0.181	0.127	0.173	777.405	762.765	0.015	0.017	0.000	0.001	0.001	0.000	0.000	0.000	0.000	0.000	0.000	0.000	0.000
99	125.173	4.231	5.116	5.045	4.037	0.594	0.499	0.437	0.451	0.216	0.259	0.208	0.247	765.791	766.460	0.024	0.023	0.000	0.000	0.001	0.001	0.000	0.000	0.000	0.000	0.000	0.000	0.000
100	144.266	4.427	4.892	4.979	4.727	0.999	1.185	1.324	1.408	0.249	0.285	0.244	0.269	951.637	908.380	0.031	0.027	0.001	0.001	0.001	0.001	0.000	0.000	0.000	0.000	0.000	0.000	0.000
101	171.339	6.521	6.938	7.189	7.054	3.597	3.531	3.259	3.974	0.198	0.241	0.181	0.238	769.286	769.509	0.027	0.030	0.000	0.000	0.001	0.001	0.000	0.000	0.000	0.000	0.000	0.000	0.000
102	175.833	5.867	6.224	6.112	5.442	0.689	0.654	0.516	0.346	0.250	0.293	0.238	0.287	775.524	776.932	0.028	0.030	0.001	0.001	0.001	0.001	0.001	0.000	0.000	0.000	0.000	0.000	0.000
103	175.833	6.535	8.102	8.094	6.366	2.040	4.783	4.845	2.448	0.214	0.245	0.348	0.352	962.701	977.316	0.069	0.069	0.001	0.001	0.001	0.001	0.001	0.000	0.000	0.000	0.000	0.000	0.000
104	176.292	5.443	7.272	7.414	5.375	0.481	0.457	0.563	0.743	0.418	0.463	0.399	0.460	715.936	722.218	0.039	0.039	0.001	0.001	0.001	0.001	0.001	0.000	0.000	0.000	0.000	0.000	0.000
105	176.574	5.066	6.194	6.094	5.089	0.519	0.513	0.868	0.831	0.376	0.331	0.361	0.329	780.798	770.442	0.040	0.039	0.001	0.001	0.001	0.001	0.001	0.000	0.000	0.000	0.000	0.000	0.000
106	176.574	5.654	6.758	6.798	5.985	0.772	0.905	0.949	0.924	0.369	0.402	0.366	0.391	749.730	749.703	0.034	0.036	0.001	0.001	0.001	0.001	0.001	0.000	0.000	0.000	0.000	0.000	0.000
107	226.306	5.128	5.252	5.276	5.422	1.088	1.066	0.902	0.644	0.369	0.368	0.362	0.356	739.684	754.981	0.016	0.017	0.000	0.000	0.000	0.000	0.000	0.000	0.000	0.000	0.000	0.000	0.000

Fig. A.3—*Continued.*

	A	B	C	D	E	F
1	**Bridge 1 Column A:**					
2						
3	**Column Quantity**	**Value**		**Metric Value**		**Notes**
4	column diameter	48	in	1.22	m	
5	column surface area	276	sf	25.68	m2	
6	number of columns	4	ea	4	ea	
7	required column casing thickness	0.375	in	0.0095	m	XS7-010e
8	column height	22	ft	6.706	m	
9	bar area	1.27	in2	0.00082	m2	US #10 bars
10	diameter of longitudinal bars	1.272	in	0.0323	m	US #10 bars
11	number of longitudinal bars	28	ea	28	ea	
12	percent transverse reinforcement	1.59	%	1.59	%	
13	percent long. reinforcement	2.0	%	2.0	%	
14	column dead load (bottom)	1837	k	8171	kN	
15	col gross area (Ag)	1810	in2	1.168	m2	
16	column cover	1.5	in	0.038	m	
17	total column bar volume (long.)	5.43	cf	0.154	m3	
18	total column bar weight (long.)	2662	lb	1207	kg	
19	steel (fye)	68	ksi	468843	kPa	
20	concrete (f'ce)	5.20	ksi	35853	kPa	
21	steel weight	490	lb/ft3	76973	N/m3	
22	concrete weight	150	lb/ft3	23563	N/m3	
23	steel weight estimate (BDA 11-5)	16.72	lb/ft3	268.0	kg/m3	BDA 11-5
24	total column gross volume	276.53	ft3	7.826	m3	
25						
26	**Deck Quantity**	**Value**		**Metric Value**		**Notes**
27	deck area, total	26910	sf	2500	m2	
28	deck width	39	ft	11.89	m	
29	deck depth	6	ft	1.83	m	
30	ext. span length	120	ft	36.58	m	
31	int. span length	150	ft	45.72	m	
32	deck area per column	6728	sf	625.0	m2	
33	deck area, ext. span	4680	sf	434.8	m2	
34	deck area, int. span	5850	sf	543.5	m2	
35	deck cross-sectional area	61.59	sf	5.72	m2	
36	superstructure bottom width	23	ft	7.01	m	
37	spalling strain	0.005	in/in	0.005	m/m	
38						
39	**Abutment and Joint Quantities**	**Value**		**Metric Value**		**Notes**
40	number of bearings/joint	3	ea	3	ea	bearing under each box web
41	bearing height	2	in	0.051	m	
42	expansion Joint gap	4	in	0.102	m	
43	expansion Joint blockout height	12	in	0.305	m	
44	expansion Joint blockout width	10	in	0.254	m	
45	expansion Joint blockout steel	2.995	lb/ft3	48.00	kg/m3	BDA 11-5
46	backwall steel	3.370	lb/ft3	54.00	kg/m3	BDA 11-5
47	abutment Dead Load	554.31	k	2466	kN	
48	number of shear keys	2	ea	2	ea	
49	approach slab length	30	ft	9.14	m	Caltrans standard approach slab length
50	approach slab width	39	ft	11.89	m	deck width
51	approach slab thickness	1	ft	0.30	m	
52	approach slab area	1170	sf	108.7	m2	
53	approach slab roadway volume	1170	cf	43.3	cy	
54	wing wall length	19.0	ft	5.79	m	
55	wing wall thickness	1.0	ft	0.30	m	
56	shortest wing wall height	3.0	ft	0.91	m	
57	backwall thickness	1.0	ft	0.30	m	
58	backwall height	6.0	ft	1.83	m	deck depth
59	stem wall thickness	4.0	ft	1.22	m	

Fig. A.4 Info spreadsheet.

	A	B	C	D	E	F
60	stem wall height	8.0	ft	2.44	m	
61	Shear Key thickness at top	3.0	ft	0.91	m	
62	Shear Key height	5.0	ft	1.52	m	
63	embankment slope (V/H)	2.0	-	2.0	-	
64						
65	**Column foundation Quantity**	**Value**		**Metric Value**		**Notes**
66	pile cap dimension 1	15	ft	4.57	m	
67	pile cap dimension 2	10	ft	3.05	m	
68	pile cap depth	3.25	ft	0.99	m	
69	pile cap steel reinforcement %	3.65	%	3.65	%	
70	pile cap volume	18.06	cy	13.80	m3	
71	column pile diameter	24	in	0.610	m	
72	column pile thickness	0.50	in	0.0127	m	
73	column pile fye	68	ksi	468843	kPa	
74	column pile spacing	72	in	1.829	m	3*D
75	pile length	60	ft	18.3	m	
76	number of piles	6	ea	6	ea	3x2 group
77	enlarged pile cap dimension 1	27	ft	8.23	m	original + 2*spacing
78	enlarged pile cap dimension 2	22	ft	6.71	m	original + 2*spacing
79	pile cap embedment depth	2	ft	0.61	m	
80	steel weight estimate footing	6.552	lb/ft3	105.00	kg/m3	BDA 11-5
81						
82	**Abutment foundation Quantity**	**Value**		**Metric Value**		**Notes**
83	abutment pile cap dimension 1	45	ft	13.72	m	
84	abutment pile cap dimension 2	10	ft	3.05	m	
85	abutment pile cap depth	3	ft	0.91	m	
86	abutment pile cap reinforcement %		%	0	%	
87	abutment pile diameter	24	in	0.610	m	
88	abutment pile thickness	0.5	in	0.013	m	
89	abutment pile fye	68	ksi	468843		
90	abutment pile spacing	96	in	2.438	m	4*D
91	abutment pile length	70	ft	21.34	m	
92	abutment number of piles	6	ea	6	ea	6x1 group

Fig. A.4—*Continued.*

	A	B	C	D	E	F	G	H
1	Production rates associated with each repair quantity							
2								
3	Item Name	Unit	PR mean	PR std dev	Mode	Min	Max	Notes
4	Structure excavation	CWD	1.2	0.2	1.0	1.0	2.0	Excavation (1)
5	Structure backfill	CWD	2.2	0.5	2.0	1.0	4.0	Backfill (1 to 4)
6	Temporary support (superstructure)	CWD	34.2	3.8	34.0	23.0	46.0	Submit/review temporary support (30), Install (3), Remove (1)
7	Temporary support (abutment)	CWD	33.2	3.8	33.0	22.0	45.0	Submit/review temporary support (30), Install (2), Remove (1)
8	Structural concrete (bridge)	CWD	10.0	0.7	10.0	8.0	12.0	Place forms (0 to 1), Cure (7 to 10), Strip forms (1)
9	Structural concrete (footing)	CWD	10.0	0.7	10.0	8.0	12.0	Place forms (0 to 1), Cure (7 to 10), Strip forms (1)
10	Structural concrete (approach slab)	CWD	2.0	0.3	2.0	1.0	3.0	Construct approach slab (1+1, in half-width strips)
11	Aggregate base (approach slab)	CWD	1.2	0.2	1.0	1.0	2.0	
12	Bar reinforcing steel (bridge)	CWD	1.8	0.2	2.0	1.0	2.0	Place reinforcement (1 to 2)
13	Bar reinforcing steel (footing, retaining wall)	CWD	1.8	0.2	2.0	1.0	2.0	Place reinforcement (1 to 2)
14	Epoxy inject cracks	CWD	2.0	0.3	2.0	1.0	3.0	Repair cracks with epoxy (1 to 3)
15	Repair minor spalls	CWD	2.0	0.3	2.0	1.0	3.0	Repair spalls (1 to 3)
16	Column steel casing	CWD	70.0	7.7	70.0	47.0	93.0	Submit shop plans (2), Review shop plans (30), Procure column casing (30), Set and weld (2), Grout and paint (6)
17	Joint seal assembly	CWD	2.0	0.3	2.0	1.0	3.0	Install joint seal assembly (2)
18	Elastomeric bearings	CWD	1.2	0.2	1.0	1.0	2.0	Install bearings (1)
19	Drill and bond dowel	CWD	1.2	0.2	1.0	1.0	2.0	Drill and bond dowels (1)
20	Furnish steel pipe pile	CWD	35.0	1.7	35.0	30.0	40.0	Procure piling (30 to 40)
21	Drive steel pipe pile	CWD	2.0	0.3	2.0	1.0	3.0	Drive piles (2)
22	Drive abutment pipe pile	CWD	3.0	0.3	3.0	2.0	4.0	Drive piles (3)
23	Asphalt concrete	CWD	2.0	0.3	2.0	1.0	3.0	Asphalt concrete (2)
24	Mud jacking	CWD	2.0	0.3	2.0	1.0	3.0	Mudjacking (2)
25	Bridge removal (column)	CWD	16.2	1.8	16.0	11.0	22.0	Submit/review bridge removal plan (15), Remove existing column (1)
26	Bridge removal (portion)	CWD	2.0	0.3	2.0	1.0	3.0	Demo existing / Remove (1 to 3); Use for misc removal e.g. shear keys
27	Approach slab removal	CWD	4.0	0.7	4.0	2.0	6.0	Remove approach slab (2 + 2, in half-width strips)
28	Clean deck for methacrylate	CWD	1.2	0.2	1.0	1.0	2.0	Clean bridge deck (1)
29	Furnish methacrylate	CWD	20.0	3.3	20.0	10.0	30.0	Material sampling (10), Methacrylate safety plan (10)
30	Treat bridge deck	CWD	1.2	0.2	1.0	1.0	2.0	Treat bridge deck (1)
31	Barrier rail	CWD	10.0	0.3	10.0	9.0	11.0	
32	Re-center column	CWD	100.0	3.3	100.0	90.0	110.0	

Fig. A.5 Production spreadsheet.

	A	B	C	D	E	F	G	H	I	J	K	L	M	N	O	P	Q	R	S	T	U	V	W	X	Y	Z	AA	AB	AC	AD	AE
1	Repair quantities		Structure excavation	Structure backfill	Temporary support (bridge)	Temporary support (abut.)	Structural concrete (bridge)	Structural concrete (footing)	Structural concrete (approach slab)	Aggregate base (approach slab)	Bar reinforcing steel (bridge)	Bar reinforcing steel (footing, retaining wall)	Epoxy inject cracks	Repair minor spalls	Column steel casing	Joint seal assembly (MR 4")	Elastomeri c bearing	Drill and bond dowel	Furnish steel pipe pile	Drive steel pipe pile	Drive abutment pipe pile	Asphalt concrete	Mud jacking	Bridge removal (column)	Bridge removal (portion)	Approach slab removal	Clean deck for methacryla te	Furnish methacryla te	Treat bridge deck	Barrier rail	Re-center column
2		unit	CY	CY	SF	SF	CY	CY	CY	CY	LB	LB	LF	SF	LB	LF	EA	LF	LF	EA	EA	TON	CY	CY	CY	CY	SF	GAL	SF	LF	EA
3	**Columns (max)**																														
4	PG1	DS1	0	0	0		0				0		44	27.6										0							
5		DS2	0	0	0		0				0		88	69.1										0							
6		DS3	13	13	5,265		10.24				4,624		0	0.0										10.24							
7		DS?	13	13	5,265		10.24				4,624		0	0.0										10.24							
8	PG2	DS1	0	0	0		0				0		44	27.6										0							
9		DS2	0	0	0		0				0		88	69.1										0							
10		DS3	13	13	5,850		10.24				4,624		0	0.0										10.24							
11		DS?	13	13	5,850		10.24				4,624		0	0.0										10.24							
12	PG3	DS1	0	0	0		0				0		44	27.6										0							
13		DS2	0	0	0		0				0		88	69.1										0							
14		DS3	13	13	5,850		10.24				4,624		0	0.0										10.24							
15		DS?	13	13	5,850		10.24				4,624		0	0.0										10.24							
16	PG4	DS1	0	0	0		0				0		44	27.6										0							
17		DS2	0	0	0		0				0		88	69.1										0							
18		DS3	13	13	5,265		10.24				4,624		0	0.0										10.24							
19		DS?	13	13	5,265		10.24				4,624		0	0.0										10.24							
20																															
21	**Columns (residual)**																														
22	PG5	DS1	8	8	2,633						231				4,690														60	0	
23		DS2	8	8	2,633						231				4,690														120	1	
24		DS3	0	0	2,633						0				0														120	0	
25		DS?	0	0	0						0				0														240	0	
26	PG6	DS1	8	8	2,925						231				4,690														75	0	
27		DS2	8	8	2,925						231				4,690														150	1	
28		DS3	0	0	2,925						0				0														150	0	
29		DS?	0	0	0						0				0														300	0	
30	PG7	DS1	8	8	2,925						231				4,690														75	0	
31		DS2	8	8	2,925						231				4,690														150	1	
32		DS3	0	0	2,925						0				0														150	0	
33		DS?	0	0	0						0				0														300	0	
34	PG8	DS1	8	8	2,633						231				4,690														60	0	
35		DS2	8	8	2,633						231				4,690														120	1	
36		DS3	0	0	2,633						0				0														120	0	
37		DS?	0	0	0						0				0														240	0	
38																															
39	**Abutment**																														
40	PG9	DS1	0	0			2.41		0	0	0		0	0		39									2.41	0					
41		DS2	9	9			2.41		0	0	0		12	23.4		39									2.41	0					
42		DS3	35	35			8.67		43	10	788		0	0.0		39									8.67	43					
43		DS?	43	43			8.67		43	43	788		0	0		39									8.67	43					
44	PG10	DS1	0	0			2.41		0	0	0		0	0		39									2.41	0					
45		DS2	9	9			2.41		0	0	0		12	23.4		39									2.41	0					
46		DS3	35	35			8.67		43	10	788		0	0.0		39									8.67	43					
47		DS?	43	43			8.67		43	43	788		0	0		39									8.67	43					
48																															
49	**Bearings**																														
50	PG11	DS1				2,340											3														
51		DS?				2,340											3														
52	PG12	DS1				2,340											3														
53		DS?				2,340											3														
54																															
55	**Shear Key**																														
56	PG15	DS1					0				0		20	3.0											0						
57		DS2					8.9				809		0	0											8.9						
58		DS?					8.9				809		0	0											8.9						
59	PG16	DS1					0				0		20	3.0											0						
60		DS2					8.9				809		0	0											8.9						
61		DS?					8.9				809		0	0											8.9						
62																															
63	**Approach**																														
64	PG17	DS1																				10	0								
65		DS2																				21	122								
66		DS?																				43	244								
67	PG18	DS1																				10	0								
68		DS2																				21	122								

Fig. A.6 Repair spreadsheet.

	A	B	C	D	E	F	G	H	I	J	K	L	M	N	O	P	Q	R	S	T	U	V	W	X	Y	Z	AA	AB	AC	AD	AE
1	Repair quantities		Structure excavation	Structure backfill	Temporary support (bridge)	Temporary support (abut.)	Structural concrete (bridge)	Structural concrete (footing)	Structural concrete (approach slab)	Aggregate base (approach slab)	Bar reinforcing steel (bridge)	Bar reinforcing steel (footing, retaining wall)	Epoxy inject cracks	Repair minor spalls	Column steel casing	Joint seal assembly (MR 4")	Elastomeri c bearing	Drill and bond dowel	Furnish steel pipe pile	Drive steel pipe pile	Drive abutment pipe pile	Asphalt concrete	Mud jacking	Bridge removal (column)	Bridge removal (portion)	Approach slab removal	Clean deck for methacryla te	Furnish methacryla te	Treat bridge deck	Barrier rail	Re-center column
2		unit	CY	CY	SF	SF	CY	CY	CY	CY	LB	LB	LF	SF	LB	LF	EA	LF	LF	EA	EA	TON	CY	CY	CY	CY	SF	GAL	SF	LF	EA
69		DS?																				43	244								
70																															
71	**Deck**																														
72	PG19	DS1											0														1,170	13	1,170		
73		DS2											30														2,340	26	2,340		
74		DS?											120														4,680	52	4,680		
75	PG20	DS1											0														1,463	16	1,463		
76		DS2											38														2,925	33	2,925		
77		DS?											150														5,850	65	5,850		
78	PG21	DS1											0														1,463	16	1,463		
79		DS2											38														2,925	33	2,925		
80		DS?											150														5,850	65	5,850		
81	PG22	DS1											0														1,463	16	1,463		
82		DS2											38														2,925	33	2,925		
83		DS?											150														5,850	65	5,850		
84	PG23	DS1											0														1,170	13	1,170		
85		DS2											30														2,340	26	2,340		
86		DS?											120														4,680	52	4,680		
87																															
88	**Abutment foundation**																														
89	PG24	DS1	455	330			12.0	125.0			1,088	22,113						150	700	10											
90		DS?	569	413			12.0	156.3			1,088	27,641						150	700	10											
91	PG25	DS1	455	330			12.0	125.0			1,088	22,113						150	700	10											
92		DS?	569	413			12.0	156.3			1,088	27,641						150	700	10											
93																															
94	**Column foundations**																														
95	PG26	DS1	116.3	41.4				75.0				13,264						50	840		14										
96		DS?	145.4	51.7				93.7				16,580						50	840		14										
97	PG27	DS1	116.3	41.4				75.0				13,264						50	840		14										
98		DS?	145.4	51.7				93.7				16,580						50	840		14										
99	PG28	DS1	116.3	41.4				75.0				13,264						50	840		14										
100		DS?	145.4	51.7				93.7				16,580						50	840		14										
101	PG29	DS1	116.3	41.4				75.0				13,264						50	840		14										
102		DS?	145.4	51.7				93.7				16,580						50	840		14										

Fig. A.6—*Continued.*

	A	B	C	D	E	F	G	H	I	J	K
1	Downtime associated with each damage state. This is an immediate step, with temporary measures to get traffic flowing until full repair later										
2											
3	PG	location	DS1		DS2		DS3		DS4		
4	(days)		mean	std dev	mean	std dev	mean	std dev	mean	std dev	
5											
6	**Max col drift**		minor patching		major patching		replace column				
7	PG1	col1	0.0	0.5	0.0	0.5	1.0	1.0			
8	PG2	col2	0.0	0.5	0.0	0.5	1.0	1.0			
9	PG3	col3	0.0	0.5	0.0	0.5	1.0	1.0			
10	PG4	col4	0.0	0.5	0.0	0.5	1.0	1.0			
11											
12	**Residual col drift**		column casing		re-center column?		failure (same as above)				
13	PG5	col1	1.0	1.0	1.0	1.0	1.0	1.0			
14	PG6	col2	1.0	1.0	1.0	1.0	1.0	1.0			
15	PG7	col3	1.0	1.0	1.0	1.0	1.0	1.0			
16	PG8	col4	1.0	1.0	1.0	1.0	1.0	1.0			
17											
18	**Abutment**		joint seal assembly		backwall minor		backwall, approach replace				
19	PG9	left	0.0	0.5	0.0	0.5	1.0	1.0			
20	PG10	right	0.0	0.5	0.0	0.5	1.0	1.0			
21											
22	**Bearings**		replace bearing								
23	PG11	left	1.0	1.0							
24	PG12	right	1.0	1.0							
25											
26	**Shear Key**		minor patching		replace shear key						
27	PG13	left	0.0	0.5	0.0	0.5					
28	PG14	right	0.0	0.5	0.0	0.5					
29											
30	**Approach**		AC regrade		AC and mudjacking						
31	PG15	left	0.0	0.5	0.0	0.5					
32	PG16	right	0.0	0.5	0.0	0.5					
33											
34	**Deck**		50% overlay		100% overlay						
35	PG17	span1	0.0	0.5	1.0	1.0					
36	PG18	span2	0.0	0.5	1.0	1.0					
37	PG19	span3	0.0	0.5	1.0	1.0					
38	PG20	span4	0.0	0.5	1.0	1.0					
39	PG21	span5	0.0	0.5	1.0	1.0					
40											
41	**Abutment Foundation**		enlarge and add piles								
42	PG22	left	1.0	1.0							
43	PG23	right	1.0	1.0							
44											
45	**Column Foundation**		enlarge and add piles								
46	PG24	col1	1.0	1.0							
47	PG25	col2	1.0	1.0							
48	PG26	col3	1.0	1.0							
49	PG27	col4	1.0	1.0							

Fig. A.7 Downtime spreadsheet.

Appendix B: Damage Scenarios

The following figures illustrate the basic bridge geometry and dimensions (Figs. B.1–B.3), the minor damage scenario (Fig. B.4), and major damage scenarios (Figs. B.5–B.9) developed in Chapter 6.

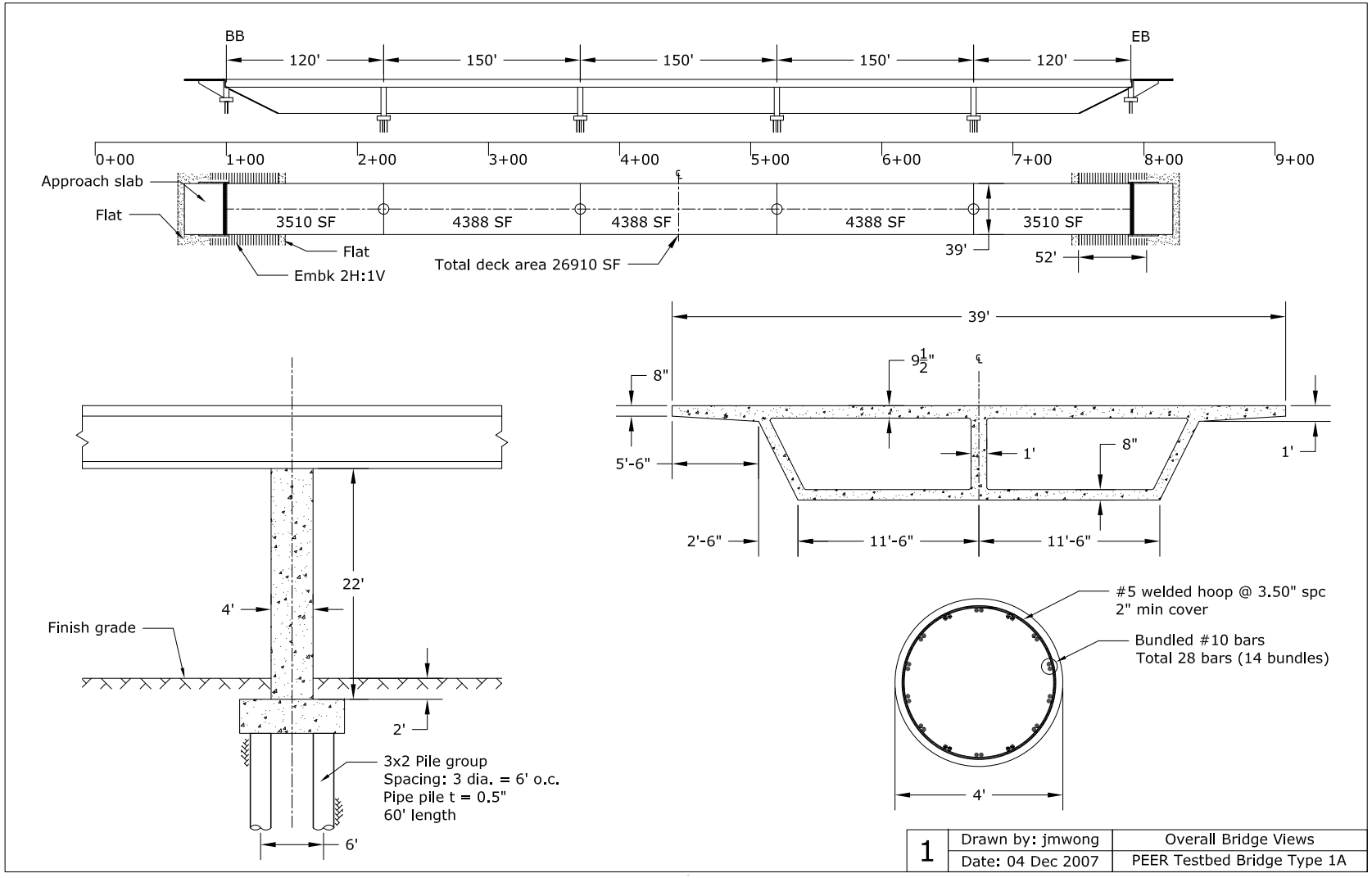

Fig. B.1 Overall bridge views.

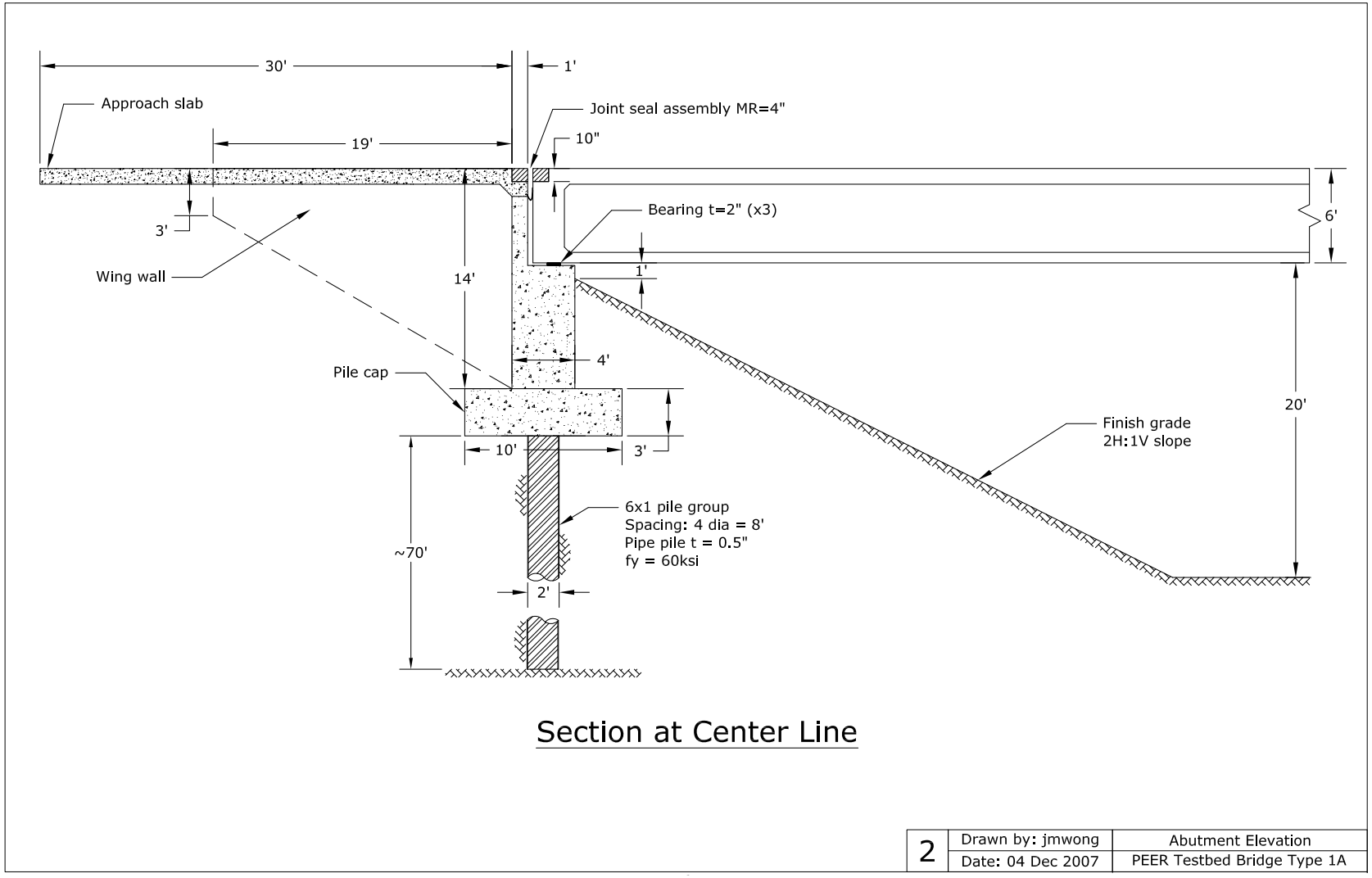

Fig. B.2 Abutment section/elevation.

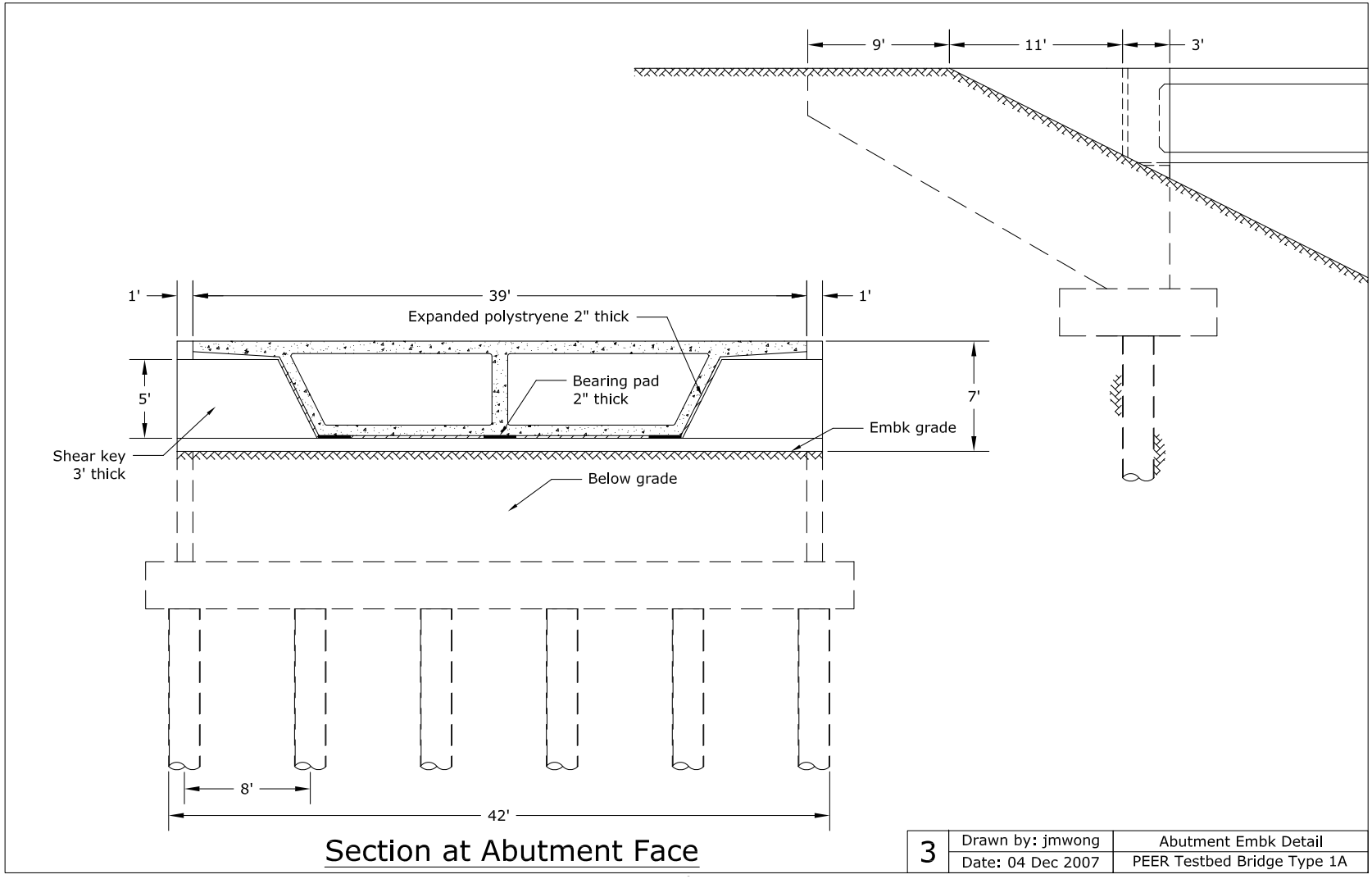

Fig. B.3 Abutment embankment detail.

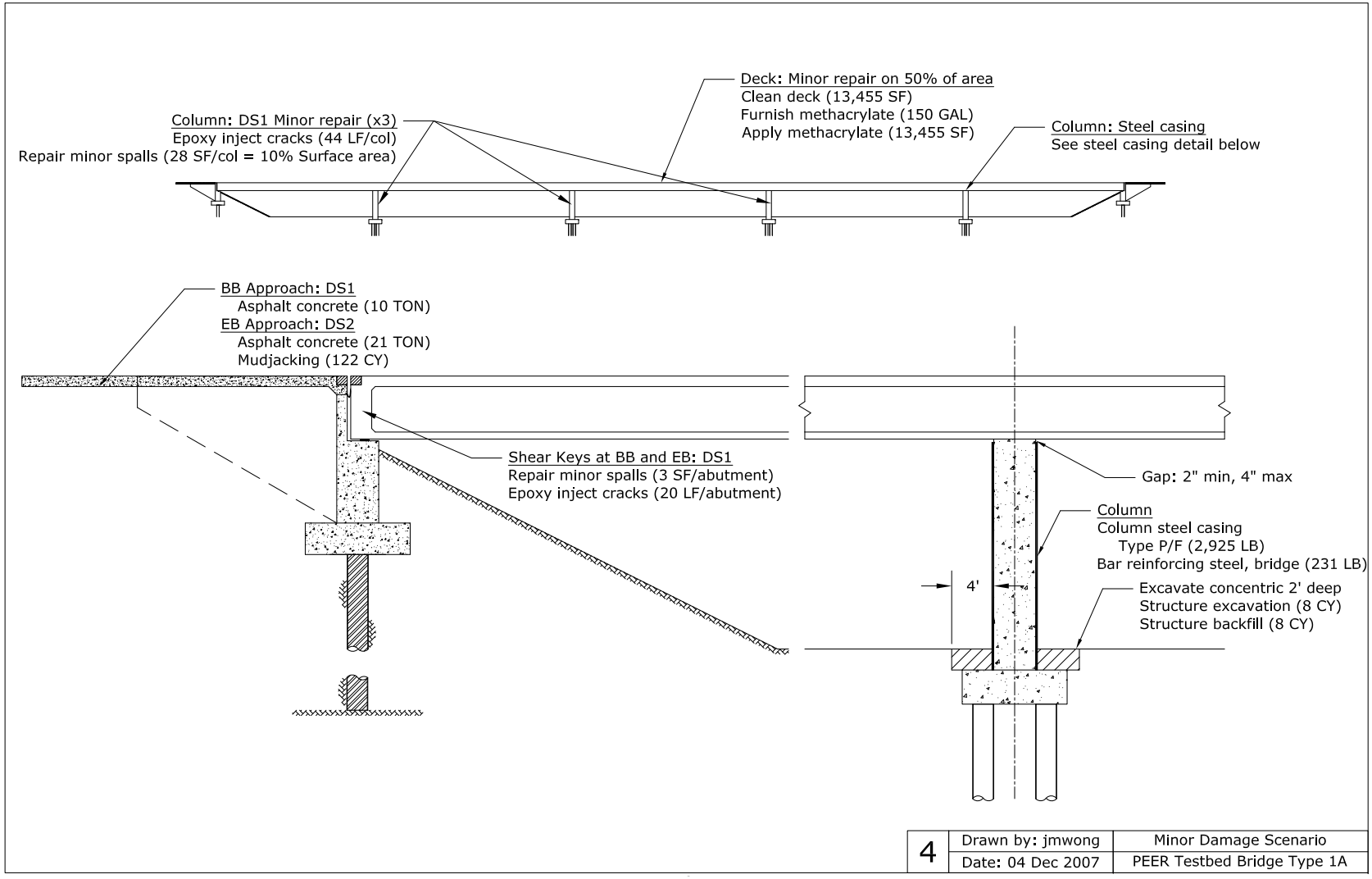

Fig. B.4 Minor damage scenario.

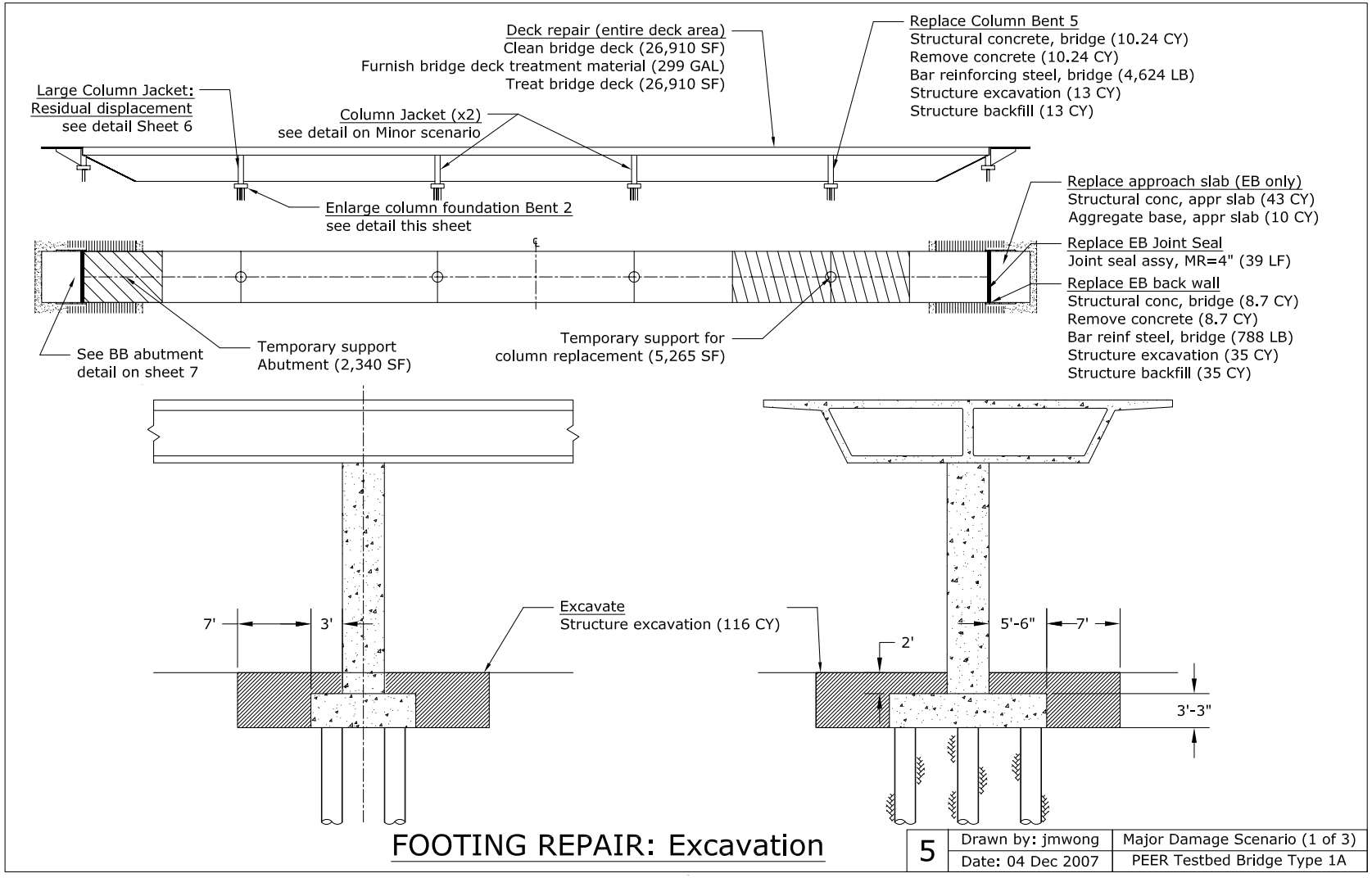

Fig. B.5 Major damage scenario 1/3.

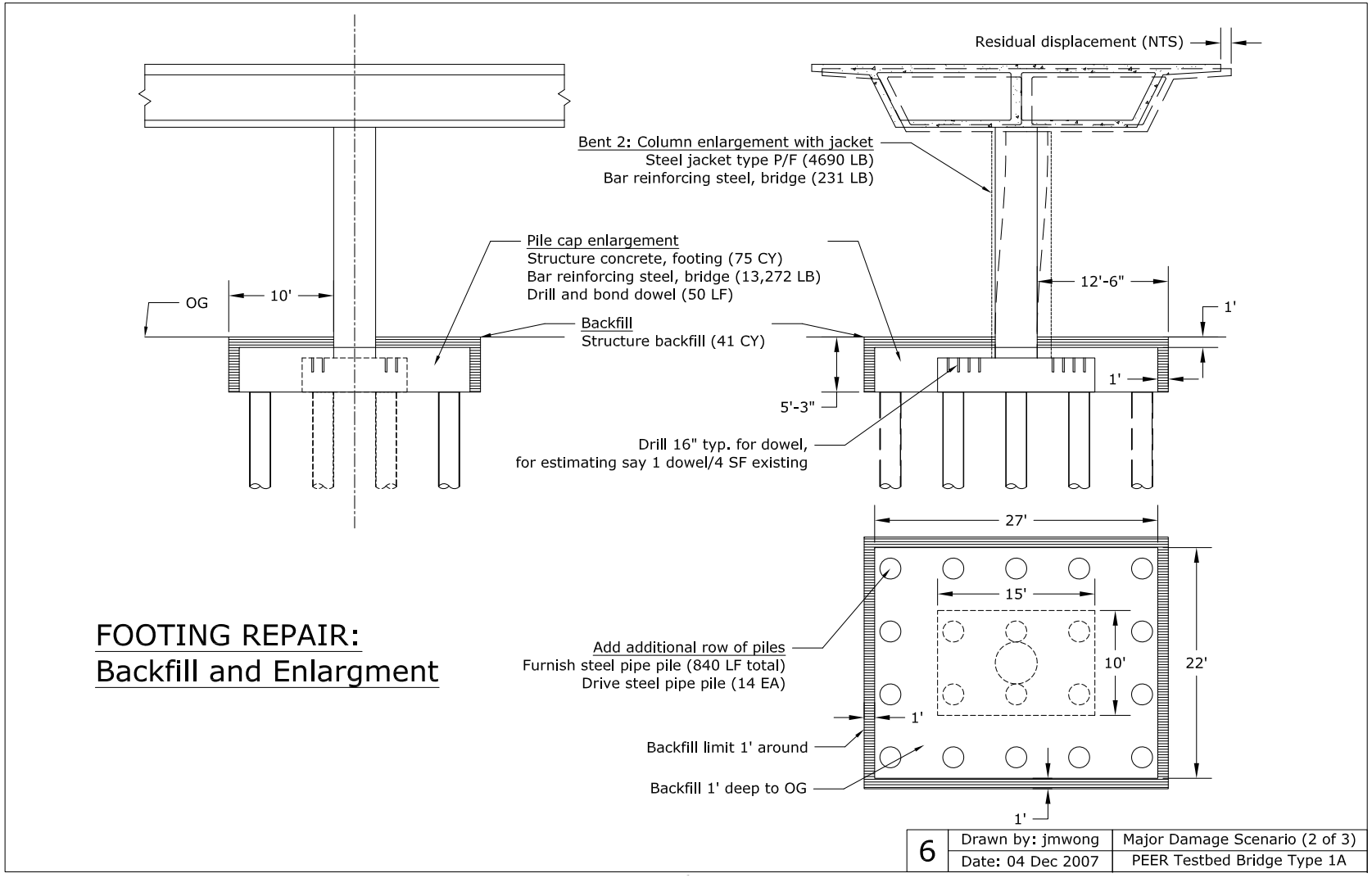

Fig. B.6 Major damage scenario 2/3.

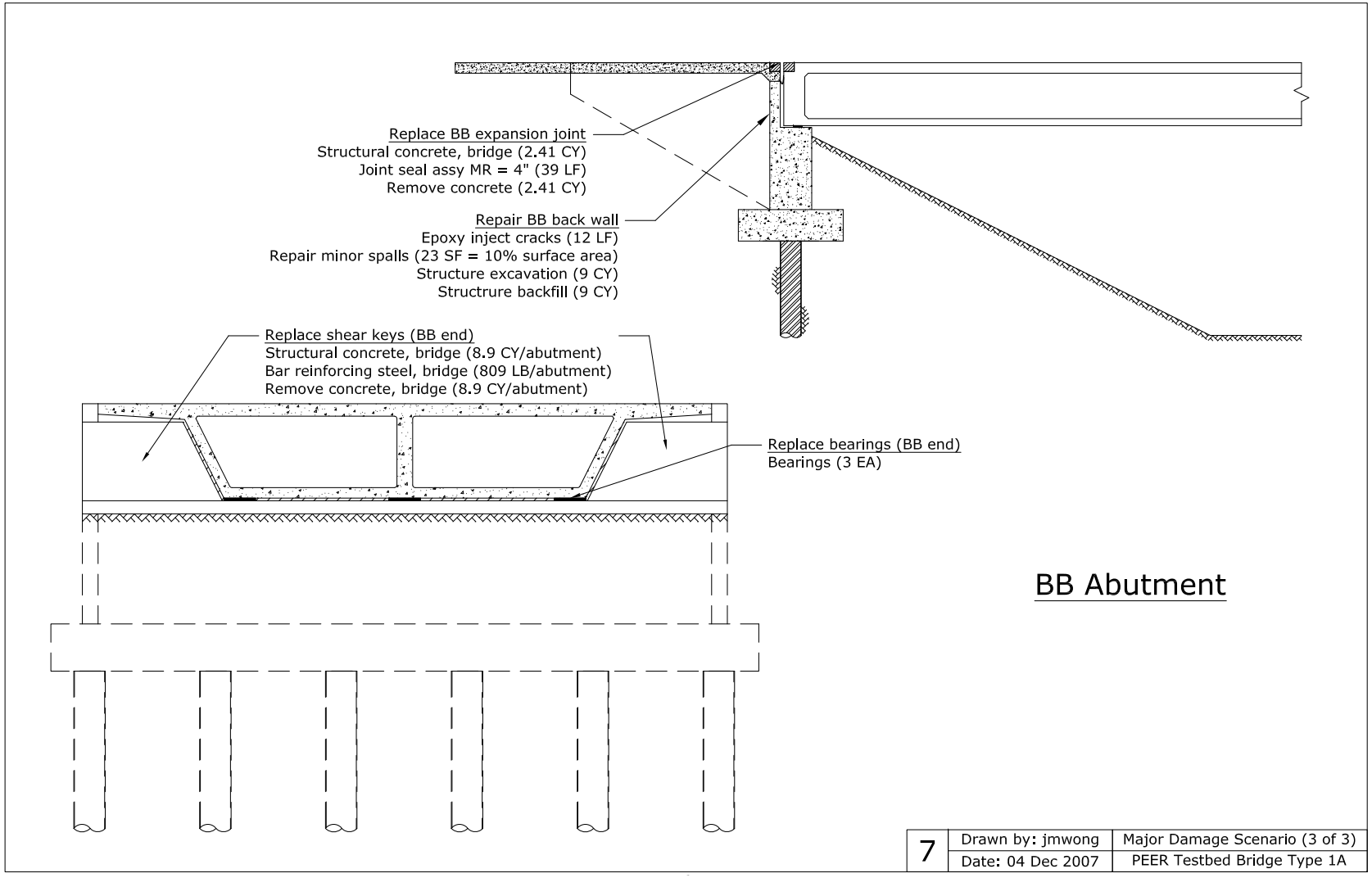

Fig. B.7 Major damage scenario 3/3.

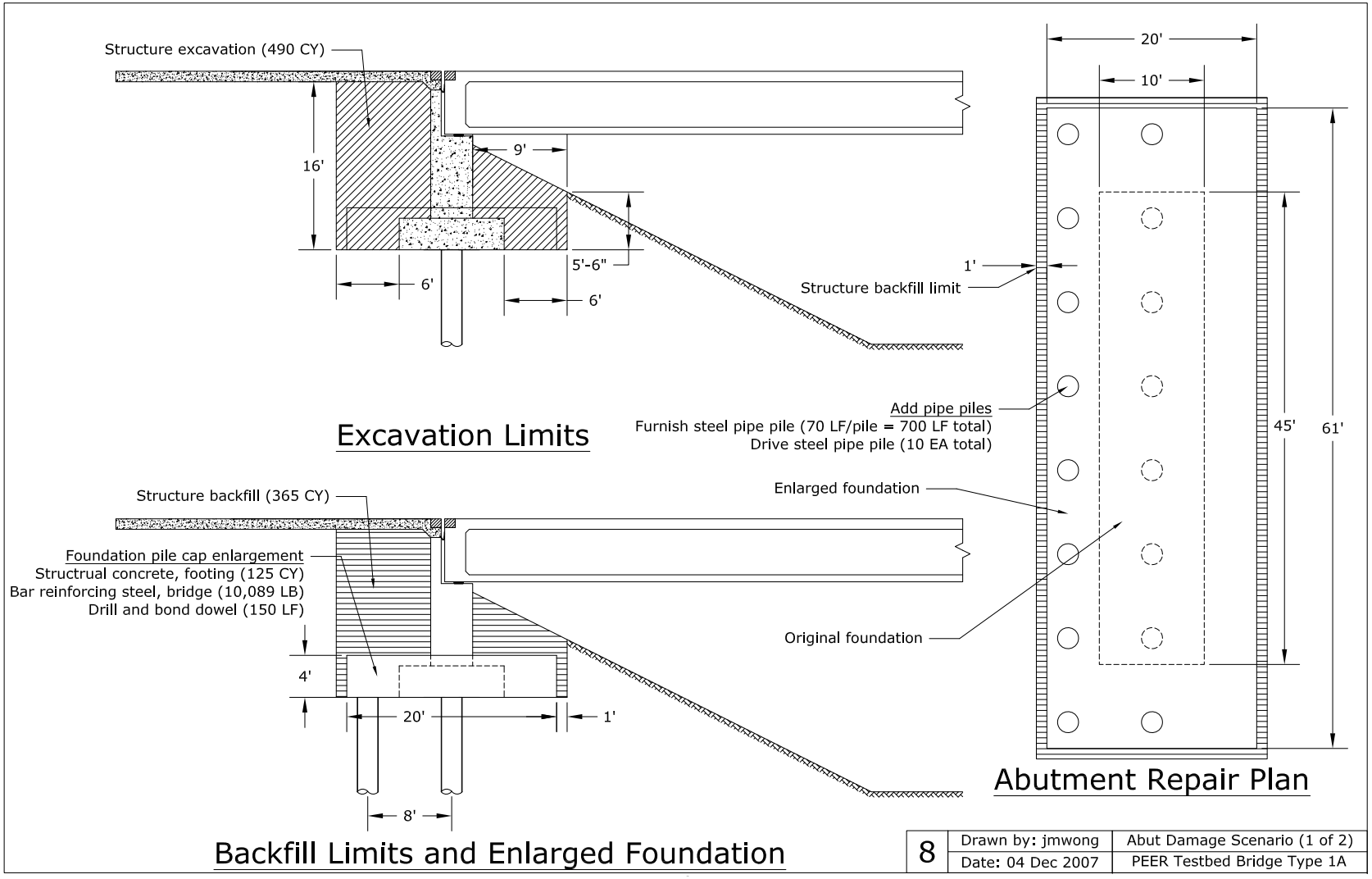

Fig. B.8 Abutment damage scenario 1/2.

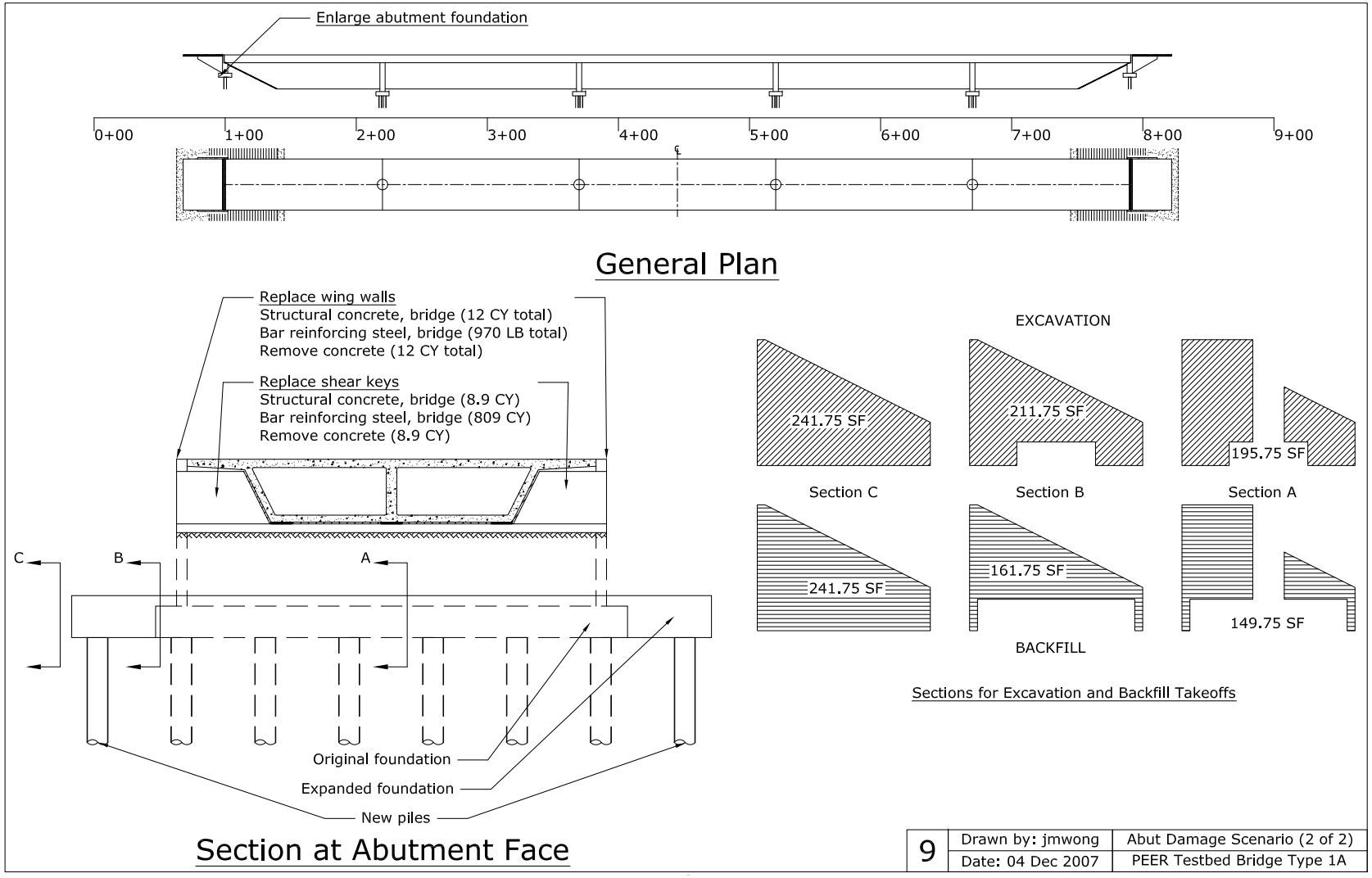

Fig. B.9 Abutment damage scenario 2/2.

Appendix C: Cost and Schedule Estimates

The repair cost estimates and schedules developed for each damage scenario in Chapter 6 are included in this appendix.

Minor Damage Scenario

RCVD BY: IN EST:
OUT EST: 10/16/2007

BRIDGE: PEER Testbed Bridge Type 11A BR. No.: DISTRICT:
TYPE: RTE:
CU: CO:
EA: PM:
LENGTH: WIDTH: AREA (SF) =

DESIGN SECTION:
OF STRUCTURES IN PROJECT : EST. NO.
PRICES BY : COST INDEX:
QUANTITIES BY: DATE:
QUANTITIES CHECKED BY: DATE:

	CONTRACT ITEMS	TYPE	UNIT	QUANTITY	PRICE	AMOUNT
1						
2						
3						
4						
5						
6	INJECT CRACK (EPOXY)		LF	132	$215.00	$28,380.00
7	REPAIR SPALLED SURFACE AREAS		SQFT	84	$300.00	$25,200.00
8						
9						
10	STRUCTURE EXCAVATION (BRIDGE)		CY	8	$250.00	$2,000.00
11	STRUCTURE BACKFILL (BRIDGE)		CY	8	$335.00	$2,680.00
12	COLUMN CASING		LB	2,925	$10.00	$29,250.00
13	BAR REINFORCING STEEL		LB	231	$6.25	$1,443.75
14						
15	CLEAN BRIDGE DECK		LF	13,455	$0.40	$5,382.00
16	FURNISH BRIDGE DECK TREATMENT MATERIAL		GAL	150	$85.00	$12,750.00
17	TREAT BRIDGE DECK		SQFT	13,455	$0.55	$7,400.25
18						
19	REPAIR SPALLED SURFACE AREAS		SQFT	6	$300.00	$1,800.00
20	INJECT CRACK (EPOXY)		LF	40	$215.00	$8,600.00
21						
22	ASPHALT CONCRETE		TON	31	$265.00	$8,215.00
23	MUDJACKING		CY	122	$380.00	$46,360.00
24						
25						
26						
27						
28						
29						
30						

SUBTOTAL	$179,461
MOBILIZATION (@ 10 %)	
SUBTOTAL BRIDGE ITEMS	
CONTINGENCIES (@ 25%)	
BRIDGE TOTAL COST	
COST PER SQ. FT.	
BRIDGE REMOVAL (CONTINGENCIES INCL.)	
WORK BY RAILROAD OR UTILITY FORCES	
GRAND TOTAL	
FOR BUDGET PURPOSES - SAY	

COMMENTS:

Fig. C.1 Minor damage cost estimate.

Major Damage Scenario

RCVD BY: IN EST:
OUT EST: 10/16/2007

BRIDGE: PEER Testbed Bridge Type 11A BR. No.: DISTRICT:
TYPE: RTE:
CU: CO:
EA: PM:
LENGTH: WIDTH: AREA (SF) =

DESIGN SECTION:
OF STRUCTURES IN PROJECT : EST. NO.
PRICES BY : COST INDEX:
QUANTITIES BY: DATE:
QUANTITIES CHECKED BY: DATE:

	CONTRACT ITEMS	TYPE	UNIT	QUANTITY	PRICE	AMOUNT
1	TEMPORARY SUPPORT		SQFT	7,605	$38.00	$288,990.00
2	CLEAN BRIDGE DECK		SQFT	26,910	$0.40	$10,764.00
3	BRIDGE REMOVAL (PORTION)		CY	30.3	$2,355.00	$71,238.75
4	STRUCTURE EXCAVATION (BRIDGE)		CY	189	$165.00	$31,185.00
5	STRUCTURE BACKFILL (BRIDGE)		CY	114	$220.00	$25,080.00
6	AGGREGATE BASE (APPROACH SLAB)		CY	10	$325.00	$3,250.00
7	FURNISH PILING (CLASS140) (ALTERNATIVE W)		LF	840	$55.00	$46,200.00
8	DRIVE PILE (CLASS 140) (ALTERNATIVE W)		EA	14	$9,000.00	$126,000.00
9	STRUCTURAL CONCRETE (BRIDGE FOOTING)		CY	75	$520.00	$39,000.00
10	STRUCTURAL CONCRETE (BRIDGE)		CY	30.3	$2,225.00	$67,306.25
11	STRUCTURAL CONCRETE, APPROACH SLAB		CY	43	$1,625.00	$69,875.00
12	BAR REINFORCING STEEL(BRIDGE)		LB	20,186	$1.35	$27,251.10
13	COLUMN CASING		LB	10,540	$10.00	$105,400.00
14	FURNISH BRIDGE DECK TREATMENT MATERIAL		GAL	299	$85.00	$25,415.00
15	TREAT BRIDGE DECK		SQFT	26,910	$0.55	$14,800.50
16	REPLACE BEARING		EA	3	$1,500.00	$4,500.00
17	INJECT CRACK (EPOXY)		LF	12	$215.00	$2,580.00
18	REPAIR SPALLED SURFACE AREAS		SQFT	23	$300.00	$6,900.00
19	JOINT SEAL ASSEMBLY (MR 4")		LF	78	275.00	$21,450.00
20	DRILL AND BOND DOWEL		LF	50	55.00	$2,750.00
21						
22						
23						
24						
25						
26						
27						
28						
29						
30						

SUBTOTAL	$989,936
MOBILIZATION (@ 10 %)	
SUBTOTAL BRIDGE ITEMS	
CONTINGENCIES (@ 25%)	
BRIDGE TOTAL COST	
COST PER SQ. FT.	
BRIDGE REMOVAL (CONTINGENCIES INCL.)	
WORK BY RAILROAD OR UTILITY FORCES	
GRAND TOTAL	
FOR BUDGET PURPOSES - SAY	

COMMENTS:

Fig. C.2 Major damage cost estimate.

Abutment Damage Scenario

RCVD BY: IN EST:
OUT EST: 10/17/2007

BRIDGE: PEER Testbed Bridge Type 11A BR. No.: DISTRICT:
TYPE: RTE:
CU: CO:
EA: PM:
LENGTH: WIDTH: AREA (SF) =

DESIGN SECTION:
OF STRUCTURES IN PROJECT : EST. NO.
PRICES BY : COST INDEX:
QUANTITIES BY: DATE:
QUANTITIES CHECKED BY: DATE:

	CONTRACT ITEMS	TYPE	UNIT	QUANTITY	PRICE	AMOUNT
1	STRUCTURE EXCAVATION (BRIDGE)		CY	490	$165.00	$80,850.00
2	STRUCTURE BACKFILL (BRIDGE)		CY	365	$115.00	$41,975.00
3	FURNISH PILING (CLASS140) (ALTERNATIVE W)		LF	700	$55.00	$38,500.00
4	DRIVE PILE (CLASS 140) (ALTERNATIVE W)		EA	10	$2,050.00	$20,500.00
5	STRUCTURAL CONCRETE (BRIDGE FOOTING)		CY	125	$520.00	$65,000.00
6	BAR REINFORCING STEEL(BRIDGE)		LB	11,868	$1.35	$16,021.80
7	DRILL AND BOND DOWEL		LF	150	$55.00	$8,250.00
8	STRUCTURAL CONCRETE (BRIDGE)		CY	21	$2,000.00	$41,800.00
9	BRIDGE REMOVAL (PORTION)		CY	21	$1,000.00	$20,900.00
10						
11						
12						
13						
14						
15						
16						
17						
18						
19						
20						
21						
22						
23						
24						
25						
26						
27						
28						
29						
30						

SUBTOTAL	$333,797
MOBILIZATION (@ 10 %)	
SUBTOTAL BRIDGE ITEMS	
CONTINGENCIES (@ 25%)	
BRIDGE TOTAL COST	
COST PER SQ. FT.	
BRIDGE REMOVAL (CONTINGENCIES INCL.)	
WORK BY RAILROAD OR UTILITY FORCES	
GRAND TOTAL	
FOR BUDGET PURPOSES - SAY	

COMMENTS:

Fig. C.3 Abutment damage cost estimate.

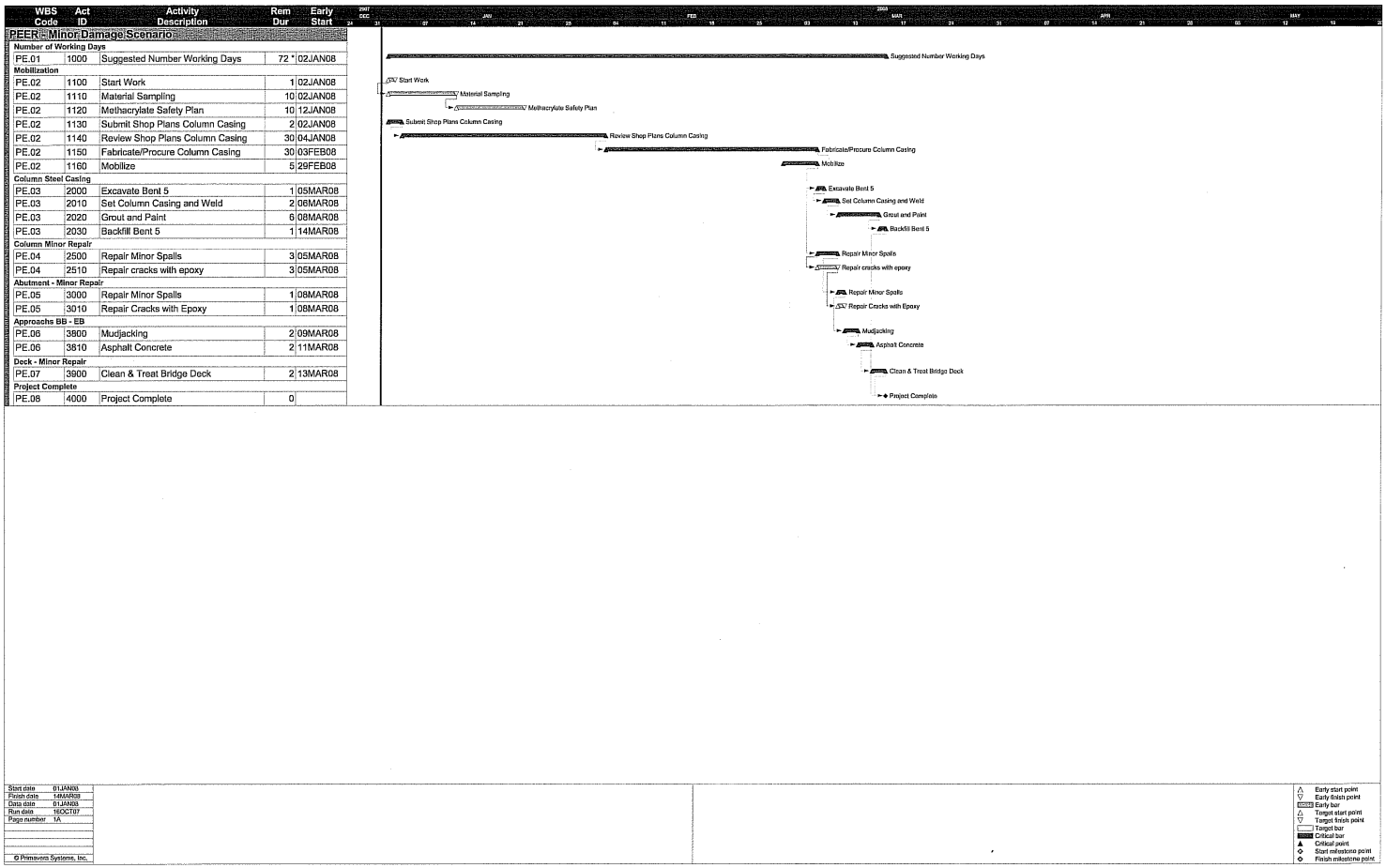

WBS Code	Act ID	Activity Description	Rem Dur	Early Start
PEER - Minor Damage Scenario				
Number of Working Days				
PE.01	1000	Suggested Number Working Days	72 *	02JAN08
Mobilization				
PE.02	1100	Start Work	1	02JAN08
PE.02	1110	Material Sampling	10	02JAN08
PE.02	1120	Methacrylate Safety Plan	10	12JAN08
PE.02	1130	Submit Shop Plans Column Casing	2	02JAN08
PE.02	1140	Review Shop Plans Column Casing	30	04JAN08
PE.02	1150	Fabricate/Procure Column Casing	30	03FEB08
PE.02	1160	Mobilize	5	29FEB08
Column Steel Casing				
PE.03	2000	Excavate Bent 5	1	05MAR08
PE.03	2010	Set Column Casing and Weld	2	06MAR08
PE.03	2020	Grout and Paint	6	08MAR08
PE.03	2030	Backfill Bent 5	1	14MAR08
Column Minor Repair				
PE.04	2500	Repair Minor Spalls	3	05MAR08
PE.04	2510	Repair cracks with epoxy	3	05MAR08
Abutment - Minor Repair				
PE.05	3000	Repair Minor Spalls	1	08MAR08
PE.05	3010	Repair Cracks with Epoxy	1	08MAR08
Approachs BB - EB				
PE.06	3800	Mudjacking	2	09MAR08
PE.06	3810	Asphalt Concrete	2	11MAR08
Deck - Minor Repair				
PE.07	3900	Clean & Treat Bridge Deck	2	13MAR08
Project Complete				
PE.08	4000	Project Complete	0	

Fig. C.4 Minor damage working days estimate.

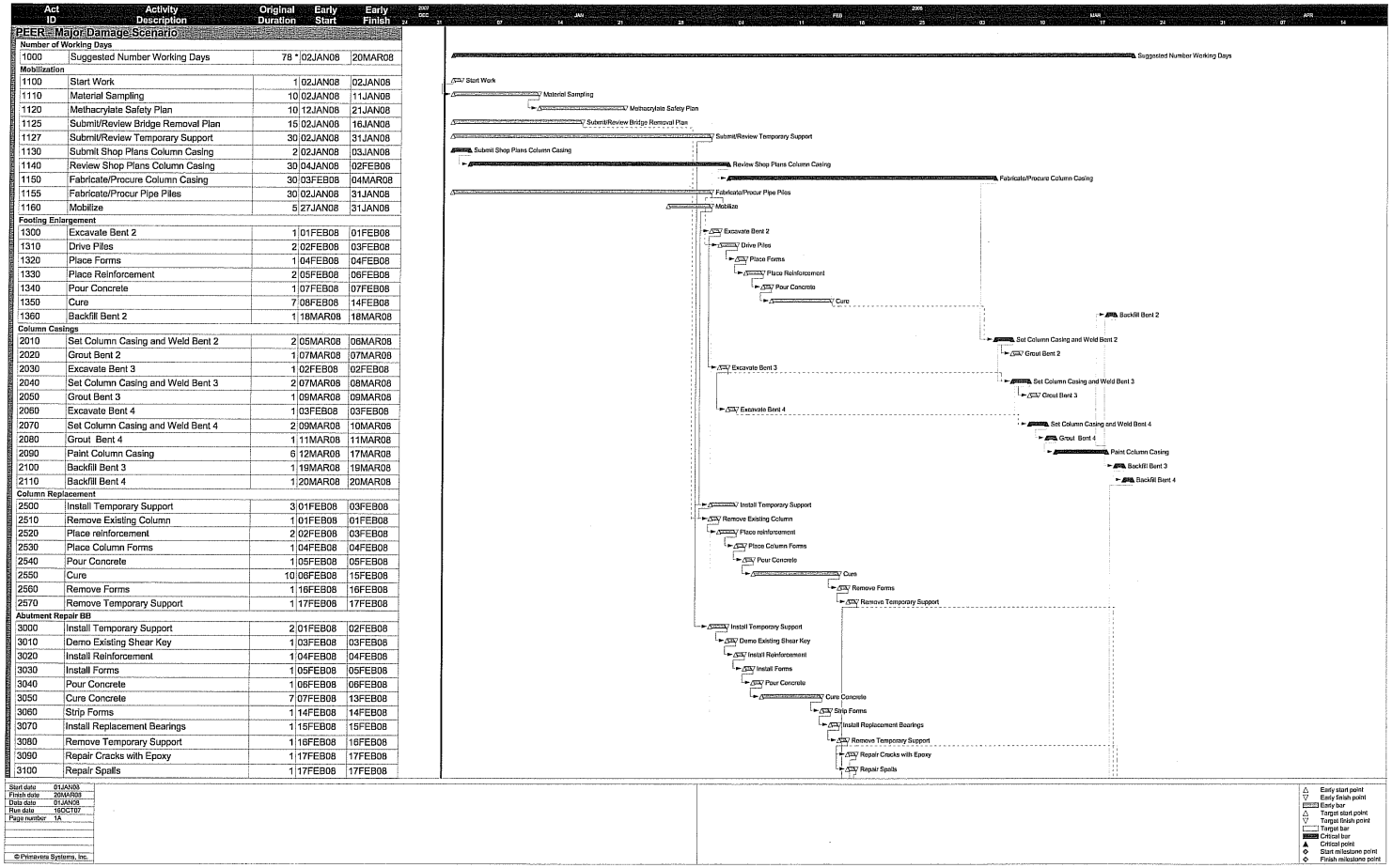

Act ID	Activity Description	Original Duration	Early Start	Early Finish
PEER - Major Damage Scenario				
Number of Working Days				
1000	Suggested Number Working Days	78 *	02JAN08	20MAR08
Mobilization				
1100	Start Work	1	02JAN08	02JAN08
1110	Material Sampling	10	02JAN08	11JAN08
1120	Methacrylate Safety Plan	10	12JAN08	21JAN08
1125	Submit/Review Bridge Removal Plan	15	02JAN08	16JAN08
1127	Submit/Review Temporary Support	30	02JAN08	31JAN08
1130	Submit Shop Plans Column Casing	2	02JAN08	03JAN08
1140	Review Shop Plans Column Casing	30	04JAN08	02FEB08
1150	Fabricate/Procure Column Casing	30	03FEB08	04MAR08
1155	Fabricate/Procur Pipe Piles	30	02JAN08	31JAN08
1160	Mobilize	5	27JAN08	31JAN08
Footing Enlargement				
1300	Excavate Bent 2	1	01FEB08	01FEB08
1310	Drive Piles	2	02FEB08	03FEB08
1320	Place Forms	1	04FEB08	04FEB08
1330	Place Reinforcement	2	05FEB08	06FEB08
1340	Pour Concrete	1	07FEB08	07FEB08
1350	Cure	7	08FEB08	14FEB08
1360	Backfill Bent 2	1	18MAR08	18MAR08
Column Casings				
2010	Set Column Casing and Weld Bent 2	2	05MAR08	06MAR08
2020	Grout Bent 2	1	07MAR08	07MAR08
2030	Excavate Bent 3	1	02FEB08	02FEB08
2040	Set Column Casing and Weld Bent 3	2	07MAR08	08MAR08
2050	Grout Bent 3	1	09MAR08	09MAR08
2060	Excavate Bent 4	1	03FEB08	03FEB08
2070	Set Column Casing and Weld Bent 4	2	09MAR08	10MAR08
2080	Grout Bent 4	1	11MAR08	11MAR08
2090	Paint Column Casing	6	12MAR08	17MAR08
2100	Backfill Bent 3	1	19MAR08	19MAR08
2110	Backfill Bent 4	1	20MAR08	20MAR08
Column Replacement				
2500	Install Temporary Support	3	01FEB08	03FEB08
2510	Remove Existing Column	1	01FEB08	01FEB08
2520	Place reinforcement	2	02FEB08	03FEB08
2530	Place Column Forms	1	04FEB08	04FEB08
2540	Pour Concrete	1	05FEB08	05FEB08
2550	Cure	10	06FEB08	15FEB08
2560	Remove Forms	1	16FEB08	16FEB08
2570	Remove Temporary Support	1	17FEB08	17FEB08
Abutment Repair BB				
3000	Install Temporary Support	2	01FEB08	02FEB08
3010	Demo Existing Shear Key	1	03FEB08	03FEB08
3020	Install Reinforcement	1	04FEB08	04FEB08
3030	Install Forms	1	05FEB08	05FEB08
3040	Pour Concrete	1	06FEB08	06FEB08
3050	Cure Concrete	7	07FEB08	13FEB08
3060	Strip Forms	1	14FEB08	14FEB08
3070	Install Replacement Bearings	1	15FEB08	15FEB08
3080	Remove Temporary Support	1	16FEB08	16FEB08
3090	Repair Cracks with Epoxy	1	17FEB08	17FEB08
3100	Repair Spalls	1	17FEB08	17FEB08

Start date	01JAN08
Finish date	20MAR08
Data date	01JAN08
Run date	16OCT07
Page number	1A

Fig. C.5 Major damage working days estimate.

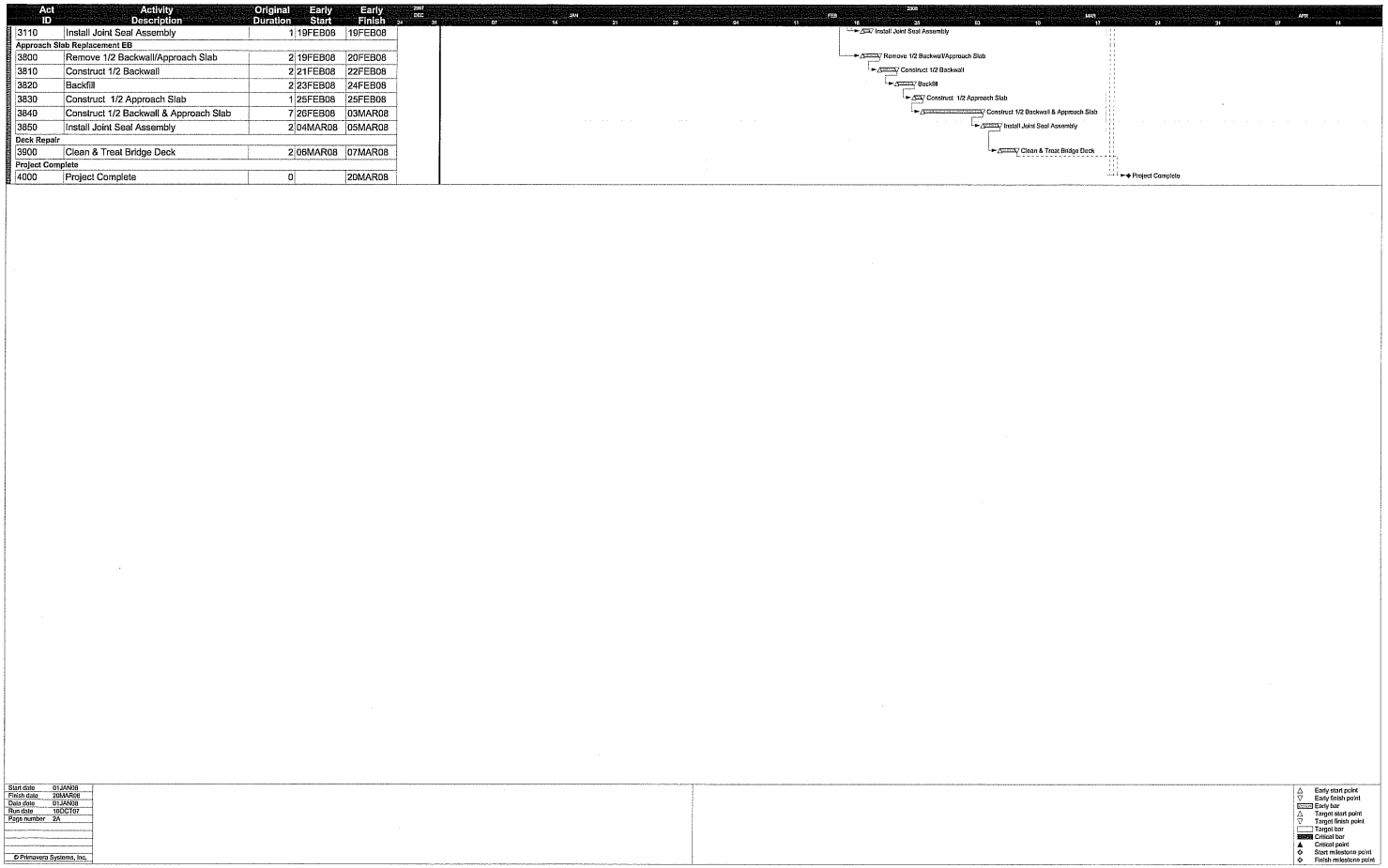

Act ID	Activity Description	Original Duration	Early Start	Early Finish
3110	Install Joint Seal Assembly	1	19FEB08	19FEB08
Approach Slab Replacement EB				
3800	Remove 1/2 Backwall/Approach Slab	2	19FEB08	20FEB08
3810	Construct 1/2 Backwall	2	21FEB08	22FEB08
3820	Backfill	2	23FEB08	24FEB08
3830	Construct 1/2 Approach Slab	1	25FEB08	25FEB08
3840	Construct 1/2 Backwall & Approach Slab	7	26FEB08	03MAR08
3850	Install Joint Seal Assembly	2	04MAR08	05MAR08
Deck Repair				
3900	Clean & Treat Bridge Deck	2	06MAR08	07MAR08
Project Complete				
4000	Project Complete	0		20MAR08

Fig. C.5—*Continued.*

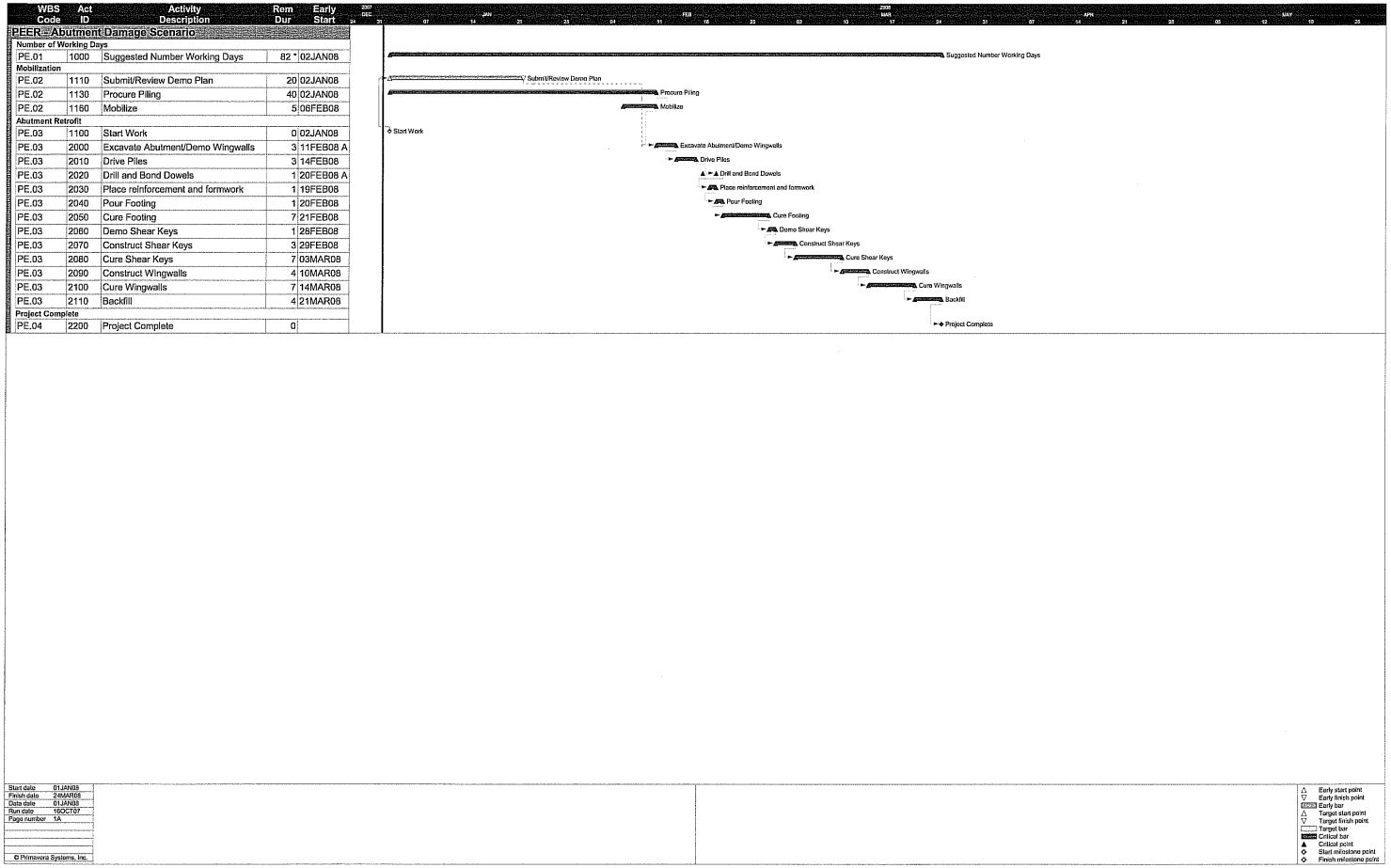

Fig. C.6 Abutment damage working days estimate.

PEER REPORTS

PEER reports are available from the National Information Service for Earthquake Engineering (NISEE). To order PEER reports, please contact the Pacific Earthquake Engineering Research Center, 1301 South 46th Street, Richmond, California 94804-4698. Tel.: (510) 665-3405; Fax: (510) 665-3420.

PEER 2007/11 *Bar Buckling in Reinforced Concrete Bridge Columns.* Wayne A. Brown, Dawn E. Lehman, and John F. Stanton. February 2008.

PEER 2007/09 *Integrated Probabilistic Performance-Based Evaluation of Benchmark Reinforced Concrete Bridges.* Kevin R. Mackie, John-Michael Wong, and Božidar Stojadinović. January 2008.

PEER 2007/08 *Assessing Seismic Collapse Safety of Modern Reinforced Concrete Moment-Frame Buildings.* Curt B. Haselton and Gregory G. Deierlein. February 2008.

PEER 2007/06 *Development of Improved Procedures for Seismic Design of Buried and Partially Buried Structures.* Linda Al Atik and Nicholas Sitar. June 2007.

PEER 2007/05 *Uncertainty and Correlation in Seismic Risk Assessment of Transportation Systems.* Renee G. Lee and Anne S. Kiremidjian. July 2007.

PEER 2007/02 *Campbell-Bozorgnia NGA Ground Motion Relations for the Geometric Mean Horizontal Component of Peak and Spectral Ground Motion Parameters.* Kenneth W. Campbell and Yousef Bozorgnia. May 2007.

PEER 2007/01 *Boore-Atkinson NGA Ground Motion Relations for the Geometric Mean Horizontal Component of Peak and Spectral Ground Motion Parameters.* David M. Boore and Gail M. Atkinson. May. May 2007.

PEER 2006/12 *Societal Implications of Performance-Based Earthquake Engineering.* Peter J. May. May 2007.

PEER 2006/11 *Probabilistic Seismic Demand Analysis Using Advanced Ground Motion Intensity Measures, Attenuation Relationships, and Near-Fault Effects.* Polsak Tothong and C. Allin Cornell. March 2007.

PEER 2006/10 *Application of the PEER PBEE Methodology to the I-880 Viaduct.* Sashi Kunnath. February 2007.

PEER 2006/09 *Quantifying Economic Losses from Travel Forgone Following a Large Metropolitan Earthquake.* James Moore, Sungbin Cho, Yue Yue Fan, and Stuart Werner. November 2006.

PEER 2006/08 *Vector-Valued Ground Motion Intensity Measures for Probabilistic Seismic Demand Analysis*. Jack W. Baker and C. Allin Cornell. October 2006.

PEER 2006/07 *Analytical Modeling of Reinforced Concrete Walls for Predicting Flexural and Coupled–Shear-Flexural Responses*. Kutay Orakcal, Loenardo M. Massone, and John W. Wallace. October 2006.

PEER 2006/06 *Nonlinear Analysis of a Soil-Drilled Pier System under Static and Dynamic Axial Loading.* Gang Wang and Nicholas Sitar. November 2006.

PEER 2006/05 *Advanced Seismic Assessment Guidelines.* Paolo Bazzurro, C. Allin Cornell, Charles Menun, Maziar Motahari, and Nicolas Luco. September 2006.

PEER 2006/04 *Probabilistic Seismic Evaluation of Reinforced Concrete Structural Components and Systems.* Tae Hyung Lee and Khalid M. Mosalam. August 2006.

PEER 2006/03 *Performance of Lifelines Subjected to Lateral Spreading.* Scott A. Ashford and Teerawut Juirnarongrit. July 2006.

PEER 2006/02 *Pacific Earthquake Engineering Research Center Highway Demonstration Project.* Anne Kiremidjian, James Moore, Yue Yue Fan, Nesrin Basoz, Ozgur Yazali, and Meredith Williams. April 2006.

PEER 2006/01 *Bracing Berkeley. A Guide to Seismic Safety on the UC Berkeley Campus.* Mary C. Comerio, Stephen Tobriner, and Ariane Fehrenkamp. January 2006.

PEER 2005/16 *Seismic Response and Reliability of Electrical Substation Equipment and Systems.* Junho Song, Armen Der Kiureghian, and Jerome L. Sackman. April 2006.

PEER 2005/15 *CPT-Based Probabilistic Assessment of Seismic Soil Liquefaction Initiation.* R. E. S. Moss, R. B. Seed, R. E. Kayen, J. P. Stewart, and A. Der Kiureghian. April 2006.

PEER 2005/14 *Workshop on Modeling of Nonlinear Cyclic Load-Deformation Behavior of Shallow Foundations.* Bruce L. Kutter, Geoffrey Martin, Tara Hutchinson, Chad Harden, Sivapalan Gajan, and Justin Phalen. March 2006.

PEER 2005/13 *Stochastic Characterization and Decision Bases under Time-Dependent Aftershock Risk in Performance-Based Earthquake Engineering.* Gee Liek Yeo and C. Allin Cornell. July 2005.

PEER 2005/12 *PEER Testbed Study on a Laboratory Building: Exercising Seismic Performance Assessment.* Mary C. Comerio, editor. November 2005.

PEER 2005/11 *Van Nuys Hotel Building Testbed Report: Exercising Seismic Performance Assessment.* Helmut Krawinkler, editor. October 2005.

PEER 2005/10 *First NEES/E-Defense Workshop on Collapse Simulation of Reinforced Concrete Building Structures.* September 2005.

PEER 2005/09 *Test Applications of Advanced Seismic Assessment Guidelines.* Joe Maffei, Karl Telleen, Danya Mohr, William Holmes, and Yuki Nakayama. August 2006.

PEER 2005/08 *Damage Accumulation in Lightly Confined Reinforced Concrete Bridge Columns.* R. Tyler Ranf, Jared M. Nelson, Zach Price, Marc O. Eberhard, and John F. Stanton. April 2006.

PEER 2005/07 *Experimental and Analytical Studies on the Seismic Response of Freestanding and Anchored Laboratory Equipment.* Dimitrios Konstantinidis and Nicos Makris. January 2005.

PEER 2005/06 *Global Collapse of Frame Structures under Seismic Excitations.* Luis F. Ibarra and Helmut Krawinkler. September 2005.

PEER 2005//05 *Performance Characterization of Bench- and Shelf-Mounted Equipment.* Samit Ray Chaudhuri and Tara C. Hutchinson. May 2006.

PEER 2005/04 *Numerical Modeling of the Nonlinear Cyclic Response of Shallow Foundations.* Chad Harden, Tara Hutchinson, Geoffrey R. Martin, and Bruce L. Kutter. August 2005.

PEER 2005/03 *A Taxonomy of Building Components for Performance-Based Earthquake Engineering.* Keith A. Porter. September 2005.

PEER 2005/02 *Fragility Basis for California Highway Overpass Bridge Seismic Decision Making.* Kevin R. Mackie and Božidar Stojadinović. June 2005.

PEER 2005/01 *Empirical Characterization of Site Conditions on Strong Ground Motion.* Jonathan P. Stewart, Yoojoong Choi, and Robert W. Graves. June 2005.

PEER 2004/09 *Electrical Substation Equipment Interaction: Experimental Rigid Conductor Studies.* Christopher Stearns and André Filiatrault. February 2005.

PEER 2004/08 *Seismic Qualification and Fragility Testing of Line Break 550-kV Disconnect Switches.* Shakhzod M. Takhirov, Gregory L. Fenves, and Eric Fujisaki. January 2005.

PEER 2004/07 *Ground Motions for Earthquake Simulator Qualification of Electrical Substation Equipment.* Shakhzod M. Takhirov, Gregory L. Fenves, Eric Fujisaki, and Don Clyde. January 2005.

PEER 2004/06 *Performance-Based Regulation and Regulatory Regimes.* Peter J. May and Chris Koski. September 2004.

PEER 2004/05 *Performance-Based Seismic Design Concepts and Implementation: Proceedings of an International Workshop.* Peter Fajfar and Helmut Krawinkler, editors. September 2004.

PEER 2004/04 *Seismic Performance of an Instrumented Tilt-up Wall Building.* James C. Anderson and Vitelmo V. Bertero. July 2004.

PEER 2004/03 *Evaluation and Application of Concrete Tilt-up Assessment Methodologies.* Timothy Graf and James O. Malley. October 2004.

PEER 2004/02 *Analytical Investigations of New Methods for Reducing Residual Displacements of Reinforced Concrete Bridge Columns.* Junichi Sakai and Stephen A. Mahin. August 2004.

PEER 2004/01 *Seismic Performance of Masonry Buildings and Design Implications.* Kerri Anne Taeko Tokoro, James C. Anderson, and Vitelmo V. Bertero. February 2004.

PEER 2003/18 *Performance Models for Flexural Damage in Reinforced Concrete Columns.* Michael Berry and Marc Eberhard. August 2003.

PEER 2003/17 *Predicting Earthquake Damage in Older Reinforced Concrete Beam-Column Joints.* Catherine Pagni and Laura Lowes. October 2004.

PEER 2003/16 *Seismic Demands for Performance-Based Design of Bridges.* Kevin Mackie and Božidar Stojadinović. August 2003.

PEER 2003/15 *Seismic Demands for Nondeteriorating Frame Structures and Their Dependence on Ground Motions.* Ricardo Antonio Medina and Helmut Krawinkler. May 2004.

PEER 2003/14 *Finite Element Reliability and Sensitivity Methods for Performance-Based Earthquake Engineering.* Terje Haukaas and Armen Der Kiureghian. April 2004.

PEER 2003/13 *Effects of Connection Hysteretic Degradation on the Seismic Behavior of Steel Moment-Resisting Frames.* Janise E. Rodgers and Stephen A. Mahin. March 2004.

PEER 2003/12 *Implementation Manual for the Seismic Protection of Laboratory Contents: Format and Case Studies.* William T. Holmes and Mary C. Comerio. October 2003.

PEER 2003/11 *Fifth U.S.-Japan Workshop on Performance-Based Earthquake Engineering Methodology for Reinforced Concrete Building Structures.* February 2004.

PEER 2003/10 *A Beam-Column Joint Model for Simulating the Earthquake Response of Reinforced Concrete Frames.* Laura N. Lowes, Nilanjan Mitra, and Arash Altoontash. February 2004.

PEER 2003/09 *Sequencing Repairs after an Earthquake: An Economic Approach.* Marco Casari and Simon J. Wilkie. April 2004.

PEER 2003/08 *A Technical Framework for Probability-Based Demand and Capacity Factor Design (DCFD) Seismic Formats*. Fatemeh Jalayer and C. Allin Cornell. November 2003.

PEER 2003/07 *Uncertainty Specification and Propagation for Loss Estimation Using FOSM Methods.* Jack W. Baker and C. Allin Cornell. September 2003.

PEER 2003/06 *Performance of Circular Reinforced Concrete Bridge Columns under Bidirectional Earthquake Loading*. Mahmoud M. Hachem, Stephen A. Mahin, and Jack P. Moehle. February 2003.

PEER 2003/05 *Response Assessment for Building-Specific Loss Estimation.* Eduardo Miranda and Shahram Taghavi. September 2003.

PEER 2003/04 *Experimental Assessment of Columns with Short Lap Splices Subjected to Cyclic Loads*. Murat Melek, John W. Wallace, and Joel Conte. April 2003.

PEER 2003/03 *Probabilistic Response Assessment for Building-Specific Loss Estimation.* Eduardo Miranda and Hesameddin Aslani. September 2003.

PEER 2003/02 *Software Framework for Collaborative Development of Nonlinear Dynamic Analysis Program.* Jun Peng and Kincho H. Law. September 2003.

PEER 2003/01 *Shake Table Tests and Analytical Studies on the Gravity Load Collapse of Reinforced Concrete Frames*. Kenneth John Elwood and Jack P. Moehle. November 2003.

PEER 2002/24 *Performance of Beam to Column Bridge Joints Subjected to a Large Velocity Pulse.* Natalie Gibson, André Filiatrault, and Scott A. Ashford. April 2002.

PEER 2002/23 *Effects of Large Velocity Pulses on Reinforced Concrete Bridge Columns.* Greg L. Orozco and Scott A. Ashford. April 2002.

PEER 2002/22 *Characterization of Large Velocity Pulses for Laboratory Testing.* Kenneth E. Cox and Scott A. Ashford. April 2002.

PEER 2002/21 *Fourth U.S.-Japan Workshop on Performance-Based Earthquake Engineering Methodology for Reinforced Concrete Building Structures*. December 2002.

PEER 2002/20 *Barriers to Adoption and Implementation of PBEE Innovations.* Peter J. May. August 2002.

PEER 2002/19 *Economic-Engineered Integrated Models for Earthquakes: Socioeconomic Impacts.* Peter Gordon, James E. Moore II, and Harry W. Richardson. July 2002.

PEER 2002/18 *Assessment of Reinforced Concrete Building Exterior Joints with Substandard Details.* Chris P. Pantelides, Jon Hansen, Justin Nadauld, and Lawrence D. Reaveley. May 2002.

PEER 2002/17 *Structural Characterization and Seismic Response Analysis of a Highway Overcrossing Equipped with Elastomeric Bearings and Fluid Dampers: A Case Study.* Nicos Makris and Jian Zhang. November 2002.

PEER 2002/16 *Estimation of Uncertainty in Geotechnical Properties for Performance-Based Earthquake Engineering.* Allen L. Jones, Steven L. Kramer, and Pedro Arduino. December 2002.

PEER 2002/15 *Seismic Behavior of Bridge Columns Subjected to Various Loading Patterns.* Asadollah Esmaeily-Gh. and Yan Xiao. December 2002.

PEER 2002/14 *Inelastic Seismic Response of Extended Pile Shaft Supported Bridge Structures.* T.C. Hutchinson, R.W. Boulanger, Y.H. Chai, and I.M. Idriss. December 2002.

PEER 2002/13 *Probabilistic Models and Fragility Estimates for Bridge Components and Systems.* Paolo Gardoni, Armen Der Kiureghian, and Khalid M. Mosalam. June 2002.

PEER 2002/12 *Effects of Fault Dip and Slip Rake on Near-Source Ground Motions: Why Chi-Chi Was a Relatively Mild M7.6 Earthquake.* Brad T. Aagaard, John F. Hall, and Thomas H. Heaton. December 2002.

PEER 2002/11 *Analytical and Experimental Study of Fiber-Reinforced Strip Isolators*. James M. Kelly and Shakhzod M. Takhirov. September 2002.

PEER 2002/10 *Centrifuge Modeling of Settlement and Lateral Spreading with Comparisons to Numerical Analyses***.** Sivapalan Gajan and Bruce L. Kutter. January 2003.

PEER 2002/09 *Documentation and Analysis of Field Case Histories of Seismic Compression during the 1994 Northridge, California, Earthquake.* Jonathan P. Stewart, Patrick M. Smith, Daniel H. Whang, and Jonathan D. Bray. October 2002.

PEER 2002/08 *Component Testing, Stability Analysis and Characterization of Buckling-Restrained Unbonded Braces™*. Cameron Black, Nicos Makris, and Ian Aiken. September 2002.

PEER 2002/07 *Seismic Performance of Pile-Wharf Connections.* Charles W. Roeder, Robert Graff, Jennifer Soderstrom, and Jun Han Yoo. December 2001.

PEER 2002/06 *The Use of Benefit-Cost Analysis for Evaluation of Performance-Based Earthquake Engineering Decisions*. Richard O. Zerbe and Anthony Falit-Baiamonte. September 2001.

PEER 2002/05 *Guidelines, Specifications, and Seismic Performance Characterization of Nonstructural Building Components and Equipment*. André Filiatrault, Constantin Christopoulos, and Christopher Stearns. September 2001.

PEER 2002/04 *Consortium of Organizations for Strong-Motion Observation Systems and the Pacific Earthquake Engineering Research Center Lifelines Program: Invited Workshop on Archiving and Web Dissemination of Geotechnical Data, 4–5 October 2001*. September 2002.

PEER 2002/03 *Investigation of Sensitivity of Building Loss Estimates to Major Uncertain Variables for the Van Nuys Testbed.* Keith A. Porter, James L. Beck, and Rustem V. Shaikhutdinov. August 2002.

PEER 2002/02 *The Third U.S.-Japan Workshop on Performance-Based Earthquake Engineering Methodology for Reinforced Concrete Building Structures*. July 2002.

PEER 2002/01 *Nonstructural Loss Estimation: The UC Berkeley Case Study.* Mary C. Comerio and John C. Stallmeyer. December 2001.

PEER 2001/16 *Statistics of SDF-System Estimate of Roof Displacement for Pushover Analysis of Buildings.* Anil K. Chopra, Rakesh K. Goel, and Chatpan Chintanapakdee. December 2001.

PEER 2001/15 *Damage to Bridges during the 2001 Nisqually Earthquake.* R. Tyler Ranf, Marc O. Eberhard, and Michael P. Berry. November 2001.

PEER 2001/14 *Rocking Response of Equipment Anchored to a Base Foundation.* Nicos Makris and Cameron J. Black. September 2001.

PEER 2001/13 *Modeling Soil Liquefaction Hazards for Performance-Based Earthquake Engineering.* Steven L. Kramer and Ahmed-W. Elgamal. February 2001.

PEER 2001/12 *Development of Geotechnical Capabilities in OpenSees.* Boris Jeremi . September 2001.

PEER 2001/11 *Analytical and Experimental Study of Fiber-Reinforced Elastomeric Isolators*. James M. Kelly and Shakhzod M. Takhirov. September 2001.

PEER 2001/10 *Amplification Factors for Spectral Acceleration in Active Regions.* Jonathan P. Stewart, Andrew H. Liu, Yoojoong Choi, and Mehmet B. Baturay. December 2001.

PEER 2001/09 *Ground Motion Evaluation Procedures for Performance-Based Design.* Jonathan P. Stewart, Shyh-Jeng Chiou, Jonathan D. Bray, Robert W. Graves, Paul G. Somerville, and Norman A. Abrahamson. September 2001.

PEER 2001/08 *Experimental and Computational Evaluation of Reinforced Concrete Bridge Beam-Column Connections for Seismic Performance*. Clay J. Naito, Jack P. Moehle, and Khalid M. Mosalam. November 2001.

PEER 2001/07 *The Rocking Spectrum and the Shortcomings of Design Guidelines.* Nicos Makris and Dimitrios Konstantinidis. August 2001.

PEER 2001/06 *Development of an Electrical Substation Equipment Performance Database for Evaluation of Equipment Fragilities*. Thalia Agnanos. April 1999.

PEER 2001/05 *Stiffness Analysis of Fiber-Reinforced Elastomeric Isolators.* Hsiang-Chuan Tsai and James M. Kelly. May 2001.

PEER 2001/04 *Organizational and Societal Considerations for Performance-Based Earthquake Engineering.* Peter J. May. April 2001.

PEER 2001/03 *A Modal Pushover Analysis Procedure to Estimate Seismic Demands for Buildings: Theory and Preliminary Evaluation.* Anil K. Chopra and Rakesh K. Goel. January 2001.

PEER 2001/02 *Seismic Response Analysis of Highway Overcrossings Including Soil-Structure Interaction.* Jian Zhang and Nicos Makris. March 2001.

PEER 2001/01 *Experimental Study of Large Seismic Steel Beam-to-Column Connections.* Egor P. Popov and Shakhzod M. Takhirov. November 2000.

PEER 2000/10 *The Second U.S.-Japan Workshop on Performance-Based Earthquake Engineering Methodology for Reinforced Concrete Building Structures.* March 2000.

PEER 2000/09 *Structural Engineering Reconnaissance of the August 17, 1999 Earthquake: Kocaeli (Izmit), Turkey.* Halil Sezen, Kenneth J. Elwood, Andrew S. Whittaker, Khalid Mosalam, John J. Wallace, and John F. Stanton. December 2000.

PEER 2000/08 *Behavior of Reinforced Concrete Bridge Columns Having Varying Aspect Ratios and Varying Lengths of Confinement.* Anthony J. Calderone, Dawn E. Lehman, and Jack P. Moehle. January 2001.

PEER 2000/07 *Cover-Plate and Flange-Plate Reinforced Steel Moment-Resisting Connections.* Taejin Kim, Andrew S. Whittaker, Amir S. Gilani, Vitelmo V. Bertero, and Shakhzod M. Takhirov. September 2000.

PEER 2000/06 *Seismic Evaluation and Analysis of 230-kV Disconnect Switches.* Amir S. J. Gilani, Andrew S. Whittaker, Gregory L. Fenves, Chun-Hao Chen, Henry Ho, and Eric Fujisaki. July 2000.

PEER 2000/05 *Performance-Based Evaluation of Exterior Reinforced Concrete Building Joints for Seismic Excitation.* Chandra Clyde, Chris P. Pantelides, and Lawrence D. Reaveley. July 2000.

PEER 2000/04 *An Evaluation of Seismic Energy Demand: An Attenuation Approach.* Chung-Che Chou and Chia-Ming Uang. July 1999.

PEER 2000/03 *Framing Earthquake Retrofitting Decisions: The Case of Hillside Homes in Los Angeles.* Detlof von Winterfeldt, Nels Roselund, and Alicia Kitsuse. March 2000.

PEER 2000/02 *U.S.-Japan Workshop on the Effects of Near-Field Earthquake Shaking.* Andrew Whittaker, ed. July 2000.

PEER 2000/01 *Further Studies on Seismic Interaction in Interconnected Electrical Substation Equipment.* Armen Der Kiureghian, Kee-Jeung Hong, and Jerome L. Sackman. November 1999.

PEER 1999/14 *Seismic Evaluation and Retrofit of 230-kV Porcelain Transformer Bushings*. Amir S. Gilani, Andrew S. Whittaker, Gregory L. Fenves, and Eric Fujisaki. December 1999.

PEER 1999/13 *Building Vulnerability Studies: Modeling and Evaluation of Tilt-up and Steel Reinforced Concrete Buildings.* John W. Wallace, Jonathan P. Stewart, and Andrew S. Whittaker, editors. December 1999.

PEER 1999/12 *Rehabilitation of Nonductile RC Frame Building Using Encasement Plates and Energy-Dissipating Devices.* Mehrdad Sasani, Vitelmo V. Bertero, James C. Anderson. December 1999.

PEER 1999/11 *Performance Evaluation Database for Concrete Bridge Components and Systems under Simulated Seismic Loads.* Yael D. Hose and Frieder Seible. November 1999.

PEER 1999/10 *U.S.-Japan Workshop on Performance-Based Earthquake Engineering Methodology for Reinforced Concrete Building Structures.* December 1999.

PEER 1999/09 *Performance Improvement of Long Period Building Structures Subjected to Severe Pulse-Type Ground Motions*. James C. Anderson, Vitelmo V. Bertero, and Raul Bertero. October 1999.

PEER 1999/08 *Envelopes for Seismic Response Vectors.* Charles Menun and Armen Der Kiureghian. July 1999.

PEER 1999/07 *Documentation of Strengths and Weaknesses of Current Computer Analysis Methods for Seismic Performance of Reinforced Concrete Members.* William F. Cofer. November 1999.

PEER 1999/06 *Rocking Response and Overturning of Anchored Equipment under Seismic Excitations.* Nicos Makris and Jian Zhang. November 1999.

PEER 1999/05 *Seismic Evaluation of 550 kV Porcelain Transformer Bushings.* Amir S. Gilani, Andrew S. Whittaker, Gregory L. Fenves, and Eric Fujisaki. October 1999.

PEER 1999/04 *Adoption and Enforcement of Earthquake Risk-Reduction Measures.* Peter J. May, Raymond J. Burby, T. Jens Feeley, and Robert Wood.

PEER 1999/03 *Task 3 Characterization of Site Response General Site Categories.* Adrian Rodriguez-Marek, Jonathan D. Bray, and Norman Abrahamson. February 1999.

PEER 1999/02 *Capacity-Demand-Diagram Methods for Estimating Seismic Deformation of Inelastic Structures: SDF Systems.* Anil K. Chopra and Rakesh Goel. April 1999.

PEER 1999/01 *Interaction in Interconnected Electrical Substation Equipment Subjected to Earthquake Ground Motions.* Armen Der Kiureghian, Jerome L. Sackman, and Kee-Jeung Hong. February 1999.

PEER 1998/08 *Behavior and Failure Analysis of a Multiple-Frame Highway Bridge in the 1994 Northridge Earthquake.* Gregory L. Fenves and Michael Ellery. December 1998.

PEER 1998/07 *Empirical Evaluation of Inertial Soil-Structure Interaction Effects.* Jonathan P. Stewart, Raymond B. Seed, and Gregory L. Fenves. November 1998.

PEER 1998/06 *Effect of Damping Mechanisms on the Response of Seismic Isolated Structures.* Nicos Makris and Shih-Po Chang. November 1998.

PEER 1998/05 *Rocking Response and Overturning of Equipment under Horizontal Pulse-Type Motions.* Nicos Makris and Yiannis Roussos. October 1998.

PEER 1998/04 *Pacific Earthquake Engineering Research Invitational Workshop Proceedings, May 14–15, 1998: Defining the Links between Planning, Policy Analysis, Economics and Earthquake Engineering.* Mary Comerio and Peter Gordon. September 1998.

PEER 1998/03 *Repair/Upgrade Procedures for Welded Beam to Column Connections.* James C. Anderson and Xiaojing Duan. May 1998.

PEER 1998/02 *Seismic Evaluation of 196 kV Porcelain Transformer Bushings.* Amir S. Gilani, Juan W. Chavez, Gregory L. Fenves, and Andrew S. Whittaker. May 1998.

PEER 1998/01 *Seismic Performance of Well-Confined Concrete Bridge Columns.* Dawn E. Lehman and Jack P. Moehle. December 2000.

ONLINE REPORTS

The following PEER reports are available by Internet only at http://peer.berkeley.edu/publications/peer_reports.html

PEER 2007/101 *Generalized Hybrid Simulation Framework for Structural Systems Subjected to Seismic Loading.* Tarek Elkhoraibi and Khalid M. Mosalam. July 2007.

PEER 2007/100 *Seismic Evaluation of Reinforced Concrete Buildings Including Effects of Masonry Infill Walls.* Alidad Hashemi and Khalid M. Mosalam. July 2007.